Genetic and Pharmacological Modulation of Alpha-Synuclein Aggregation

Dissertation
for the award of the degree
"Doctor rerum naturalium" (Dr. rer. nat.)
of the Georg-August-Universität Göttingen,
Faculty of Biology

within the doctoral program Molecular Physiology of the Brain
of the Georg-August University School of Science (GAUSS)

submitted by
Diana Fernandes Lázaro
from Santarém, Portugal
Göttingen 2017

Thesis Committee

Prof. Dr. Tiago Outeiro (1st Reviewer)
Neurodegeneration and Restorative Research, University Medical Center Göttingen

Prof. Dr. Markus Zweckstetter (2nd Reviewer)
German Center for Neurodegenerative Diseases (DZNE) Göttingen

Prof. Dr. Silvio Rizzoli
Neuro-and Sensory Physiology, University Medical Center Göttingen

Extended Thesis Committee Members

Dr. Sebastian Kügler
Neurology, AG Viral Vectors, University Medical Center, Göttingen

Prof. Dr. Gerhard Braus
Molecular Microbiology and Genetics and Göttingen Center for Molecular Biosciences (GZMB), Institute of Microbiology and Genetics, Georg-August-Universität, Göttingen

Prof. Dr. Thomas Dresbach
Anatomy and Embryology Kreuzbergring University Medical Center Göttingen

Date of oral examination: June 21st, 2017

Posso ter defeitos, viver ansioso e ficar irritado algumas vezes,
Mas não esqueço de que minha vida
É a maior empresa do mundo…
E que posso evitar que ela vá à falência.
Ser feliz é reconhecer que vale a pena viver
Apesar de todos os desafios, incompreensões e períodos de crise.
Ser feliz é deixar de ser vítima dos problemas e
Se tornar um autor da própria história…
É atravessar desertos fora de si, mas ser capaz de encontrar
Um oásis no recôndito da sua alma…
É agradecer a Deus a cada manhã pelo milagre da vida.
Ser feliz é não ter medo dos próprios sentimentos.
É saber falar de si mesmo.
É ter coragem para ouvir um "Não"!!!
É ter segurança para receber uma crítica,
Mesmo que injusta…

Pedras no caminho?
Guardo todas, um dia vou construir um castelo…

by Fernando Pessoa

Affirmation

I hereby declare that I have written this thesis entitled "*Genetic and Pharmacological Modulation of Alpha-Synuclein Aggregation*" independently and with no other sources and aids other than quoted. This thesis has not been submitted elsewhere for any academic degree.

_____

Diana Fernandes Lázaro

Göttingen, April 12th, 2017

This work was accomplished in the group of Prof. Dr. Tiago F. Outeiro at the Department of Experimental Neurodegeneration, Georg-August-Universität Göttingen.

List of publications included in this thesis:

Lázaro DF, Rodrigues EF et al. Systematic comparison of the effects of alpha-synuclein mutations on its oligomerization and aggregation. PLoS Genet. 2014 Nov.

Lázaro DF#, Moree B#, Yin G#**,** Munari F, Strohäker T, Giller K, Becker S, Outeiro TF, Zweckstetter M, Salafsky J. Small Molecules Detected by Second-Harmonic Generation Modulate the Conformation of Monomeric α-Synuclein and Reduce its Aggregation in Cells. J Bio Chem. 2015 Sep. (#equal contribution)

Lázaro DF#, Dias M#, Carija A, Navarro S, Madaleno CS, Tenreiro S, Ventura S, Outeiro TF. The effects of the novel A53E alpha-synuclein mutation on its oligomerization and aggregation. Acta Neuropathologica Communications. 2016 Dez. (#equal contribution)

Acknowledgements

Obviously, all the people that I acknowledge here are very important to me. They were either my guides through this “crazy” journey of a PhD, or they were companions along the journey that helped me keep things on the right track.

First of all, I would like to thank Prof. Tiago Outeiro for all his support. He is an inspiring person, with whom I had the great pleasure to work with. I am truly thankful for your words of encouragement throughout all these years.

To Prof. Silvio Rizzoli and Prof. Markus Zweckstetter, I thank them for the opportunity to discuss my work and for the valuable feedback and suggestions they provided.

I would like to thank Prof. Dr. Jochen Klucken for the opportunity to spend some days in his lab in Erlangen.

I am also thankful to Dr. Daniel Kaganovich for giving me the opportunity to visit his laboratory in Jerusalem, and use excellent tools and microscopes in his group.

To Sonja Reisenauer, Ellen Gerhardt and Christiane Fahlbusch, for being the bridge between English and German, and for helping me also with various non-related issues of daily life in Germany. All of us are very lucky to have you in the lab! Your constant support was one of the key ingredients for me, to have come this far, I have not doubts!

To Éva Szegö for all the kind help with the animal experiments, and for the time that I took away from her busy schedule. Thank you so much!

To Dr. Niels Kruse, for his constant help with some important experiments. Thank you so much for always analyzing my samples and for your interest in the project.

To my lovely Shantal López. You know how much I like you! Thank you for being such a dedicated, and motivated person, but mostly, for your golden heart. I wish you all the best that the world can give!

To Prof. Michael Hausser, with whom I never had the pleasure to work with, but with whom I had extremely pleasant scientific and non-scientific conversations.

To my friend, and swimming partner Tiago Coimbra. Everything became so much more fun since we meet! Thank you for your constant support, for the stimulating cultural programs, and for the long talks in the cold. You know that I will be always here for you.

To my parents, for letting me fly… It is not easy to be away from them for all these years. Thank you for always supporting and believing in me! Words will never translate how grateful, and lucky I am to have you both in my life!

To my brother, Filipe, and my "sister" Inês, for being so many times the bridge between these two countries. For your concerns and worries.

To my grandmother, for being such an inspiring person! For your contagious energy, your smile, your sweetness, and craziness. To my grandfather, that is no longer physically with us, but I believe that he is still looking out for me… Thank you both! Those little moments that we shared together, as simple as drinking lemonade or playing cards, are priceless!

I also need to thank to all the little stones and extra challenges I had to face along the way… Those things just make me a BETTER, a WISER and a STRONGER person!

Finally, to YOU! Words will never be enough to express my gratitude, and how much you mean to me! During this journey, which was not always easy… you were always there for me, *no matter how far*. Thank you for being my shoulder, motivation and inspiration. I am so lucky to have you in my life!!!

Thank you all!!

Table of Contents

Table of Contents ..... *viii*

II. List of Figures ..... *x*

III. List of Tables ..... *xi*

IV. List of Abbreviations ..... *xii*

Abstract *1*

1. Introduction *3*

1.1. Protein Folding and Misfolding **3**

1.2. Cellular Quality Control Mechanisms **5**

1.2.1. Molecular Chaperones 6

1.2.2. Ubiquitin proteasome system (UPS) 7

1.2.3. Autophagy-Lysosome Pathway 8

1.2.4. Protein compartmentalization 9

1.3. Protein Misfolding diseases **12**

1.4. Parkinson's Disease **13**

1.4.1. Protein aggregation in PD 15

1.4.2. Etiology of PD 16

1.4.2.1. The synuclein family of proteins 17

1.4.2.2. aSyn Structure 18

1.4.2.3. aSyn aggregation and cytotoxic species 19

1.4.2.3.1. Mutations in aSyn 21

1.4.2.3.2. aSyn Posttranslational Modifications 23

1.4.2.3.3. Putative functions of aSyn 25

1.4.2.3.4. Prion-like spreading of aSyn pathology 28

1.4.2.4. Synphilin-1: an aSyn-interacting protein 31

1.5. *In vitro* studies of aSyn **33**

1.6. Cell-based models of aSyn aggregation **34**

2. Aims of the study *38*

3. Results *39*

3.1. Systematic comparison of the effects of alpha-synuclein mutations on its oligomerization and aggregation 39

3.2. Small Molecules Detected by Second-Hamonic Generation Modulate the Conformation of Monomeric a-Synuclein and Reduce Its Aggregation in Cells 58

3.3. The effects of the novel A53E alpha-synuclein mutation on its oligomerization and aggregation 71

4. Discussion 88

4.1. The urgency for standardization of models and observations 88

4.2. Distinguishing aSyn species and their cellular effects 88

4.3. Modulation of aSyn aggregation by proline residues 90

4.4. Position 53: the effect of the charge 91

4.5. Phosphorylation and other PTMs: the need for additional in depth studies 92

4.6. Better treatments for a brighter future 93

5. Conclusion 96

6. Annex 98

6.1. Supporting Information 98

6.2. Additional file 101

7. References 104

8. Curriculum vitae 121

II. List of Figures

Figure 1.1 The free energy landscape of protein folding (left) and aggregation (right). 4
Figure 1.2 Deregulation of proteostasis due to protein misfolding. 5
Figure 1.3 Schematic representation of a mammalian cell showing two misfolded proteins compartments.....10
Figure 1.4 Mitotic cells have asymmetric inheritance of JUNQ and IPOD. 11
Figure 1.5 Different methods for amyloid protein characterization 13
Figure 1.6 Afflicted region in PD patients.....14
Figure 1.7 Lewy Bodies and Lewy Neurites in the SN of PD patients 15
Figure 1.8 Human aSyn. A. 19
Figure 1.9 Schematic model of the process of aSyn aggregation.. 20
Figure 1.10 aSyn sequence. 22
Figure 1.11 Schematic representation of some of the known PTMs in aSyn. 23
Figure 1.12 Model for aSyn-mediated membrane remodeling and curvature induction 26
Figure 1.13 Schemating of a physiological folding pathway for aSyn. 27
Figure 1.14 Schematic model of the role of aSyn in regulating presynaptic vesicle cycling. 28
Figure 1.15 Spreading of aSyn.....29
Figure 1.16 Proposed mechanisms for aSyn propagation.....31
Figure 1.17 Schematic representation of the domains of Sph1 and Sph1A.....32
Figure 1.18 SHG principal.....34
Figure 1.19 Schematic model of aSyn aggregation 35
Figure 1.20 Schematic representation of the SynT structure.....36

III. List of Tables

Table 1. Genes associated with PD. 17

IV. List of Abbreviations

3D	Three-dimensional
%	Percent
aSyn	alpha-Synuclein
A	Alanine
aa	Amino acids
Aβ	Amyloid β-peptide
AD	Alzheimer's disease
aSyn	alpha-Synuclein
ATP	Adenosinetriphosphate
bSyn	beta -Synuclein
CMA	Chaperone Mediated Autophagy
D	Aspartic Acid
DA	Dopamine
DNA	Deoxyribonucleic acid
E	Glutamic acid
ER	Endoplasmic Reticulum
ERAD	Endoplasmic Reticulum Associated degradation
FRET	Fluorescence Resonance Energy Transfer
FTIR	Fourier transform infrared spectroscopy
G	Glycine
gSyn	gama-synuclein
H	Histidine
HSP	Heat-Shock Protein
IPOD	Insoluble Protein Deposit
JUNQ	JUxta Nuclear Quality control compartment
K	Lysine
kDa	kilo Dalton
L	Leucine
L-DOPA	L-3,4-dihydroxypheny-lalanine
LBs	Lewy Body

LN	Lewy Neurite
LRRK2	Leucine-rich-repeat-kinase 2
MTOC	Microtubule Organizing Center
MPTP	1-methyl-4-phenyl-1,2,3,6-tetrahydropyridine
N	Asparagine
NAC	Non-Abeta Component
NMR	Nuclear Magnetic Resonance
P	Proline
PD	Parkinson's disease
PET	Positron-emission tomography
PFFs	Preformed Fibrils
FRAP	Fluorescence Recovery After Photobleaching
FLIP	Fluorescence Loss in Photobleaching
pH	potentia Hydrogenii
PK	Proteinase K
PrP	Prion protein
PrP^{C}	Cellular conformation
PrP^{Sc}	Scrapie isoform
PTM	Post-Translational Modification
Q	Glutamine
S	Serine
SN	*Substantia nigra*
SNARE	Soluble N-ethylmaleimide–sensitive factor attachment protein receptor
Sph1	Synphilin-1
SynT	aSyn linked with a truncated non-fluorescent fragment of EGFP
T	Threonine
TH	Tyrosine Hydroxylase
ThioS	Thioflavin S
ThioT	Thioflavin T
TEM	Transmission Electron Microscopy
UPS	Ubiquitin-Proteasome-System
WT	Wild-Type

Abstract

Several neurodegenerative disorders, such as Parkinson's disease (PD), are characterized by the deposition of misfolded and aggregated forms of a particular protein in different areas of the brain. Understanding the molecular mechanisms of neurodegenerative diseases are extremely important to prevent and stop such debilitate diseases.

PD is a movement related disorder that primarily affects aged individuals, but mutations on alpha-Synuclein (aSyn) gene (*SNCA)* have been identified in an early- and juvenile-onset of the disease.

aSyn is a small an intrinsically disorder protein, that binds to membrane and lipids. It is the major component of Lewy Bodies (LBs) and Lewy Neurites (LN) in the surviving neurons in parkinsonian brains. However, the molecular mechanisms that lead to the selective degeneration of dopaminergic neurons from the *substantia nigra pars compacta* are still unclear. aSyn aggregation is an important process for the pathology. In pathological conditions, aSyn aggregates, forming oligomeric species that can rapidly convert into amyloid fibrils. Amyloid fibrils made up of aSyn then deposit in LBs, along with several other proteins and lipids. A combination of *in vitro*, cell and animal models studies has been useful to investigate not only aSyn aggregation intermediates, but also the toxic mechanisms.

Over the years, the number of models in the PD field increased significantly, but has not generated consensus with respect to the best models to use. Thus, it is important to choose the appropriate models to investigate a particular question of interest. Roughly, the PD models can be divided into two categories: those based on genetic alterations and those based on the effect of toxins. For the purpose of this thesis, I will focus on the genetic models. Due to our limited understanding of the molecular mechanisms underlying disease, cell-based models constitute a powerful tool to mimic important aspects of basic aSyn biology (such as aggregation and toxicity), and afford unique opportunities to test the effect of possible therapeutic strategies. A number of molecular dysfunctions have been associated with PD. These include defects in mitochondrial function, defects in degradation systems (ubiquitin–proteasome and autophagy), increased production of reactive oxygen species, or impairment of intracellular trafficking. However, the lack of systematic comparisons

makes it difficult to interpret and reconcile the relevance of results obtained using different models.

This study focuses mainly on the exploitation of two cell-based systems that try to model the oligomerization and aggregation of aSyn. The Bimolecular Fluorescence complementation assay enables us to visualize the dimerization and oligomerization of aSyn in living cells. To model aSyn aggregation, manipulations of the C-terminal region have been useful, as they promote the formation of LBs-like inclusions that can be readily detected by immunostaining. Thus, using these two models, we performed a systematic comparison to investigate the effects of genetic alterations on aSyn oligomerization and aggregation, and how these impacted on selected cellular functions. In addition, we investigated the effects of small molecules on the conformation and aggregation of aSyn, as this is thought to be a possible target for therapeutic intervention.

Overall, our studies demonstrated the usefulness of the two cell-based models for studying specific aspects of aSyn aggregation and for the screening of drugs that may lead to the identification of novel therapeutic strategies for PD and other synucleinopathies.

1. Introduction

1.1. Protein Folding and Misfolding

Life relies on a series of fundamental biological processes like those governing the folding of biomolecules, such as proteins and nucleic acids. Depending on their primary amino acid (aa) sequences, proteins can be particularly unstable when they are formed, and the surrounding environment is critical to determine the proper folding of the polypeptide chain during and after translation. Different types of forces contribute to the folding process. These include hydrogen bonding (between amide and carbonyl groups), hydrophobic forces, electrostatic forces, and Van der Waals forces (Anfinsen 1973; Dobson 2003). The conjugation of the various forces according to the environment culminates with the folding of the protein, and the achievement of the functional native conformation, that is normally the most thermodynamically stable under physiological conditions.

The ability of a polypeptide to fold to a specific structure has evolved since the beginning of life. Levinthal proposed that the folding of a protein can not be a random process but rather follow a particular "pathway" to shorten the time required to for the protein to reach the native state, otherwise the folding process would take longer than the age of the Universe (known as the Levinthal paradox) (Levinthal 1968; Honig 1999). The nature of the folding reactions is determined by the potential energy surface, and by the thermodynamics laws. Proteins can cross a number of different energy landscapes, like in funnel-like shape, with the low-energy state (folded) closer to the bottom of the funnel (Onuchic et al. 1997) (Figure 1.1).

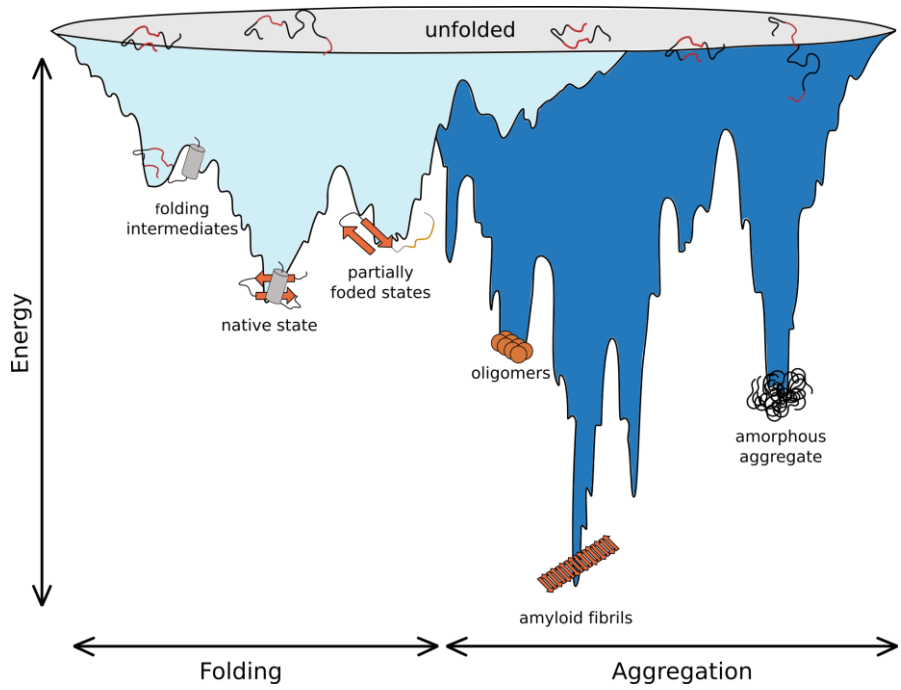

Figure 1.1 The free energy landscape of protein folding (left) and aggregation (right). Protein folding requires intramolecular connections that roughly resemble as a funnel in which non-native conformations occupy low energy levels. When proteins start to fold into amorphous structures, toxic oligomers or ordered amyloid fibrils will be produced with a lower free energy than the native state. Adapted from (Hartl et al. 2011).

Despite tremendous progress in the field of structural biology, predicting the conformation of a specific polypeptide chain still a challenge, due to our limited understanding of the rules governing protein folding (Dobson 2003; Dobson 2001). In the cell, to avoid misfolding and proteotoxicity, molecular chaperones, folding catalysts, and other protein quality control systems (e.g. the ubiquitin proteasome system and autophagy-lysosomal pathway), act to either refold the unfolded or disordered regions of a protein, or to target them for destruction. When misfolded proteins escape these quality control systems, or when they establish undesired/aberrant interactions, problems and diseases can arise.

Protein conformation, function, and localization can be modulated by internal and external signals, such as posttranslation modifications (PTMs), ligand binding, molecular recognition, or environmental changes (Beltrao et al. 2013).

1.2. Cellular Quality Control Mechanisms

Protein quality control mechanisms, highly conserved among all eukaryotes, ensure that each protein is properly folded or degraded to ensure the normal protein homeostasis (proteostasis) and the normal functioning of the cell. Thus, strategies aimed at maintaining or restoring homeostasis can be valuable for preventing disease.

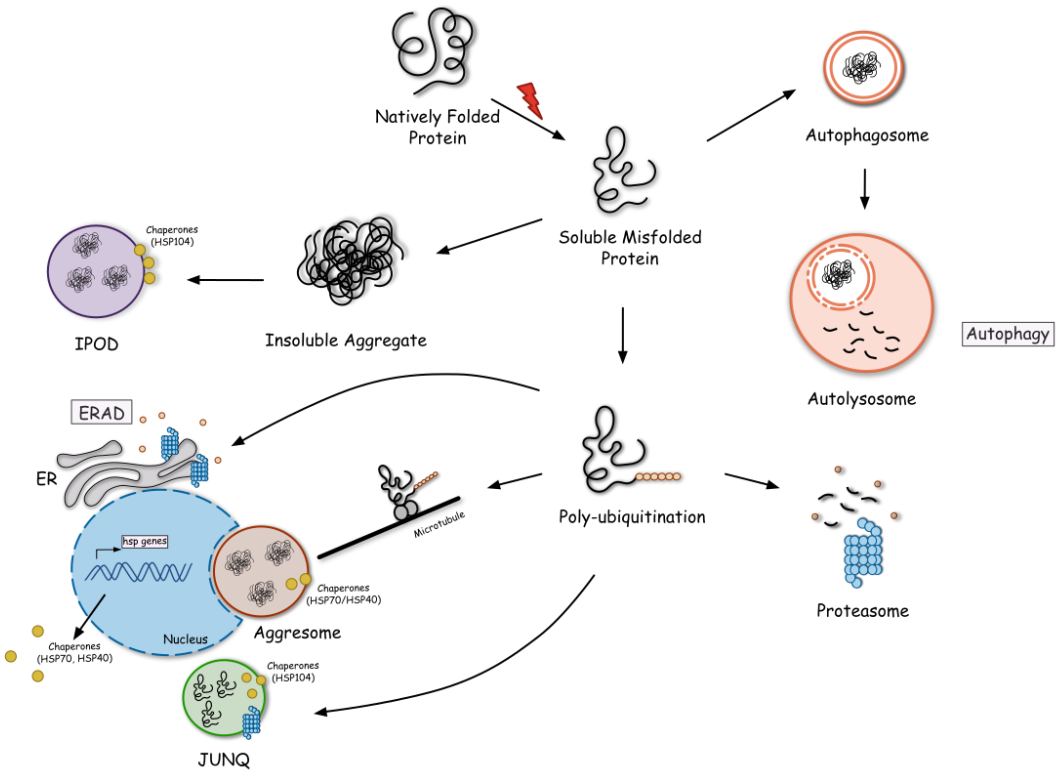

Figure 1.2 Deregulation of proteostasis due to protein misfolding. Proteins can acquire their native state or, upon environmental challenges and/or mutations, they may acquire a misfolded state. Here, proteins can be refolded with the aid of molecular chaperones, or degraded by cellular degradation mechanisms such as ERAD, proteasome, or autophagy. Alternatively, proteins can be redirected to the JUNQ compartment for ulterior refolding or degradation, or to the IPOD or aggresome, to be permanently sequestered.

When the cell is challenged or stressed, the stress response is proportional to the stress encountered, to enable a proper response to protein misfolding (Morimoto, 2008). Heat, oxidative, osmotic, or pH stress are examples of types of stresses that can affect proteostasis (Morimoto, 2008). Aging can also affect proteostasis due to the progressive failure of cellular quality control systems, and can lead to the accumulation of potentially harmful, aggregation-prone protein species.

1.2.1. Molecular Chaperones

The folding of a proteins in living cells is a great challenge due to the crowded macro-molecular environment of the cell, which favors protein misfolding and aggregation (Ellis 2001). To prevent illegitimate inter- and intramolecular interactions, and protect hydrophobic aa side chains, the folding process of some proteins is assisted by molecular chaperones. Molecular chaperones are proteins designed to effectively reduce the tendency of non-native proteins to aggregate, both in *de novo* synthesis or in stress conditions, to promote correct interactions within themselves and with other polypeptides (Frydman et al. 1996). In contrast to what happens in the process of protein assembly (the ordered association of several polypeptide chains), protein aggregation describes a disordered, non-specific association, which the cells need to prevent by all means (Walter et al. 2002). Chaperones can be regulated by various co-factors and some act in an energy dependent manner where ATPase activity works through cycles of binding and release of the substrate. Chaperones are found in all compartments of the cell where folding and other conformational adjustments need to occur (Walter et al. 2002).

Heat Shock protein (HSPs), one type of molecular chaperones, play a critical role in the recovery of cells from heat stress, and in cytoprotection from subsequent insults (Nollen et al. 2002). For example, cells that have lost their ability to regulate cell growth, such as tumor cells, normally express high levels HSP proteins (Jaattela 1999). This might indicate that chaperones can suppress or buffer the effect of mutations.

In the process of *de novo* protein folding or refolding, the cooperative work between the Heat Shock protein 70 (Hsp70) system, small chaperones, chaperonins, and the Heat Shock protein 90 (Hsp90) system takes place (Sin et al. 2015). By binding to hydrophobic segments, Hsp70 can stabilize and prevent protein misfolding and aggregation, in an ATP-dependent manner. Then, the substrate can be transferred to other systems (such as chaperonins), where the folding takes place and the three-dimensional (3D) structure is acquired (Sin et al. 2015). Hsp70 also assists membrane translocation of organellar and secretory proteins, and the activity of regulatory proteins (Mayer et al. 2005).

Importantly, depletion of Hsp70 has been associated with PD. *In vitro*, Hsp70 significantly increases the lag phase of aSyn aggregation (Roodveldt et al. 2009). The

inhibitory effect of Hsp70 depends on the ratio between Hsp70/aSyn, and on the relative levels of aSyn and ATP, or ADP (Roodveldt et al. 2009). One important aspect for the Hsp70-mediated inhibition of aSyn aggregation is the presence of the Hip co-chaperone (Roodveldt et al. 2009). Hip stabilizes the ADP-bound state of Hsp70 and assists Hsp70 in protein folding (Nollen et al. 2001). Alone, Hip can also bind to unfolded proteins and prevent their aggregation (Nollen et al. 2001). *In vivo*, in drosophila, Hsp70 was shown to reduce aSyn toxicity, but could not prevent the accumulation of amyloid-like aggregates (Auluck et al, 2002).

1.2.2. Ubiquitin proteasome system (UPS)

We still do not fully understand how misfolded proteins are discriminated from the correct folded counterparts. However, this is a crucial step in cellular homeostasis. Polypeptides that enter the secretory pathway are first received at the endoplasmic reticulum (ER) (Braakman et al. 2011). The ER is responsible for the addition of specific PTMs and, later, for targeting proteins to specific organelles or to the outside of the cell. So, it is no surprise, that the ER-associated degradation (ERAD) pathway cooperates tightly with the ubiquitin-proteasome system (UPS) to prevent the accumulation of misfolded proteins (Figure 1.2). This is a joint effort of selection, production, and transportation of misfolded proteins from the ER to the cytosol for degradation (Guerriero et al. 2012).

The UPS is the major degradation pathways for short-lived proteins, such as those that regulate cell division, signal transduction, and gene expression (Kraft et al. 2010). For that, there are two consecutive steps: ubiquitylation and proteasomal degradation (Hershko et al. 1998). Ubiquitylation is a common and reversible PTM where the small protein ubiquitin, a highly conserved protein of 76 aa, is ligated to a lysine residue in a substrate protein (Klein et al. 2016). After the recognition of eligible proteins, these can be mono- or poly-ubiquitinated (at least four ubiquitin molecules are added) (Weissman 2001), in an ATP-dependent process that starts with the attachment of ubiquitin to the polypeptide chain, in an ordered three-step process. The ubiquitin-activating enzyme (E1) transfers ubiquitin to an ubiquitin-carrier protein (E2) and, finally, the ubiquitin molecules are transferred to lysine residues in

the target substrate in a reaction catalyzed by the ubiquitin protein ligase (E3) (Ciechanover et al. 1980; Hershko et al. 1980).

The ligation of multiple ubiquitin groups to a substrate protein leads to the formation of a polyubiquitin chain. This is a complex process in which at least seven different types of ubiquitin linkages can be established (K6, K11, K27, K29, K33, K48 or K63) (Kim et al. 2007; Ikeda et al. 2008). The exact conformation of the polyubiquitin chain will determine the fate of the substrate. For example, K48 chains generally target the substrate for degradation via the proteasome (Klein et al. 2016). However, ubiquitylation can have other roles besides proteasomal degradation. These include as cell-cycle control, differentiation, apoptosis, transcriptional regulation, and immune response. It has been reported that K63-linked ubiquitin chains do not act as a proteasome-targeting signal *in vivo*, as K48 (Nathan et al. 2013). Instead, these chains are implicated in macroautophagy (Kraft et al. 2010), and play an important role in signaling, endocytosis, and DNA repair (Ikeda et al. 2008). Also, K63-polyubiquitinated proteins do not co-localize with proteasomes in cells (Newton et al. 2008).

The 26S proteasome complex is the most common form in cells, and is functionally and structurally divided into two parts: the 19S cap, and the core formed by the 20S proteasome (Inobe et al. 2014). The 19S subunit recognizes the substrates, unfolds the polypeptides and guides them through the channel to the proteolytic core (Inobe et al. 2014). The 20S core is responsible for the proteolytic activity and has three peptidase activities: chymotrypsin-like (Tyrosine or Phenylalanine at position 1), trypsin-like (Arginine or Lysine at position 1), and caspase-like, that cleaves the substrate into short peptides (Bedford et al. 2010).

1.2.3. Autophagy-Lysosome Pathway

A second proteolytic system is commonly referred to as autophagy ("self-eating" in Greek). This system eliminates cytosolic components, organelles, long-lived proteins, and pathogens, *via* lysosomes. It is also involved in starvation and stress responses (Kraft et al. 2010). Autophagy can be divided in three categories: macroautophagy, microautophagy and chaperone-mediated autophagy (CMA). Both macro- and microautophagy involve dynamic membrane readjustments to engulf of the cytoplasm. In macroautophagy, commonly referred to as autophagy, the double

membrane forms a vesicle that engulfs the material- autophagosome. When the autophagosome fuses with an endosome or lysosome, it gives rise to the autolysosome where the hydrolytic enzymes will act (Figure 1.2) (Yang et al. 2009).

In microautophagy, small particles from the cytosol are internalized by the lysosome through the invagination of its own membrane. CMA is particularly associated with lysosomal degradation. Unlike other degradation systems, it is based on the recognition of a specific aa sequence - KFERQ - which is present in around 30% of cytoplasmic proteins (Dice 1990). HSP70 recognizes this aa sequence, and Hsc70 binds and delivers the proteins to the CMA receptor at the lysosome.

If the capacities of the refolding machinery and 26S proteasome are overwhelmed and exceeded, misfolded proteins can accumulate in cellular inclusions.

1.2.4. Protein compartmentalization

When misfolded proteins exceed the degradation capacity of the quality control systems, proteins can have one of two fates: they can either accumulate, or be compartmentalized in the cell. Compartmentalization can be a cellular strategy, by spatially sequestering misfolded proteins into defined compartments, the deal with proteins that can then be either refolded or permanently sequestered (Figure 1.2). There are specific types of such compartments, evolutionary conserved from yeast to mammals, which accumulate proteins according to their solubility state the juxtanuclear quality control (JUNQ) and the insoluble protein deposit (IPOD) (Figure 1.3) (Kaganovich et al. 2008; Weisberg et al. 2012).

The JUNQ compartment sequesters mobile, misfolded polypeptides in a detergent-soluble state, as well as 26S proteasomes and Hsp104 (Kaganovich et al. 2008).

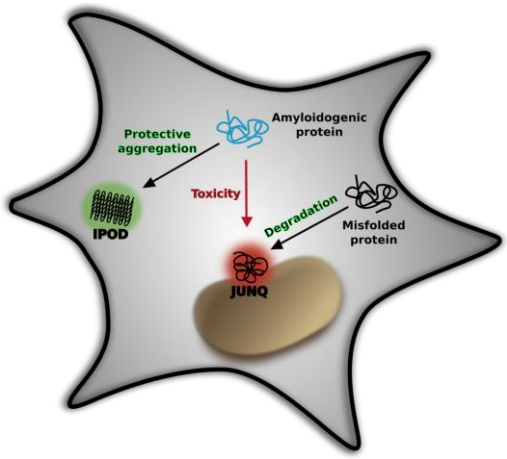

Figure 1.3 Schematic representation of a mammalian cell showing two misfolded proteins compartments. Proteins can be sorted into two different quality control compartments, the JUNQ or the IPOD, based on their ubiquitination state.

The IPOD accumulates insoluble proteins at the periphery of the cells, typically adjacent to the pre-autophagosomal structure. Do to the insoluble material this compartment is immobile (Miller et al. 2015). Vimentin is an intermediate filament protein that establishes mitotic polarity in mitotic cells, by confining/encaging proteins in JUNQ, mediating asymmetric partitioning during (Figure 1.4) (Ogrodnik et al. 2014). This mechanism represents an important strategy for cellular rejuvenation. Asymmetric segregation in single-cell organisms (as *Saccharomyces cerevisiae*) potentiates the rejuvenation of the emerging generation by preventing the inheritance of damaged factors (Ogrodnik et al. 2014). The ability of mother cells to retain damaged factors such as DNA, lipids, and proteins, must be carefully regulated to isolate them or to filter several aging factors (Nystrom et al. 2014; Lai et al. 2002; Aguilaniu et al. 2003; Lindner et al. 2008). In this fascinating process, the mother cell generates younger daughter cells where the clock of aging not only stops but is also completely reset (Nystrom et al. 2014).

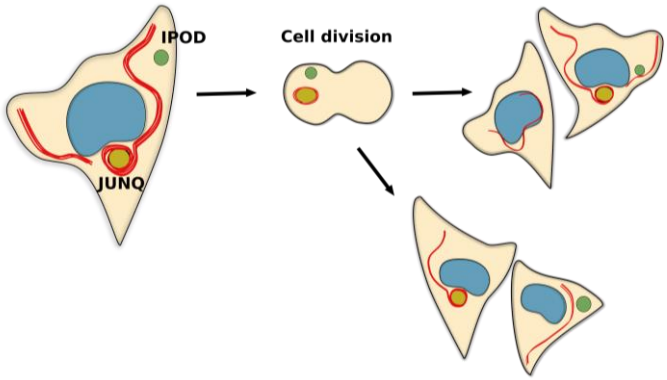

Figure 1.4 Mitotic cells have asymmetric inheritance of JUNQ and IPOD. In mammalian the cytoskeleton, and intermediate filaments provide the scaffold for asymmetric inheritance of inclusions, in contrast to IPOD inclusions, which are not partitioned as effectively during mitosis. Adapted from (Ogrodnik et al. 2014).

Another type of compartments are the aggresomes, localized at the microtubule organizing center (MTOC) (Figure 1.2) These periocentriolar cytoplasmic structures are typically formed when the proteasome can not clear misfolded proteins properly (Johnston et al. 1998), and transports them via dynein/dynactin complex to their final destination (Figure 1.2) (Johnston et al. 2002). Interestingly, the JUNQ shares several properties with the aggresomes, like the localization, the presence of ubiquitinated proteins and chaperones (Kaganovich et al. 2008). However, neither the JUNQ nor the IPOD are localized in the spindle pole body (the microtubule organizing center in yeast cells, equivalent to the centrosome), unlike the aggresome, which co-localizes with MTOC (Johnston et al. 2002).

However, the idea of protein sequestration as an alternative cellular defense was recently challenged. Instead, compartmentalization could be an early response to stress or to toxic misfolded species into transient and dynamic structures called “Q bodies” or cytosolic stress-induced aggregates (CytoQ) (Escusa-Toret et al. 2013). The recruitment of misfolded proteins into Q-bodies is an active process that relies on molecular chaperones (Escusa-Toret et al. 2013). However, these structures are not necessary targets for degradation but may improve cell fitness, using the same factors that promote folding (Escusa-Toret et al. 2013). The formation and the movement of the Q-bodies are independent of the cytoskeleton, but involve the cortical ER (tubular system analogous to the ER network in higher eukaryotes) and chaperones (Escusa-Toret et al. 2013).

If all these systems fail, in mitotic cells, the asymmetric division known as replicative rejuvenation, can still be an option. Studies in bacteria and yeast showed that aging mother cells retain damaged proteins, where the daughter cells are freed of these proteins (Lindner et al. 2008; Liu et al. 2010; Coelho et al. 2013; Ogrodnik et al. 2014).

1.3. Protein Misfolding diseases

Misfolded proteins compromise not only the integrity of the cellular proteome, but also cell viability. Despite a lack of similarity in aa sequence, there are approximately 50 disorders associated with misfolding of normally soluble, functional peptides and proteins, and their subsequent conversion into aggregates (Knowles et al. 2014).

The accumulation of aggregated proteins in the brain is a hallmark shared by several neurodegenerative diseases, like Parkinson's (PD), Alzheimer's (AD) and Huntington's disease. Interestingly, these protein aggregates share common characteristics, like a fibrillar structure that shares similar morphology and size. They display a characteristic cross-beta structure X-ray diffraction pattern, revealing that the core structure is composed of β-sheets in which the β-strands run approximately perpendicular to the long fibril axis, and the inter-strand hydrogen bonds run approximately parallel to the long fibril axis (Sunde et al. 1998). Furthermore, fibrils exhibit yellow-green birefringence upon binding of the dye Congo red (Khurana et al. 2001) and other specific optical properties upon binding to other dyes like Thioflavin T (ThioT) (Chiti et al. 2006) (Figure 1.5) These aggregates are also thermally stable, SDS- and protease-resistant. In vitro, amyloid fibrils are formed through a nucleation-dependent polymerization process (Figure 1.5) (Serio et al. 2000).

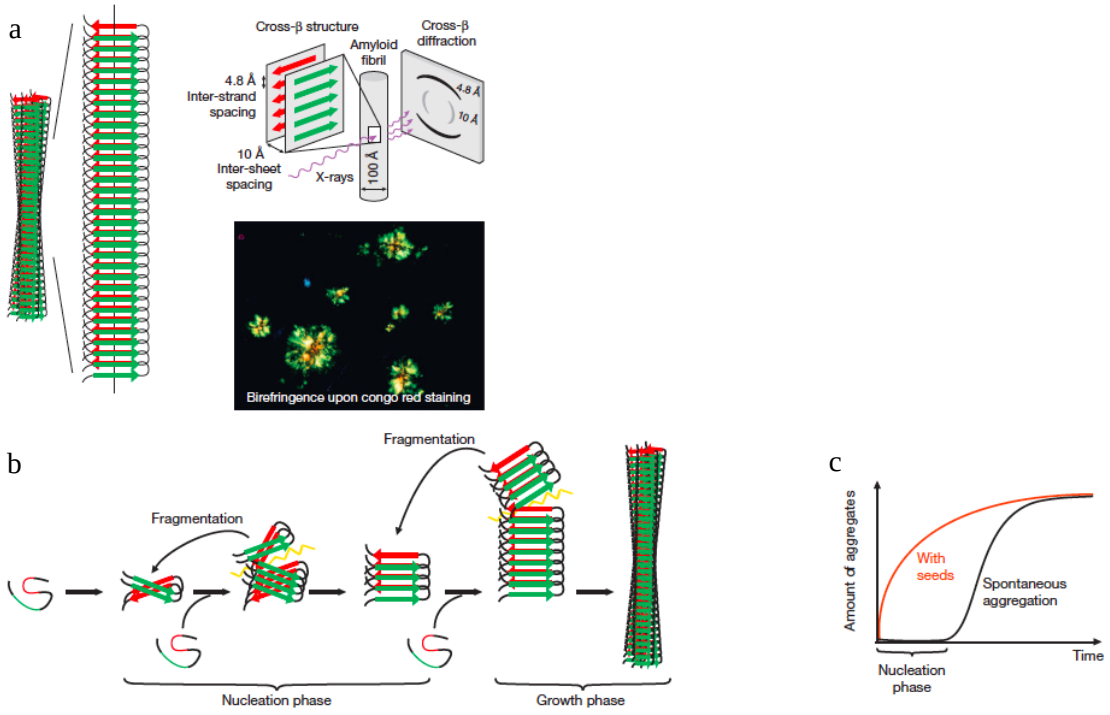

Figure 1.5 Different methods for amyloid protein characterization. (a) Amyloid proteins forms filaments composed of sheets of β-strands, that because of their arrangement it produces a distinctive cross-β X-ray diffraction pattern, reflecting the characteristic spacing between the β-sheets and the β-strands. Using Congo red dye in combination with cross-polarizes light technique is possible to distinguish the presence of fibrils. **(b)** Amyloid formation initiates with a slow nucleation phase (formation of seeds), and the monomers and the oligomers can bond to the ends of the initial amyloid seed. The fibril can grow, and eventually break, producing more seeds. **(d)** *In vitro*, the nucleation phase can be shortened by the addition of pre-formed exogenous seeds. Adapted from (Jucker et al. 2013)

Typically, amyloid formation in mammals occurs with aging and is commonly associated with protein misfolding diseases (Selkoe 2003; Chiti et al. 2006).

1.4.Parkinson's Disease

PD is the most common progressive motor disorder, and the second most prevalent neurodegenerative disorder, after AD, affecting around 1% of the worldwide population at the age of 60, and 4-5% of people over 85 (de Lau et al. 2006). PD was first described in 1817 by the english physician James Parkinson, in his "An Essay on the Shaking Palsy", as a movement-related disorder (Parkinson 2002). PD is characterized by the progressive loss of dopaminergic neurons in Substantia Nigra pars compacta (SN) (Figure 1.6).

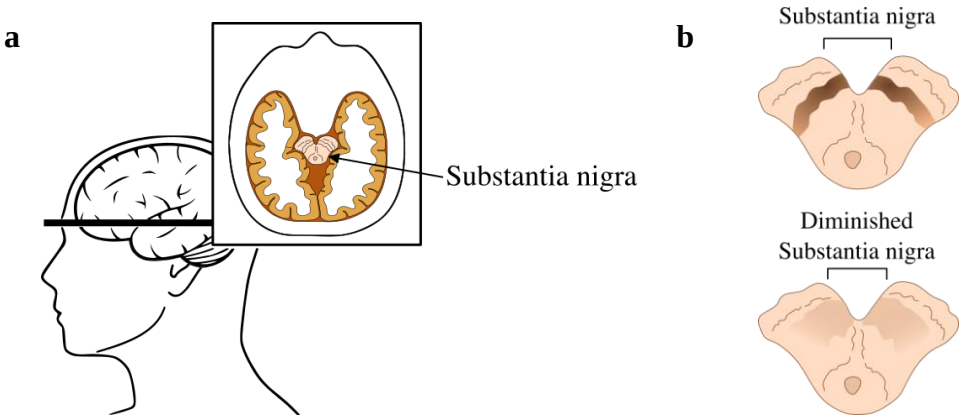

Figure 1.6 Afflicted region in PD patients. (a) Cut section, showing the localization of SN. **(b)** In PD patients there is a depletion of pigmented dopaminergic neurons localized in the SN.

These neurons form the nigrostriatal dopaminergic pathway that primarily projects to the putamen, and are enriched with neuromelanin (Marsden 1983) and iron (Forno et al. 1974). The loss of these dopaminergic neurons leads to dopamine (DA) deficiency, responsible for the major cardinal symptoms in PD: muscle rigidity, bradykinesia, resting tremor, and postural instability. At the onset of symptoms, it is estimated that about 80% of putamental DA is depleted, and about 60% of SN dopaminergic neurons are lost (Dauer et al. 2003). In addition, about 30- 50% of non- DA cells are lost in the final stages of PD, including monoaminergic cells, cholinergic cells, and hypocretin cells, which are associated with cognitive deficits, gait problems and sleep disorders (Zarow et al. 2003; Hilker et al. 2005; Thannickal et al. 2007). Furthermore, other symptoms at the psychiatric level, such as anxiety and depression, dysautonomic symptoms (as hypotension and constipation), olfactory dysfunction, and seborrheic dermatitis can also arise (Checkoway et al. 1999). However, these symptoms precede the tremor or bradykinesia.

The underlying causes for massive neuronal cell loss are still unknown, and the symptoms of PD can be, albeit transiently treated by replacement of DA (via levadopa), DA agonists, monoamine oxidase B or catechol-O-methyltransferase inhibitors, and N-methyl-D-aspartate receptor antagonists (Groiss et al. 2009; Litim et al. 2015). In some particular cases, deep brain stimulation is also a possibility (Benabid et al. 1987).

1.4.1. Protein aggregation in PD

The neuropathological hallmark of idiopathic PD is the presence of concentric hyaline cytoplasmic inclusions called Lewy bodies (LBs) and Lewy neurites (LN), first described in 1912 by Friedrich Lewy (Figure 1.7) (Goedert et al. 2013). This pathological hallmark can occur in the brainstem, basal forebrain, autonomic ganglia and, in higher concentrations, in the SN and locus coeruleus (Mezey et al. 1998). Nevertheless, LBs have also been observed in the brains of asymptomatic individuals (Nussbaum et al. 1997) and in 10-15% of healthy, aged individuals (Gibb et al. 1988; Conway et al. 2000).

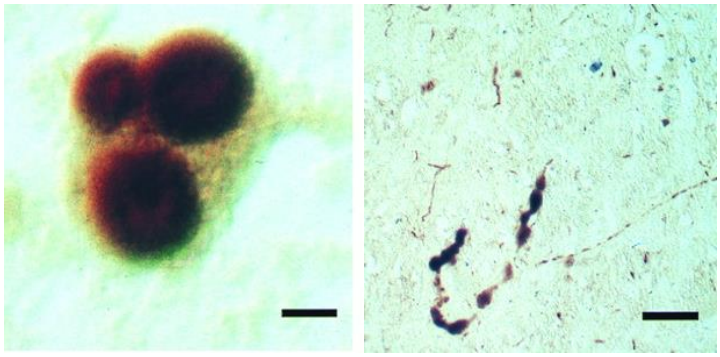

Figure 1.7 Lewy Bodies and Lewy Neurites in the SN of PD patients. Immunohistochemistry for aSyn and ubiquitin**.** Scale bar: 10 µm and 90 µm respectively. From (Spillantini et al. 1998).

LBs are composed of a large number of molecules including synphilin-1 (Sph1) (Wakabayashi et al. 2000), heat-shock proteins (Hsp90, Hsp70, Hsp40) (Auluck et al. 2002; McLean et al. 2002; Uryu et al. 2006)), p62 (Kuusisto et al. 2003), sphingomyelin (den Jager 1969), tau (Ishizawa et al. 2003), ubiquitin (Lowe et al. 1988), and others. However, the most abundant protein component of LBs is alpha-Synuclein (aSyn) (Figure 1.7) (Spillantini et al. 1997). LBs are not exclusive in PD, and are also present in diseases such as Dementia with LBs (Spillantini et al. 1998), sporadic AD, Down's syndrome, Hallervorden-Spatz syndrome, and neurodegeneration with iron accumulation type 1 in the brain (Arawaka et al. 1998; Ebrahimi-Fakhari et al. 2011). Thus, these disorders are referred to as synucleinopathies (Arawaka et al. 1998; Lippa et al. 1998).

1.4.2. Etiology of PD

The majority of PD cases are sporadic/idiopathic and most likely triggered by a combination of aging, genetic, and environmental factors. In fact, the exposure to certain pesticides like 1-methyl-4-phenyl-1, 2, 3, 6,-tetrahydropyridine (MPTP) or paraquat, results in the degeneration of dopaminergic neurons and in chronic parkinsonism (Di Monte et al. 2002). Interestingly, in monkeys treated with MPTP, it was observed that the depletion of striatal terminals precedes the death of dopaminergic neurons in the SN (Herkenham et al. 1991).

Genetic predisposition also plays a role in the disease, and familial forms of PD can manifest in two ways: *autosomal dominant* or *recessive*. Initial studies on twins reveled that the concordance rate among monozygotic and dizygotic twins was similar overall. Nevertheless, in early-onset cases (before 50 years), the rate in monozygotic twins was significantly higher (100%) compared to dizygotic twins (17%) (Tanner et al. 1999).

With the improvement of imaging methods, such as PET (positron-emission tomography), it became clear that striatal dopaminergic dysfunction was significantly higher in monozygotic than in dizygotic twin pairs (55%, 18%, respectively), even in pre-symptomatic cases (Burn et al. 1992; Piccini et al. 1999). Although, familial PD accounts for only a minority of all PD cases, the understanding of the underlying genetic alterations provides tremendous insight into the molecular pathogenesis of the disease (Thomas et al. 2007).

Several genes have been linked to PD, and the list will potently continue to grow in coming years, as more powerful studies are conducted (Table 1).

Locus	Gene	Description	Reference
PARK 1/4	*SNCA*	Presynaptic/nuclear protein	(Polymeropoulos et al. 1997)
PARK2	*Parkin*	Ubiquitin ligase	(Kitada et al. 1998)
PARK3	SPR(?)		(Gasser et al. 1998)
PARK5	*UCH-L1*	Ubiquitin protease	(Liu et al. 2002)
PARK6	*PINK1*	Mitochondrial protein kinase	(Hatano et al. 2004)
PARK7	*DJ-1*	Multifunctional protein	(Bonifati et al. 2003)
PARK8	LRRK2	Leucine-rich repeat kinase 2	(Gasser 2009)
PARK9	ATP13A2	Lysosomal ATPase	(Ramirez et al. 2006)
PARK10	(?)		(Li et al. 2002)
PARK11	GIGYF2		(Lautier et al. 2008)
PARK12	(?)		(Pankratz et al. 2002)
PARK13	Omi/HTRA2	Serine Protease	(Strauss et al. 2005)
PARK14	PLA2G6	Phospholipase	(Paisan-Ruiz et al. 2009)
PARK15	FBXO7	F-box protein	(Shojaee et al. 2008)
PARK16	(?)		(Satake et al. 2009)
PARK17	VPS35	Retromer Complex	(Wider et al. 2008)
PARK18	EIF4G1	Translation Initiation Factor	(Chartier-Harlin et al. 2011)
PARK19	DNAJC6	DNAJ/HSP40 homolog, Subfamily C, Member 6	(Edvardson et al. 2012)
PARK20	SYNJ1	Synaptojanin 1	(Krebs et al. 2013; Quadri et al. 2013)
PARK21	DNAJC13	DNAJ/Hsp40 Homolog, Subfamily C, Member 13	(Vilarino-Guell et al. 2014)
PARK22	CHCHD2	Coiled-coil-helix-coiled-coil-helix domain containing 2	(Funayama et al. 2015)
PARK23	VPS13C	Vacuolar protein sorting 13 homolog C	(Lesage et al. 2016)

Table 1. Genes associated with PD.

1.4.2.1. The synuclein family of proteins

aSyn belongs to a family with three different gene products: a-, beta (b)- and gamma (g)-Syn. These proteins have been described in vertebrates, and seem to be

highly conserved among distantly related vertebrate species (Maroteaux et al. 1988; Jakes et al. 1994; George et al. 1995). Knockout of a-,b-, or gSyn in mice is not lethal, although some electrophysiological abnormalities have been described (Abeliovich et al. 2000; Chandra et al. 2004). aSyn and bSyn are predominantly expressed in the neocortex, hippocampus, striatum, thalamus, and cerebellum (Nakajo et al. 1993; Iwai et al. 1995). Additionally, aSyn can be found in fluids such as the cerebrospinal fluid, saliva, and blood plasma (El-Agnaf et al. 2003; Tokuda et al. 2006; Devic et al. 2011). Recently, it was showed that the expression of human wild-type (WT) bSyn protein leads to the formation of proteinase K (PK) resistant aggregates, and loss of dopaminergic neurons in primary neuronal cultures and in rats, suggesting that bSyn may also play a role in the neurodegenerative process (Taschenberger et al. 2013). gSyn, is the least conserved and the smallest member of the synuclein family, and is expressed in the brain, in the ovary, testis, colon, and heart (Clayton et al. 1998).

1.4.2.2. aSyn Structure

aSyn is a small protein of 140 aa, highly negatively charged, thermally stable, and is usually functionally divided into three domains (Figure 1.8).

aSyn was first discovered in the electric organ of *Torpedo californica*, and named synuclein for its cellular localization within synaptic nerve terminals and within the nuclear compartment (Maroteaux et al. 1988). However, aSyn was not consistently found in the nucleus in several subsequent studies, and this is still a subject of debate.

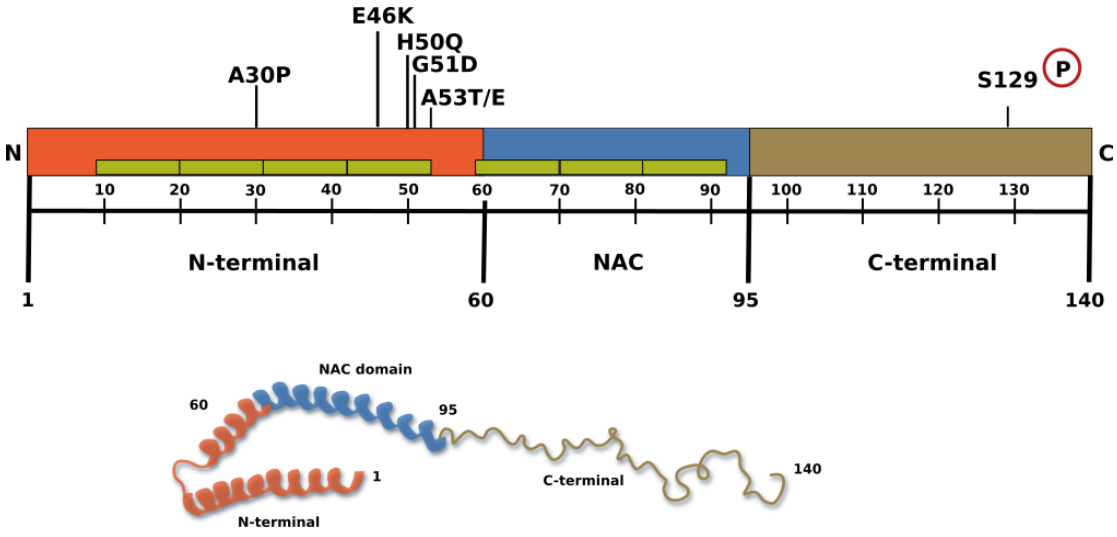

Figure 1.8 Human aSyn. A. Schematic representation of the structure of human aSyn showing the three distinct domains (N- terminal, non-b-amyloid component (NAC), and C-terminal domain). Aa positions are indicated at the bottom. Green boxes represent the imperfect hexameric KTKEGV repeats. The lines show the familial mutations in PD context and the sites of aSyn phosphorylation. Adapted from (Gallegos et al. 2015)

The N-terminal domain is a highly-conserved region with a series of imperfect hexameric (KTKEGV) repeats. This unstructured region adopts amphipathic α-helical structure in the presence of lipids or some detergents (Davidson et al. 1998; Eliezer et al. 2001; Mihajlovic et al. 2008). All the familial mutations described in aSyn are located in the N-terminal domain, suggesting that this region has an important cellular function (Fig. 1.8).

The central hydrophobic domain of aSyn is also referred as the NAC region. This amyloidogenic region has the ability to change conformation from random coil to β-sheet structure (Sykes et al. 1990; Serpell et al. 2000), and to form Aβ-like protofibrils and fibrils (Harper et al. 1997; Harper et al. 1999). The C-terminal region is the least conserved in the synuclein family, and is variable in size and sequence. This is a highly acidic domain composed of proline, glutamate, and aspartate residues (Amer et al. 2006), and has been proposed to confer chaperone-like activity to the protein (Kim et al. 2000; Souza et al. 2000; Park et al. 2002).

1.4.2.3. aSyn aggregation and cytotoxic species

Understanding the mechanisms involved in the aggregation process of aSyn is crucial to identify the toxic species that trigger diseases. A widely accepted hypothesis posits that aSyn oligomers and protofibrils are the cytotoxic species, and that the larger insoluble aggregates are cytoprotective (Caughey et al. 2003; Winner et al. 2011). As stated above, aSyn is a disordered protein in solution. This lack of defined secondary and tertiary structure allows aSyn to adopt multiple conformations. Thus, it is still not clear how native unfolded aSyn acquires a structure that is prone to nucleation and aggregation (Figure 1.9).

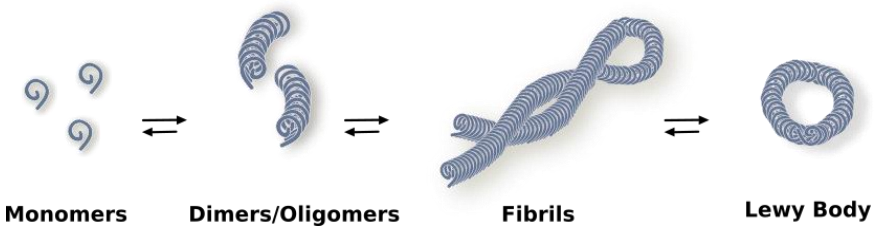

Figure 1.9 Schematic model of the process of aSyn aggregation. When monomeric aSyn interacts with itself, in ways we do not fully understand, it starts to aggregate producing oligomers, and later amyloid fibrils, in a nucleation-dependent manner. The accumulation of aSyn in LBs is a primary hallmark of PD and other synucleinopathies. We still do not know precisely which of the various species of aSyn are responsible for cellular toxicity and neurodegeneration.

The driving forces for these interactions are primarily due to the hydrophobic stretch in the middle of the aSyn sequence, constituted by 12 aa (VTGVTAVAQKTV) (Giasson et al. 2001). After these initial interactions, monomers start to aggregate, and form oligomeric species, which are soluble and non-fibrillar. When oligomers reach a critical concentration, they are rapidly converted into protofilaments, protofibrils and, finally, into amyloid fibrils, of high molecular weight.

The environment around aSyn can trigger its aggregation (Figure 1.9). Polyamines (like putrescine, spermidine, and spermine) (Antony et al. 2003), low pH (pH 4 or 5), and increasing salt concentrations (Hoyer et al. 2002), among others, are external known factors that accelerate the rate of aSyn fibrillation. The fibril elongation rate is correlated with protein concentration (Wood et al. 1999), which is in line with multiplication of *SNCA*.

The C-terminus of aSyn stabilizes long-range interactions within the protein by shielding the central region and preventing aggregation (Bertoncini et al. 2005). When the C-terminus is truncated, the aggregation progresses faster (Hoyer et al. 2004). However, two recent reports challenge this concept by suggesting that aSyn predominantly exists in a stable tetrameric state, with low propensity to aggregate. Furthermore, the dissociation of the tetramer into monomeric subunits would promote the formation of toxic aggregates (Bartels et al. 2011; Wang et al. 2011).

1.4.2.3.1. Mutations in aSyn

The first gene linked to familial forms of PD was *SNCA* when, in 1997, a point mutation was identified in aSyn (the protein encoded by the *SNCA* gene), in an Italian family and in three unrelated Greek families with autosomal dominant inheritance of PD (Polymeropoulos et al. 1997). This mutation consists in the substitution of an alanine for a tyrosine at position 53 (A53T). In solution, A53T is more thermodynamically stable than WT aSyn, and has higher propensity to aggregate, due to an increase in β-sheet formation (Coskuner et al. 2013). Moreover, A53T mutant aSyn alters mitochondrial morphology, and the proteins involved in mitochondrial fission and fusion, in an age-dependent manner, in mice (Xie et al. 2012).

One year later, another mutation was found in a German family, and consisted in the substitution of an alanine for a proline at position 30 (A30P) (Kruger et al. 1998). *In vitro*, A30P reduces membrane and vesicle binding capacity, slows down fibrillation kinetics compared to the WT aSyn, and promotes protofibrillar and oligomeric accumulation (Conway et al. 2000; Jo et al. 2002). Also, overexpression A30P aSyn interferes with the process of tyrosine hydroxylase (TH) synthesis, and impairs neurite and axonal regeneration in damaged midbrain dopaminergic neurons (Kim et al. 2014; Tonges et al. 2014).

The E46K mutation was identified in a Spanish family with autosomal dominant parkinsonism that showed dementia and visual hallucinations (Zarranz et al. 2004). Recently, another case in a 60-year-old male, from Bolivia, with a familial history of autosomal dominant PD was reported (Pimentel et al. 2015). Thus, mutation was shown to increase rate of fibrillization, similar to A53T (Choi et al. 2004; Greenbaum et al. 2005). In transgenic mice, it leads to intracytoplasmic neuronal inclusions in an age-dependent manner (Emmer et al. 2011). Furthermore, E46K can significantly enhanced phosphorylation on S129 in yeast, mammalian cells, and in the mouse brain (Mbefo et al. 2015). In addition, it increased the ability of aSyn to bind to negatively charged liposomes, in contrast to the A30P or A53T mutations (Choi et al. 2004) (Figure 1.10).

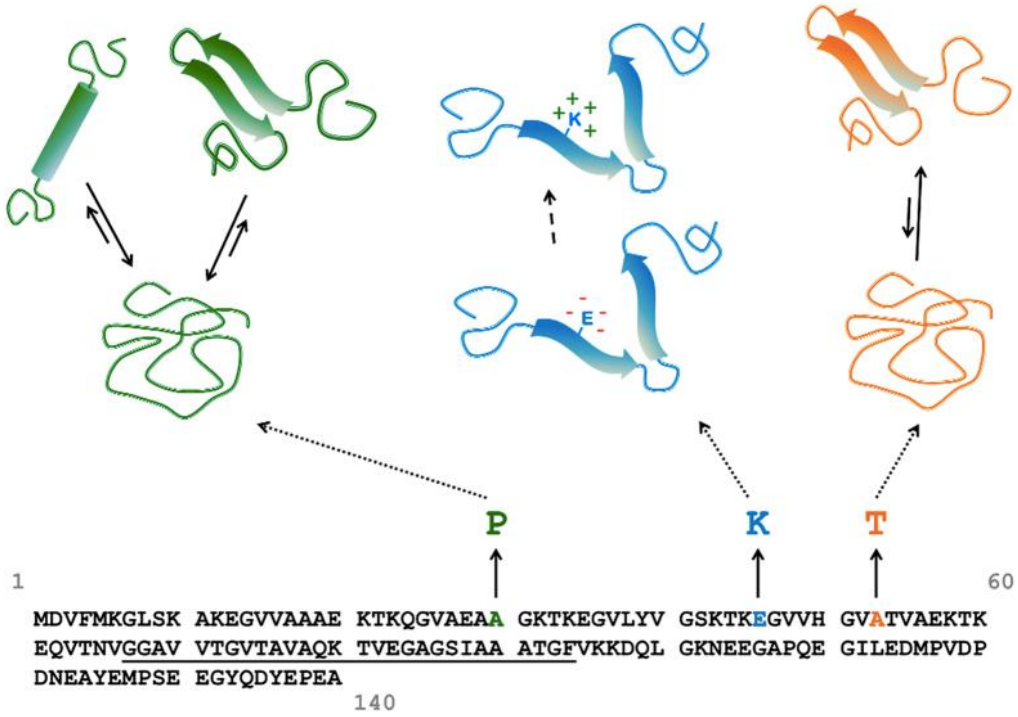

Figure 1.10 aSyn sequence. Examples of familial point mutations and their possible effects on aSyn conformation. From (Tosatto et al. 2015).

In 2013, two studies reported another aSyn mutation - H50Q (Appel-Cresswell et al. 2013; Proukakis et al. 2013). H50Q mimics late-onset idiopathic PD with a positive response to levodopa (Kiely et al. 2015). It accelerates the aggregation (Ghosh et al. 2013; Khalaf et al. 2014; Rutherford et al. 2014), causes an increase of the flexibility of the C-terminal region, which indicates that H50Q can mediate long-range interactions (Chi et al. 2014). In cell culture, H50Q increases aSyn secretion and cell death, and induces increased mitochondrial fragmentation in hippocampal neurons (Khalaf et al. 2014; Xiang et al. 2015).

In the same year, the G51D nutation was found to associate with an unusual PD phenotype (Kiely et al. 2013; Lesage et al. 2013), with early disease onset. *In* vitro, G51D oligomerization occurs slowly and the fibrils are more toxic than those formed by WT aSyn (Lesage et al. 2013). G51D impairs membrane binding, and increases mitochondrial fragmentation (Fares et al. 2014).

The most recent mutation (A53E) was discovered in a 36 years old Finish patient with atypical PD. The patient had a dense accumulation of *SNCA* inclusions in the striatum, and severe cortical pathology (Pasanen et al. 2014). *In vitro*, A53E attenuates aSyn aggregation and amyloid formation without altering the

secondary structure, and causes the accumulation of oligomers like the A30P mutation (Ghosh et al. 2014). This suggests that a negatively charged side chain from the glutamic acid may affect aSyn structure and, consequently, the fibrillation process. Furthermore, A53E reduces membrane-binding affinity compared to A53T and WT (Ghosh et al. 2014), and enhances toxicity in mitochondria (Rutherford et al. 2015).

In summary, the fact that all the reported PD-associated aSyn mutations are concentrated in the N-terminal region of the protein (Figure 1.8), suggests that this region is important in the process of aSyn aggregation and toxicity.

In addition to point mutations, multiplications of the *SNCA* gene (duplications and triplications) appear to confer a functional gain of cytotoxicity to aSyn, clearly showing a dosage effect on disease progression (Singleton et al. 2003; Chartier-Harlin et al. 2004; Ibanez et al. 2004). Polymorphisms in the promoter region of *SNCA*, also play a role in PD by increasing aSyn expression (Holzmann et al. 2003).

1.4.2.3.2. aSyn Posttranslational Modifications

aSyn is known to undergo various types of PTMs. These include phosphorylation in S129 (Fujiwara et al. 2002), ubiquitination (Shimura et al. 2001), sumoylation (Dorval et al. 2006), C-terminal truncations (Li et al. 2005), or nitration (Giasson et al. 2000). However, it is not clear how these PTMs affect aSyn structure, folding, and how they modulate disease pathogenesis. Interestingly, most known sites of aSyn PTMs are localized in the C-terminal tail, including phosphorylation (Y125, S129, Y133 and Y136), truncation (D115, D119, P120, E130 and D135), ubiquitination (K96), and sumoylation (K96, K102) (Figure 1.11).

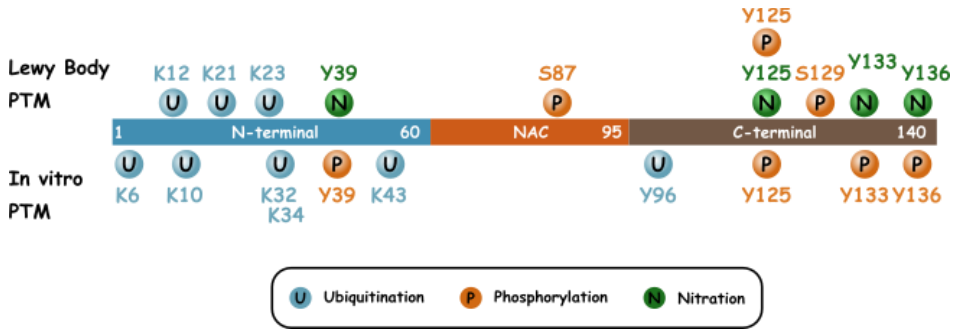

Figure 1.11 Schematic representation of some of the known PTMs in aSyn. Adapted from (Schmid et al. 2013)

Phosphorylation at S129 (pS129) has been intensively studied since approximately 90% of aSyn in LBs is thought to be phosphorylated (Fujiwara et al. 2002; Anderson et al. 2006). This suggests a close interaction between aSyn pS129 and its aggregation. Phosphorylated aSyn on tyrosine 39 (pY39) and 125 (pY125) has been also reported in human brains, although, no correlation was established among increased levels of phosphorylation and the pathological condition (Chen et al. 2009; Mahul-Mellier et al. 2014).

Several *in vivo* and *in vitro* studies attempted to clarify the consequences of aSyn phosphorylation by blocking (S129A) or mimic (S129D/E) phosphorylation. However, the conclusions turned out to be conflicting. In *Drosophila*, S129D aSyn was associated with pathology (Chen et al. 2005; Chen et al. 2009), but in yeast, rat, and *Caenorhabditis elegans* S129E had no effect. In addition, in budding yeast, S129A increases aSyn toxicity (Fiske et al. 2011; Sancenon et al. 2012). Moreover, in rats expressing aSyn in SN, S129A showed to be toxic, while S129D either was protective (Gorbatyuk et al. 2008) or had no effect (Azeredo da Silveira et al. 2009). Regarding the correlation between pS129 aSyn and aggregation is also not consensual. Most of the studies performed in cell lines reported an increase formation of soluble oligomers (Smith et al. 2005; Arawaka et al. 2006; Takahashi et al. 2007; Kragh et al. 2009; Wu et al. 2011), and in yeast, S129A is more toxic, and forms more inclusions and higher molecular oligomeric species than WT or S129E (Sancenon et al. 2012; Tenreiro et al. 2014).

Tyrosine phosphorylation is known to be a very rapid process, difficult to evaluate *in vivo*. The only study in human brain tissue showed that the levels of pY125 decrease with age and PD pathology (Chen et al. 2009). However, a recent study did not observe any significant differences in the levels of pY125 between PD brains and controls (Mahul-Mellier et al. 2014). Nevertheless, tyrosine phosphorylation (Y125, Y133, and Y136) can suppress eosin-induced oligomerization (Negro et al. 2002).

S87 (in addition to Y39) is the residue outside the C-terminal region that is phosphorylation (pS87) in rat, mice and human brains (Paleologou et al. 2010). *In vitro* studies demonstrated that pS87, inhibits aSyn fibrillization, and significant reduces aSyn binding to membranes, which is not the case of (Paleologou et al. 2010). However, depending on the model, the outcomes are different (Kim et al. 2006; Waxman et al. 2008; Paleologou et al. 2010).

Ubiquitin and the small ubiquitin-related modifier (SUMO) share structural similarities (Eckermann 2013). SUMO preferentially targets lysine residues at 96 and 102 sites of aSyn. *In vitro,* aSyn aggregation and fibrillation can be delayed or even blocked by sumoylation (Krumova et al. 2011).

1.4.2.3.3. Putative functions of aSyn

Assessing the normal function of aSyn has been challenging, not only because it is an intrinsically disordered protein that shifts between conformations, but also because it is a promiscuous protein that interacts and interferes with a lot of biological/cellular processes. In addition, the model systems available only partially recapitulate the symptoms and molecular pathologies associated with the disease. Furthermore, these models generally rely on aSyn overexpression, which adds another layer of complexity (for example, compensatory mechanisms) to the interpretation of its pathogenic and physiological roles.

The cellular localization of aSyn is thought to be regulated throughout brain development, during neuronal migration, maturation and synaptogenesis (Hsu et al. 1998; Murphy et al. 2000). In animal models, like rodents, aSyn levels are low in early embryogenesis (prior to E15), but increases in later stages of neuronal development (E18) extending into the postnatal period (P7) (Hsu et al. 1998). Also, increase levels of aSyn in pre-synapses are involved in critical stages of development, such as learning and synaptic plasticity (Maroteaux et al. 1988; George et al. 1995; Clayton et al. 1998; Hsu et al. 1998; Murphy et al. 2000). A recent study performed with professional musicians reveled up-regulation of some genes after music performance. In the list, dopaminergic neurotransmission-related genes were consistently identified. Around 26% of the *SNCA* co-expression network, was found to be up-regulated along with *SNCA*, suggesting that music performance may modulate the biological pathways of aSyn (Kanduri et al. 2015).

aSyn exists in a dynamic equilibrium between a soluble and a membrane-bound state (Roy 2009). The interaction between aSyn and lipid surfaces is believed to be a key features both in physiological and pathological condition. The N-terminal region of aSyn can adopt α-helical secondary structure upon binding to detergent micelles, liposomes (Davidson et al. 1998) or to negatively charged lipids or membranes (Jao et al. 2004; Jao et al. 2008). The membrane binding likely occurs via

the 11-mer sequences, as truncation of this domain drastically reduces lipid binding (Bisaglia et al. 2006; Burre 2015). N-terminal acetylation of aSyn can also increase its helical folding propensity, membrane binding affinity, and resistance to aggregation (Fauvet et al. 2012; Kang et al. 2012; Maltsev et al. 2012). aSyn not only binds to membranes, but it can induce membrane curvature and membrane tubulation, similar to amphiphysin (curvature-inducing protein involved in endocytosis) (Figure 1.12) (Varkey et al. 2010). These membrane-curvature changes can have a significant impact on the fusogenic properties of synaptic vesicles. For example, vesicles that have a high curvature, favors fusion with flat target membranes (Auluck et al. 2010). Interestingly, aSyn can aggregate faster in the presence of brain membranes, than in the presence of cytosolic fractions (Lee et al. 2002).

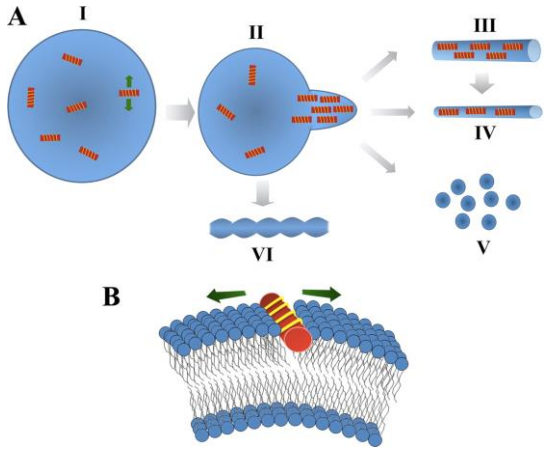

Figure 1.12 Model for aSyn-mediated membrane remodeling and curvature induction. (I) When aSyn binds to a single vesicle **(II)** the curvature strain causes initiation of a membrane tubule. The shape of the tube **(V)** is dependent of the concentration and orientation of the protein bound molecules on the membrane **(III, IV)** with higher concentrations favoring more curved structures. **(V)** Vesicular structures could originate from smaller membrane tubes or directly from large vesicles **(II). B**. Insertion of aSyn helical structure on intact vesicles occurs at the phosphate level. From (Varkey et al. 2010)

The mechanism by which membranes can be disrupted by aSyn is still intensely debated. Nevertheless, the formation of pore-like structures within the lipid bilayer (Lashuel et al. 2002), and the observation of donut-shaped complexes by atomic force and electron microcopy (Quist et al. 2005) have been reported. Mutations in aSyn also alter its phospholipid binding affinities. A30P and G51D decrease lipid affinity (Ysselstein et al. 2015).

Another role attributed to aSyn is its association with lipid metabolism. aSyn has been reported to bind to fatty acids (Sharon et al. 2001), to organize membrane components (Sharon et al. 2001), to regulate phospholipid composition (Adamczyk et al. 2007), and to inhibit phospholipase D1 and D2 *in vitro* and *in vivo* (Ahn et al. 2002; Outeiro et al. 2003). This implies that aSyn may be implicated in cleavage of membrane lipids and membrane biogenesis.

aSyn can interfere with neuronal membrane trafficking, affecting both Ras analog in brain (Rab) GTPases and certain N-ethylmaleimide-sensitive factor attachment protein (SNAP) receptors (SNAREs) (Amaya et al. 2015). SNAREs are a family of proteins that act in membrane fusion (Bonifacino et al. 2004; Jahn et al. 2006). aSyn directly promotes presynaptic SNARE-complex assembly via a nonclassical chaperone activity (Burre et al. 2010). aSyn is able to act as a SNARE chaperone when bound to the membrane, which can adopt α-helical conformation, and associates into multimers on the membrane surface. The multimers are the active forms that will promote SNARE complex assembly (Figure 1.13) (Burre et al. 2014).

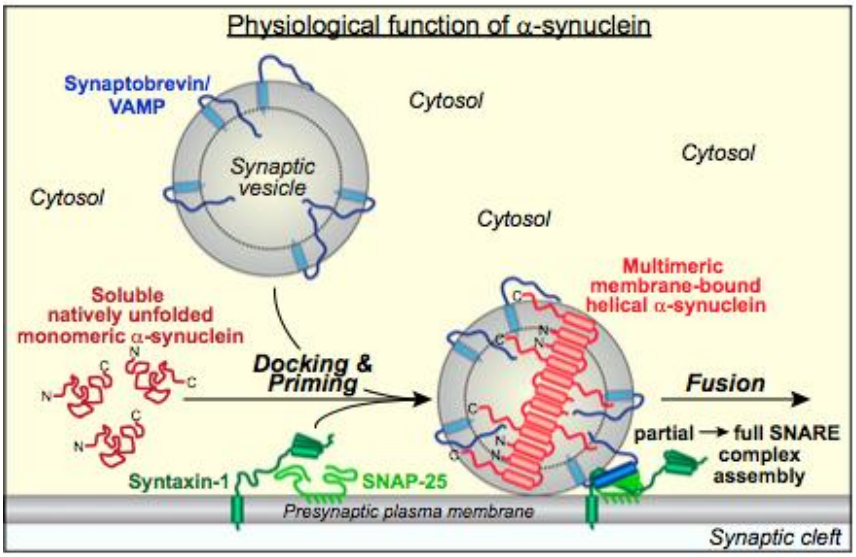

Figure 1.13 Schemating of a physiological folding pathway for aSyn. Native unstructured monomeric aSyn binds to synaptic vesicles during docking and priming of the vesicles. As a result of membrane binding, aSyn promotes SNARE complex assembly during docking and priming of synaptic vesicles. From (Burre et al. 2014)

The loss of dopaminergic neurons in the SN in PD results in a deficiency of DA signaling. In this context, it was hypothesized that aSyn could be related with DA biosynthesis and metabolism. aSyn inhibits DA synthesis by downregulating tyrosine

hydroxylase (TH) (Gao et al. 2007), limiting the conversion of tyrosine conversion to L-3,4-dihydroxypheny-lalanine (L-DOPA) (Baptista et al. 2003). This likely occurs via reducing TH phosphorylation and activation, which would lead to the activation of protein phosphatase 2A (Peng et al. 2005; Liu et al. 2008). Furthermore, aSyn affects the vesicular DA transporter VMAT2. aSyn knockout mice showed increased density of VMAT2 molecules *per* vesicle, and altered DA release (Abeliovich et al. 2000).

Expression of aSyn decreases the rate of DA release without changing DA levels or clearance/uptake mediated by dopamine transporter (Figure 1.14) (Yavich et al. 2005; Larsen et al. 2006). This shows that aSyn can acts as a negative regulator of DA release, by modulating vesicle function upon synaptic stimulation.

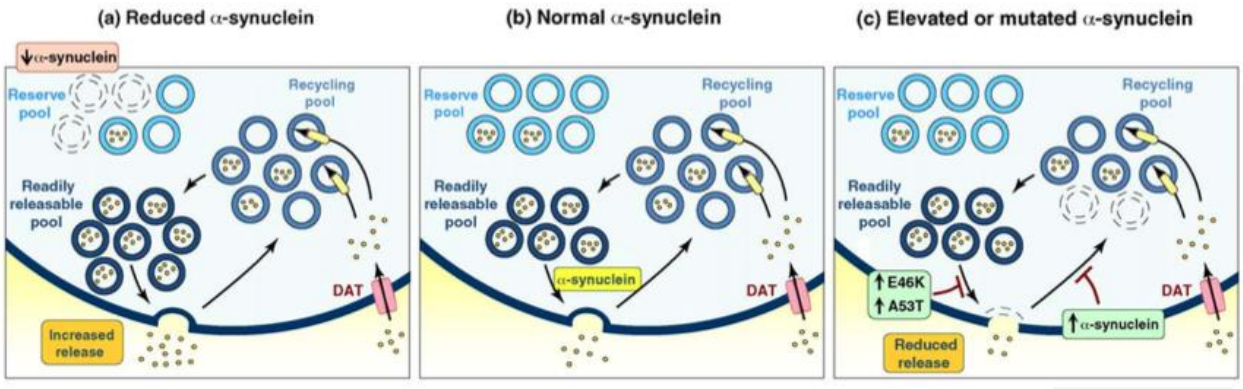

Figure 1.14 Schematic model of the role of aSyn in regulating presynaptic vesicle cycling. (a) When the levels of aSyn are low, the availability of vesicles in the reserve pool decreases and more vesicles are become available to be released. This increases dopamine release. **(b)** Under physiological conditions aSyn is regulates the vesicle docking and fusion. **(c)** Elevated levels of aSyn (or E46K and A53T), aSyn reduces dopamine release. From (Venda et al. 2010)

1.4.2.3.4. Prion-like spreading of aSyn pathology

In the past few years, there was an increase of reports establish an analogy between the prion diseases with synucleinopathies, suggesting that aSyn can behave in a prion-like manner. The prion protein (PrP) can act both as normal and as infectious pathogenic agents, unlike conventional pathogenic organisms (as viruses, bacteria, or yeast) (Prusiner 1982). The non-viral pathogens can spread/transmit within and between species upon changes in protein conformation: the cellular form of PrP (PrP^{C}) is rich in α-helices, and converts into the scrapie isoform (PrP^{Sc}) that is rich in β-sheet structure). Additionally, PrP^{Sc} will act as a template/seed and recruit

PrP^{c} into aggregates, by triggering its conversion into PrP^{Sc} (Riek et al. 1996; Wille et al. 2009). However, in synucleinopathies, the prion-like terminology only indicates that aSyn might share some features with prions, albeit without having infectious properties.

According to the "Braak hypothesis", the topography of Lewy pathology is correlated with the extent and severity of PD symptoms. The chronological appearance of PD symptoms starts with a pre-symptomatic phase characterized by olfactory deficits, sleep disturbances, and constipation (LBs/LN are restricted to the peripheral enteric system, olfactory bulb, and the caudal brainstem), followed by the motor symptom phase (Lewy pathology appears in SN). The final phase is characterized by cognitive decline and psychiatric symptoms (LBs reach the neocortex) (Figure 1.15) (Braak et al. 2003).

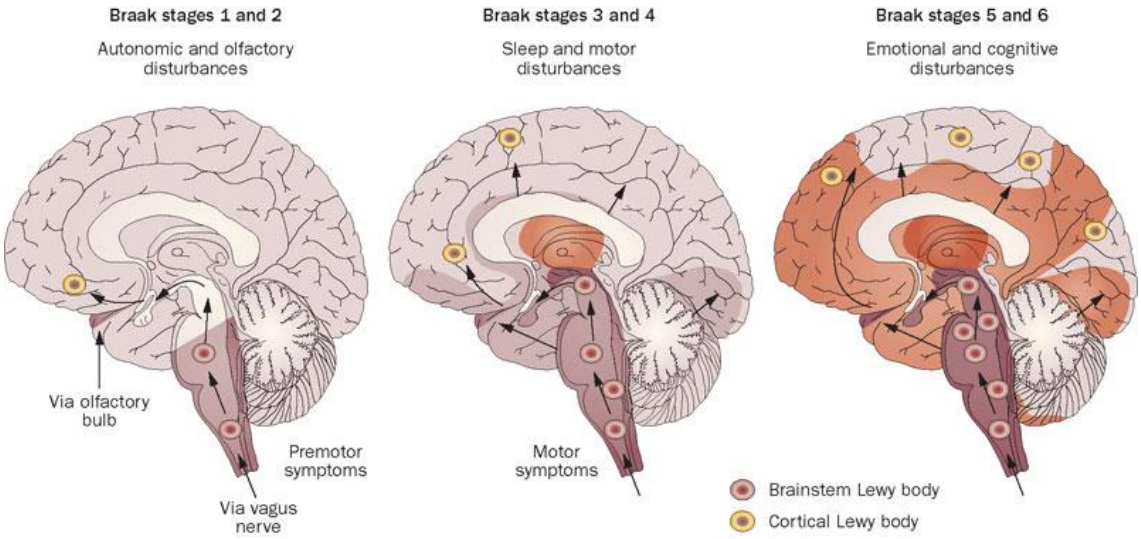

Figure 1.15 Spreading of aSyn. The Braak staging system hypothesizes that PD initiates in the olfactory bulb and the medulla oblongata and the dispersion of Lewy pathology into cortical regions (Doty 2012).

Furthermore, grafts of embryonic mesencephalic neurons in PD patients were found to present LBs years after transplant (Kordower et al. 2008; Kordower et al. 2008; Brundin et al. 2010), consistently with the proposed Braak hypothesis (Braak et al. 2006). The ability of fibrillar aSyn to self-propagate and spread, suggests that cell-to-cell transmissions plays a role in disease progression (Braak et al. 2003; Angot et al. 2010). Intracerebral inoculation of aSyn preformed fibrils (PFFs) initiates a rapidly

progressive onset of neurological symptoms and death in A53T aSyn transgenic (tg) mice, by enhancing the conversion of endogenous aSyn into LBs (Luk et al. 2012). Also, single intrastriatal injection of misfolded aSyn seeds into mice was able to initiate a neurodegenerative cascade by the accumulation of intracellular LBs/LN, loss of SN DA neurons, and impaired motor coordination. Thus, aSyn is sufficient to induce the cardinal behavioral and pathological features of sporadic PD (Luk et al. 2012). In line with Braak's hypothesis, a recent study showed that in mice injected with aSyn PFFs in the olfactory bulb aSyn was able to spread gradually from the injected site to multiple olfactory and non-olfactory brain regions that are affected in PD (Rey et al. 2016). Another interesting study showed that intragastrical administration of rotenone (an inhibitor of complex I of the mitochondrial respiratory chain) induces a progressive accumulation of aSyn in the enteric nervous system, arising sequentially to the dorsal motor nucleus of the vagus, the spinal cord and the SN in mice (Pan-Montojo et al. 2010). These observations reinforce the idea that PD can start in the periphery and progress until it reaches the brain.

Converging lines of evidence suggest that aSyn is released and taken up by neuronal cells. It is present in the cerebrospinal fluid, blood plasma, and saliva, in normal and affected patients (El-Agnaf et al. 2003; El-Agnaf et al. 2006; Al-Nimer et al. 2014). The mechanism by which aSyn is released is unclear. Thus, a better understanding of the mechanisms involved would be important for the potential identification of novel biomarkers and targets for therapeutic intervention. aSyn transfer has been proposed to occur via direct release, exosomes, endocytosis, and tunneling nanotubes (Figure 1.16).

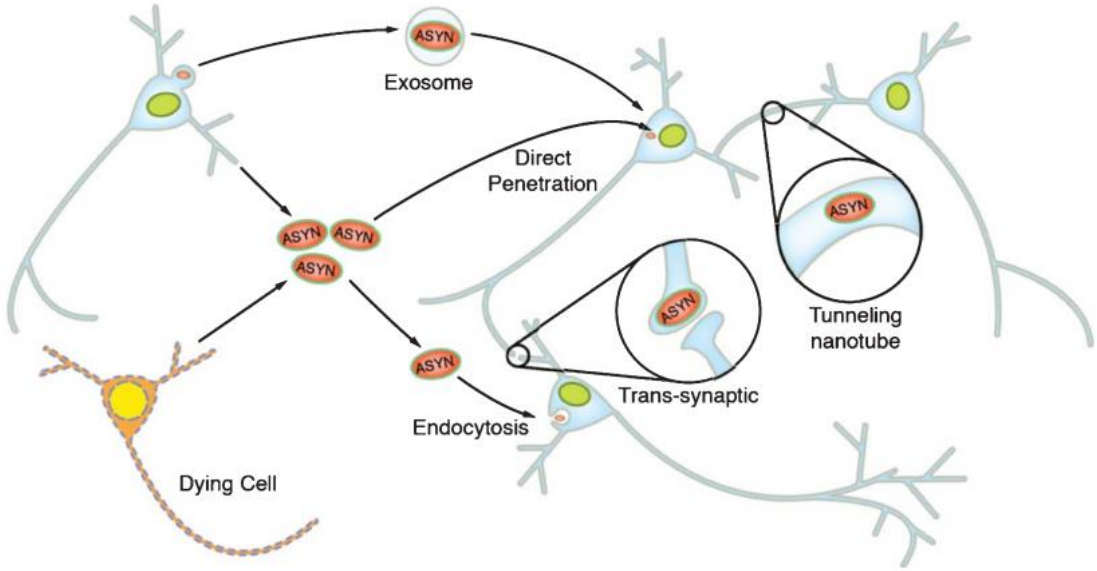

Figure 1.16 Proposed mechanisms for aSyn propagation. Several mechanisms have been proposed for the transfer of aSyn between neurons and induce disease to other brain regions. Once released to the extracellular environment, via exocytic pathway or via exosomes, these species can enter other neurons by direct penetration, or by endocytosis. The other two mechanisms possible ways involve a direct interaction between the host and the target cell and can occur by the formation of tunneling nanotubes or by trans-synaptic transmission. From (Wales et al. 2013)

1.4.2.4. Synphilin-1: an aSyn-interacting protein

aSyn binds to a number of ligands and proteins, which likely can alter its conformation. Sph1 belongs to this list of molecules, and was first identified as an aSyn-interacting protein in a yeast two-hybrid screen (Engelender et al. 1999). This was also confirmed by fluorescence resonance energy transfer (FRET) studies in mammalian cells (Kawamata et al. 2001), where co-expression of a domain of aSyn and Sph1 results in the formation of cytoplasmic inclusions that resemble LBs (Engelender et al. 1999). As a consequence, it was considered a candidate PD gene (since it binds to aSyn, potentiates aSyn aggregation, and is present in LBs). However, variability within the Sph1 locus is a rare cause of the disease. No coding change in the open reading frame has been found in the gene (Farrer et al. 2001), except for a point mutation (substitution of an arginine by a cysteine at position 621-R621C) in two sporadic PD patients (Marx et al. 2003). However, this connection has not been found in other synucleinopathies (Wakabayashi et al. 2000), and is even less consensual in AD (Wakabayashi et al. 2000; Iseki et al. 2002).

Sph1 is a protein with 919 amino acids, composed of different domains thought to form the basis of its function. It exists predominantly as a 90 kDa protein, but can also occur as a 120 kDa isoform. Smaller fragments of Sph1 are also detected in the human brain, and may represent proteolytically processed forms, or alternately spliced species (Murray et al. 2003) (Figure 1.17).

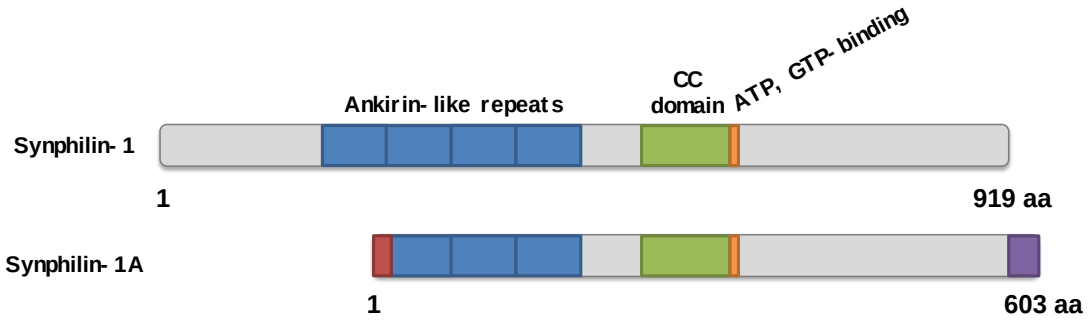

Figure 1.17 Schematic representation of the domains of Sph1 and Sph1A. Sph1 and Sph1A are structurally different in their exon and have different start codons.

Sph1 is a neuronal protein, enriched in presynaptic nerve terminals (Ribeiro et al. 2002). It is present in cerebellar Purkinje, nigral and hippocampal pyramidal neurons, in the human brain (Engelender et al. 2000; Ribeiro et al. 2002; Murray et al. 2003), and is also located within the central core of the LBs (while aSyn is in the periphery), and in glial cytoplasmic inclusions (Wakabayashi et al. 2000; Murray et al. 2003; Smith et al. 2010). This suggests that Sph1 deposition in LBs is not a secondary event, and may participate in their formation. Curiously, Sph1 does not seem to be present in LN, which may suggest heterogeneous composition and function (Wakabayashi et al. 2000). In terms of homology, human Sph1 sequence is 86% similar to mouse, but this number increases to 96% if the comparison focuses in the central portion of the protein - the ankyrin-like repeats and the coiled-coil domain (so-called protein-protein interaction domain) (Kruger 2004) (Figure 1.17).

Biochemical fractionation studies of human brain tissue revealed that Sph1 is predominantly soluble and is present in lipid bound fractions (Murray et al. 2003). At the ultrastructural level, Sph1 inclusions are membrane bound, and appear to include lipid-derived materials (den Jager 1969; O'Farrell et al. 2001), suggesting that the high lipid content facilitates protein incorporation into LBs, since it is known that

lipids are present in LBs (Gai et al. 2000), and that aSyn interacts with lipids and can associate with vesicular membranes (Davidson et al. 1998; Jensen et al. 1998).

1.5. *In vitro* studies of aSyn

Escherichia coli is routinely used to produce recombinant aSyn for *in vitro* studies that have been instrumental for our understanding of the structural properties and fibrillization of the protein. *In vitro*, unfolded monomeric aSyn tends to acquire transient structure that is prone to aggregate. After the initial lag phase, monomeric aSyn is converted to oligomeric species that then act as nuclei/seeds that rapidly assemble into protofilaments and protofibrils. Finally, the process reaches a plateau when amyloid fibrils are the majority of the polymers in solution. The kinetic properties of aSyn amyloid formation follow a sigmoidal curve and can be monitored using thioflavin T binding assay (Figure 1.5C) (Plotegher et al. 2014).

Several other methods are used to characterize and identify amyloid fibrils. These include, but are not limited to, Fourier transform infrared (FTIR) spectroscopy, nuclear magnetic resonance (NMR), or transmission electron microscopy (TEM).

FTIR provides evidence of the secondary structure distribution rather than precise structural details. Suspensions of aSyn fibrils display FTIR signal at 1630–1635 cm−1 (vibrational frequencies of intramolecular parallel β-sheets) (Kaylor et al. 2005; Qin et al. 2007). However, the resolution of FTIR analysis is low compared to NMR, since this powerful tool reports on atomic resolution (Jensen et al. 2014).

The resolution of TEM resolution is limited not only by the electron wavelength but also by the staining procedure. Information regarding aSyn fibril length and periodicity can be estimated, but diameter measurements are strongly biased by the grains of uranyl acetate salt. Therefore, TEM experiments are typically used to qualitatively evaluate aggregate morphology (Heise et al. 2005; Plotegher et al. 2014).

The capacity to detect and monitor conformational changes in real time is essential to understand the relationship between structure and biological function. A well-established technique in physics and chemistry, called Second-Harmonic generation (SHG), offers a highly sensitive method for studying structure and conformational changes upon ligand binding (Salafsky 2006). SHG is a nonlinear optical technique in which two photons with equal energy (ω- the fundamental)

generate one photon with twice the energy (2ω- second harmonic) (Figure 1.18) (Salafsky 2006; Moree et al. 2015).

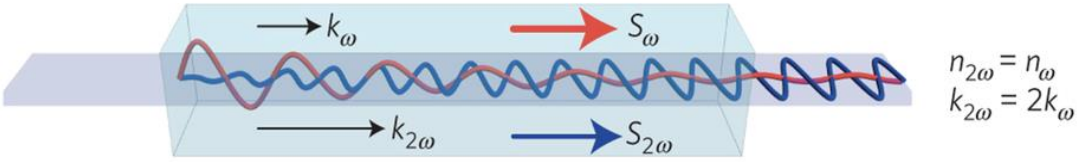

Figure 1.18 SHG principal. Conventional phase-matching for SHG ($k_{2\omega} = 2k_\omega$), where the fundamental and harmonic waves possess the same index of refraction and co-propagate along the same direction. Adapted from (Lan et al. 2015).

When a ligand binds and alters the conformation of a protein, this causes a change in the time and space averaged orientation of the second-harmonic-active moiety, resulting in alteration of the light intensity. However, for this process to occur it is not allowed to use media with inversion symmetry, since it produces SHG (Salafsky 2006; Moree et al. 2015). Therefore, this technique can serve as a starting point for basic studies on protein folding and conformational change. In addition, SHG can also be useful for drug screening at the molecular level.

1.6. Cell-based models of aSyn aggregation

A big effort has been made over the years to link the *in vitro* aggregation properties of aSyn to its biological and pathological significance. aSyn aggregation is one of the hallmarks of synucleinopathies, so the study of this process is crucial to understand the pathological mechanisms underlying LBs formation (Figure 1.19). Several cellular models have been developed to aid in addressing this question. However, unlike many proteins prone to aggregate, aSyn does not readily aggregate when overexpressed in cell cultures.

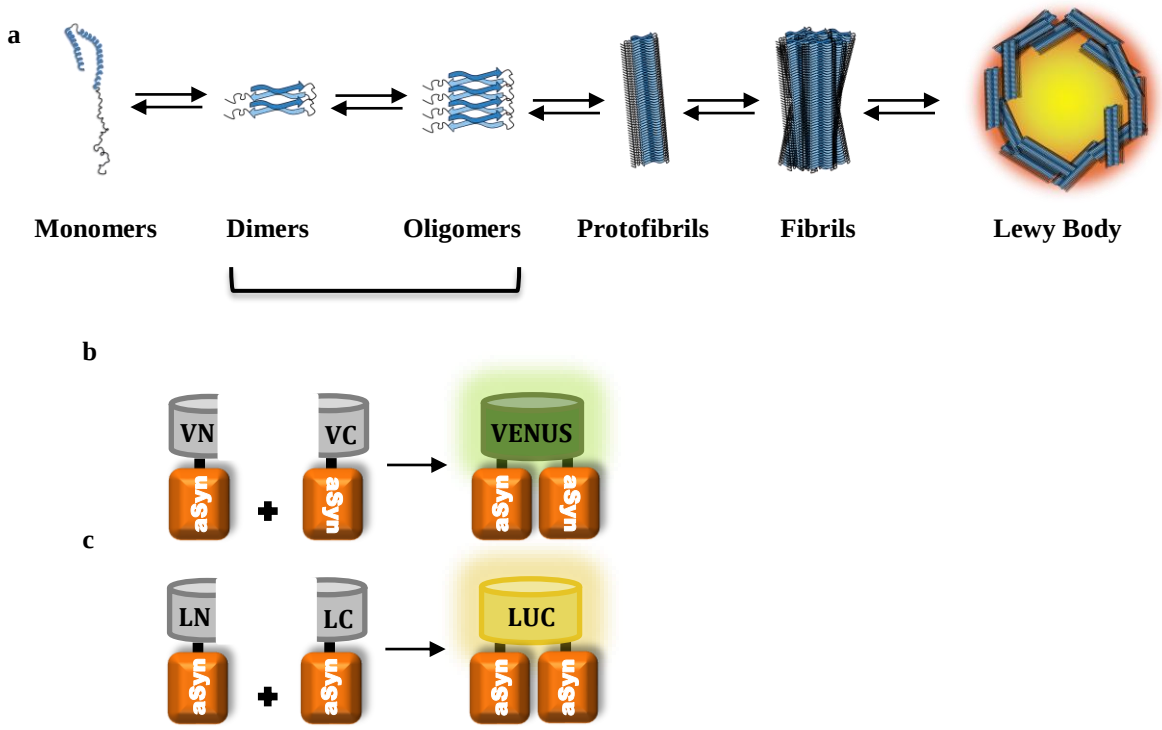

Figure 1.19 Schematic model of aSyn aggregation. Summary of aSyn aggregation models. **(a) Schematic model of aSyn aggregation.** Propose mechanism of aSyn aggregation. **(b) Schematic representation of Venus BiFC.** This model allows *in vivo* visualization of aSyn complex. **(c) Representation of humanized Gaussia luciferase (hGLuc) constructs.** Non-bioluminescent halves of hGLuc are fused to aSyn. Upon aSyn interaction, luminescence can be measure either inter or extracellular.

It is likely that the self-interaction of aSyn into dimers is the primary event underlying the formation of higher molecular weight species. The formation of those initial species is thought to be the rate-limiting step for aSyn aggregation (Krishnan et al. 2003; Roostaee et al. 2013). Therefore, mimicking the initial steps of aSyn aggregation in cells is of great interest. One approach to enable the visualization of protein dimers in living cells is the Bimolecular Fluorescence Complementation assay (BiFC) (Kerppola 2006). This system involves the association of two non-fluorescent fragments of a fluorescent protein, reconstituting the functional fluorophore. This method allows the direct visualization of protein-protein interactions in the context of a living cell, and therefore, their subcellular localization.

The BiFC assay has been applied for the study of aSyn dimerization by fusing each of the fluorescent protein fragments to either to N- and/or C-terminus of aSyn (Figure 1.9b). When aSyn interacts, and forms dimers/oligomers, the two non-fluorescent fragments can assemble, and generate fluorescence. aSyn dimers and oligomers are detected in the cell nucleus, and these species led to a significant

increase in cytotoxicity (Outeiro et al. 2008). aSyn dimerization was shown to be reversible, for example by the overexpression of Hsp70, that selectively impacts on high molecular weight species, and reducing cytotoxicity (Outeiro et al. 2008).

A similar concept for the assessment of protein-protein interactions is the split luciferase assay. The principle is similar to that of the BiFC assay, but in this case the luciferase protein is split into N- and C-terminal fragments, that are then fused to the protein of interest. In this case, however, the readout is a luminescence, and not fluorescence (Figure 1.8c). The split luciferase assay has the advantage that it enables a more readily detection of protein dissociation (Remy et al. 2006).

Another useful cell model in the study of aSyn aggregation consists on the co-expression of aSyn linked with a truncated, non-fluorescent fragment of EGFP (SynT) together with Sph1 (Figure 1.20) (McLean et al. 2001).

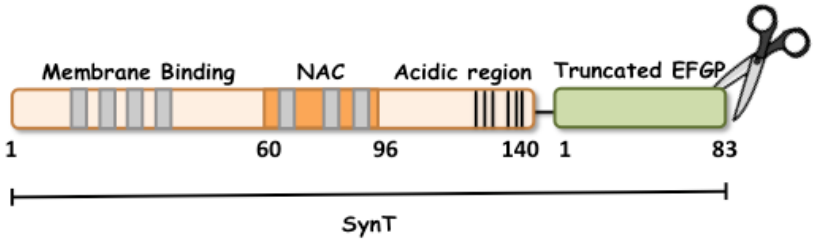

Figure 1.20 Schematic representation of the SynT structure. The initial 83 aa of EGFP are fused at the C-terminus of aSyn. This construction enables the visualization of aSyn cytoplasmatic inclusions that resemble LBs, upon immunostaining.

Using this model, it was shown that alterations in the C-terminus of aSyn increase its potential to form intracellular inclusions, as this was not simply due to the EGFP fragment used. Fusion of the same 83 aa of EGFP with tubulin or synaptophysin did not induce the formation of protein inclusions (McLean et al. 2001).

All of these cell models have their limitations, since no cell-based assay is able to recapitulate the *in vivo* physiology of aSyn (Astashkina et al. 2012). However, these "living test tubes" facilitate the interpretation of the effect of single events/pathways, mutations, or drugs/small compounds, on aSyn aggregation and, therefore, are extremely valuable for these studies.

2. Aims of the study

Synucleinopathies are a group of neurodegeneration disorders that share a common feature of misfolding and aggregation of aSyn. In order to achieve a better understanding of the molecular mechanisms underlying the disease, it is crucial to conduct systematic analyses of the cellular effects of aSyn. In this context, we decided to assess the effects of aSyn aggregation in cellular models of synucleinopathies. To achieve this, we focused on the systematic comparison of selected aSyn mutants described.

The main goal of this project was to provide novel insight into the molecular determinants of aSyn aggregation in cultured human cells, and to investigate potential therapeutic approaches that modulate the process of aSyn aggregation. To this end, the specific aims of this thesis were to:

Aim 1. Establish a base knowledge regarding the cellular effects of aSyn

Aim 2. Test the effects of small molecules on aSyn aggregation

3. Results

3.1. Systematic comparison of the effects of alpha-synuclein mutations on its oligomerization and aggregation

Diana F. Lázaro, Eva F. Rodrigues, Ramona Langohr, Hedieh Shahpasandzadeh, Thales Ribeiro, Patrícia Guerreiro, Ellen Gerhardt, Katharina Kröhnert, Jochen Klucken, Marcos D. Pereira, Blagovesta Popova, Niels Kruse, Brit Mollenhauer, Silvio O. Rizzoli, Gerhard H. Braus, Karin M. Danzer, Tiago F. Outeiro

Experiments	Done by
Analysis of mutations effect on aSyn oligomerization, in Figure 2.	Eva F. Rodrigues and Thales Ribeiro
Analysis of aSyn mutation effects in the inclusion formation, in Figure 3.	Diana F. Lázaro and Thales Ribeiro
Analysis of aSyn-GFP variants in yeast, in Figure 5.	Hedieh Shahpasandzadeh
Analysis of aSyn native conformation, and solubility state, Figure 6.	Eva F. Rodrigues
Analysis of fine structure of aSyn inclusions, in Figure 6.	Diana F. Lázaro and Katharina Kröhnert
Thioflavin staining, in Figure 6.	Diana F. Lázaro
Analysis of aSyn bPCA, in Figure 7.	Ramona Langohr
Analysis of aSyn secretion, in Figure 8.	Dr. Niels Kruse
Analysis of aSyn toxicity and the inverse correlation, in Figure 8.	Diana F. Lázaro
Analysis of aSyn partially co-localizes with endosomes/lysosomes, in Figure 9.	Diana F. Lázaro
Analysis of Golgi morphology, in Figure 10.	Diana F. Lázaro
Analysis of BiP levels, in Figure 10.	Diana F. Lázaro and Eva F. Rodrigues

Status of the manuscript: published (PLoS Genet. 2014 Nov 13;10(11):e1004741)

OPEN ACCESS Freely available online

PLOS | GENETICS

Systematic Comparison of the Effects of Alpha-synuclein Mutations on Its Oligomerization and Aggregation

Diana F. Lázaro[1], Eva F. Rodrigues[1], Ramona Langohr[2], Hedieh Shahpasandzadeh[3], Thales Ribeiro[4], Patrícia Guerreiro[1,5], Ellen Gerhardt[1], Katharina Krohnert[6], Jochen Klucken[7], Marcos D. Pereira[4], Blagovesta Popova[3], Niels Kruse[8], Brit Mollenhauer[8,9], Silvio O. Rizzoli[6], Gerhard H. Braus[3], Karin M. Danzer[2], Tiago F. Outeiro[1,4]*

1 Department of NeuroDegeneration and Restorative Research, Center for Nanoscale Microscopy and Molecular Physiology of the Brain University Medical Goettingen, Goettingen, Germany, 2 Department of Neurology, Ulm University, Ulm, Germany, 3 Georg August University, Institute for Microbiology and Genetics Dept. of Molecular Microbiology and Genetics, Goettingen, Germany, 4 Laborato´rio de Citotoxicidade e Genotoxicidade, Departamento de Bioquı´mica - Instituto de Quı´mica Universidade Federal do Rio de Janeiro, Rio de Janeiro, Brazil, 5 Instituto de Medicina Molecular, Faculdade de Medicina da Universidade de Lisboa, Lisboa, Portugal, 6 Department of Neuro and Sensory Physiology, University of Go¨ttingen Medical Center c/o European Neuroscience Institute Go¨ttingen, Go¨ttingen, Germany, 7 Department of Molecular Neurology, University Hospital Erlangen, Friedrich-Alexander University Erlangen-Nu¨rnberg, Erlangan, Germany, 8 Institute for Neuropathology, University Medical Center Goettingen, Goettingen, Germany, 9 The Department for neurosurgery at UMG and Paracelsus-Elena-Klinik, Kassel, Germany

Abstract

Aggregation of alpha-synuclein (ASYN) in Lewy bodies and Lewy neurites is the typical pathological hallmark of Parkinson's disease (PD) and other synucleinopathies. Furthermore, mutations in the gene encoding for ASYN are associated with familial and sporadic forms of PD, suggesting this protein plays a central role in the disease. However, the precise contribution of ASYN to neuronal dysfunction and death is unclear. There is intense debate about the nature of the toxic species of ASYN and little is known about the molecular determinants of oligomerization and aggregation of ASYN in the cell. In order to clarify the effects of different mutations on the propensity of ASYN to oligomerize and aggregate, we assembled a panel of 19 ASYN variants and compared their behaviour. We found that familial mutants linked to PD (A30P, E46K, H50Q, G51D and A53T) exhibited identical propensities to oligomerize in living cells, but had distinct abilities to form inclusions. While the A30P mutant reduced the percentage of cells with inclusions, the E46K mutant had the opposite effect. Interestingly, artificial proline mutants designed to interfere with the helical structure of the N-terminal domain, showed increased propensity to form oligomeric species rather than inclusions. Moreover, lysine substitution mutants increased oligomerization and altered the pattern of aggregation. Altogether, our data shed light into the molecular effects of ASYN mutations in a cellular context, and established a common ground for the study of genetic and pharmacological modulators of the aggregation process, opening new perspectives for therapeutic intervention in PD and other synucleinopathies.

Citation: Lázaro DF, Rodrigues EF, Langohr R, Shahpasandzadeh H, Ribeiro T, et al. (2014) Systematic Comparison of the Effects of Alpha-synuclein Mutations on Its Oligomerization and Aggregation. PLoS Genet 10(11): e1004741. doi:10.1371/journal.pgen.1004741

Editor: Daniel Kaganovich, Hebrew University of Jerusalem, Israel

Received May 27, 2014; Accepted September 9, 2014; Published November 13, 2014

Copyright: 2014 La´zaro et al. This is an open-access article distributed under the terms of the Creative Commons Attribution License, which permits unrestricted use, distribution, and reproduction in any medium, provided the original author and source are credited.

Data Availability: The authors confirm that all data underlying the findings are fully available without restriction. All relevant data are within the paper and its Supporting Information files.

Funding: This work was supported by the DFG Center for Nanoscale Microscopy and Molecular Physiology of the Brain (CNMPB). The funders had no role in study design, data collection and analysis, decision to publish, or preparation of the manuscript.

Competing Interests: The authors have declared that no competing interests exist.

* Email: touteir@gwdg.de

Introduction

Alpha-synuclein (ASYN) is an abundant neuronal protein whose normal function is still elusive, but seems to be related to SNARE-complex assembly [1]. Misfolding and aggregation of ASYN in proteinaceous inclusions, known as Lewy bodies (LBs), are associated with Parkinson's disease (PD) and other neurodegen-erative disorders known as synucleinopathies [2,3]. PD is the second most common neurodegenerative disease, affecting ap-proximately 1% of the population over 65 years of age [4], and is therefore a growing problem in the aging population. Both point mutations [5,6,7] and multiplications [8,9,10,11] of the SNCA gene, encoding for ASYN, have been linked to autosomal-dominant forms of PD. More recently, GWAS studies identified the SNCA locus as a strong risk factor underlying PD [12,13], and two additional familial mutations (G51D and H50Q) were recently identified [14,15,16]. The H50Q mutation is associated with late-onset parkinsonism, and the patients exhibit similar pathological features to those observed for patients carrying E46K or A53T mutations [17]. The G51D mutation is associated with early onset of disease [15].

Over the years, numerous in vitro and in vivo studies confirmed the toxic potential of both wild type (WT) and PD-linked ASYN mutants [18,19]. In vitro, these ASYN mutations alter the aggregation process and interfere with oligomerization, fibril formation, and subcellular distribution [20,21,22]. Upon overex-pression, ASYN induces aggregation and cytotoxicity [23], disrupts vesicular transport [24,25], causes mitochondrial deficits, impairs autophagy [26], increases sensitivity to oxidative stress [27], impairs vesicle recycling, neuronal plasticity and synaptic

Author Summary

The accumulation of aggregated proteins in the brain is common across several neurodegenerative disorders. In Parkinson's disease (PD), the protein alpha-synuclein (ASYN) is the major component of aggregates known as Lewy bodies. It is currently unclear whether protein aggregates are protective or detrimental for neuronal function and survival. The present hypothesis is that smaller aggregated species, known as oligomers, might constitute the toxic forms of ASYN. Several mutations in ASYN cause familial forms of PD. In the laboratory, artificial mutations have been designed to enable the study of the aggregation process. However, different studies relied on the use of different model systems, compromising the interpretation of the effects of the mutations. Here, we addressed this by (i) assembling a panel of 19 ASYN variants and (ii) by performing a systematic comparison of the effects of the mutations in mammalian cell models. Interestingly, our study enabled us to correlate oligomerization and aggregation of ASYN in cells. Altogether, our data shed light into the molecular determinants of ASYN aggregation, opening novel avenues for the identification of modulators of ASYN aggregation, which conceal great hopes towards the development of strategies for therapeutic intervention in PD and other synucleinopathies.

integrity [28] as well as the folding/refolding of SNARE proteins [29]. Several animal models have also been generated based on the overexpression of either wild type or mutant ASYN, but the phenotypes reported are quite diverse [30,31,32].

Posttranslational modifications (PTM) in the context of PD are also controversial. The majority of ASYN in LBs isolated from PD patients is phosphorylated at serine-129 (S129) but whether this is a cause or a consequence of aggregation is unclear [33,34,35]. Other ASYN residues like serine-87 (S87) and tyrosines-125, -133 and -136 (Y125, Y133 and Y136) can be also phosphorylated [36]. SUMOylation, another type of PTM that modulates protein-protein interactions, affects subcellular localization, stability and solubility of target proteins [37,38]. Engineered mutants of ASYN to prevent SUMOylation enhanced the tendency to aggregate in cell-based assays and increase cytotoxicity in dopaminergic neurons of the substantia nigra (SN), in vivo [38].

Although aggregation of ASYN is recognized as a central process in synucleinopathies, it is still unclear whether inclusions are toxic or protective [39]. Actually, accumulating evidence suggests ASYN oligomers may constitute the toxic species, rather than mature aggregates [40,41]. To overcome these limitations, engineered mutation is a simple way to understand the putative effects impact of determine residues in the context of PD. Several artificial proline mutants of ASYN (A56P, A30P/A76P double mutant, and A30P/A56P/A76P triple mutant (TP) display impaired propensity to fibrilize [40]. A similar effect was reported for mutants disrupting the formation of salt bridges between b-strands of ASYN (E35K and E57K) [41], which increases the formation of oligomers when compared with WT ASYN.

Nevertheless, conflicting results obtained in different cell and animal models, and the limited existence of systematic studies comparing the behaviour of WT and ASYN mutants in the same model systems, complicate our understanding of the molecular determinants of ASYN aggregation and toxicity. Here, we conducted a systematic comparison of the effects of PD-linked and engineered ASYN mutants in two established cell-based models of ASYN oligomerization [42] and aggregation [43]. Our findings establish the effects of the different mutants studied and pave the way for the identification of genetic and pharmacological modulators of the various processes studied, opening new perspectives for the design of therapeutic strategies aimed at targeting specific steps of the ASYN aggregation process.

Results

Design and generation of ASYN mutants

To investigate the molecular determinants of ASYN oligomer-ization and aggregation in a cellular context, we used site-directed mutagenesis to generate a panel of 19 ASYN point mutants including five mutations associated with familial PD (A30P, E46K, H50Q, G51D and A53T) and others known to interfere with different aspects of ASYN biology (Fig. 1 and Table S1). Then, we analysed the behaviour of each mutant in established paradigms of ASYN oligomerization (Fig. 2A) or aggregation (Fig. 3A).

Effect of mutations on ASYN oligomerization

In order to assess the effect of ASYN mutations on oligomer-ization, we used a variant of the Bimolecular Fluorescence Complementation (BiFC) assay we previously described [42], based on the reconstitution of functional Venus fluorescent protein promoted by the interaction between, at least, two ASYN molecules, that enables us to directly visualize the formation of ASYN dimeric/oligomeric species (hereforth referred to as oligomeric species for simplicity) in living cells (Fig. 2A) [42]. We have previously demonstrated that the efficiency of the ASYN BiFC assay is identical in different cell lines, including HEK cells [42]. Using epifluorescence microscopy we found that, as expected, all the ASYN variants formed oligomers in HEK cells

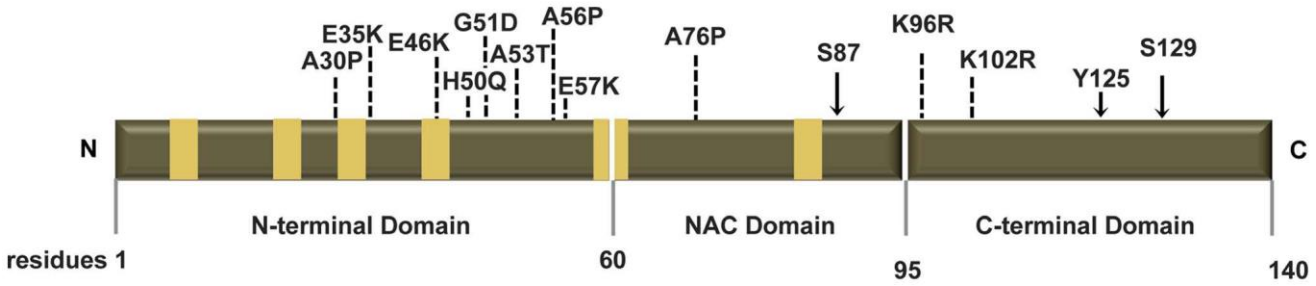

Figure 1. Human ASYN. Scheme representing the structure of human ASYN with the three distinct domains (N-terminal, NAC and C-terminal). Amino acid residues are indicated in the bottom. Brown bars inside protein domains represent the imperfect hexameric KTKEGV repeats. Arrows indicate the sites of phosphorylation and the broken lines show the mutated sites.
doi:10.1371/journal.pgen.1004741.g001

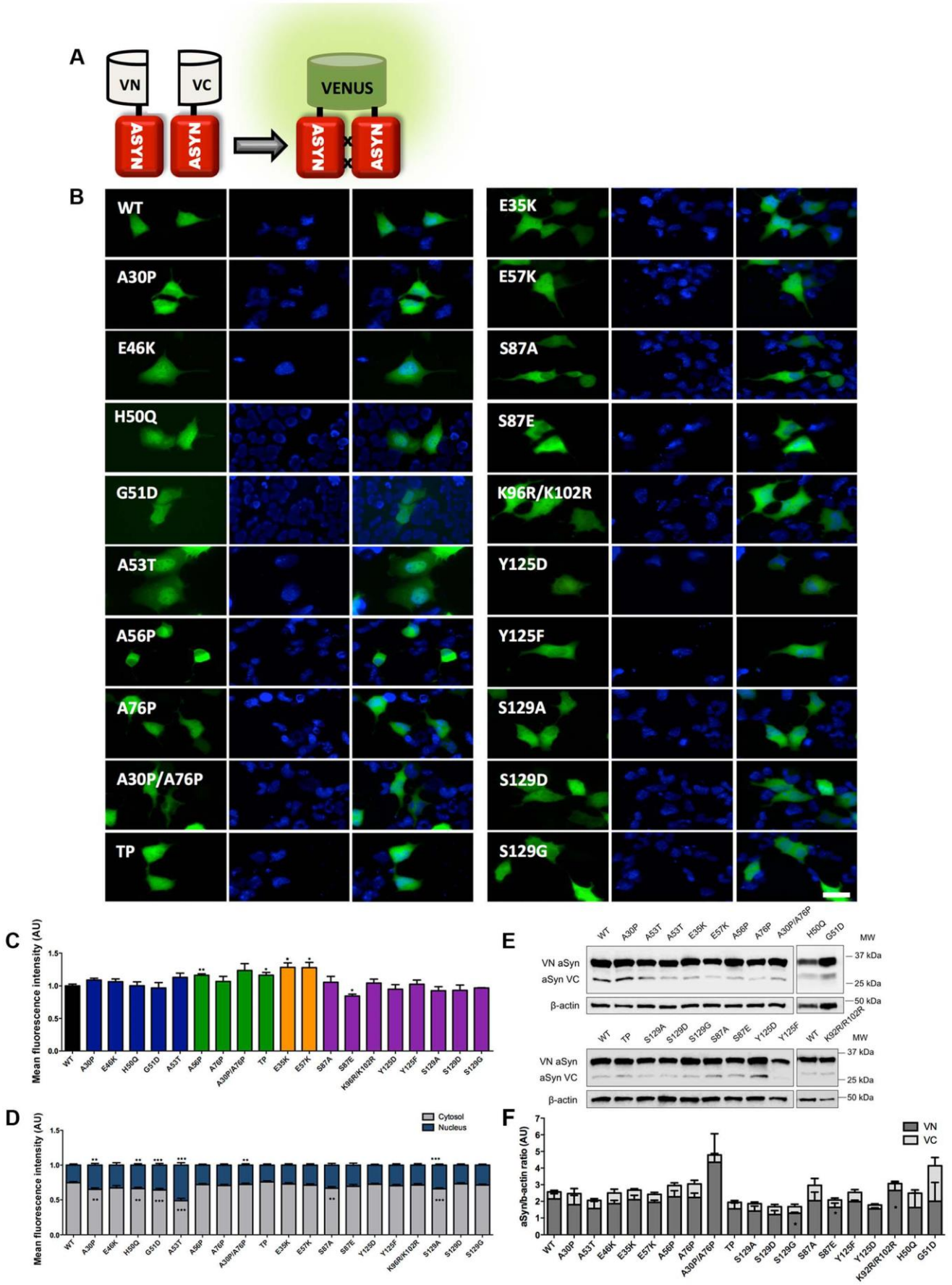
A
VN
VC
VENUS
ASYN
ASYN
ASYN
ASYN
B
WT
A30P
E46K
H50Q
G51D
A53T
A56P
A76P
A30P/A76P
TP
E35K
E57K
S87A
S87E
K96R/K102R
Y125D
Y125F
S129A
S129D
S129G
C
Mean fluorescence intensity (AU)
D
Cytosol
Nucleus
Mean fluorescence intensity (AU)
E
MW
VN aSyn
aSyn VC
β-actin
37 kDa
25 kDa
50 kDa
F
aSynb-actin ratio (AU)
VN
VC

Figure 2. Mutations effect on ASYN oligomerization. A. Schematic representation of Bimolecular Fluorescence Complementation assay (BiFC). ASYN BiFC constructs in anti-parallel orientation. B. Representative pictures of ASYN oligomerization. HEK-293 cells overexpressing VN-ASYN and ASYN-VC constructs. The green fluorescence results from the reconstitution of the Venus fluorophore, promoted by the interaction of the proteins of interest. Scale bar: 10 mm. C. Oligomerization efficiency. Mean fluorescence intensity of cells expressing different ASYN mutants was assessed 24 hours post-transfection, using a microcapillary system (GuavaeasyCyte HT system). For each sample 25,000 events were counted. D. Intracellular distribution of oligomeric ASYN. Nuclear and cytoplasmic venus fluorescence intensities in HEK-293 cells were quantified using ImageJ. The graph demonstrates an increase in nuclear fluorescence in cells expressing ASYN mutants. For each experiment.25 cells were analysed. E-F. Levels of ASYN. E. Representative immunoblot showing the expression levels of ASYN. F. Immunoblot analysis of the expression levels of VN-ASYN and ASYN-VC from all the mutations studied in HEK-293 cells. Student's t test (*p,0.05, **p,0.01, ***p,0.001). n = 3. doi:10.1371/journal.pgen.1004741.g002

(Fig. 2B and C). One striking observation was that the PD-linked mutant A53T promoted the strongest increase (,50%) in the accumulation of ASYN oligomers in the nucleus (Figure 2B and D).

To compare the extent to which different ASYN variants promoted oligomerization we used flow cytometry to measure the fluorescence intensities of cells expressing the different mutants. We observed an increase in fluorescence intensity for proline and lysine mutants. This increase was around 16.3% for A56P mutant, and 16.5% for the TP mutant (Fig. 2C). In the case of A30P/A76P double mutant (DP) and single A76P mutant we observed a trend towards an increase in fluorescence intensity, but the increase was not statistically significant. Likewise, we found a 28.4% increase in oligomerization for the E35K mutant, and 28.1% for the E57K mutant. In contrast, we found that the S87E mutant, mimicking phosphorylation at S87, reduced oligomerization by,16%. To investigate whether these effects were explained by differences in the levels of ASYN, we performed immunoblot analysis. We found that the levels of VN-ASYN decreased for almost all mutants (statistically significant for G51D, S129D and S87A) and increased for H50Q, A30P/A76P and K96R/K102R (Fig. 2E, F). Interest-ingly, there was no correlation between the levels of the mutants and the fluorescence signal, suggesting the effects observed were intimately correlated with the effects of the mutations on oligomerization, and not due to differences in the levels of expression of the various ASYN mutants.

Effect of mutations on ASYN aggregation

In parallel, we asked whether the selected mutations altered ASYN inclusion formation. For this, we took advantage of an established paradigm of ASYN aggregation based on the co-expression of SynT and synphilin-1, an ASYN-interacting protein that is also present in LBs (Fig. 3A) [43]. As previously established, human neuroglioma cells (H4) were co-transfected with plasmids encoding each of the SynT variants and synphilin-1 and inclusion formation was assessed 48 hours post-transfection. Since the inclusion pattern was heterogeneous, we defined four categories (cells without inclusions, with ,5 inclusions, with more than 5 and less than 9 inclusions, or $10 inclusions) in order to obtain a more precise assessment of the effects of the mutations. For the PD-linked mutants, we found that A30P increased the percentage of cells without inclusions to ,70% when compared to WT ASYN. In contrast, the E46K and G51D mutations dramatically increased the percentage of cells with inclusions to ,90% and ,80%, respectively (Fig. 3B, C and Fig. S1).

In the case of the proline mutants, we observed that all four mutants reduced the percentage of cells displaying inclusions (Fig. 3B, C and Fig. S1).

For the E35K and E57K mutants, the number and the size of the inclusions varied. Both mutants promoted an increase to ,70– 80% of cells with inclusions (Fig. 3B, C and Fig. S1). While we predominantly observed the presence of small inclusions with the E57K mutant, we detected a mix of small and larger inclusions with the E35K mutant (Fig. 3B).

We also investigated the effect of phosphorylation on ASYN inclusion formation. For this, we screened mutants that block (S87A, Y125F, S129A and S129G) or mimic (S87E, Y125D and S129D) phosphorylation. We found that mimicking phosphoryla-tion on S87 resulted in a marked decrease in the number of inclusions per cell, with ,80% of the transfected cells displaying no inclusions (p,0.01 Fig. 3C, Fig. S1A). No significant effect was observed with the S87A mutant, suggesting the S87 may normally exist, at least in our cell model, mostly unphosphorylated. Also, no significant differences were observed for Y125D, S129A, S129G, or S129D mutants, when compared to WT SynT. However, we found the Y125F mutation and SUMOylation-deficient mutant (K96R/K102R) mutation induced an altered inclusion pattern, with the accumulation of inclusions of different sizes, similar to that observed with the lysine mutant.

Immunoblot analysis showed that the levels of ASYN varied depending on the particular mutant being expressed, but we only found a significant increase in the levels of the S129G mutant (Fig. 3D and E). Interestingly, we found a trend towards a decrease in the levels of mutants that promoted accumulation of inclusions or changed the size of the inclusions (E46K, E57K and K96R/K102R).

Based on the results obtained in the oligomerization and aggregation paradigms, we decided to focus on seven ASYN mutations (A30P, E46K, A53T, E35K, E57K, TP and Y125F) that had the most pronounced effects for subsequent analysis (Table S2 and Fig. 4). We examined these selected ASYN mutants using different assays, including toxicity measurements, biochem-ical analysis of ASYN, ASYN secretion, degradation pathways, and Golgi and ER stress (Fig. 4), in order to obtain detailed information on the cellular effects of specific types of ASYN accumulations.

ASYN toxicity and aggregation in yeast

We started by investigating the toxicity of the selected variants of ASYN by taking advantage of the budding yeast as a model of synucleinopathies, as previously described [23,44]. In conditions where the expression of ASYN was induced, using galactose-containing media, we found that almost all mutations induced toxicity similar to WT ASYN (Fig. 5A). In line with the observation in H4 cells, the TP mutant did not form inclusions and the A30P mutant strongly impaired inclusion formation (Fig. 3B-C and 5B-C). Neither of these mutants was toxic in yeast (Fig. 5A) [23,44]. Importantly, we found no significant differences in the levels of expression of all variants tested, ruling out the possibility that toxicity and/or inclusion formation were due to differences in the levels of expression of ASYN (Fig. 5D).

Characterization of ASYN species

To further assess the biochemical nature of the ASYN species visualized by the BiFC assay, we employed non-denaturing polyacrylamide gel electrophoresis (native-PAGE). Immunoblot analysis showed a smear, which is indicative of the accumulation of oligomeric species of various sizes (Fig. 6A).

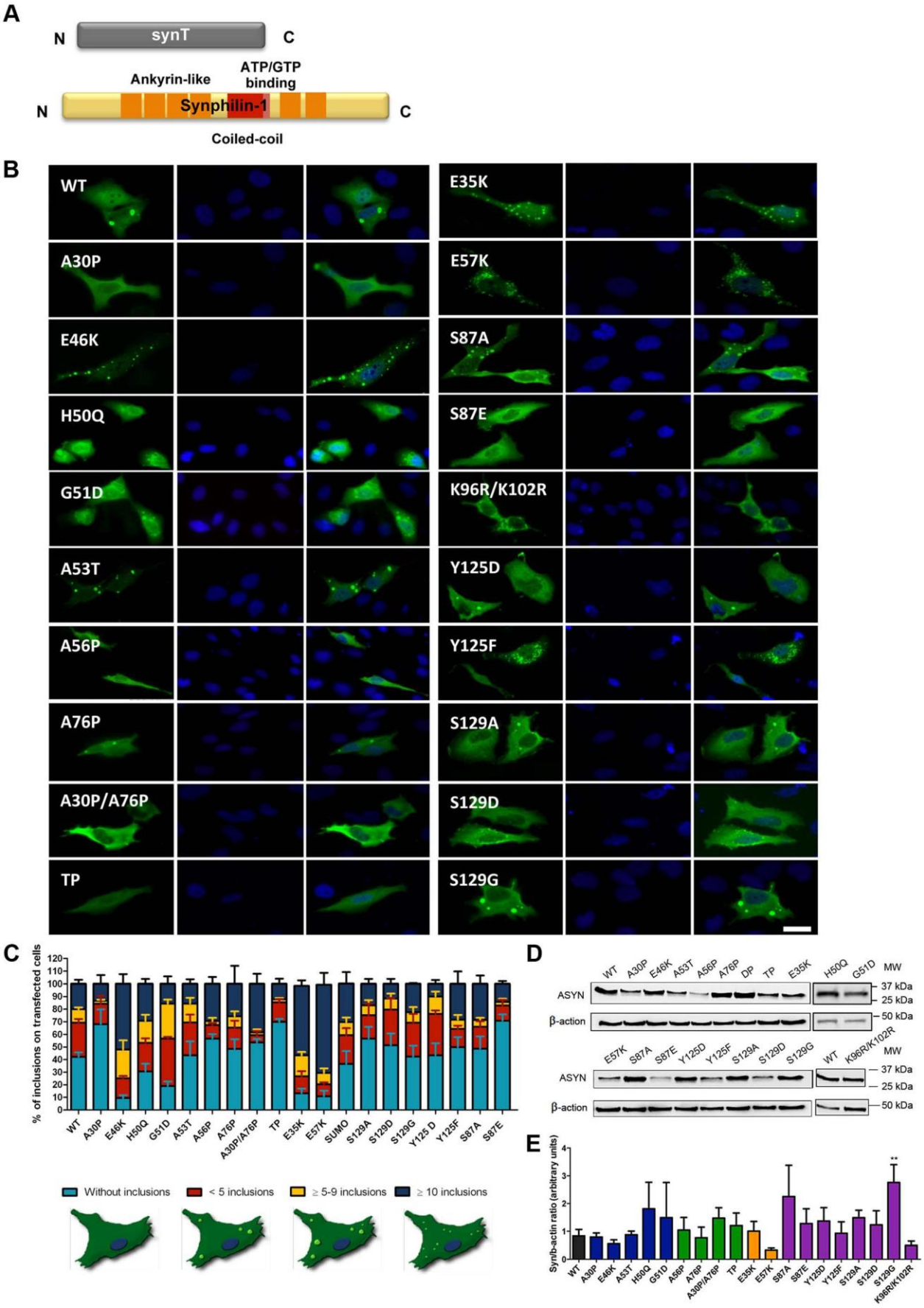
A
N
synT
C
Ankyrin-like
ATP/GTP binding
N
Synphilin-1
C
Coiled-coil
B
WT
A30P
E46K
H50Q
G51D
A53T
A56P
A76P
A30P/A76P
TP
E35K
E57K
S87A
S87E
K96R/K102R
Y125D
Y125F
S129A
S129D
S129G
C
% of inclusions on transfected cells
Without inclusions
< 5 inclusions
≥ 5-9 inclusions
≥ 10 inclusions
D
MW
ASYN
β-action
37 kDa
25 kDa
50 kDa
E
Syn/b-actin ratio (arbitrary units)

Figure 3. ASYN mutation effects in the inclusion formation. A. Constructs used in the aggregation model. This model consists of co-expressing SynT together with synphilin-1. B. Inclusion pattern in H4 cells. Different SynT mutants resulted in the formation of distinct inclusion formation in human H4 cells. Scale bar: 10 ㎜. C. Inclusion quantification..50 cells were scored per experiment and classified in different groups according to the pattern of inclusions. Representative cells were drawn to show type of inclusions present in each categories. Lysine mutants (E35K, E57K) increase the percentage of cells with inclusions and the number of inclusions per cell, whereas A30P and proline mutants reduce percentage of cells with inclusions and also the number of inclusions per cell. D-E. Levels of ASYN. Immunoblot analysis of the expression levels of ASYN. Student's t test (*p,0.05, **p,0.01, ***p,0.001). n = 3.
doi:10.1371/journal.pgen.1004741.g003

In order to characterize the structure of the ASYN inclusions formed in H4 cells, we used stimulated emission depletion (STED) super resolution microscopy (Fig. 6B). STED provided unprecedented access to the fine structure of the ASYN inclusions in the cytoplasm. We focused on selected mutants that displayed extreme patterns of aggregation (Fig. 3) and found that both smaller and larger inclusions are highly compact. For the TP mutant, only diffuse signal was detected, confirming the inability of this mutant to accumulate in inclusions that can be resolved by light microscopy techniques (Fig.6B).

It is widely established that LBs are primarily composed of amyloid filaments of ASYN [2]. To determine whether the inclusions formed by the different ASYN mutants were composed of amyloid-like fibrils, we used thioflavin S (thioS), a dye that binds specifically to amyloid-like structures [26,45]. We verified that large inclusions formed by WT or mutant ASYN stained positive for thioS, whereas small inclusions did not (Fig. 6C). Also, thioS stained the inner part of the inclusions (marked with arrow head) (Fig. 6C), suggesting the accumulation of mature amyloid-like structures in the inner part of the inclusions. To further characterize these different types of ASYN aggregates, we assessed the detergent solubility of the inclusions formed by the selected ASYN mutants. Interestingly, we observed that TP and E57K accumulated a smaller fraction of Triton X-100 insoluble ASYN species (Fig. 6D and E).

Intra- and extracellular partitioning of ASYN oligomers

To assess the effect of the selected mutations on the distribution of ASYN oligomers inside and outside cells, we used a previously described bioluminescent protein complementation assay (bPCA) that enables the detection of oligomeric species with great sensitivity [46]. In this assay, reconstitution of Gaussia princeps luciferase activity upon ASYN oligomerization was used as a readout [47] (Fig. 7A). Consistent with the results obtained with the Venus-based BiFC assay (Fig. 2A), we detected reconstitution of luciferase activity with all mutants tested. However, we observed a strong increase in intracellular (Fig. 7B) and extracellular (Fig. 7C) luciferase activity with the TP and Y125F ASYN mutants when compared to WT ASYN. This indicates that not only these mutations are able to promote increased formation of oligomers inside cells, but also in the extracellular space.

To determine if these mutants also promoted the release of oligomeric species we calculated the ratio of luciferase activity in the media compared to that in cells. Interestingly, we found that familiar mutants A30P and A53T showed an increased ratio of luciferase activity outside versus inside cells suggesting that these mutants also promote the secretion of ASYN oligomers (Fig. 7D). We confirmed these differences were not simply due to the accumulation of increased levels of mutant ASYN, since the levels of expression were identical for all mutants tested (Fig. 7E-F).

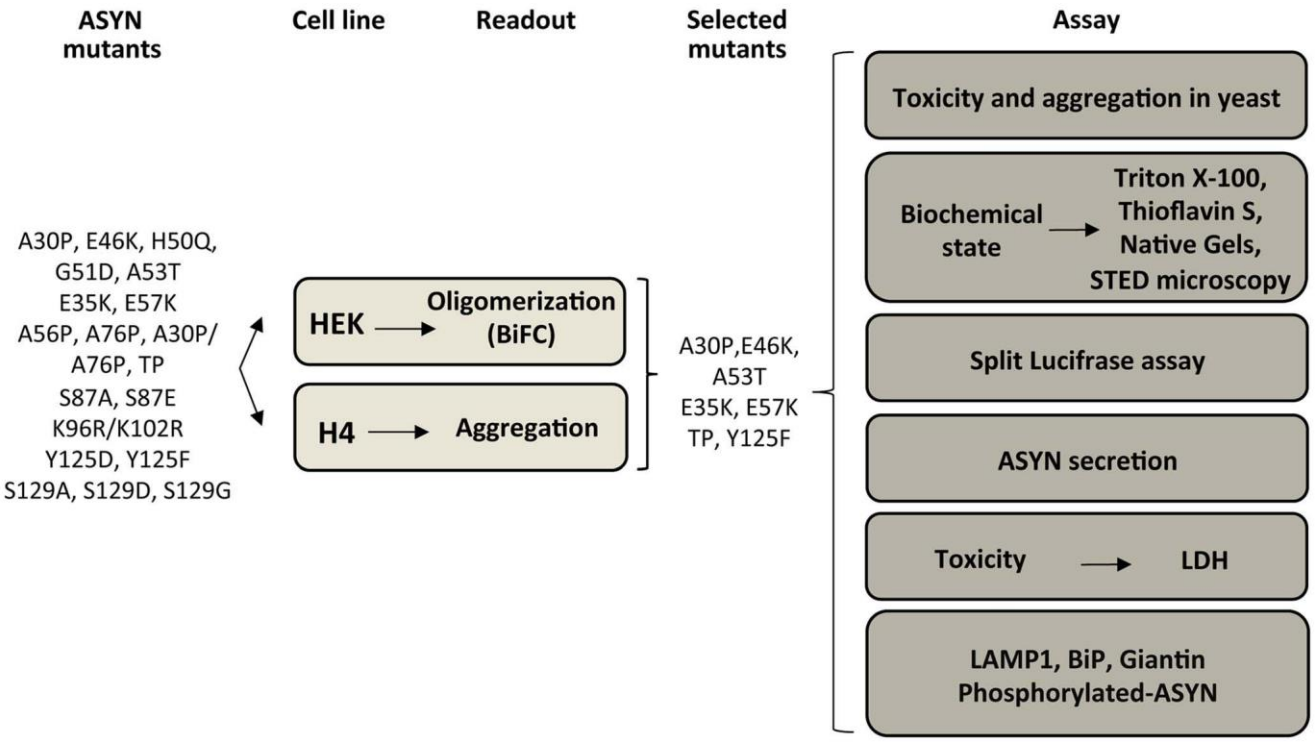

Figure 4. Experimental design. WT and ASYN mutants were subjected to a variety of assays as depicted in the schematic. doi:10.1371/journal.pgen.1004741.g004

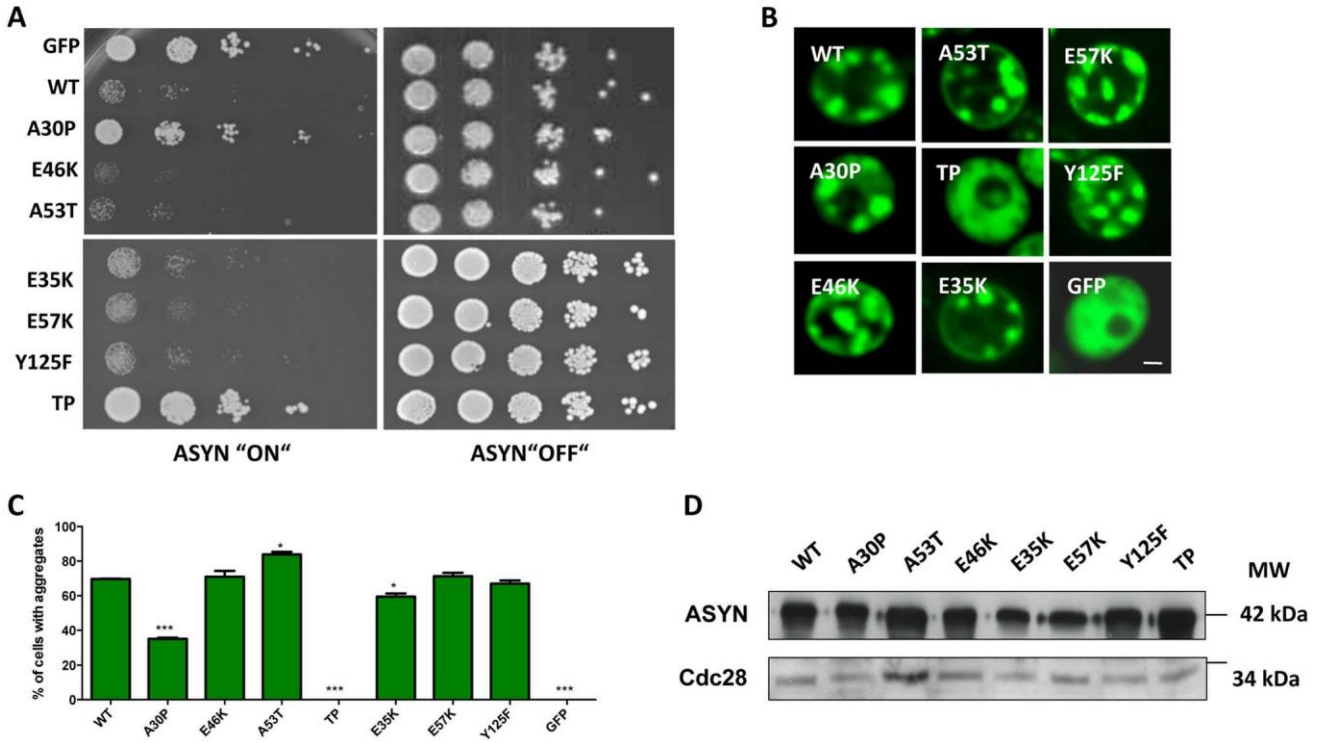

Figure 5. High-copy expression of a-synuclein-GFP variants in yeast. A. Yeast cells expressing GAL1-driven ASYN-GFP variants from 2 m plasmids were spotted in 10-fold dilutions on selection plates containing 2% glucose (control) or 2% galactose. After incubation for 3 days at 30uC the plates were photographed. Expression of GFP from the same promoter was used as a control. B. Live-cell fluorescence microscopy of yeast cells expressing ASYN-GFP. Yeast cells, pre-grown to mid-log phase, were induced in galactose-containing medium and examined for aggregates at 6 hours of induction. GFP-expressing cells were used as control. Scale bar: 1 mM. C. Aggregate quantification of yeast cells, expressing ASYN-GFP. For each strain, the number of cells displaying cytoplasmic foci is presented as percent of the total number of cells counted. For quantification of aggregation at least 300 cells were counted per strain and per experiment. GFP-expressing cells were used as a control. Student's t test (*p,0.05, **p,0.01, ***p,0.001). D. Protein levels of ASYN-GFP variants. Expression of ASYN-GFP variants was induced for 6 hours in galactose-containing medium. Equal amounts of crude protein extracts were used for Western analysis with anti-ASYN antibody and anti-cdc28 antibody as a loading control. n = 2.
doi:10.1371/journal.pgen.1004741.g005

ASYN secretion is inversely correlated with toxicity

ASYN is a cytosolic protein, but recent studies detected both monomeric and oligomeric forms of ASYN in human cerebrospi-nal fluid and plasma at low nanomolar concentrations, in both PD and control individuals [48,49].

To complement the observations with the bioluminescence complementation assay, we asked whether the selected ASYN mutants were differentially released from cells using the aggrega-tion paradigm described above (Fig. 3A). In this case, we measured the levels of ASYN in the culture medium using a highly sensitive electrochemiluminescence-based immunoassay [50]. We detected extracellular ASYN with all variants tested (Fig 8A).

Next, to demonstrate that the release of ASYN was not caused by membrane leakage from unhealthy or dying cells, we performed LDH toxicity measurements in the same media. In fact, in the aggregation paradigm, we observed an inverse correlation between ASYN release and cytotoxicity, where the TP and Y125F mutants appeared as the most toxic forms (Fig. 8B and C).

Effect of ASYN mutants on lysosomal degradation

Knowing that ASYN is predominantly degraded by lysosomal pathways and, therefore, requires intact lysosomal function, we used lysosomal associated membrane protein 1 (LAMP-1) as a marker to establish the relationship with aggregation formation. We observed that LAMP-1 partially co-localized with ASYN inclusions (Fig. 9A), suggesting that at least some types of inclusions might be degraded in lysosomes. Interestingly, we observed that some inclusions formed by two of the mutations that primarily accumulated thioS-negative inclusions (E57K and Y125F, Fig. 6B) stained positive for LAMP-1 at the periphery (Fig. 9B), reinforcing the idea that specific types of ASYN inclusions are degraded in lysosomes.

Golgi fragmentation and ER stress

Given that fragmentation of Golgi apparatus (GA) has been described in several neurodegenerative diseases [51,52,53], we next investigated the cellular consequences of the accumulation of ASYN oligomers or inclusions on this organelle. For this, we examined the morphological integrity of the GA using fluores-cence microscopy of cells immunostained for Giantin, an endogenous transmembrane protein of the cis and medial Golgi complex (Fig. 10). We defined three types of Golgi structures (non-fragmented, diffuse and fragmented). In general, we observed that in the ASYN oligomerization model there was an increased percentage of cells displaying fragmented Golgi, in comparison to what was observed in the aggregation model (Fig.10 A-B and Fig. S2). In particular, we found a statistically significant increase in the percentage of cells displaying fragmentation of the GA for the

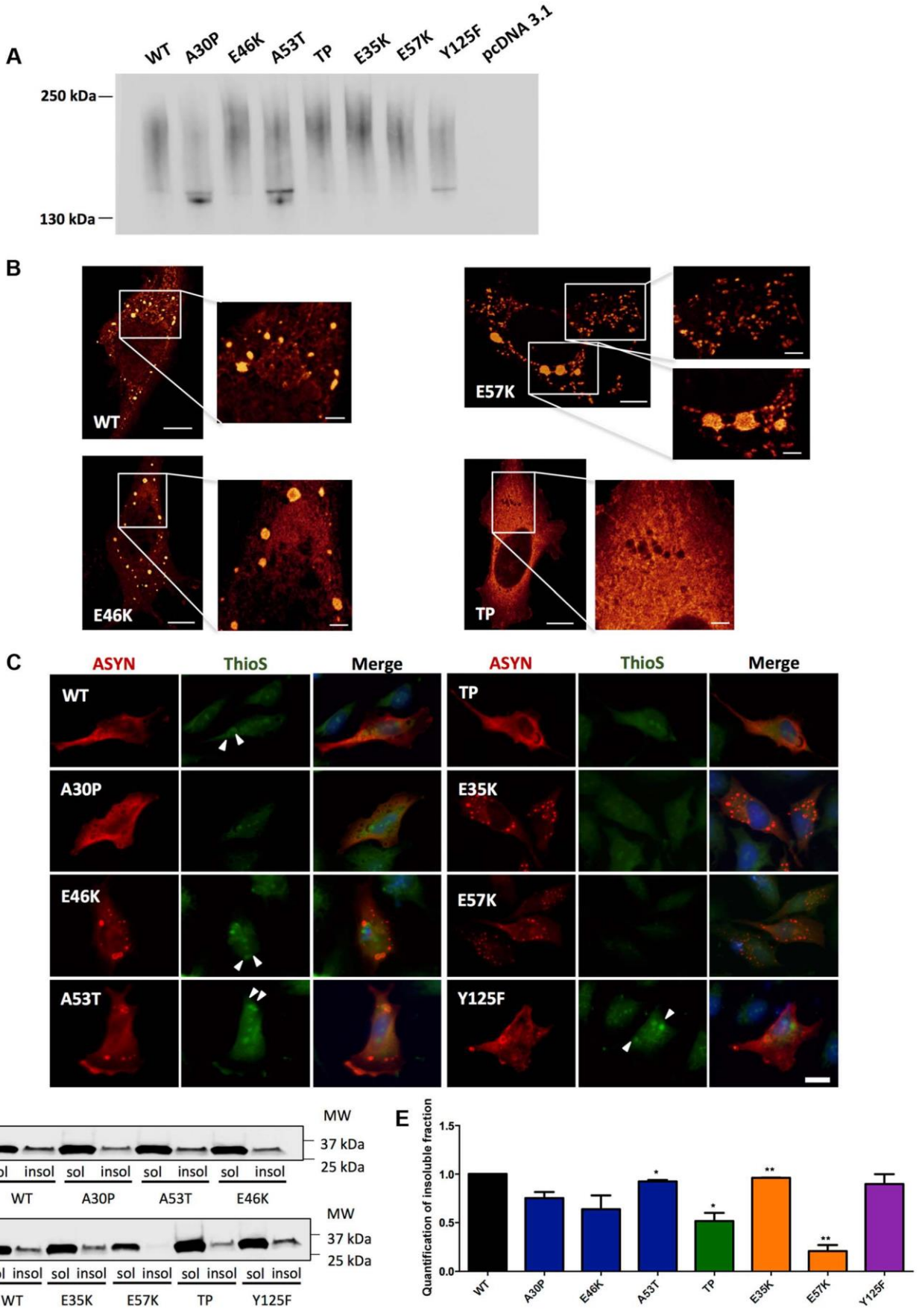
A
WT
A30P
E46K
A53T
TP
E35K
E57K
Y125F
pcDNA 3.1
250 kDa
130 kDa
B
WT
E57K
E46K
TP
C
ASYN
ThioS
Merge
WT
A30P
E46K
A53T
TP
E35K
E57K
Y125F
D
MW
37 kDa
25 kDa
sol insol sol insol sol insol sol insol
WT A30P A53T E46K
MW
37 kDa
25 kDa
sol insol sol insol sol insol sol insol sol insol
WT E35K E57K TP Y125F
E
Quantification of insoluble fraction
1.5
1.0
0.5
0.0
WT
A30P
E46K
A53T
TP
E35K
E57K
Y125F

Figure 6. ASYN biochemical state. A. Native Gels. Immunoblot analysis of native PAGE of cells transfected with the BiFC constructs in HEK 293 cells. Smears indicate the presence of oligomeric species of ASYN with different sizes. n = 2. B. STED microscopy. Selected mutants were imaged in order to characterize the fine structure of the inclusions. C. Thioflavin S staining. H4 cells expressing selected SynT mutants were incubated with ThioS in order to reveal beta sheet-rich structures. Some of the inclusions display amyloid-like properties, with increased staining in the inner part of the inclusions, indicated with arrow heads (c). Scale bar: 10 mm. D-E. Triton X-100 solubility assay and quantification. H4 cells show that all mutants form detergent insoluble species. Student's t test (*p,0.05, **p,0.01, ***p,0.001). n = 2. Quantification of insoluble fraction shows a decrease in TP and E57K mutants.
doi:10.1371/journal.pgen.1004741.g006

E35K and E57K mutants (Fig. 10A and Fig. S2A). In the ASYN aggregation paradigm, the GA displayed normal compact morphology near the nucleus (Fig. 10B and Fig. S2B).

Recent studies showed that endoplasmic reticulum (ER) stress, together with deficient protein degradation, plays a crucial role in the death of dopaminergic cells [54]. Under ER stress conditions, BiP is upregulated and preferentially binds to misfolded proteins in the ER [55]. We observed that oligomeric forms of ASYN promoted an increase in the levels of BiP (E46K and A53T mutants)(Fig.10C and D) whereas no differences were detected in the aggregation paradigm (Fig.10 E).

Taken together, these results suggest oligomeric forms of ASYN are more capable of promoting Golgi fragmentation and ER stress than aggregated forms.

Effect of mutations on ASYN phosphorylation

Accumulating evidence implicates phosphorylation on ASYN aggregation and toxicity [56]. However, it is unclear whether mutations in ASYN affect the typical pattern of phosphorylation. Using the oligomerization assay, we investigated whether ASYN was differentially phosphorylated on S129 (Fig. S3). Interestingly, we detected a significant increase in S129 phosphorylation in the E35K mutant, and only a trend towards an increase for the familial mutants and E57K (Fig. S3). The results shows that phosphorylation of ASYN on S129 is altered in the context of specific mutations known to affect the aggregation of the protein.

Discussion

Given the central role of ASYN in PD and other synucleino-pathies, and the uncertainty about the precise molecular mechanisms leading to neurodegeneration, we sought to take advantage of various cellular systems in order to systematically compare a set of ASYN mutants according to their effects on different cell functions.

Our systematic analysis enabled us to directly compare the effects of the selected mutations in terms of oligomerization and aggregation (Fig. 11). We observed that all 19 mutations tested enabled the formation of ASYN oligomers, as assessed by the BiFC system and biochemical methods. Interestingly, we found the different mutants resulted in the accumulation of different types of inclusions.

While we did not detect significant differences in the oligomer-ization induced by familial PD mutations, the A30P mutant displayed a reduced propensity to form inclusions, in contrast to the E46K and G51D mutants, which enhanced inclusion formation when compared with WT ASYN. The fact that we observed a decrease in the number of inclusions with the A30P might be related to the long-range contacts between the N and C-termini, shielding the central domain, which is known to promote aggregation, and reducing the formation of the same types of inclusions observed with WT or other mutants. On the other hand, the robust increase of inclusion formation observed with the E46K mutant might be due to the location of the mutation within the KTKEGV repeats that are involved in alpha-helix formation [57]. The charge difference introduced by the mutation could enhance the destabilization of the protein structure, leading to an increased propensity to aggregate, as reported previously [57]. Recent studies showed that the G51D mutation attenuates aSyn aggregation *in vitro* [58,59]. However, we observed a different trend in our cell models, where G51D increased the number of aSyn inclusions per cell, as observed with the E46K mutant. This might be explained by differences in the cellular environment in the different models, but might also be due to the presence of synphilin-1 in the particular model we used for aSyn aggregation. The same might apply to the H50Q mutant since, in contrast to other studies, we did not observe any difference in comparison to WT aSyn [59]. For the A53T mutant we found increased presence of oligomeric species in the nucleus, but no differences in terms of the aggregation pattern. Thus, additional studies on the effect of ASYN in the nucleus will be important.

The use of engineered mutants enables the exploration of the structural determinants of ASYN physiology in the cell. Artificial proline mutations were designed to impair fibrillization *in vitro* and promote the formation of soluble oligomers [40]. Indeed, in our cell models, the proline mutants resulted in increased oligomerization (Fig. 2B and C) and lowered the propensity to form inclusions. In particular, the TP mutant increased oligomer-ization as assessed by BiFC and bPCA, and reduced inclusion formation. These observations were also confirmed in yeast cells, where the A30P formed fewer inclusions, and the TP mutant completely blocked inclusion formation. However, in contrast to what was observed in primary neurons, worms, and in flies [40], the proline mutants failed to promote increased cytotoxicity in yeast cells. One possibility is that yeast process the species formed by the proline mutants in a distinct manner, explaining the lower levels of toxicity.

The lysine mutants (E35K and E57K) were designed to disrupt salt bridges between the b-strands of ASYN and to interfere with its binding to lipid membranes [41]. We found both mutants increased ASYN oligomerization and promoted distinct inclusion patterns. The lack of thioS staining suggests the inclusions may represent either off-pathway or immature species that cannot proceed towards the formation of mature amyloid-like inclusions. Interestingly, in cells where we could detect inclusions formed by the E57K mutant, these appeared surrounded by LAMP1, suggesting they were targeted to lysosomal degradation.

Post-translational modifications (PTMs) are important modula-tors of the structural and functional properties of proteins in health and pathological conditions. Several lines of evidence suggest that phosphorylation of ASYN may play an important role in regulating its aggregation, fibrillogenesis, Lewy body formation, and neurotoxicity *in vivo*. In addition, it appears that, *in vivo*, less than 5% of ASYN is normally phosphorylated [60] and that this occurs predominantly in the C-terminus (S129 and Y125) but also in the NAC domain (S87). However, there is still no consensus on the effects of phosphorylation due to existing contradictory results [56,61,62,63]. S87 is located in the NAC region, which is crucial for ASYN aggregation and fibrillogenesis [64] and is also the region involved in interactions with other proteins [62]. Our study supports the importance the NAC domain in the formation of ASYN inclusions, as the S87E phosphomimic mutant induced

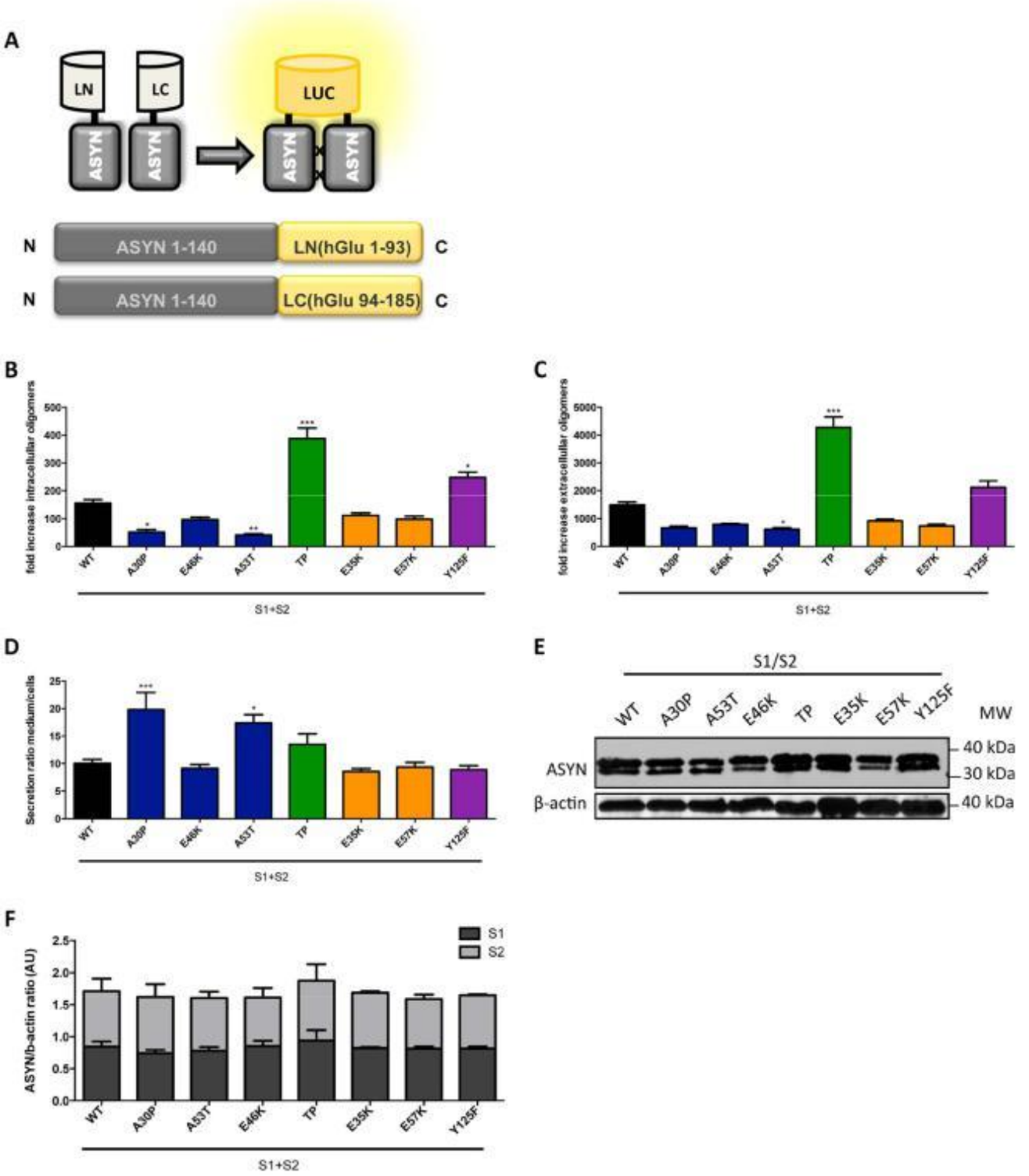

Figure 7. ASYN bPCA. A. Schematic representation of the ASYN bPCA constructs. Non-bioluminescent halves of humanized Gaussia luciferase (hGLuc) were fused to ASYN monomers. B-C. Intact cells (intracellular) and medium (extracellular) from H4 cells co-transfected with S1 and S2 were assayed for luciferase activity 48 hours post-transfection. Intracellular (B) and extracellular (C) TP displayed a 3-fold increase in luciferase activity compared to WT. n = 12. Student's t test (*p,0.05, **p,0.01, ***p,0.001) D. Ratio of luciferase activity in media compared to cells was expressed. n = 12, Student's t test (*p,0.05, **p,0.01, ***p,0.001) E-F. Levels of ASYN. Immunoblot analysis of the expression levels of ASYN showing similar levels. n = 3.
doi:10.1371/journal.pgen.1004741.g007

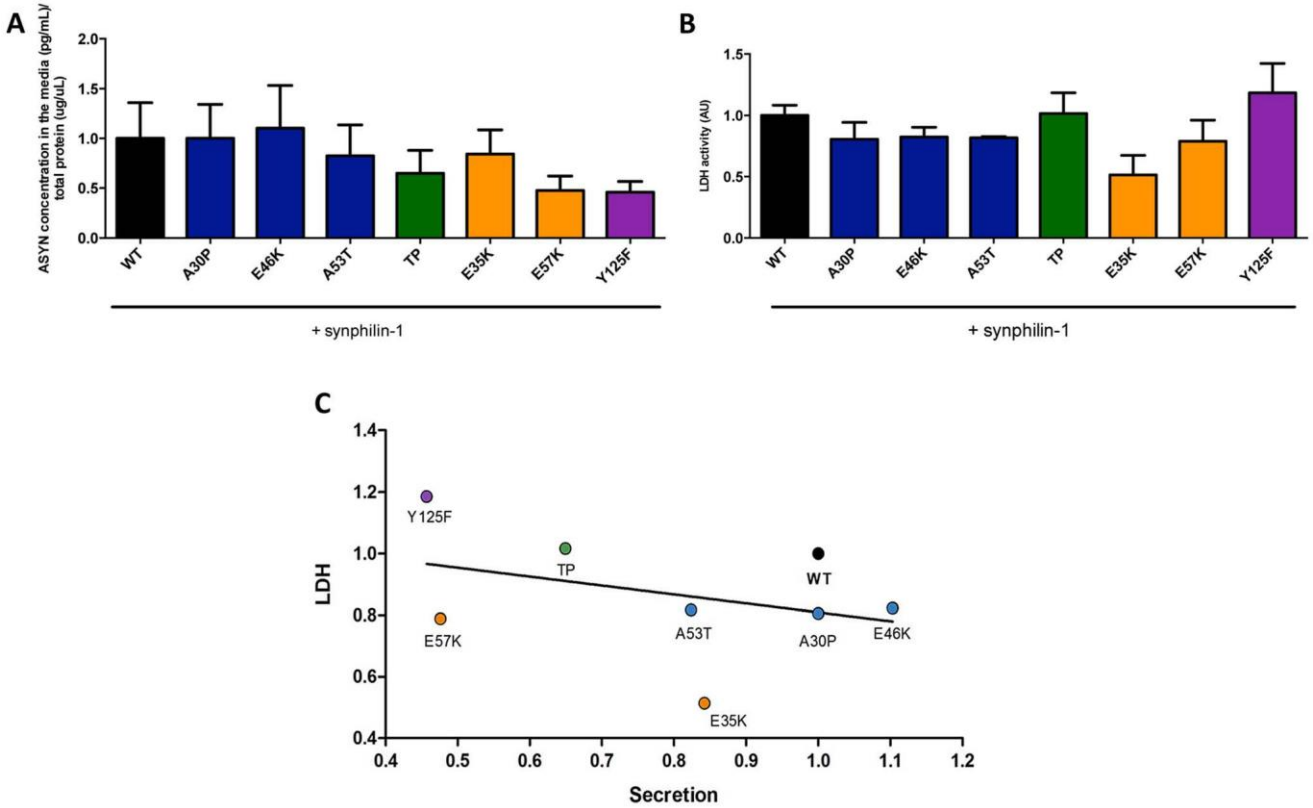

Figure 8. ASYN secretion is inversely correlated with toxicity. A. Secretion of ASYN. B. Toxicity measurements. Medium from H4 cells were collected to determine the secretion and the percentage cytotoxicity for each mutant. To measure the release of ASYN, an ELISA assay was performed. Using the same media we also measured the release of lactate dehydrogenase as a measure of cytotoxicity. We observed that these values were inversely correlated with those obtained in the release/secretion experiments. A decrease trend particularly for TP and Y125F detected in terms of secretion, was higher in toxicity. n = 3. C. Correlation between Secretion and Toxicity. The graph shows the inverse trend in secretion and toxicity.
doi:10.1371/journal.pgen.1004741.g008

different effects than those observed with the S87A mutant (Fig. 3B and C). This is in line with in vitro experiments where the S87E mutant inhibits ASYN aggregation [62]. Again, this effect on the formation of cytoplasmic inclusions might be attributed to changes in the conformation when binding to membranes, as other studies suggested [63]. Moreover, a recent study showed that S87E ASYN reduces aggregation and is less toxic [62].

Detecting significant levels of Y125-P in ASYN in human brain tissues has proven difficult [65]. Our results indicate, in the context of living cells, Y125-P ASYN exhibits similar aggregation properties to WT ASYN, in accordance with what was observed in other systems [65]. We also observed the accumulation of small inclusions for the Y125F mutant that were similar to those formed by the lysine mutants.

Recently, it was shown that when SUMO acceptor sites in ASYN (K96R/K102R) are modified, SUMOylation is strongly impaired, leading to increased inclusion formation and toxicity [38]. In our study, we observed only a 10% increase in the percentage of cells displaying inclusions and, interestingly, we observed the accumu-lation of smaller inclusions. These small inclusions promoted by several mutants tested (E35K, E57K, Y125F and SUMOylation mutants, Fig.3B) might represent intermediate species in the aggregation process of ASYN that fail to mature and may, therefore, lead to proteasomal impairment. To gain insight into the cellular consequences of different types of ASYN accumulations, we selected representative mutations for additional studies.

ASYN overexpression and/or aggregation can affect the secretory pathway. One of the consequences observed is the disruption of the Golgi and impairment ER-to-Golgi trafficking. Fragmentation of this organelle has been reported in neurode-generative disorders [51,52], including PD [53], and it was shown that it occurs in the cells accumulating prefibrillar ASYN aggregates [66]. Indeed, we observed the same trend in our study, where increased Golgi fragmentation was observed in the oligomerization model, particularly with E35K and E57K ASYN. Furthermore, we observed increased levels of BiP with familial mutants of ASYN in the oligomerization model. This was not detected in the aggregation model, further supporting the concept that oligomers are detrimental and disturb proteostasis by affecting the normal intracellular trafficking.

Autophagy is a catabolic process that is involved in the control of cellular damage in response to genetic perturbations, aging, and/or environmental toxins. Our study also underscores the interplay between ASYN inclusion formation and autophagy since we found the lysosomal marker LAMP-1 surrounding and concealing mature inclusions, as judged by thioS staining (Fig. 9B). Again, this reinforces the idea that aggregates per se might not be directly harmful to cells but, instead, might constitute an effort for cells to remove abnormal proteins from the cytoplasm.

Altogether, the systematic assessment of the effects of different ASYN mutations on its oligomerization and aggregation in cellular models allowed us to address, for the first time, the effect of the selected mutations on a panel of readouts that reflect important aspects of the biology/pathobiology of the protein. While additional studies using alternative models will be important to further dissect

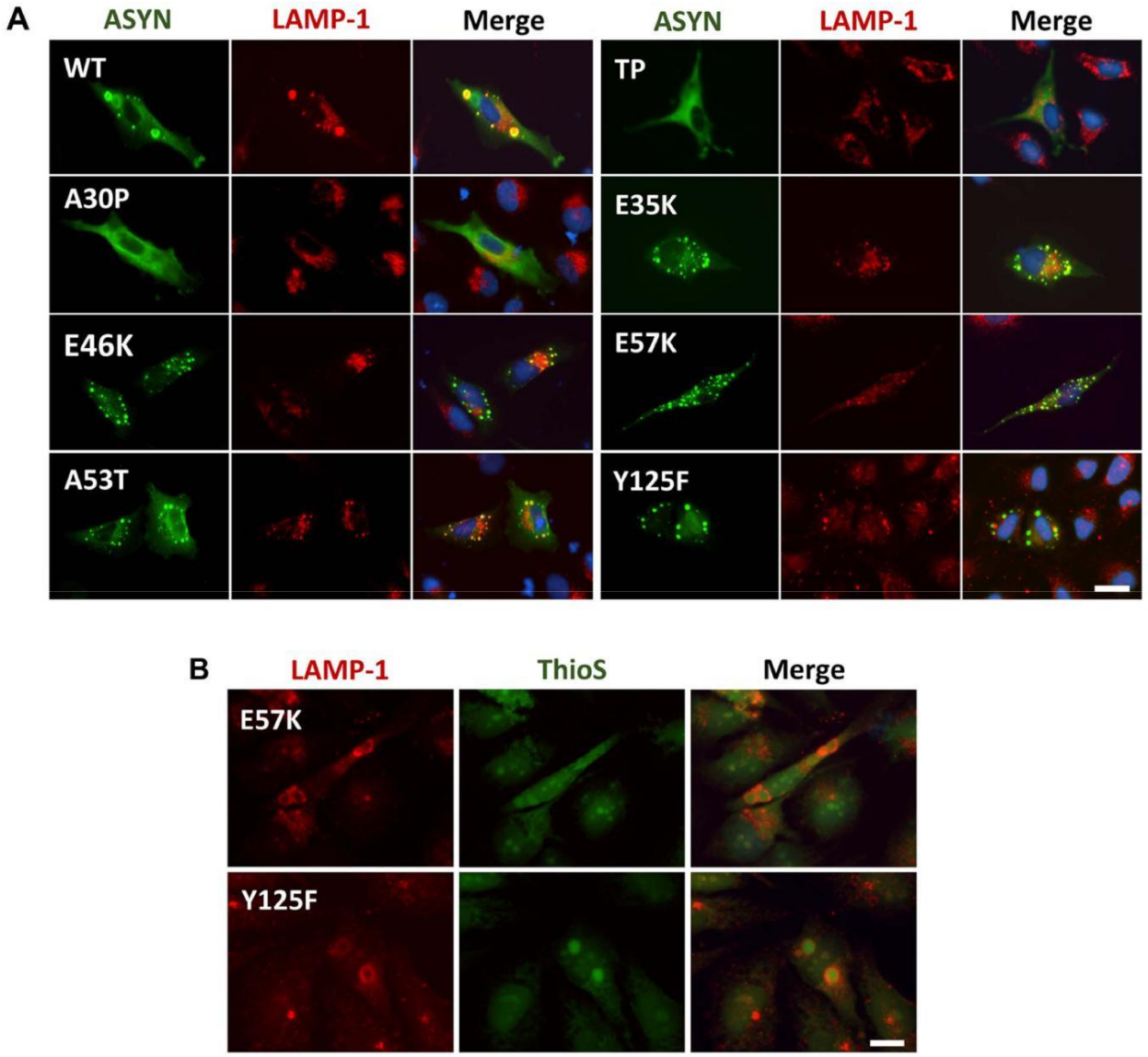

Figure 9. ASYN partially co-localizes with endosomes/lysosomes. A. Immunocytochemistry analysis of H4 cells expressing selected ASYN mutants. Partial co-localization of ASYN and LAMP1 suggests interplay between lysosomal degradation and ASYN inclusion formation. B. E57K and Y125F inclusions co-localize with lysosomal marker LAMP-1. We detected the presence of endosomes/lysosomes surrounding the aggregates in E57K and Y125F. This indicates that, maybe this could be the preferential via for degradation for these mutations. Scale bar: 10 mm. doi:10.1371/journal.pgen.1004741.g009

the effects of mutations, our study establishes the foundation for testing hypotheses that may open novel opportunities for the development of therapeutic strategies for synucleinopathies.

Materials and Methods

Primer design

The primers were designed according to the manufacturer's instructions using the QuickChange Primer Design Program and the web-based program Primer X (Table S1).

Generation of the mutant ASYN constructs

Site-directed mutagenesis using QuickChange II Site-Directed Mutagenesis Kit (Agilent Technologies, SC, USA) was performed following the manufacturer's instructions. Mutagenesis were performed in the plasmids encoding the ASYN-Venus BiFC system [42] or SynT [43] and confirmed by DNA sequencing. Also, fusion constructs ASYN-hGLuc1 (S1) and ASYN-hGLuc2 (S2) were generated as described previously [42].

Yeast plasmids expressing GFP (pME3759), human wild-type ASYN-GFP (pME3763), A30P-GFP (pME3764), A53T-GFP (pME3765) and TP-GFP (pME3942) from galactose-inducible promoter (GAL1) were described previously [67]. Plasmids harboring E46K-GFP (pME4085), E35K-GFP (pME4086), E57K-GFP (pME4087) and Y125F-GFP (pME4088) were gener-ated by site-directed mutagenesis using the same primers as above. Plasmid pME3763 was used as a template for generation of the desired amino acid substitutions.

Cell culture

Human neuroglioma cells (H4) were maintained in Opti-MEM I Reduced Serum Medium (Life Technologies- Gibco, Carlsbad,

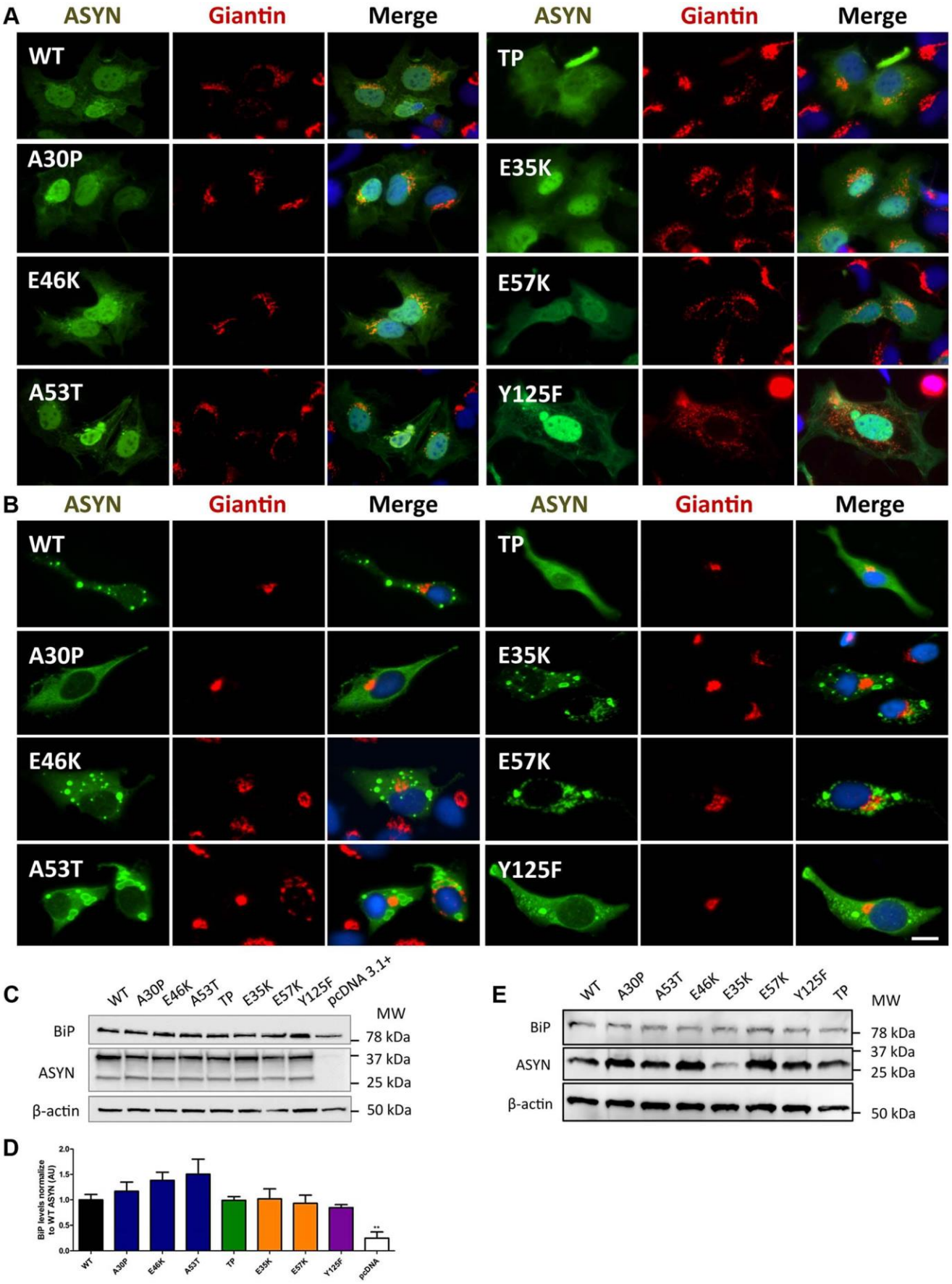
A
ASYN
Giantin
Merge
WT
TP
A30P
E35K
E46K
E57K
A53T
Y125F
B
C
WT
A30P
E46K
A53T
TP
E35K
E57K
Y125F
pcDNA 3.1+
MW
BiP
78 kDa
ASYN
37 kDa
25 kDa
β-actin
50 kDa
D
BiP levels normalize to WT ASYN (AU)
2.0
1.5
1.0
0.5
0.0
**
E

Figure 10. A-B morphology analysis of Golgi apparatus. The morphology of the Golgi apparatus in.50 cells was analysed and quantified. We observed that, in the BiFC assay, E35K and E57K mutants displayed increased Golgi fragmentation (A). In the aggregation model, Golgi morphology appeared normal, displaying a compact appearance near the nucleus (B). Levels of BiP in the oligomerization assay (C) and in the aggregation model (E), assessed by immunoblot analysis and respective quantifications (D and E). n = 3. Student's t test (*p,0.05, **p, 0.01, ***p,0.001).
doi:10.1371/journal.pgen.1004741.g010

CA, USA) and Human Embryonic Kidney 293 (HEK) cells were grown in Dulbecco's Modified Eagle Medium (DMEM, Life Technologies-Invitrogen, Carlsbad, CA, USA). Both media were supplemented with 10% Fetal Bovine Serum Gold (FBS) (PAA, Co¨lbe, Germany) and 1% Penicillin-Streptomycin (PAN, Aiden-bach, Germany). The cells were grown at 37uC in an atmosphere of 5% CO_2.

Cell transfection

HEK cells. The cells were plated in 24-well plates (Costar, Corning, New York, USA) the day before. Thirty minutes before the transfection the cells were incubated in Opti-MEM (Life Technologies-Invitrogen, Carlsbad, CA, USA) and subsequently transfected with equimolar amounts of the plasmids using Metafectene (Biotex, Munich, Germany) according to the manufacturer's instructions. Five hours after transfection, the medium was replaced. Twenty-four hours after transfection the cells were collected or stained for further analysis.

H4 cells. Twenty-four hours prior to transfection, the cells were plated in 35 cm dish (Ibidi, Munich, Germany) or in 12-well plates (Costar, Corning, New York, USA). Equal amount of the plasmids encoding ASYN and synphilin-1 were transfected using FuGENE6 Transfection Reagent (Promega, Madison, USA) in a ration of 1:3 according to the manufacturer's instructions. Forty-eight hours after the transfection, the media were collected and frozen for further experiments. Additional, cells were subjected to immunocytochemistry, for studying ASYN inclusions.

Gaussia luciferase protein-fragment complementation assay

For the bioluminescence complementation assay with ASYN-hGLuc1 (S1) and ASYN-hGLuc2 (S2) constructs, the cells were transfected as described above and conditioned media was collected 48 hours post-transfection and centrifuged for 5 minutes at 3000 g to eliminate floating cells before being used.

Forty-eight hours after transfection, culture media was trans-ferred to a new 96 well plate (Costar, Corning, NY, USA). Cells were washed with PBS and replaced with serum- and phenol-red free media. Luciferase activity from protein complementation was measured for conditioned media and live cells in an automated plate reader at 480 nm with a signal integration time of 2 seconds following the injection of the cell permeable substrate, Coelenter-azine (20 mM) (PJK, Kleinblittersdorf, Germany).

Yeast cell culture conditions

Yeast strain W303-1a (MATa; ura3-1; trp1D 2; leu2-3,112; his3-11,15; ade2-1; can1-100) was used for transformation performed by standard lithium acetate protocol. All strains were grown in Synthetic Complete medium lacking uracil (SC-Ura), supplemented with 2% raffinose or 2% galactose. ASYN expression was induced by shifting yeast cells cultured overnight in raffinose to galactose medium (OD600 = 0.1).

Overnight cultures of yeast strains were grown in SC-Ura medium containing 2% raffinose. For induction of the GAL1 promoter, cells were inoculated in SC-Ura medium containing 2%

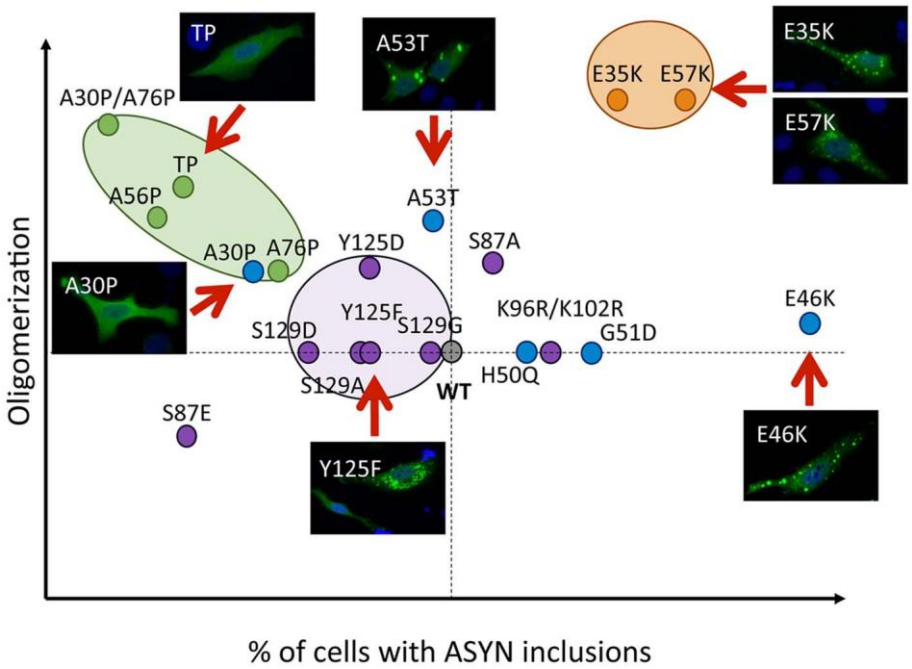

Figure 11. Correlation between the effects of ASYN mutations on oligomerization and inclusion formation. The graph depicts how mutations affect oligomerization and inclusion formation, enabling the selection of mutants with different effects. Values were attributed to ASYN mutations according to the results from the two models (oligomerization and inclusion formation) using WT ASYN as reference (center of the graph). doi:10.1371/journal.pgen.1004741.g011

galactose to an OD600 = 0.1 and incubated for 6 h. Cell extracts were prepared and the protein concentrations were determined with a Bradford assay. Immunoblotting was performed following standard procedures using anti-ASYN monoclonal antibody (AnaSpec, CA, USA) or Cdc28 polyclonal antibody (Santa Cruz Biotechnologies, Santa Cruz, CA, USA) as a loading control.

Spotting assays

To analyse cell growth on solid media, cultures were grown to mid-log phase in SC-Ura medium containing raffinose. Cells were normalized to equal densities, serially diluted 10-fold starting with an OD600 of 0.1, and spotted on SC-Ura plates containing either 2% glucose or 2% galactose. After 3 days incubation at 30uC the plates were photographed.

Fluorescence microscopy and quantifications of yeast cells

Yeast cell cultures were grown in SC-Ura medium containing 2% raffinose until mid-log phase and transferred to SC-Ura medium supplemented with 2% galactose. Expression was induced for 6 h and fluorescent images were obtained with Zeiss Observer. Z1 microscope equipped with CSU-X1 A1 confocal scanner unit (YOKOGAWA), QuantEM:512SC (Photometrics) digital camera and SlideBook 5.0 software package (Intelligent Imaging Innova-tions). For quantification of aggregation at least 300 cells were counted per strain and per experiment. For each strain, the number of cells displaying cytoplasmic foci was reported to the total number of cells counted and displayed as percentage on a column chart.

Immunocytochemistry

Twenty-four or forty-eight hours after transfection, cells (HEK or H4) were washed with PBS and fixed with 4% paraformal-dehyde (PFA) for 10 minutes at room temperature (RT), followed by a permeabilization step with 0.5% Triton X-100 (Sigma-Aldrich, St. Louis, MO, USA) for 20 minutes at RT. After blocking in 1.5% normal goat serum (PAA, Co¨lbe, Germany)/ DPBS for 1 hour, cells were incubated with primary antibody. Primary antibodies used were: mouse anti-ASYN (1:1000, BD Transduction Laboratory, New Jersey, USA) or rabbit anti-ASYN (1:1000, Abcam, Boston, USA), rabbit anti-LAMP-1 (1:1000, Abcam, Boston, USA), anti-Giantin (1:1000, Abcam, Boston, USA) for 3 hours or overnight and secondary antibody (Alexa Fluor 488 donkey anti-mouse IgG and/or Alexa Fluor 555 goat anti rabbit IgG, (Life Technologies-Invitrogen, Carlsbad, CA, USA) for 2 hours at RT. Finally, cells were stained with Hoechst 33258 (Life Technologies- Invitrogen, Carlsbad, CA, USA) (1:5000 in DPBS) for 5 minutes, and maintained in PBS for epifluorescence microscopy.

STED microscopy

For STED microscopy, H4 cells were plated in 15 mm coverslips. Forty-eight hours after transfection, the cells were washed with PBS and fixed with 4% PFA for 30 minutes at RT. The cells were rinse with quenching buffer (PBS +100 mM of Ammonium Chloride (Sigma-Aldrich, St. Louis, MO, USA)) for 15 minutes. After washing, the cells were permeabilized and blocked (2% BSA and 0.1% Triton X-100, in PBS) for 20 minutes. Cells were then incubated with primary antibodies against ASYN (1:2000, BD Transduction Laboratory, New Jersey, USA) in the permeabilization-blocking solution diluted 1:2 with PBS for 1 hour at RT. Finally, we incubated the cells with a secondary goat anti-mouse antibody labeled with Atto 647N (5 mg/mL; Sigma-Aldrich, St. Louis, MO, USA). STED images were taken with a Leica TCS STED system (Leica Microsystems) with a 100X oil objective (1.4 numerical aperture, NA, 1003 HCX PL APO CS oil; Leica Microsystems). For excitation, we used a 635 nm diode laser, and for the depletion donut (130 mW with the 1003 objective) we used a Spectra-Physics MaiTai multiphoton laser at 750 nm (Newport Spec- tra-Physics). Scans were performed at 1,000 Hz and the final images represent an average of 96 scans (STED) (average performed line-by-line) with the pinhole set at 47 mm. STED images were obtained at 20.20620.20 nm pixels.

Thioflavin S staining

After staining with secondary antibody, cells were incubated with freshly prepared 0.05% Thioflavin S (Sigma-Aldrich, St. Louis, MO, USA) for 5 minutes. Cells were then washed with 80% EtOH for 5 minutes and, finally, stained with Hoechst 33258, washed and maintained in PBS for fluorescence microscopy.

Quantification of nuclear and cytoplasmic fluorescence intensities

Nuclear and cytoplasmic fluorescence intensities were quanti-fied using ImageJ software (http://rsbweb.nih.gov/ij/). Using the freehand tool the nucleus and cytosol were selected and the respective intensities were measured. The results reflect the counting of 25 cells per experiment.

Quantification of ASYN inclusions

Transfected cells were detected and scored based on the ASYN inclusions pattern and classified into four groups: cells without inclusions, less than five inclusions (,5 inclusions), between five to nine inclusions ($5–9 inclusions) and more than ten inclusions ($ 10 inclusions). Results were expressed as the percentage of the total number of transfected cells obtained from three independent experiments for each mutation.

Quantification of Golgi fragmentation

Transfected HEK and H4 cells were scored based on the morphology of the Golgi apparatus and classified into three groups: non-fragmented, diffused and fragmented. Results were expressed as the percentage of the total number of transfected cells. Three independent experiments were performed.

Western blot analyses

HEK and H4 cells were lysed with Radio-Immunoprecipitation Assay (RIPA) lysis buffer (50 mM Tris pH 8.0, 0.15 M NaCl, 0.1% SDS, 1% NP40, 0.5% Na-Deoxycholate), 2 mM EDTA and a Protease Inhibitor Cocktail (1 tablet/10 mL) (Roche Diagnostics, Mannheim, Germany). To detect phosphorylated-ASYN was added Phosphatase Inhibitor Cocktail (1 tablets/10 mL) (Roche Diagnostics, Mannheim, Germany). Protein concentration was determined using the Bradford assay (BioRad Laboratories, Hercules, CA, USA) and the gels were loaded with 40 mg protein after denaturation for 10 minutes at 100uC in protein sample buffer (125 mM of 1 M Tris HCl pH 6.8, 4% SDS 0,5% Bromphenol blue, 4 mM EDTA 20% Glycerol 10% b-Mercapto ethanol).

The samples were separated on 12% SDS-polyacrylamide gels (SDS-PAGE) with a constant voltage of 110 V using Tris-Glycine SDS 0.5% running buffer (250 mM Tris, 200 mM Glycin, 1% SDS, pH 8.3) for 60 minutes.

The transfer was carried out to nitrocellulose membrane (Protran, Schleicher and Schuell, Whatman GmbH, Dassel,

Germany) for 90 minutes with constant current at 0.3 A using Tris-Glycine transfer buffer.

Membranes were blocked with 5% (w/v) skim milk (Fluka, Sigma-Aldrich, St. Louis, MO, USA) in 1xTBS-Tween (50 mM Tris, 150 mM NaCl, 0.05% Tween, pH 7.5) for 60 minutes at RT.

Membranes were further incubated with the primary antibody, either mouse anti-ASYN (1:1000, BD Biosciences, San Jose, CA, USA) or rabbit anti-ASYN (1:1000, Santa Cruz Biotechnologies, Santa Cruz, CA, US), anti-BiP (BD Biosciences, San Jose, CA, USA) and 1:1000 mouse anti-b-actin (Sigma-Aldrich, St. Louis, MO, USA) in 3% Albumin Bovine Fraction V (BSA)/TBS-Tween (NZYTech, Lisbon, Portugal), at RT for 3 hours or overnight at 4uC.

After washing three times in TBS-Tween for five minutes, the membranes were incubated for 1 hour with secondary antibody, anti-mouse IgG, or anti-rabbit IgG, horseradish peroxidase labeled secondary antibody (GE Healthcare, Bucks, UK) at 1:10000 in 3% milk/TBS-Tween.

Detection was done using Luminol Reagent and Peroxide Solution (Millipore, Billerica, MA, USA) and applied to the membrane 1 minute before scanning with in AlphaImager FluoroChem software (AlphaInnotech).

Protein levels were quantified using ImageJ and normalized to the b-actin levels.

H4 cells transfected with ASYN-hGLuc constructs were washed with cold PBS to remove excess cell culture media. Cell lysis buffer (20 mM NaCl, 0,6% Deoxycholate, 0,6% Igepal, 25 mM Tris pH 8.0, Protease Inhibitor Cocktail tablet, 1 tablet/10 mL) was added on human H4 cells in 60 mm dishes and incubated on ice for 10 minutes. After cell scraping samples were centrifuged for 10 minutes at 13,000 g. Lysates were resolved by electrophoresis on a 4–12% Bis-Tris gradient gel (NuPAGE Novex Bis-Tris Gel, Life Technologies, Darmstadt, Germany) according to manufacturer's instructions using NuPAGE MOPS buffer. After transfer to nitrocellulose membrane (Protran, Schleicher and Schuell, What-man GmbH, Dassel, Germany) membranes were blocked in 1x Roti Block (Roth, Carlsbad, Germany) for 1 hour at RT. The forward steps were similar as describe above.

Assessment of ASYN phosphorylation

The blots were directly removed from the blotting chamber and fixed in 0.4% PFA in PBS for 30 minutes. The membranes were briefly boiled in PBS, washed very short in TBS-Tween with phosphatase inhibitor (25 mM B-Glycerolphosphat, 5 mM NaF, 1 mM Na_3VO_4), and then were blocked in 5% BSA/TBS-Tween with phosphatase inhibitor for at least 1 hour (in the cold room). Anti-S129 phosphorylation ASYN 1:1000, WAKO, Richmond, Virginia, USA) was prepared in 5% BSA/TBS-Tween with phosphatase inhibitor and incubated overnight in the cold room. After washing tree times with TBS-Tween with phosphatase inhibitor for 10 minutes, the membranes were incubated with secondary antibody (anti-mouse IgG) for 1,5 hours at RT. Finally they were washed and revealed as previously described.

Native PAGE

For native PAGE, samples were lysed with detergent-free lysis buffer (50 mM Tris HCl pH 7.4, 175 mM NaCl, 5 mM EDTA pH 8.0 and Protease Inhibitor Cocktail tablet, 1 tablet/10 mL). Native-PAGE was run with detergent-free Tris-Glycine running buffer (250 mM Tris and 200 mM Glycin) and in protein sample buffer (1 M Tris HCl pH 6.8, Glycerol 100%, 0,4% Bromophenol blue).

Detergent solubility experiments

The H4 cells were plated and transfected as previously describe. Using 80 mL lysing buffer 1 (25 mM Tris pH 7.5, 150 mM NaCl, 1 mM EDTA, 1% Triton X-100, K tablet of EDTA Protease Inhibitor) the cells were harvested and centrifuged at 100.000 g for 30 minutes at 4uC. Supernatants were collected (soluble fraction) and the pellets (insoluble fraction) were washed with cold PBS and transferred to new tubes.

Once again, the samples were centrifuged at 14.000 rpm for 10 minutes at 4uC and the pellets were resuspended in 50 mL lysing buffer 2 (75 mM Tris pH 6.8, 3% SDS, 15% Glycerin, 3.75 mM EDTA pH 7.4). Finally, the samples were sonicated (10 pulse/ second) and a western blot was run as previously described.

The $\frac{\text{insoluble}}{\text{insoluble fraction}}$ fraction was calculated as: insoluble fraction z soluble fraction and then normalized for ASYN WT.

Flow cytometry

HEK cells were plated and imaged after twenty-four hours, as described above. Then, cells were trypsinized, neutralized with growth medium, centrifuged (1500 g at 5uC) and the pellet was reconstituted in 7-aminoactinomycin D (7-AAD, Life Technolo-gies- Invitrogen, Carlsbad, CA, USA) prepared 1:1000 in PBS. The fluorescence was measured using a microcapillary system (GuavaeasyCyte HT system, Millipore). 25000 events were counted per sample.

ASYN levels in the culture medium

A detailed description of the assay procedure has been published before [50]. [50]96-well Multi-Array standard plates (Meso Scale Discovery, Gaithersburg, MD, USA) were coated with 30 ml of MJF1 clone 12.1 (kindly provided by Liyu Wu, Epitomics, Burlingame, CA, USA) as capture antibodies at 3 mg/ ml dissolved in PBS buffer and incubated overnight at 4uC without shaking. All washing steps were done three times with 150 ml PBS-T (PBS supplemented with 0.05% Tween-20). After washing away the capture antibodies plates were blocked with 1% BSA/PBS-T for 1 h at RT with shaking at 300 rpm. Standards and biosamples collected from H4 cells were diluted in 1% BSA/PBS-T and applied in 25 ml volumes. Incubation was done for 1 h (RT, 700 rpm). Plates were washed again and 25 ml Sulfo-TAG labelled ASYN (BD Biosciences, Heidelberg, Germany) were applied at 1 mg/ml. After a final washing 150 ml 2x Read Buffer T (MSD) were applied to the wells and plates were read in a Sector Imager 6000 (MSD).

Toxicity assays – LDH release

For lactate dehydrogenase (LDH) cytotoxicity assay (Roche Diagnostics, Mannheim, Germany) the reaction mixture were prepared according to the manufacturer. The growth media from H4 cells were plated in triplicates in a 96 well plate, in a ratio 1:1 with the reaction mixture. The absorbance measurements were performed in a TECAN Infinite 200 Pro plate reader at 490 nm. To determine the percentage cytotoxicity, the average absorbance values were subtracted with the average absorbance value obtained in the background control. The percentage of toxicity was calculated as indicated by the manufacturer.

Statistical analyses

Data were analysed using GraphPad Prism 5 (San Diego California, USA) software and were expressed as the mean 6 SEM of at least three independent experiments. The values of

ASYN mutations from flow cytometry were normalized to WT ASYN and mean values for each experiment were determined. Statistical differences from WT ASYN were calculated using unpaired Student t-test. Significance was assessed for p#0.05, where * corresponds to p#0.05, ** corresponds to p#0.01 and *** corresponds to p#0.001.

Supporting Information

Table S1 Primers used in the site directed mutagenesis. Primer used to performed site-directed mutagenesis and generated all the mutants versions of ASYN used in this study.
(PDF)

Table S2 Summary of the effects of the mutations on ASYN oligomerization and aggregation. The table resume the effects that each mutation had in the two systems analyze regarding the WT. In grey it is highlight the mutations that we used for further analysis.

(PDF)

Figure S1 Statistical analysis of ASYN inclusion formation. A. Cells without inclusions. B. Cells with less than five inclusions. C. Cells with more than 5 and less than 10 inclusions. D. Cells with more than ten inclusions. Student's t test (*p,0.05, **p,0.01, ***p,0.001). n = 3.
(PDF)

Figure S2 Morphological analysis of Golgi apparatus. A. Oligomerization paradigm B. Aggregation model paradigm. Student's t test (*p,0.05, **p,0.01, ***p,0.001). n = 3.
(PDF)

Figure S3 Phosphorylation state of ASYN on S129. A-B Phosphorylation of ASYN in the BiFC assay. E35K and E57K showed an increase of S129 ASYN phosphorylation. Student's t test (*p,0.05, **p,0.01, ***p,0.001). n = 3. B. Levels of ASYN S129 phosphorylation in the aggregation model.
(PDF)

Author Contributions

Conceived and designed the experiments: TFO KMD. Performed the experiments: DFL EFR RL HS KK BP NK TR. Analyzed the data: DFL EFR KK BP NK KMD TFO. Contributed reagents/materials/analysis tools: EG PG SOR BM GHB MDP TFO. Wrote the paper: DFL KMD BP NK MDP JK TFO.

References

1. Burre J, Sharma M, Tsetsenis T, Buchman V, Etherton MR, et al. (2010) Alpha-synuclein promotes SNARE-complex assembly in vivo and in vitro. Science 329: 1663–1667.
2. Spillantini MG, Schmidt ML, Lee VM, Trojanowski JQ, Jakes R, et al. (1997) Alpha-synuclein in Lewy bodies. Nature 388: 839–840.
3. Goedert M, Spillantini MG, Del Tredici K, Braak H (2013) 100 years of Lewy pathology. Nat Rev Neurol 9: 13–24.
4. de Rijk MC, Tzourio C, Breteler MM, Dartigues JF, Amaducci L, et al. (1997) Prevalence of parkinsonism and Parkinson's disease in Europe: the EURO-PARKINSON Collaborative Study. European Community Concerted Action on the Epidemiology of Parkinson's disease. J Neurol Neurosurg Psychiatry 62: 10–15.
5. Polymeropoulos MH, Lavedan C, Leroy E, Ide SE, Dehejia A, et al. (1997) Mutation in the alpha-synuclein gene identified in families with Parkinson's disease. Science 276: 2045–2047.
6. Kruger R, Kuhn W, Muller T, Woitalla D, Graeber M, et al. (1998) Ala30Pro mutation in the gene encoding alpha-synuclein in Parkinson's disease. Nat Genet 18: 106–108.
7. Zarranz JJ, Alegre J, Gomez-Esteban JC, Lezcano E, Ros R, et al. (2004) The new mutation, E46K, of alpha-synuclein causes Parkinson and Lewy body dementia. Ann Neurol 55: 164–173.
8. Singleton AB, Farrer M, Johnson J, Singleton A, Hague S, et al. (2003) alpha-Synuclein locus triplication causes Parkinson's disease. Science 302: 841.
9. Chartier-Harlin MC, Kachergus J, Roumier C, Mouroux V, Douay X, et al. (2004) Alpha-synuclein locus duplication as a cause of familial Parkinson's disease. Lancet 364: 1167–1169.
10. Ibanez P, Bonnet AM, Debarges B, Lohmann E, Tison F, et al. (2004) Causal relation between alpha-synuclein gene duplication and familial Parkinson's disease. Lancet 364: 1169–1171.
11. Farrer M, Kachergus J, Forno L, Lincoln S, Wang DS, et al. (2004) Comparison of kindreds with parkinsonism and alpha-synuclein genomic multiplications. Ann Neurol 55: 174–179.
12. Simon-Sanchez J, Schulte C, Bras JM, Sharma M, Gibbs JR, et al. (2009) Genome-wide association study reveals genetic risk underlying Parkinson's disease. Nat Genet 41: 1308–1312.
13. Nalls MA, Plagnol V, Hernandez DG, Sharma M, Sheerin UM, et al. (2011) Imputation of sequence variants for identification of genetic risks for Parkinson's disease: a meta-analysis of genome-wide association studies. Lancet 377: 641– 649.
14. Kiely AP, Asi YT, Kara E, Limousin P, Ling H, et al. (2013) alpha-Synucleinopathy associated with G51D SNCA mutation: a link between Parkinson's disease and multiple system atrophy? Acta Neuropathol 125: 753– 769.
15. Lesage S, Anheim M, Letournel F, Bousset L, Honore A, et al. (2013) G51D alpha-synuclein mutation causes a novel parkinsonian-pyramidal syndrome. Ann Neurol 73: 459–471.
16. Proukakis C, Dudzik CG, Brier T, MacKay DS, Cooper JM, et al. (2013) A novel alpha-synuclein missense mutation in Parkinson disease. Neurology 80: 1062–1064.
17. Khalaf O, Fauvet B, Oueslati A, Dikiy I, Mahul-Mellier AL, et al. (2014) The H50Q mutation enhances alpha-synuclein aggregation, secretion and toxicity. J Biol Chem 289: 21856–21876.
18. Marques O, Outeiro TF (2012) Alpha-synuclein: from secretion to dysfunction and death. Cell Death Dis 3: e350.
19. Lashuel HA, Overk CR, Oueslati A, Masliah E (2013) The many faces of alpha-synuclein: from structure and toxicity to therapeutic target. Nat Rev Neurosci
14: 38–48.
20. Conway KA, Lee SJ, Rochet JC, Ding TT, Williamson RE, et al. (2000) Acceleration of oligomerization, not fibrillization, is a shared property of both alpha-synuclein mutations linked to early-onset Parkinson's disease: implications for pathogenesis and therapy. Proc Natl Acad Sci U S A 97: 571–576.
21. Fredenburg RA, Rospigliosi C, Meray RK, Kessler JC, Lashuel HA, et al. (2007) The impact of the E46K mutation on the properties of alpha-synuclein in its monomeric and oligomeric states. Biochemistry 46: 7107–7118.
22. Goncalves S, Outeiro TF (2013) Assessing the Subcellular Dynamics of Alpha-synuclein Using Photoactivation Microscopy. Mol Neurobiol 47: 1081–1092.
23. Outeiro TF, Lindquist S (2003) Yeast cells provide insight into alpha-synuclein biology and pathobiology. Science 302: 1772–1775.
24. Cai H, Reinisch K, Ferro-Novick S (2007) Coats, tethers, Rabs, and SNAREs work together to mediate the intracellular destination of a transport vesicle. Dev Cell 12: 671–682.
25. Murphy DD, Rueter SM, Trojanowski JQ, Lee VM (2000) Synucleins are developmentally expressed, and alpha-synuclein regulates the size of the presynaptic vesicular pool in primary hippocampal neurons. J Neurosci 20: 3214–3220.
26. Klucken J, Poehler AM, Ebrahimi-Fakhari D, Schneider J, Nuber S, et al. (2012) Alpha-synuclein aggregation involves a bafilomycin A 1-sensitive autophagy pathway. Autophagy 8: 754–766.
27. Hernandez-Vargas R, Fonseca-Ornelas L, Lopez-Gonzalez I, Riesgo-Escovar J, Zurita M, et al. (2011) Synphilin suppresses alpha-synuclein neurotoxicity in a Parkinson's disease Drosophila model. Genesis 49: 392–402.
28. Bonini NM, Giasson BI (2005) Snaring the function of alpha-synuclein. Cell 123: 359–361.
29. Vekrellis K, Xilouri M, Emmanouilidou E, Rideout HJ, Stefanis L (2011) Pathological roles of alpha-synuclein in neurological disorders. Lancet Neurol
10: 1015–1025.
30. McDowell K, Chesselet MF (2012) Animal models of the non-motor features of Parkinson's disease. Neurobiol Dis 46: 597–606.
31. Low K, Aebischer P (2012) Use of viral vectors to create animal models for Parkinson's disease. Neurobiol Dis 48: 189–201.
32. Bezard E, Przedborski S (2011) A tale on animal models of Parkinson's disease. Mov Disord 26: 993–1002.
33. Fujiwara H, Hasegawa M, Dohmae N, Kawashima A, Masliah E, et al. (2002) alpha-Synuclein is phosphorylated in synucleinopathy lesions. Nat Cell Biol 4: 160–164.
34. Okochi M, Walter J, Koyama A, Nakajo S, Baba M, et al. (2000) Constitutive phosphorylation of the Parkinson's disease associated alpha-synuclein. J Biol Chem 275: 390–397.

35. Paleologou KE, Schmid AW, Rospigliosi CC, Kim HY, Lamberto GR, et al. (2008) Phosphorylation at Ser-129 but not the phosphomimics S129E/D inhibits the fibrillation of alpha-synuclein. J Biol Chem 283: 16895–16905.
36. Taschenberger G, Garrido M, Tereshchenko Y, Bahr M, Zweckstetter M, et al. (2012) Aggregation of alphaSynuclein promotes progressive in vivo neurotoxicity in adult rat dopaminergic neurons. Acta Neuropathol 123: 671–683.
37. Dorval V, Fraser PE (2006) Small ubiquitin-like modifier (SUMO) modification of natively unfolded proteins tau and alpha-synuclein. J Biol Chem 281: 9919– 9924.
38. Krumova P, Meulmeester E, Garrido M, Tirard M, Hsiao HH, et al. (2011) Sumoylation inhibits alpha-synuclein aggregation and toxicity. J Cell Biol 194: 49–60.
39. Shults CW (2006) Lewy bodies. Proc Natl Acad Sci U S A 103: 1661–1668.
40. Karpinar DP, Balija MB, Kugler S, Opazo F, Rezaei-Ghaleh N, et al. (2009) Pre-fibrillar alpha-synuclein variants with impaired beta-structure increase neurotoxicity in Parkinson's disease models. EMBO J 28: 3256–3268.
41. Winner B, Jappelli R, Maji SK, Desplats PA, Boyer L, et al. (2011) In vivo demonstration that alpha-synuclein oligomers are toxic. Proc Natl Acad Sci U S A 108: 4194–4199.
42. Outeiro TF, Putcha P, Tetzlaff JE, Spoelgen R, Koker M, et al. (2008) Formation of toxic oligomeric alpha-synuclein species in living cells. PLoS ONE 3: e1867.
43. McLean PJ, Kawamata H, Hyman BT (2001) Alpha-synuclein-enhanced green fluorescent protein fusion proteins form proteasome sensitive inclusions in primary neurons. Neuroscience 104: 901–912.
44. Tenreiro S, Munder MC, Alberti S, Outeiro TF (2013) Harnessing the power of yeast to unravel the molecular basis of neurodegeneration. J Neurochem 127: 438–452.
45. Lee HJ, Lee SJ (2002) Characterization of cytoplasmic alpha-synuclein aggregates. Fibril formation is tightly linked to the inclusion-forming process in cells. J Biol Chem 277: 48976–48983.
46. Danzer KM, Ruf WP, Putcha P, Joyner D, Hashimoto T, et al. (2011) Heat-shock protein 70 modulates toxic extracellular alpha-synuclein oligomers and rescues trans-synaptic toxicity. FASEB J 25: 326–336.
47. Remy I, Michnick SW (2006) A highly sensitive protein-protein interaction assay based on Gaussia luciferase. Nat Methods 3: 977–979.
48. Borghi R, Marchese R, Negro A, Marinelli L, Forloni G, et al. (2000) Full length alpha-synuclein is present in cerebrospinal fluid from Parkinson's disease and normal subjects. Neurosci Lett 287: 65–67.
49. El-Agnaf OM, Salem SA, Paleologou KE, Cooper LJ, Fullwood NJ, et al. (2003) Alpha-synuclein implicated in Parkinson's disease is present in extracellular biological fluids, including human plasma. FASEB J 17: 1945–1947.
50. Kruse N, Schulz-Schaeffer WJ, Schlossmacher MG, Mollenhauer B (2012) Development of electrochemiluminescence-based singleplex and multiplex assays for the quantification of alpha-synuclein and other proteins in cerebrospinal fluid. Methods 56: 514–518.
51. Gonatas NK, Stieber A, Gonatas JO (2006) Fragmentation of the Golgi apparatus in neurodegenerative diseases and cell death. J Neurol Sci 246: 21–30.
52. Fan J, Hu Z, Zeng L, Lu W, Tang X, et al. (2008) Golgi apparatus and neurodegenerative diseases. Int J Dev Neurosci 26: 523–534.
53. Fujita Y, Ohama E, Takatama M, Al-Sarraj S, Okamoto K (2006) Fragmentation of Golgi apparatus of nigral neurons with alpha-synuclein-positive inclusions in patients with Parkinson's disease. Acta Neuropathol 112: 261–265.
54. Holtz WA, O'Malley KL (2003) Parkinsonian mimetics induce aspects of unfolded protein response in death of dopaminergic neurons. J Biol Chem 278: 19367–19377.
55. Hetz C (2012) The unfolded protein response: controlling cell fate decisions under ER stress and beyond. Nat Rev Mol Cell Biol 13: 89–102.
56. Chen L, Feany MB (2005) Alpha-synuclein phosphorylation controls neurotoxicity and inclusion formation in a Drosophila model of Parkinson disease. Nat Neurosci 8: 657–663.
57. Pandey N, Schmidt RE, Galvin JE (2006) The alpha-synuclein mutation E46K promotes aggregation in cultured cells. Exp Neurol 197: 515–520.
58. Fares MB, Ait-Bouziad N, Dikiy I, Mbefo MK, Jovicic A, et al. (2014) The novel Parkinson's disease linked mutation G51D attenuates in vitro aggregation and membrane binding of alpha-synuclein, and enhances its secretion and nuclear localization in cells. Hum Mol Genet 23: 4491–4509.
59. Rutherford NJ, Moore BD, Golde TE, Giasson BI (2014) Divergent effects of the H50Q and G51D SNCA mutations on the aggregation of alpha-synuclein. J Neurochem. E-pub ahead of print. doi:10.1111/jnc.12806
60. Trexler AJ, Rhoades E (2010) Single molecule characterization of alpha-synuclein in aggregation-prone states. Biophys J 99: 3048–3055.
61. Chen L, Periquet M, Wang X, Negro A, McLean PJ, et al. (2009) Tyrosine and serine phosphorylation of alpha-synuclein have opposing effects on neurotoxicity and soluble oligomer formation. J Clin Invest 119: 3257–3265.
62. Oueslati A, Paleologou KE, Schneider BL, Aebischer P, Lashuel HA (2012) Mimicking phosphorylation at serine 87 inhibits the aggregation of human alpha-synuclein and protects against its toxicity in a rat model of Parkinson's disease. J Neurosci 32: 1536–1544.
63. Paleologou KE, Oueslati A, Shakked G, Rospigliosi CC, Kim HY, et al. (2010) Phosphorylation at S87 is enhanced in synucleinopathies, inhibits alpha-synuclein oligomerization, and influences synuclein-membrane interactions. J Neurosci 30: 3184–3198.
64. El-Agnaf OM, Jakes R, Curran MD, Middleton D, Ingenito R, et al. (1998) Aggregates from mutant and wild-type alpha-synuclein proteins and NAC peptide induce apoptotic cell death in human neuroblastoma cells by formation of beta-sheet and amyloid-like filaments. FEBS Lett 440: 71–75.
65. Hejjaoui M, Butterfield S, Fauvet B, Vercruysse F, Cui J, et al. (2012) Elucidating the role of C-terminal post-translational modifications using protein semisynthesis strategies: alpha-synuclein phosphorylation at tyrosine 125. J Am Chem Soc 134: 5196–5210.
66. Gosavi N, Lee HJ, Lee JS, Patel S, Lee SJ (2002) Golgi fragmentation occurs in the cells with prefibrillar alpha-synuclein aggregates and precedes the formation of fibrillar inclusion. J Biol Chem 277: 48984–48992.
67. Petroi D, Popova B, Taheri-Talesh N, Irniger S, Shahpasandzadeh H, et al. (2012) Aggregate clearance of alpha-synuclein in S. cerevisiae depends more on autophagosome and vacuole function than on the proteasome. J Biol Chem 287: 27567–27579.

3.2. Small Molecules Detected by Second-Hamonic Generation Modulate the Conformation of Monomeric a-Synuclein and Reduce Its Aggregation in Cells

Ben Moree#, Guowei Yin#, **Diana F. Lázaro#**, Francesca Munari, Timo Strohaker§, Karin Giller, Stefan Becker, Tiago F. Outeiro, Markus Zweckstetter, and Joshua Salafsky.

#equal contribution

Experiments	Done by
Analysis of BIOD303 inhibition on a-synuclein inclusion formation in an H4 neuronal cell model, in Figure 7.	Diana F. Lázaro
Analysis of proteasome activity in H4 cells, in Figure 8	Diana F. Lázaro
Analysis of insoluble a-synuclein levels with BIOD303 in H4 cells, in Figure9	Diana F. Lázaro
All other experiment were performed by the other authors	

Status of the manuscript: published (J Biol Chem. 2015 Nov 13;290(46):27582-93.)

THE JOURNAL OF BIOLOGICAL CHEMISTRY VOL. 290, NO. 46, pp. 27582–27593, November 13, 2015
© 2015 by The American Society for Biochemistry and Molecular Biology, Inc. Published in the U.S.A.

Author's Choice

Small Molecules Detected by Second-Harmonic Generation Modulate the Conformation of Monomeric a-Synuclein and Reduce Its Aggregation in Cells*

Received for publication, September 2, 2015 Published, JBC Papers in Press, September 22, 2015, DOI 10.1074/jbc.M114.636027

Ben Moree[‡1], Guowei Yin[§1], Diana F. Lázaro[¶ 1], Francesca Munari[§], Timo Strohaker[§], Karin Giller[§], Stefan Becker[§], Tiago F. Outeiro[¶ 2], Markus Zweckstetter[§**2], and Joshua Salafsky[‡3]**

*From [‡]Biodesy, Inc., South San Francisco, California 94080, the [§]Max Planck Institute for Biophysical Chemistry, Am Fassberg 11, 37077 Go¨ttingen, Germany, the [¶]Center for Nanoscale Microscopy and Molecular Physiology of the Brain, University Medical Center, 37075 Go¨ttingen, Germany, the Department of Neurodegeneration and Restorative Research, University Medical Center Go¨ttingen, 37073 Go¨ttingen, Germany, and the **German Center for Neurodegenerative Diseases (DZNE), 37077 Go¨ttingen, Germany*

Background: *a*-Synuclein aggregation is associated with Parkinson disease.

Results: Small molecules were identified by second-harmonic generation (SHG) that change *a*-synuclein conformation *in vitro* and reduce the aggregation of protein in cells.

Conclusion: Conformation plays a role in *a*-synuclein aggregation in cells.

Significance: Small molecules that modulate the conformation of *a*-synuclein and reduce its aggregation could be developed into therapeutics for Parkinson disease.

Proteins are structurally dynamic molecules that perform specialized functions through unique conformational changes accessible in physiological environments. An ability to specifically and selectively control protein function via conformational modulation is an important goal for development of novel therapeutics and studies of protein mechanism in biological networks and disease. Here we applied a second-harmonic generation-based technique for studying protein conformation in solution and in real time to the intrinsically disordered, Parkinson disease related protein a-synuclein. From a fragment library, we identified small molecule modulators that bind to monomeric -synuclein *in vitro* and significantly reduce *a*-synuclein aggregation in a neuronal cell culture model. Our results indicate that the conformation of -synuclein is linked to the aggregation of protein in cells. They also provide support for a therapeutic strategy of targeting specific conformations of the protein to suppress or control its aggregation.

The regulation of protein activity and function through changes in protein conformation is a central theme in biology. Diverse biological processes such as enzyme catalysis, allostery, and protein-protein interactions are all governed by conforma-tional changes (1–3). Classical biochemical experiments on enzyme catalysis led to the development of the structure-function paradigm, whereby the structure of a protein determines its function (4, 5). However, this paradigm has been challenged by the discovery of intrinsically disordered proteins (IDPs)[4] (6, 7).

IDPs exist as a highly dynamic ensemble of conformations and thus do not populate a dominant and stable three-dimensional structure. IDPs as a class are estimated to comprise 15– 45% of all eukaryotic proteins and include both proteins that lack a folded structure as well as those that have disordered regions, such as loops and linkers, of greater than 30 amino acids in length (8). Although they are natively unstructured, IDPs may adopt secondary and tertiary structures upon binding ligands or other proteins (9).

The protein *a*-synuclein is a 140-residue IDP that is highly enriched in the brain (10). Although the precise cellular function of *a*-synuclein is not completely understood, it is thought to promote SNARE complex assembly and play a role in regulating synaptic vesicle levels and dopamine release at the pre-synaptic terminal (11–13). The aggregation and accumulation of *a*-synuclein in neurons is associated with a number of neurodegenerative diseases known as synucleinopathies. One such example is Parkinson disease (PD), which is a characterized by the progressive loss of dopaminergic neurons in the *substantia nigra* of the midbrain and by the presence of Lewy bodies, which are comprised mainly of aggregated *a*-synuclein fibrils (14). Mutations in *a*-synuclein have also been linked to both sporadic and rare forms of early onset PD, providing further evidence that the protein is implicated in the pathogenesis of

• This work was supported in part by Deutsche Forschungsgemeinschaft (DFG) Grant ZW 71/2-2,3-2 (to M. Z.) and in part by three Rapid Response Innovation Award grants (to J. S.) and Biodesy from the Michael J. Fox Foundation for Parkinson's Research. B. M. is an employee of Biodesy, Inc. J. S. is the Founder and Chief Scientific Officer of Biodesy, Inc.

Author's Choice—Final version free via Creative Commons CC-BY license.

1. These authors contributed equally to this manuscript.
2. Supported by the DFG Center for Nanoscale Microscopy and Molecular Physiology of the Brain.
3. To whom correspondence should be addressed: 384 Oyster Point Blvd., 8, South San Francisco, CA 94080. Tel.: 650-871-8716; E-mail: joshua. salafsky@biodesy.com.

[2] The abbreviations used are: IDP, intrinsically disordered protein; SHG, second-harmonic generation; PcTS, phthalocyanine tetrasulfonate; Ro3, rule of three; PD, Parkinson disease; PRE, paramagnetic relaxation enhancement; MTSL, oxy-2,2,5,5-tetramethyl-D-pyrroline-3-methyl)-methanethio-sulfonate; DMSO, dimethyl sulfoxide.

Downloaded from http://www.jbc.org/ by guest on October 9, 2016

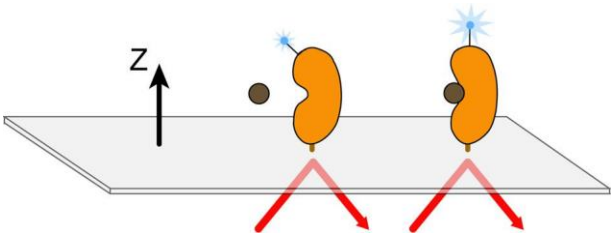

FIGURE 1. **Schematic of second-harmonic generation.** Incident laser light strikes the surface and through total internal reflection creates an evanescent wave that decays away from the surface. Labeled protein is bound to the surface and the SHG signal magnitude depends on the orientation of the dye label relative to the surface normal (*z* axis). A conformational change that re-orients the average, net orientation of the label toward or away from the normal results in a signal change.

the disease (15–18). *In vitro*, *a*-synuclein adopts a wide range of conformations from compact to fully extended (19 –21). Inter-actions between the N and C termini appear to stabilize the protein predominantly in a compact, monomeric conformation that is non-toxic (19). The process by which the protein proceeds from monomer to oligomers and fibrillar aggregates is currently the subject of intense scrutiny (22–24). Growing evidence suggests that oligomers of *a*-synuclein, formed prior to the larger aggregates found in the brains of patients with the disease, may be neurotoxic *in vivo* (20, 22). Irrespective of the toxic species, monomeric *a*-synuclein is an attractive therapeutic target for small molecules that modulate *a*-synuclein conformation as it is the most upstream form of the protein in the aggregation process. However, the intrinsic disorder of the pro-tein makes it difficult to screen by conventional techniques and few molecules are known to bind specifically to the protein (25–32).

To overcome the challenges associated with traditional small molecule screening of *a*-synuclein, we developed a novel sec-ond-harmonic generation (SHG)-based screen to identify com-pounds that directly modulate the conformation of monomeric *a*-synuclein. SHG is a nonlinear optical technique (33, 34) in which two photons of equal energy are combined by a nonlinear material or molecule to generate one photon with twice the energy. Because the intensity of the SHG signal is highly sensitive to the angular orientation of second-harmonic active molecules tethered to a surface, the technique can be applied to study structure and conformational changes. (35–38). Although biological molecules are not usually second-harmonic active, they can be rendered so through the incorporation of a second-harmonic active dye molecule (39). Once tethered to a surface, a labeled second-harmonic active protein irradiated by a fundamental light beam produces an SHG signal whose intensity depends sensitively on the tilt angle of the dye with respect to the surface (Fig. 1). The SHG intensity is the coherent superposition of scattered second-harmonic light orientationally averaged across the molecules in the irradiated ensemble. When the protein molecules undergo a conformational change upon ligand binding, this causes a change in the orientational distribution of the second-harmonic active moiety, leading to a change in the intensity of light. Changes in SHG intensity therefore correspond with high orientational sensitivity to conformational changes at the attachment site of the second-harmonic active probe. In addition, conformational changes can be classified by their response in both magnitude and direction relative to baseline (for a more detailed explanation of the theoretical background for SHG, please see the "Experimental Procedures").

In the study presented here, we used an SHG-based fragment screen to identify novel conformational modulators of *a*-synuclein. We subsequently used these modulators, which include a compound we named BIOD303 and its analogs, to probe the biological chemistry of monomeric *a*-synuclein. We demonstrate that these molecules bind to the protein by both SHG and NMR spectroscopy and by paramagnetic relaxation enhancement (PRE). We also show definitively by SHG that these molecules induce a conformational change in *a*-sy-nuclein. Finally, we demonstrate that these modulators reduce *a*-synuclein aggregation in a human neuronal cell model. Taken together, our results demonstrate that modulation of *a*-synuclein conformation by small molecules can significantly reduce the aggregation of the protein in cells. In addition, our results demonstrate that SHG can sensitively study the biolog-ical mechanism of ligand-protein interactions and enable the identification of novel ligands for drug discovery and basic research.

Experimental Procedures

a-Synuclein Purification and Labeling—A single-site cysteine mutant (A90C) of *a*-synuclein was constructed and labeled with the second-harmonic active dye SHG2-maleimide (thiol-reactive, available from Biodesy), and conjugated to the protein according to the manufacturer's instructions. The incorporation of a single label at A90C was confirmed by mass spectrometry.

SHG Instrumentation and Measurements—Our instrument comprises a mode-locked Ti:Sapphire oscillator, which pro-vides the fundamental beam necessary to generate the second-harmonic signal (high peak power). For these experiments, we used a Mira 900 Ti:Sapphire ultrafast oscillator (Coherent Inc., Santa Clara, CA) pumped by a Millenia V DPSS laser (Spectra-Physics Corp., Santa Clara, CA). The fundamental was passed through a half-wave plate to select *p*-polarization (used for all the experiments described here), and focused into a Dove prism for total internal reflection at a spot size of 100 *m*m. The second-harmonic light was collected by a lens, separated from the fundamental using a dichroic mirror and wavelength filters, and directed into a PMT module with a built-in pre-amplifier for photon counting (Hamamatsu, Bridgewater, NJ). A custom electronics board was used to digitize the signal and the data were sent to a computer running customized control and data collection software (Labview, National Instruments Corp., Austin, TX). For these experiments, a microscope slide with protein was coupled to a prism using BK7 index matching fluid (Cargille, Cedar Grove, NJ) and the prism itself was secured onto a one-dimensional translation stage capable of 1-*m*m randomly addressable precision (Renishaw, Parker-Hannifin Corp., Rohnert Park, CA). A silicone template defined 16 wells on each slide. Each of the 16 wells is read in sequence by translating the stage via the control software. The instrument was also outfitted with a single-channel liquid injector (Cavro,

Downloaded from http://www.jbc.org/ by guest on October 9, 2016

Tecan Systems, Inc., San Jose, CA) that delivered a liquid bolus (in the screening experiments, spermine).

α-Synuclein Assay Slide Preparation—A custom 2-mm thick silicone template with adhesive backing (Arrowleaf Research, Bend, OR) was applied to commercially available aldehyde derivatized glass microscope slides (Xenobind, Xenopore, Hawthorne, NJ). Each silicone template defined 16 wells whose spacing and diameter equals those of a standard 384-well plate format. Stock solutions of second-harmonic active dye-labeled *α*-synuclein were diluted to 5 *m*M final concentration (below the threshold for oligomer formation (40)) in PBS and allowed to adsorb to the glass surface in each well by incubating at room temperature for 30 min. After allowing the protein to adsorb, the slide was placed on the instrument and each well was scanned via SHG to determine the amount of signal in each well. Unbound protein was then removed by washing five times with 20 *m*l of PBS. A post-wash well scan was then performed.

Maybridge Library Screening—The Maybridge Rule of Three (Ro3) fragment library contains 1,000 pharmacophores of $95% purity that conform to the rule of three standard (molec-ular mass 300 Da, ClogP 3, and the number of hydrogen bond donor and acceptors 3) (41). Each compound has a stated solubility of up to 1 mM in PBS. Because fragments typically possess lower potency than larger compounds, they were screened at 1 mM final concentration. For screening experiments, each compound from the library was solubilized at 50 mM in DMSO and diluted in PBS to produce a final concentration of 2 mM (4% DMSO). Each compound (2 mM) was then injected into a well containing an equal volume of buffer to produce a final concentration of 1 mM compound in the well. To ensure that a buffer mismatch did not occur, the buffer used during screening was PBS 4% DMSO. The slide was then loaded onto the instrument stage, baseline signal was measured in real time, and spermine was injected at 5 mM while reading the SHG signal. In these experiments, baseline signals were monitored for 8 s, followed by spermine injection, and the SHG signal was recorded for an additional 8 s. For the screen, each well was loaded with 5 *m*M *α*-synuclein, washed out after binding to the surface, and preincubated with one compound from the Maybridge Ro3 library for 30 min at 1 mM. Spermine was then added to each well at 5 mM and the resulting change in SHG signal was measured. Compounds that inhibited the spermine-induced conformational change as measured by SHG were re-tested. A similar procedure was used to test the BIOD303 analogs.

Dose-response Curves—To measure the dose-response curves of spermine (Sigma) and BIOD303, serial dilutions of each con-centrated stock compound were prepared. Each compound was added to a well to produce the indicated final concentration. For spermine, the range of concentrations tested was 10 *m*M, 30 *m*M, 100 *m*M, 300 *m*M, 1 mM, 3 mM, and 10 mM. For BIOD303 the concentration range was 5 *m*M, 32.5 *m*M, 62.5 *m*M, 125 *m*M, 250 *m*M, 500 *m*M, and 1 mM. Concentrations were then converted to logarithmic scale and the percent change at each concentration was plotted in Prism (GraphPad Software, La Jolla, CA) using a non-linear regression fit for log (agonist) *versus* normalized response. The data were normalized so that the values for the lowest concentration and the highest concentration were set to 0 and 100%, respectively. EC_{50} values were calculated empirically using the software.

Compound Injections—BIOD303, spermine, spermidine, and phthalocyanine tetrasulfonate (PcTS, Sigma) were all freshly prepared as stock solutions at the indicated concentrations in PBS. Compounds from the Maybridge library were also pre-pared in PBS at the indicated concentrations. To determine the change in SHG signal that a given compound produced, the baseline signal of *α*-synuclein was measured for 10 s followed by compound injection. The change in SHG intensity was recorded for 90 s after compound addition. Where appropriate, the buffer was supplemented with DMSO to prevent buffer mismatch.

Quantifying Changes in SHG Intensity—Control experiments were performed on each compound to empirically determine the time required for each compound to produce a maximal response (t_{max}). For all experiments except those using PcTS the maximal response measured by SHG occurred within 30 s after compound addition. For the PcTS experiments, the maximal response occurred 45 s after compound addition. To calculate the percent change in SHG intensity (% SH), the sec-ond-harmonic intensity measured just prior to injection (I_{t0}) was subtracted from the second-harmonic intensity at t_{max} (I_{tmax}) and then divided by the initial second-harmonic inten-sity (I_{t0}) according to Equation 1.

$$\%\Delta_{SH} = (I_{t,max} - I_{t0})/I_{t0} \qquad \text{(Eq. 1)}$$

All experiments included a control buffer injection that was used to determine the threshold for SHG intensity change, which was calculated in a similar manner. The net SHG intensity change for each compound was then reported by subtracting the buffer threshold value from the SHG intensity value produced by compound addition. The resulting value was reported as the percent change in SHG intensity resulting from compound addition.

NMR Spectroscopy—NMR spectra were acquired at 15 °C on a Bruker Avance 600 NMR spectrometer using a triple-resonance cryoprobe equipped with *z* axis self-shielded gradient coils. *α*-Synuclein and BIOD303 or the analog compounds were dissolved in 50 mM HEPES, 100 mM NaCl buffer containing 2% DMSO. Low temperature (15 °C) inhibits the rate of aggregation of *α*-synuclein and ensures the species under study is in the monomeric form. *α*-Synuclein-ligand binding was measured using two-dimensional ^{1}H-^{15}N heteronuclear single quantum coherence experiments. Chemical shift perturbations $s^{1}H^{15}N$ were calculated according to $[(\Delta\sigma^{2}H)^{2} + (0.2\ \Delta\sigma^{15}N)^{2}]^{0.5}$, where $\Delta\sigma^{1}H$ and $\Delta\sigma^{15}N$ are the observed changes in the ^{1}H and ^{15}N dimensions. PRE was measured using spin-labeled A90C *α*-synuclein. Spin labeling with oxy-2,2,5,5-tetramethyl-D-pyrroline -3-methyl)- methanethio-sulfonate (MTSL, Toronto Research Chemicals, Toronto) was carried out as described (42). PRE effects were measured from the peak intensity ratios between two ^{1}H-^{15}N heteronuclear single quantum coherence spectra in the absence and presence of a 10-fold excess (compared with protein) of DTT. To exclude contributions from DMSO, the chemical shifts and PREs in the presence of ligand were compared with those observed upon

Downloaded from http://www.jbc.org/ by guest on October 9, 2016

addition of the same amount of DMSO without ligand. Data processing was performed using the software packages NMRPipe/NMRDraw (43), Topspin (Bruker), and Sparky (62).

Cell Culture—Human neuroglioma cells (H4) were maintained in Opti-MEM I Reduced Serum Medium (Life Technologies-Gibco) supplemented with 10% fetal bovine serum Gold (FBS) (PAA, Colbe, Germany) at 37 °C in an atmosphere of 5% CO_2.

Cell Transfection—H4 Cells were plated in 12-well plates (Costar, Corning, New York) 1 day prior to transfection. On the subsequent day, cells were transfected with FuGENE 6 Transfection Reagent (Promega, Madison, WI) according to the manufacturer's instructions with equal amounts of plasmids encoding a C terminally modified *a*-synuclein (SynT construct) and synphilin-1 as previously described (44 – 46). Twenty-four hours after the transfections, the cells were treated with different compounds at different concentrations (0, 10, 100, or 500 *m*M). DMSO was used as the vehicle. Twenty-four hours later the cells were subjected to immunocytochemistry to examine *a*-synuclein inclusion formation.

Immunocytochemistry—After transfection, cells were washed with PBS and fixed with 4% paraformaldehyde for 10 min at room temperature. Cells were then permeabilized with 0.5% Triton X-100 (Sigma) for 20 min at room temperature and blocked in 1.5% normal goat serum (PAA)/PBS for 1 h. Cells were then incubated for 3 h with mouse anti-ASYN primary antibody (1:1000, BD Transduction Laboratories, NJ), and afterward with a secondary antibody (Alexa Fluor 488 donkey anti-mouse IgG) for 2 h at room temperature. Finally, cells were stained with Hoechst 33258 (Life Technologies-Invitrogen) (1:5000 in PBS) for 5 min and maintained in PBS for epifluorescence microscopy.

Quantification of a-Synuclein Inclusions—Experiments were performed as previously described (44). Briefly, transfected cells were detected and scored based on the *a*-synuclein inclusions pattern and classified as presented. Results were ex-pressed as the percentage of the total number of transfected cells. A minimum of 50 cells were counted per condition.

Immunoblotting—Twenty-four hours after H4 cells co-ex-pressing *a*-synuclein (SynT) and synphilin-1 were treated with BIOD303, the cells were lysed with radioimmunoprecipitation assay (RIPA) lysis buffer (50 mM Tris, pH 8.0, 0.15 M NaCl, 0.1% SDS, 1% Nonidet P-40, 0.5% sodium deoxycholate), 2 mM EDTA and a protease inhibitor mixture (1 tablet/10 ml, Roche Diagnostics, Mannheim, Germany). Using the Bradford assay (Bio-Rad Laboratories), the protein concentration was deter-mined and the gels were loaded with 30 *m*g of protein. The samples were denatured for 5 min at 99 °C in protein sample buffer (125 mM Tris-HCl, pH 6.8, 4% SDS 0.5% bromphenol blue, 4 mM EDTA, 20% glycerol, 10% *b*-mercaptoethanol).

The samples were separated on 12% SDS-PAGE with a constant voltage of 110 V using Tris glycine, SDS 0.5% running buffer (250 mM Tris, 200 mM glycine, 1% SDS, pH 8.3) for 90 min and transferred to a nitrocellulose membrane (Protran, Schleicher and Schuell, Whatman GmbH, Dassel, Germany) for 120 min with constant current at 0.3 A using Tris glycine transfer buffer.

Membranes were blocked with 5% (w/v) skim milk (Fluka, Sigma) in 1 TBS-Tween (50 mM Tris, 150 mM NaCl, 0.05% Tween, pH 7.5) for 60 min at room temperature. Afterward, membranes were incubated with the primary antibody, mouse anti-ASYN (1:1000, BD Biosciences, San Jose, CA), and 1:5000 mouse anti-GAPDH (Cell Signaling, Danvers, MA) in 3% albumin bovine fraction V/TBS (NZYTech, Lisbon, Portugal) overnight at 4 °C. After washing three times in TBS-Tween, the membranes were incubated for 2 h with secondary antibody, either anti-mouse IgG-or anti-rabbit IgG-horseradish peroxidase (GE Healthcare, Bucks, United Kingdom) at 1:10,000 in 3% milk/TBS-Tween. Detection was performed using Luminol Reagent and peroxide solution (Millipore, Billerica, MA). Protein levels were quantified using ImageJ and normalized to the GAPDH levels.

Proteasome Activity Reporter Assay— H4 cells expressing SynT synphilin were transfected with a plasmid encoding GFP-u, a reporter of proteasome activity (47). After 24 h, cells were treated with different concentrations of BIOD303. Cells were imaged using an Olympus IX81-ZDC microscope system (Olympus Germany, Hamburg, Germany) and analyzed using the Olympus Scan^R Image Analysis Software.

Triton X-100 Solubility Assay—Experiments were performed as previously described (44). Briefly, H4 cells transiently co-transfected with *a*-synuclein (SynT) and synphilin-1 were treated with vehicle (DMSO) or BIOD303 (10, 100, or 500 *m*M). After 24 h, cells were washed with cold PBS and lysed in lysis buffer (PBS supplemented with protease and phosphatase inhibitor mixture tablets, Roche Applied Science). Samples were sonicated three times for 30 s and incubated on ice for 1 min between each sonication step. Total protein concentration was measured and 1% of Triton X-100 was added to 150 *m*g of the protein extracts. Samples were incubated at 4 °C for 30 min and the Triton X-100-insoluble (InsoI) fraction was separated from the soluble (Sol) fraction by centrifugation at 100,000 *g* for 1 h at 4 °C. The insoluble fraction was resuspended in 40 *m*l of lysis buffer containing 2% SDS and sonicated twice for 30 s with 1-min incubation on ice between each sonication step. Both fractions were run on an SDS-PAGE for immunoblotting analysis. A representative membrane is shown (*n* 3).

Theoretical Background of SHG—The intensity of SHG light generated from a population of SHG molecules under irradiation by a fundamental beam, for a given polarization combina-tion of the input and output beams, is given as:

$$I_{SH} = G\,(\chi^{(2)})^2 I^2 \quad \text{(Eq. 2)}$$

where I_{SH} is the measured second-harmonic intensity, G is a function that depends on the experimental geometry, polariza-tion of the fundamental and second-harmonic beams, refractive indices, angle of incidence, optical wavelengths, and the symmetry-allowed elements of the tensor nonlinear susceptibility $x^{(2)}$, and I is the intensity of the fundamental light. $x^{(2)}$ connects the microscopic properties of the second-harmonic active molecules to the observed second-harmonic intensity as,

$$x^2 = N_s \langle a^{(2)} \rangle \quad \text{(Eq. 3)}$$

where N_s is the surface density of the second-harmonic active molecules and the angle brackets denote an orientational aver-

Downloaded from http://www.jbc.org/ by guest on October 9, 2016

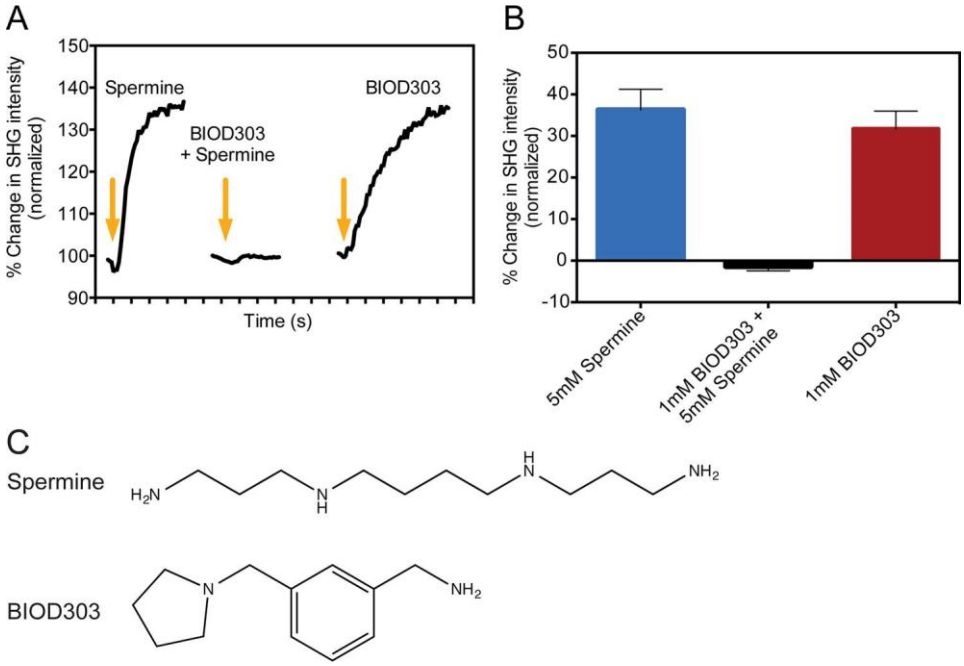

FIGURE 2. **SHG results of the -synuclein assay and Maybridge Ro3 fragment library screen.** *A, left*, the SHG response for *α*-synuclein upon addition of 5 mM spermine. *Middle*, the SHG response of *α*-synuclein upon addition of 5 mM spermine after preincubation with 1 mM BIOD303. *Right*, the SHG response of *α*-synuclein upon addition of 1 mM BIOD303. The *arrows* denote compound addition. Each interval on the time axis is 10 s. *B,* quantification of the mean percent change in SHG intensity for 5 mM spermine, 5 mM spermine addition after preincubation with 1 mM BIOD303, and 1 mM BIOD303. The change in SHG intensity is plotted as the percent change normalized to preinjection levels. *C,* the chemical structures of spermine (*top*) and the compound BIOD303 (*bottom*). For all figures *error bars* mean± S.E., *n*= 3.

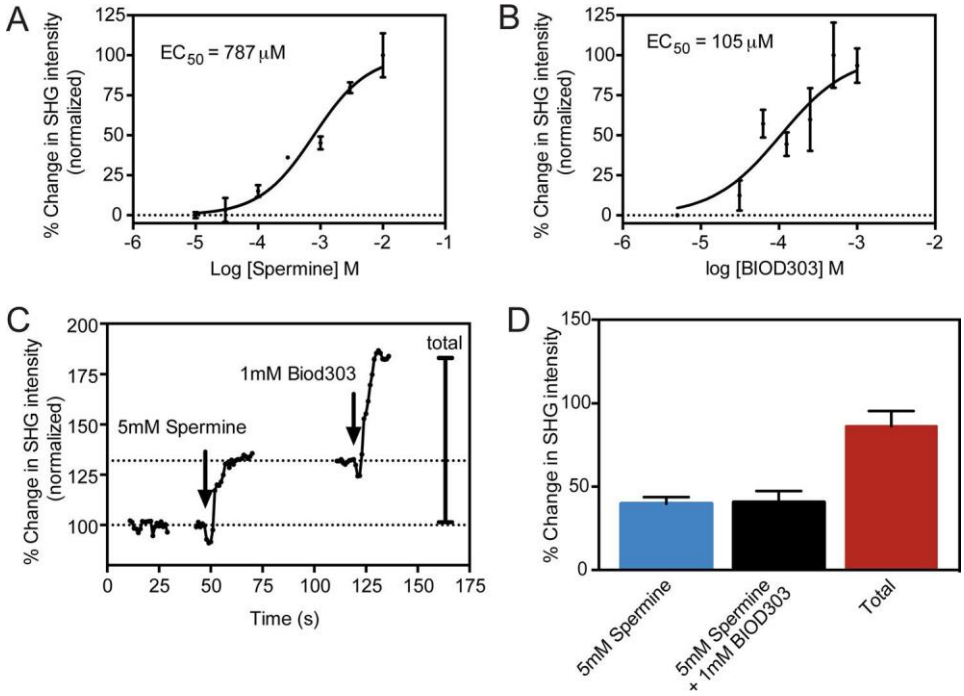

FIGURE 3. **BIOD303 induces a distinct conformation in -synuclein compared with spermine.** *A,* dose-response curves of spermine; and *B,* BIOD303 on *α*-synuclein conformation as measured by SHG. *C,* a representative trace showing the SHG response from a competition experiment in which 5 mM spermine is injected onto *α*-synuclein prior to BIOD303 addition. *Left*, the SHG response for *α*-synuclein upon addition of buffer. *Middle*, the SHG response upon addition of 5 mM spermine onto *α*-synuclein. *Right*, the SHG response of *α*-synuclein upon addition of 1 mM BIOD303 after injecting 5 mM spermine. The *arrows* denote compound addition. The *dotted lines* on the graph represent the baseline level for normalization of the percent change in SHG intensity. Only the portion of the kinetic trace up to the SHG intensity plateau is shown. *D,* quantification of the mean percent change in SHG intensity for 5 mM spermine, 1 mM BIOD303 addition after preincubation with 5 mM spermine, and the total percent change for the original SHG baseline signal after both injections. Change in SHG intensity plotted as percent change normalized to preinjection levels. For all figures *error bars* S.E. *n* 5.

age over $\alpha^{(2)}$, the molecular nonlinear polarizability, a property of the second-harmonic active molecule that determines the probability of producing one second-harmonic photon from two photons of the fundamental beam. In solution phase with isotropic molecular orientation, SHG vanishes, as seen from Equation 3, but at surfaces this symmetry is broken, producing

October 9, 2016

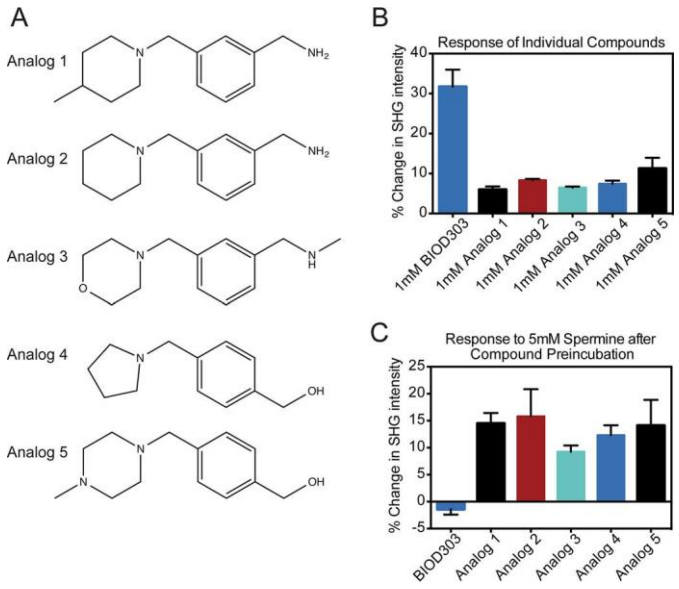

FIGURE 4. **BIOD303 is a highly specific inhibitor of the spermine-induced conformational change in -synuclein.** *A,* chemical structures of the top five scoring BIOD303 analogs from the Maybridge Ro3 library as determined by the program SimFinder. *B,* quantification of the conformational change of *a*-synuclein upon exposure to the top five scoring chemical analogs of BIOD303. Each analog was added at 1 mM final concentration and the change in SHG intensity was measured. Representative data indicating the typical SHG response for 1 mM BIOD303 addition is included for comparison pur-poses. Changes in SHG intensity are plotted as the percent change normal-ized to pre-injection levels. *C,* quantification of conformational change in the analog-spermine competition assay. The indicated BIOD303 analog was pre-incubated with 1 mM *a*-synuclein and the change in SHG intensity upon expo-sure to 5 mM spermine was measured. Representative data indicating the typical SHG response from the BIOD303 5 mM spermine competition assay is included for comparison purposes. Changes in SHG intensity are plotted as a percent change. For all experiments *error bars* S.E. *n* 3.

a net orientation and allowing SHG. The requirements for gen-erating second-harmonic light are thus as follows: the mole-cules must possess second-harmonic activity (a non-zero $a^{(2)}$) and a net, average orientation. Non-centrosymmetric mole-cules with a large difference dipole moment between the ground and excited states often possess second-harmonic activity. Equation 3 can be expressed further as,

$$\chi_{s,ijk}{}^{(2)} = N_2 < T_{ii'}T_{jj'}T_{kk'} > \alpha^{(2)}{}_{i'j'k'} \qquad \text{(Eq. 4)}$$

where $a^{(2)}{}_{i\,j\,k}$ is the molecular nonlinear polarizability mea-sured in the cartesian coordinate frame of the molecule. It is common for planar second-harmonic active molecules, such as dye molecules with aromatic heterocycles, to exhibit nonlinear polarizability in a single plane, such as *x z* , and mirror symme-try perpendicular to the *x* axis of the molecule. If molecular orientation is also isotropic in the plane of the surface, as is commonly the case, by symmetry only three terms of $x_{s,ijk}{}^{(2)}$ contribute to the observed SHG, $x_{ppp}{}^{(2)}$ $x_{pss}{}^{(2)}$ $x_{sps}{}^{(2)}$. Furthermore, the nonlinear polarizability is often dominated by a single element, *i.e.* $\alpha'_{z'z'z'}{}^{(2)}$. Then $x^{(2)}$ is given by,

$$\chi_{pss}{}^{(2)} = \chi_{pss}{}^{(2)} = \frac{1}{2}N_s(cos\theta sin^2\theta)^2\alpha_{z'z'z'}{}^{(2)} \qquad \text{(Eq.6)}$$

$$\chi_{ppp}{}^{(2)} = N_S(cos\theta sin^3\theta)^2\alpha_{z'z'z'}{}^{(2)} \qquad \text{(Eq.5)}$$

TABLE 1
Quantification of BIOD303 analog data

	% Change	
Compound	**Compound only**	**Competition assay**
BIOD303	31.7 4.3%	1.4 1.1%
Analog 1	6.0 0.8%	14.5 1.9%
Analog 2	8.3 0.4%	15.8 5.1%
Analog 3	6.5 0.3%	9.2 1.7%
Analog 4	7.4 0.8%	12.3 1.9%
Analog 5	11.2 2.7%	14.1 4.8%

where *p* and *s* denote the polarizations parallel and perpendicular to the plane of incidence and *u* is the angle between the molecular *z* axis and the surface normal (48). The observed SHG intensity of the labeled protein from Equation 2 is thus directly related to the orientationally averaged tilt angle *u* of the second-harmonic active moiety in the laboratory frame. For example, SHG is often measured using total internal reflection geometry. Under total internal reflection excitation at the critical angle, under *p*-polarized excitation and detection, and with a population of oriented molecules that have a single dominant element in nonlinear polarizability $\alpha_{Z'Z'Z'}$ and a narrow orientational distribution, the SHG intensity $I_{SH}{\approx}\cos^6\theta$. With this sensitivity to tilt angle, at a mean tilt angle of 45°, for example, and a population of oriented molecules, conformational changes of 1° or less could be resolved with typical experimental noise of ~1%. For a dye of 1-nm length, this corresponds to a conformational arc of sub-Ångstrom length, which gives the technique great sensitivity.

Results

Ligand-induced a-Synuclein Conformational Change Analysis—We began by examining the conformational change of *a*-synuclein upon addition of the tool compound spermine, which has previously been shown to bind to the C-terminal domain of *a*-synuclein and induce a change in the conforma-tion of the protein from a closed to an open form (19, 40). Addition of 5 mM spermine to labeled *a*-synuclein resulted in an instantaneous increase in the SHG signal intensity (Fig. 2*A*, *left trace*). We measured the change in the SHG intensity at 5 mM spermine to be 36.3 5.0% (Fig. 2*B*). We also tested two other known binders, spermidine and PcTS (25, 40, 49), and confirmed they also induced conformational change upon binding *a*-synuclein (3 mM spermidine 19.9±2.4%; 10 μM PcTS= -79.5± 6.2%, data not shown). Next, we tested each compound from the Maybridge Ro3 fragment library for an ability to inhibit the *a*-synuclein conformational change upon spermine addition. A hit was defined as complete abolishment of the spermine-induced signal change following preincubation of the test compound. One compound from the library, BIOD303, completely prevented spermine-induced conforma-tional change at a concentration of 1 mM as measured by SHG (-1.4±1.1%; Fig. 2*A*, *middle trace*; Fig. 2*B*).

We next sought to determine by SHG if BIOD303 could induce a conformational change in *a*-synuclein on its own. As shown in Fig. 2*A* (*right trace*), addition of 1 mM BIOD303 to *a*-synuclein changed the SHG baseline signal immediately. We measured the change in SHG intensity to be 31.7±4.3% and classified the response of the compound by direction of signal

Downloaded from http://www.jbc.org/ by guest on October 9, 2016

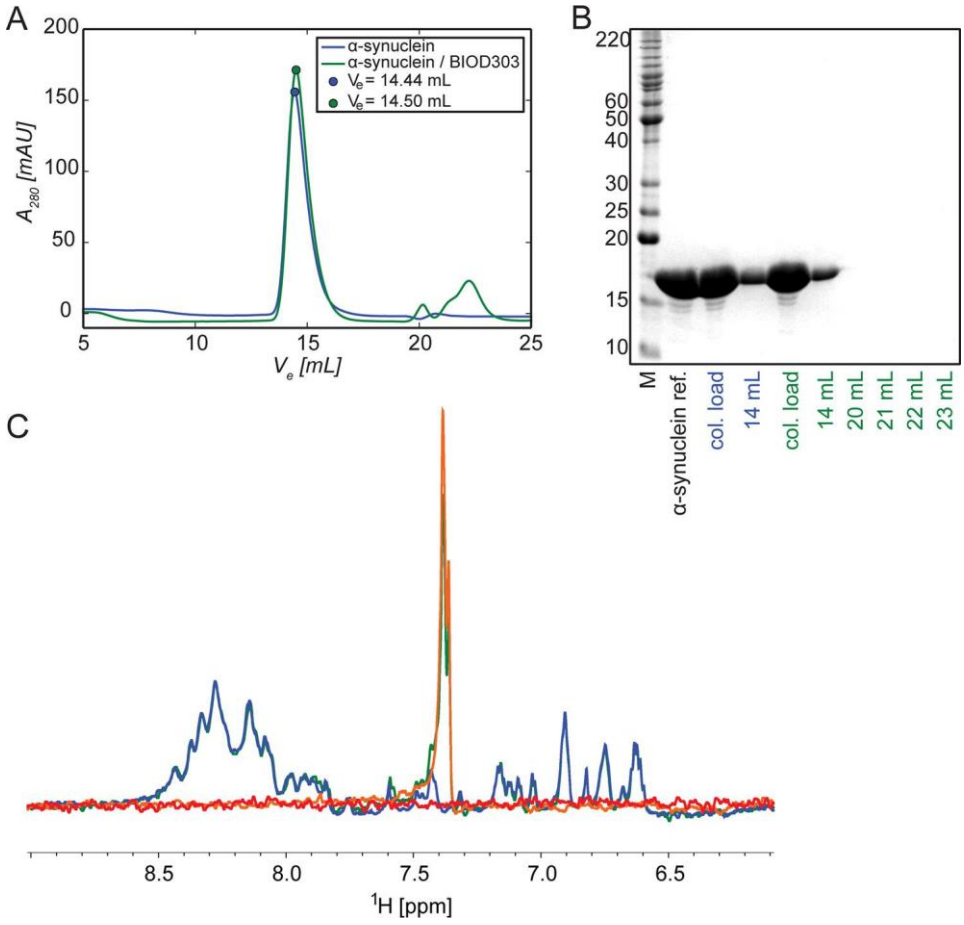

FIGURE 5. **Addition of a 5-fold excess of BIOD303 to -synuclein does not alter its monomeric conformation in solution.** *A,* elution profile of *α*-synuclein (100 *m*M) in the absence (*blue*) and presence (*green*) of 5-fold excess of BIOD303 (500 *m*M) shows comparable retention behavior and elution at a volume of 14 ml on a Superdex 200 10/300 GL size exclusion column. *B,* different elution fractions of size exclusion chromatography and the column loads were analyzed by reducing SDS-PAGE and compared with an *α*-synuclein standard. *C,* ^{1}H NMR spectra of *α*-synuclein (30 *m*M) in the absence (*blue*) and presence (*green*) of 5-fold excess of BIOD303 (150 *m*M) as well as BIOD303 (150 *m*M, *orange*) and HEPES buffer (*red*) as controls. Spectra were recorded at 700 MHz.

relative to baseline, magnitude, and kinetics, to be similar to that of spermine (Fig. 2*B*). Although different conformational changes generally produce different changes in SHG magnitude, direction, or kinetics, they can lead to a similar change, as observed when BIOD303 and spermine bind to the protein. Only a single site (A90C) is labeled, so the angular change at this particular site may be similar although the overall conformations are distinct. Moreover, spermine and BIOD303 are not chemically similar (Fig. 2*C*).

To better understand the relationship between spermine and BIOD303, we determined the EC_{50} of both compounds for *α*-synuclein conformational modulation using SHG. We obtained a dose-response curve (Fig. 3*A*) for spermine and determined its EC_{50} to be 787 μM (log EC_{50} −3.13), in agree-ment with previous values (40). We also measured the dose response of BIOD303 by SHG (Fig. 3*B*) and determined its EC_{50} to be 105 *m*M (log EC_{50} −3.98). Thus, BIOD303 has a ∼7.5-fold higher affinity for *α*-synuclein than spermine, which suggests that BIOD303 can potentially outcompete spermine in binding to *α*-synuclein.

To determine whether BIOD303 was competing with sperm-ine for binding to *α*-synuclein, we repeated our original com-petition experiments except that we reversed the order of com-pound addition. In this experiment, if both ligands at a saturating dose bind to and produce the same conformation of *α*-synuclein, addition of BIOD303 subsequent to spermine would not be expected to change the SHG signal. As seen in Fig. 3*C*, addition of 5 mM spermine to *α*-synuclein resulted in a 39.8±4.1% increase in SHG signal of *α*-synuclein, similar to previous results. Interestingly, subsequent addition of 1 mM BIOD303 to the same sample resulted in a further 40.7±6.7% increase in the SHG intensity of *α*-synuclein suggesting that BIOD303 causes a different conformational change upon bind-ing *α*-synuclein than spermine. If the time scale for protein and dye re-orientation back to the original apo state is slower than BIOD303 binding, *i.e.* the reaction is not at equilibrium, this would account for the additional change observed when BIOD303 is introduced after spermine. Thus the data suggests the lack of response in the original competition experiment from the screen is due to direct inhibition of spermine by BIOD303 and not because the sensitivity of the assay has reached a maximal response.

Next, we wanted to determine whether fragments chemically similar to BIOD303 could also modulate the conformation of *α*-synuclein. We used the ranking program SimFinder (50) to select the five most closely related chemical analogs of BIOD303 from the Ro3 library (Fig. 4*A*). The addition of each individual analog at 1 mM resulted in a smaller increase in SHG

Downloaded from http://www.jbc.org/ by guest on October 9, 2016

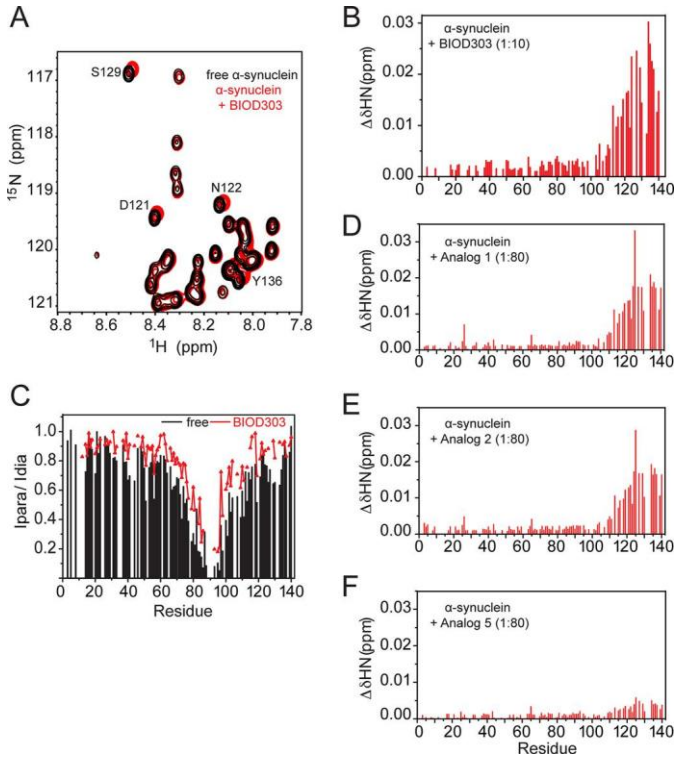

FIGURE 6. **BIOD303 binds to the C-terminal domain of -synuclein and attenuates intramolecular long-range contacts.** *A*, detail of the superposi-tion of ^{1}H-^{15}N NMR spectra of 100 μM *a*-synuclein in the absence (*black*) and presence (*red*) of BIOD303. *B*, chemical shift perturbation analysis of ^{1}H-^{15}N resonances of *a*-synuclein in the presence of BIOD303 at a 1:10 molar ratio. *C*, profile of PRE of amide protons in MTSL-labeled A90C *a*-synuclein (100 *m*M) in the absence (*black*) and presence (*red*) of BIOD303 (3 mM). *D–F*, chemical shift perturbation analysis of ^{1}H-^{15}N resonances of *a*-synuclein in the presence of analogs 1 (*D*), 2 (*E*), and 5 (*F*), at a molar ratio of 1:80.

intensity than BIOD303, indicating modulation of *a*-synuclein conformation (Fig. 4*B*, Table 1), but they did not fully block spermine binding in the competition assay (Fig. 4*C*, Table 1). These data support the exclusion of the analogs as hits in the original screen and suggest that the magnitude and direction of SHG responses can be used to distinguish structure-activity relationships, by measuring the degree to which ligands induce or prevent conformational change. In addition, these results demonstrate that BIOD303 is the most specific and potent inhibitor of spermine-induced conformational change from this series of compounds.

NMR Analysis of the Ligand-induced a-Synuclein Conformational Changes—To obtain further insight into the *a*-synuclein-BIOD303 interaction, we used NMR spectroscopy. NMR resonances are sensitive probes of protein-protein and protein-ligand interactions and can provide a description of interaction interfaces and binding affinities (51). First, the influence of BIOD303 on the aggregation state of *a*-synuclein was tested. To this end, we compared the elution profile of *a*-synuclein on a Superdex 200 10/300 GL in the absence and presence of a 5-fold excess of BIOD303 (Fig. 5, *A* and *B*). The presence of BIOD303 did not change the retention time, indicating that *a*-synuclein remains predominantly monomeric. Consistent with this hypothesis, the overall signal intensity in a one-dimensional NMR spectrum of *a*-synuclein was not attenuated upon addition of a 5-fold molar excess of BIOD303 (Fig. 5*C*). Next, BIOD303 was exposed to ^{15}N-labeled *a*-synuclein and changes in chemical shifts were followed by two-dimensional ^{1}H-^{15}N correlation spectra of *a*-synuclein (Fig. 6*A*). Significant changes in NMR signals (~0.01%) were observed for residues Gly-111 to Ala-140 of *a*-synuclein (Fig. 6, *A* and *B*) at a 10:1 compound: protein molar ratio. A similar perturbation profile had been observed upon addition of spermine to *a*-synuclein (40), indicating that both BIOD303 and spermine bind to the C-terminal domain of *a*-synuclein.

We also tested analogs 1, 2, and 5 for binding to *a*-synuclein. The analysis of chemical shift differences suggest that analogs 1 and 2 bind *a*-synuclein more weakly than BIOD303 at 12-fold molar excess to *a*-synuclein (data not shown). No chemical shift was detected for analog 5 at 12-fold molar excess to *a*-synuclein, although chemical shift perturbation at the C terminus was observed at 80-fold molar ratio. The residual binding of analogs 1 and 2 at the *a*-synuclein C terminus was also emphasized at 80-fold molar ratio of compound:protein (Fig. 6, *D–F*). These data further corroborate our initial screening results and suggest that SHG is highly sensitive to even weak protein-ligand interactions.

Next, we studied the consequences of BIOD303 binding on the conformational ensemble populated by *a*-synuclein in solution using PRE. The interaction between a specifically attached paramagnetic nitroxide radical and nearby protons (less than ≈ 25 Å) causes broadening of their NMR signals because of an increase in transverse relaxation rate (19). This effect has an r^{-6} dependence on the electron-proton distance and thus allows the detection of long-range interactions in proteins. To observe transient long-range contacts within *a*-synuclein in the presence of BIOD303, we attached a paramagnetic MTSL label at position 90 in *a*-synuclein. A comparison of the PRE profiles of MTSL-A90C *a*-synuclein in the absence and presence of BIOD303 revealed decreased paramagnetic broadening at residues 40 – 46 and the C-terminal region covering residues 124 – 136 (Fig. 6*C*). Thus, BIOD303 binds to a similar site as spermine or to one with substantial overlap with it, and induces a conformational change by attenuating the long-range interactions in *a*-synuclein.

Effect of BIOD303 on a-Synuclein Aggregation in Cells—Because both SHG and PRE data indicated that BIOD303 altered the conformation of monomeric *a*-synuclein *in vitro*, we investigated the effect of BIOD303 on *a*-synuclein aggregation in cells. To do so, we tested BIOD303 in an established human H4 neuronal cell model of *a*-synuclein aggregation and inclusion formation (45, 46). In this model, a C terminally modified version of *a*-synuclein (SynT) is co-expressed with synphilin-1, resulting in the formation of LB-like, detergent-insoluble inclusions. The addition of 500 μM BIOD303 to H4 cells significantly increased the percentage of cells without *a*-synuclein inclusions (*, p= 0.0172, Student's t test) as shown by the absence of *a*-synuclein inclusions compared with control cells (Fig. 7). The effect on *a*-synuclein inclusion formation was dose dependent (data not shown). Analogs 1 and 2 also reduced inclusion formation (*, p 0.0203, 0.0477 respectively, Student's t test), although to a lesser extent than BIOD303, consistent with the SHG and NMR data. Analog 5, which exhibited weak binding by NMR, had no effect on inclusion forma-

Downloaded from http://www.jbc.org/ by guest on October 9, 2016

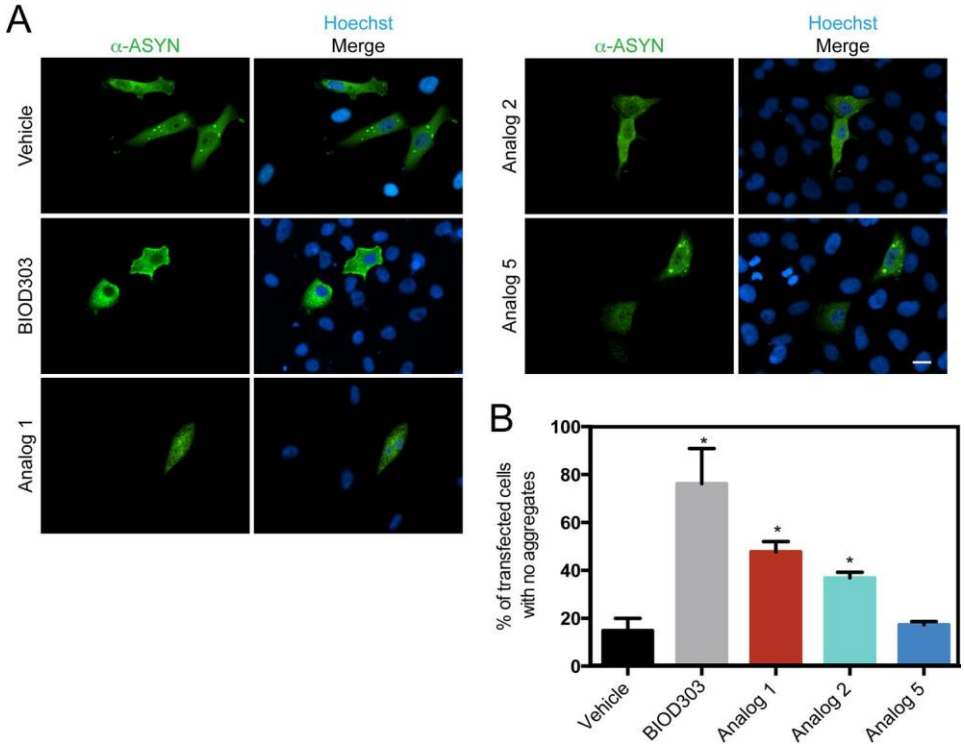

FIGURE 7. **BIOD303 inhibits -synuclein inclusion formation in an H4 neuronal cell model.** *A,* representative images of transfected H4 cells treated with 500 μM of each compound. The staining for *a*-synuclein or the merge of *a*-synuclein and DNA (Hoechst) are indicated above the image. The compound addition is shown to the *left* of each image row. *Scale bar* 20 μM. *B,* bar graph showing the percentage of H4 cells with no *a*-synuclein inclusions upon treatment with 500 μM of each compound. Student's *t* test (*, *p* 0.05). *Error bars* S.E. *n* =2.

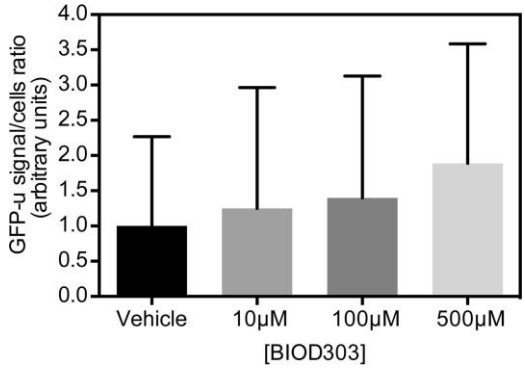

FIGURE 8. **BIOD303 does not significantly alter proteasome activity in H4 cells.** H4 cells expressing SynT+ synphilin were transfected with a plasmid encoding GFP-u, a reporter of proteasome activity. Twenty-four hours after transfection, cells were treated with different concentrations of BIOD303. No significant differences could be detected between treated and untreated cells. *Error bars*= S.E. *n*=2.

tion (*p* value 0.7365, Student's *t* test). These results demon-strate that BIOD303 and analogs 1 and 2 directly target *a*-synuclein and reduce inclusion formation in a cellular context.

Because inclusion formation is a complex, multistep process we further investigated the mechanism by which BIOD303 reduced *a*-synuclein inclusion formation. We began by deter-mining whether BIOD303 affected proteasome activity, which in turn could affect *a*-synuclein inclusion formation. To address this we used an unstable version of GFP (GFPu) that is targeted for proteasomal degradation (47). If proteasome activity is compromised, GFP-u accumulates in the cell, leading to an increase in fluorescence signal. In our experiments, we found no significant difference in the GFP signal of control cells compared with cells treated with different concentrations of BIOD303, suggesting that proteasome activity was not significantly affected (Fig. 8).

To assess whether the observed effect on inclusion formation was indeed due to a change in the biochemical state of *a*-synuclein, we performed Triton X -100 solubility assays. We found that BIOD303 reduced the amount of detergent-insoluble *a*-synuclein compared with control cells (*, *p* 0.0424, Student's *t* test) (Fig. 9, *A* and *B*), without changing the total levels of *a*-synuclein expression (Fig. 9, *C* and *D*), as assessed in a model where SynT and synphilin-1 are expressed in a 1:1 ratio (hence the slight difference in the apparent size on the SDS- PAGE when compared with the detergent solubility assay) . This result, in combination with the *in vitro* biochemical and SHG experiments, indicates that BIOD303 reduces *a*-synuclein inclusion formation in cells, by binding to and directly modulating the conformation of monomeric *a*-synuclein.

Discussion

Here we present an SHG-based approach to study and identify protein-small molecule conformational changes. Our goal was to test the hypothesis that modulating the monomeric *a*-synuclein conformation can affect aggregation of the protein in cells. SHG has previously been used to study the natural polarizability of biological materials such as collagen. In the pioneering studies by Freund *et al.* (52), SHG was used to demonstrate the highly ordered, anisotropic organization of collagen fibers in rat tail tendon. The intrinsic SHG activity of bio-

Downloaded from http://www.jbc.org/ by guest on October 9, 2016

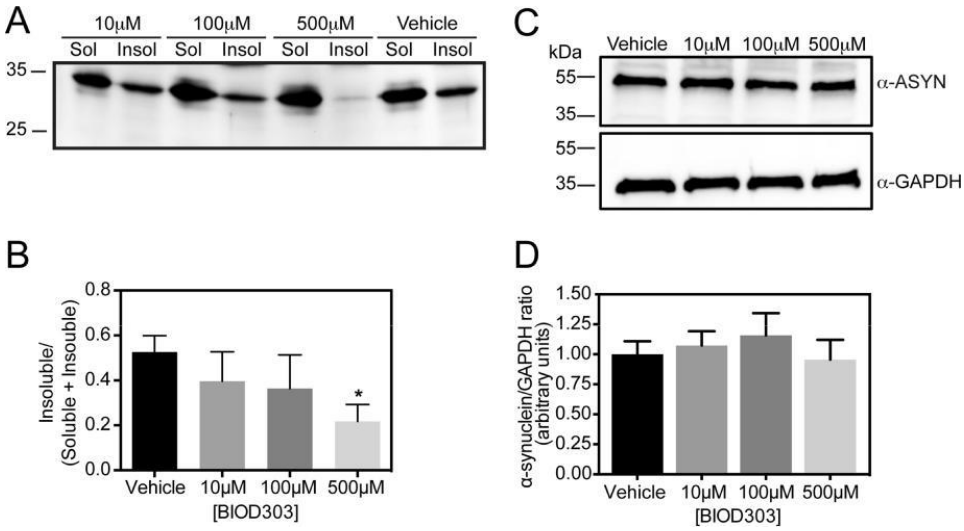

FIGURE 9. **BIOD303 reduces the level of insoluble -synuclein in H4 cells.** *A,* a representative Western blot of the Triton X-100 solubility assay comparing the soluble and insoluble fractions of *α*-synuclein upon BIOD303 treatment. Cells treated with 500 *μ*M BIOD303 show a significant reduction in the amount of *α*-synuclein in the insoluble (*Insol*) fraction. *B,* bar graph quantifying the ratio of insoluble *α*-synuclein to total *α*-synuclein from the Triton X-100 solubility assay. H4 cells treated with different concentrations of BIOD303 show a dose-dependent reduction in the amount of *α*-synuclein in the insoluble (*Insol*) fraction. Student's *t* test; *, <*p* 0.05. *n*=3. *C,* representative immunoblot; and *D,* quantification showing that expression levels of *α*-synuclein do not change upon treatment with BIOD303. *Error bars* S.E. *n* =3.

logical materials has also been demonstrated in other biological samples including tetra fish keratocytes and the nematode *Caenorhabditis elegans* (53, 54). Other applications of SHG include study of the cell membrane potential through the exogenous incorporation of organic second-harmonic active membrane dyes (55). The technique presented here renders a protein second-harmonic active by coupling a second-harmonic active dye to it via standard chemistries. Conjugation with an second-harmonic active probe offers the key advantage that the target protein can be modified either randomly at lysine residues using amine labeling or site specifically at either naturally occurring or engineered cysteine residues via maleimide labeling. In addition, attaching the protein directly to a surface ensures that the requirement for noncentrosymmetric orientation of the dye, necessary for SHG, is met. Taken together, the approach described here should allow the study of virtually any biological target via SHG.

To probe the role of conformation in *α*-synuclein aggregation and PD pathogenesis, we used SHG to identify a single compound, BIOD303, as a potent conformational modulator of the protein *in vitro*. The fragment appears to bind to a conformation of monomeric *α*-synuclein distinct from that bound by spermine, and it significantly reduces *α*-synuclein aggregation in a neuronal cell model. BIOD303 is distinct from other previ-ously identified *α*-synuclein aggregation inhibitors such as cur-curmin, epigallocatechin gallate, and hydroxyquinolines, which are known pan-assay interference compounds (26, 29, 56 –58) in that it specifically binds to monomeric *α*-synuclein. In addition, BIOD303 has drug-like properties and appears to be an excellent starting point for medicinal chemistry efforts. The ability of SHG to identify BIOD303 and distinguish it from closely related analogs that bind to an IDP target that is chal-lenging to screen against, for which few specific ligands are known, illustrates the sensitivity of the technique. As the magnitude and sign of the measured SHG change depend on the specific conformation and therefore the tilt angle of the label produced by binding each ligand, the technique can also classify ligands by the different conformations to which they bind. Pro-teins exist in an ensemble of conformations, particularly in the case of IDPs such as *α*-synuclein. Many of these conformations are short-lived and represent only minor populations in the total ensemble, yet they may nonetheless be crucially important to the function of a protein and also unique across a protein family. Therefore, a key potential advantage of conformational modulators as therapeutics is that they can target specific, conserved con-formations and thereby act more selectively (1, 59 – 61). In summary, our results indicate that the conformation of monomeric *α*-synuclein plays an important, possibly decisive, role in the aggregation of the protein, and presumably PD pathogenesis. As shown here, small molecules that modulate *α*-synuclein conformation can be identified rapidly by SHG. By modulating the con-formation of the monomeric protein, selective therapeutics directed to suppressing protein aggregation and PD pathogenesis at the earliest stage could be developed.

Author Contributions—B. M. performed the SHG experiments, data analysis, and wrote the paper. G. Y. performed NMR data acquisition and NMR analysis. D. F. L. performed cell culture experiments, analysis, and wrote the paper. T. S. performed the SEC and NMR experiments. F. M. performed NMR data acquisition and analysis. K. G. contributed sample preparations. S. B. supervised sample production and wrote the paper. T. F. O. supervised the cell culture work and wrote the paper. M. Z. supervised the NMR work and wrote the paper. J. S. designed and supervised the project, performed the screen, and wrote the paper.

Acknowledgments—We thank Ryan McGuinness for assistance with the SHG screen. J. S. gratefully acknowledges Richard Ulevitch for helpful suggestions and discussions. We also thank Prof. Dr. Thomas Myer and Anke Gregus for technical assistance.

Downloaded from http://www.jbc.org/ by guest on October 9, 2016

References

1. Goodey, N. M., and Benkovic, S. J. (2008) Allosteric regulation and catal-ysis emerge via a common route. *Nat. Chem. Biol.* **4,** 474 – 482
2. Goh, C. S., Milburn, D., and Gerstein, M. (2004) Conformational changes associated with protein-protein interactions. *Curr. Opin. Struct. Biol.* **14,** 104 –109
3. Henzler-Wildman, K., and Kern, D. (2007) Dynamic personalities of pro-teins. *Nature* **450,** 964 –972
4. Koshland, D. E., Jr., Ray, W. J., Jr., and Erwin, M. J. (1958) Protein structure and enzyme action. *Fed. Proc.* **17,** 1145–1150
5. Fischer, E. (1894) Einfluss der configuration auf die wirkung der enzyme. *Ber. Dtsch. Chem. Ges.* **27,** 2985–2993
6. Wright, P. E., and Dyson, H. J. (1999) Intrinsically unstructured proteins: re-assessing the protein structure-function paradigm. *J. Mol. Biol.* **293,** 321–331
7. Uversky, V. N. (2015) Intrinsically disordered proteins and their (disor-dered) proteomes in neurodegenerative disorders. *Front. Aging Neurosci.***7,** 18
8. Tompa, P. (2012) Intrinsically disordered proteins: a 10-year recap. *Trends Biochem. Sci.* **37,** 509 –516
9. Uversky, V. N. (2014) Introduction to intrinsically disordered proteins (IDPs). *Chem. Rev.* **114,** 6557– 6560
10. Fauvet, B., Mbefo, M. K., Fares, M. B., Desobry, C., Michael, S., Ardah,
    a. T., Tsika, E., Coune, P., Prudent, M., Lion, N., Eliezer, D., Moore, D. J., Schneider, B., Aebischer, P., El-Agnaf, O. M., Masliah, E., and Lashuel,

    A. (2012) *α*-Synuclein in central nervous system and from erythrocytes, mammalian cells, and *Escherichia coli* exists predominantly as disordered monomer. *J. Biol. Chem.* **287,** 15345–15364
53. Bendor, J. T., Logan, T. P., and Edwards, R. H. (2013) The function of *α*-synuclein. *Neuron* **79,** 1044 –1066
54. Chandra, S., Gallardo, G., Ferna´ndez-Chaco´n, R., Schlu¨ter, O. M., and Su¨dhof, T. C. (2005) Alpha-synuclein cooperates with CSP*α* in preventing neurodegeneration. *Cell* **123,** 383–396
55. Burre´, J., Sharma, M., Tsetsenis, T., Buchman, V., Etherton, M. R., and Sudhof, T. C. (2010) *α*-Synuclein promotes SNARE-complex assembly *in vivo* and *in vitro*. *Science* **329,** 1663–1667
56. Spillantini, M. G., Schmidt, M. L., Lee, V. M., Trojanowski, J. Q., Jakes, R., and Goedert, M. (1997) *α*-Synuclein in Lewy bodies. *Nature* **388,** 839 – 840
57. Polymeropoulos, M. H., Lavedan, C., Leroy, E., Ide, S. E., Dehejia, A., Dutra, A., Pike, B., Root, H., Rubenstein, J., Boyer, R., Stenroos, E. S., Chandrasekharappa, S., Athanassiadou, A., Papapetropoulos, T., Johnson,
    3: G., Lazzarini, A. M., Duvoisin, R. C., Di Iorio, G., Golbe, L. I., and Nussbaum, R. L. (1997) Mutation in the *α*-synuclein gene identified in families with Parkinson's disease. *Science* **276,** 2045–2047
58. Singleton, A. B., Farrer, M., Johnson, J., Singleton, A., Hague, S., Kachergus, J., Hulihan, M., Peuralinna, T., Dutra, A., Nussbaum, R., Lincoln, S., Crawley, A., Hanson, M., Maraganore, D., Adler, C., Cookson, M. R., Muenter, M., Baptista, M., Miller, D., Blancato, J., Hardy, J., and Gwinn-Hardy, K. (2003) *α*-Synuclein locus triplication causes Parkinson's disease. *Science* **302,** 841
59. Simo´n-Sa´nchez, J., Schulte, C., Bras, J. M., Sharma, M., Gibbs, J. R., Berg, D., Paisan-Ruiz, C., Lichtner, P., Scholz, S. W., Hernandez, D. G., Kruger, R., Federoff, M., Klein, C., Goate, A., Perlmutter, J., Bonin, M., Nalls, M. A., Illig, T., Gieger, C., Houlden, H., Steffens, M., Okun, M. S., Racette, B. A., Cookson, M. R., Foote, K. D., Fernandez, H. H., Traynor, B. J., Schreiber, S., Arepalli, S., Zonozi, R., Gwinn, K., van der Brug, M., Lopez, G., Chanock,
    J., Schatzkin, A., Park, Y., Hollenbeck, A., Gao, J., Huang, X., Wood,
    W., Lorenz, D., Deuschl, G., Chen, H., Riess, O., Hardy, J. A., Singleton,

    A. B., and Gasser, T. (2009) Genome-wide association study reveals ge-netic risk underlying Parkinson's disease. *Nat. Genet.* **41,** 1308 –1312
18. Eliezer, D., Kutluay, E., Bussell, R., Jr., and Browne, G. (2001) Conformational properties of *α*-synuclein in its free and lipid-associated states. *J. Mol. Biol.* **307,** 1061–1073
19. Bertoncini, C. W., Jung, Y.-S., Fernandez, C. O., Hoyer, W., Griesinger, C., Jovin, T. M., and Zweckstetter, M. (2005) Release of long-range tertiary interactions potentiates aggregation of natively unstructured *α*-synuclein. *Proc. Natl. Acad. Sci. U.S.A.* **102,** 1430 –1435
20. Winner, B., Jappelli, R., Maji, S. K., Desplats, P. A., Boyer, L., Aigner, S., Hetzer, C., Loher, T., Vilar, M., Campioni, S., Tzitzilonis, C., Soragni, A., Jessberger, S., Mira, H., Consiglio, A., Pham, E., Masliah, E., Gage, F. H., and Riek, R. (2011) *In vivo* demonstration that *α*-synuclein oligomers are toxic. *Proc. Natl. Acad. Sci. U.S.A.* **108,** 4194 – 4199
21. Conway, K. A., Harper, J. D., and Lansbury, P. T. (2000) Fibrils formed *in vitro* from *α*-synuclein and two mutant forms linked to Parkinson's dis-ease are typical amyloid. *Biochemistry* **39,** 2552–2563
22. Karpinar, D. P., Balija, M. B., Kugler, S., Opazo, F., Rezaei-Ghaleh, N., Wender, N., Kim, H.-Y., Taschenberger, G., Falkenburger, B. H., Heise, H., Kumar, A., Riedel, D., Fichtner, L., Voigt, A., Braus, G. H., Giller, K., Becker, S., Herzig, A., Baldus, M., Ja¨ckle, H., Eimer, S., Schulz, J. B., Griesinger, C., and Zweckstetter, M. (2009) Pre-fibrillar *α*-synuclein variants with impaired *β*-structure increase neurotoxicity in Parkinson's dis-ease models. *EMBO J.* **28,** 3256 –3268
23. Lashuel, H. A., Overk, C. R., Oueslati, A., and Masliah, E. (2013) The many faces of *α*-synuclein: from structure and toxicity to therapeutic target. *Nat. Rev. Neurosci.* **14,** 38 – 48
24. Conway, K. A., Lee, S. J., Rochet, J. C., Ding, T. T., Williamson, R. E., and Lansbury, P. T., Jr. (2000) Acceleration of oligomerization, not fibrillization, is a shared property of both alpha-synuclein mutations linked to early-onset Parkinson's disease: implications for pathogenesis and therapy. *Proc. Natl. Acad. Sci. U.S.A.* **97,** 571–576
25. Lamberto, G. R., Binolfi, A., Orcellet, M. L., Bertoncini, C. W., Zweckstet-ter, M., Griesinger, C., and Fernandez, C. O. (2009) Structural and mech-anistic basis behind the inhibitory interaction of PcTS on *α*-synuclein amyloid fibril formation. *Proc. Natl. Acad. Sci. U.S.A.* **106,** 21057–21062
26. Ehrnhoefer, D. E., Bieschke, J., Boeddrich, A., Herbst, M., Masino, L., Lurz, R., Engemann, S., Pastore, A., and Wanker, E. E. (2008) EGCG redirects amyloidogenic polypeptides into unstructured, off-pathway oligomers. *Nat. Struct. Mol. Biol.* **15,** 558 –566
27. Braga, C. A., Follmer, C., Palhano, F. L., Khattar, E., Freitas, M. S., Romao, L., Di Giovanni, S., Lashuel, H. A., Silva, J. L., and Foguel, D. (2011) The anti-Parkinsonian drug selegiline delays the nucleation phase of *α*-synuclein aggregation leading to the formation of nontoxic species. *J. Mol. Biol.* **405,** 254 –273
28. Kritzer, J. A., Hamamichi, S., McCaffery, J. M., Santagata, S., Naumann,
    T. A., Caldwell, K. A., Caldwell, G. A., and Lindquist, S. (2009) Rapid selection of cyclic peptides that reduce *α*-synuclein toxicity in yeast and animal models. *Nat. Chem. Biol.* **5,** 655– 663
29. Su, L. J., Auluck, P. K., Outeiro, T. F., Yeger-Lotem, E., Kritzer, J. A., Tardiff, D. F., Strathearn, K. E., Liu, F., Cao, S., Hamamichi, S., Hill, K. J., Caldwell, K. A., Bell, G. W., Fraenkel, E., Cooper, A. A., Caldwell, G. A., McCaffery, J. M., Rochet, J. C., and Lindquist, S. (2010) Compounds from an unbiased chemical screen reverse both ER-to-Golgi trafficking defects and mitochondrial dysfunction in Parkinson's disease models. *Dis. Model Mech.* **3,** 194 –208
30. Tardiff, D. F., Jui, N. T., Khurana, V., Tambe, M. A., Thompson, M. L., Chung, C. Y., Kamadurai, H. B., Kim, H. T., Lancaster, A. K., Caldwell,
    K. A., Caldwell, G. A., Rochet, J. C., Buchwald, S. L., and Lindquist, S. (2013) Yeast reveal a "druggable" Rsp5/Nedd4 network that ameliorates *α*-synuclein toxicity in neurons. *Science* **342,** 979 –983
31. Chung, C. Y., Khurana, V., Auluck, P. K., Tardiff, D. F., Mazzulli, J. R., Soldner, F., Baru, V., Lou, Y., Freyzon, Y., Cho, S., Mungenast, A. E., Muf-fat, J., Mitalipova, M., Pluth, M. D., Jui, N. T., Schule, B., Lippard, S. J., Tsai, L.-H., Krainc, D., Buchwald, S. L., Jaenisch, R., and Lindquist, S. (2013) Identification and rescue of *α*-synuclein toxicity in Parkinson patient-derived neurons. *Science* **342,** 983–987
32. To´th, G., Gardai, S. J., Zago, W., Bertoncini, C. W., Cremades, N., Roy,
    S. L., Tambe, M. A., Rochet, J.-C., Galvagnion, C., Skibinski, G., Fink-beiner, S., Bova, M., Regnstrom, K., Chiou, S.-S., Johnston, J., Callaway, K., Anderson, J. P., Jobling, M. F., Buell, A. K., Yednock, T. A., Knowles, T. P., Vendruscolo, M., Christodoulou, J., Dobson, C. M., Schenk, D., and Mc-Conlogue, L. (2014) Targeting the Intrinsically Disordered Structural En-semble of *α*-Synuclein by Small Molecules as a Potential Therapeutic Strategy for Parkinson's Disease. *PLoS ONE* **9,** e87133
33. Heinz, T. F., Tom, H. W. K., and Shen, Y. R. (1983) Determination of

Downloaded from http://www.jbc.org/ by guest on October 9, 2016

molecular orientation of monolayer adsorbates by optical second-harmonic generation. *Phys. Rev. A* **28,** 1883–1885

34. Zhuang, X., Miranda, P. B., Kim, D., and Shen, Y. R. (1999) Mapping molecular orientation and conformation at interfaces by surface nonlinear optics. *Phys. Rev. B* **59,** 12632–12640
35. Salafsky, J. S. (2006) Detection of protein conformational change by opti-cal second-harmonic generation. *J. Chem. Phys.* **125,** 074701
36. Salafsky, J. S. (2007) Second-harmonic generation for studying structural motion of biological molecules in real time and space. *Phys. Chem. Chem. Phys.* **9,** 5704 –5711
37. Salafsky, J. S., and Cohen, B. (2008) A second-harmonic-active unnatural amino acid as a structural probe of biomolecules on surfaces. *J. Phys. Chem. B* **112,** 15103–15107
38. Moree, B., Connell, K., Mortensen, R. B., Liu, C. T., Benkovic, S. J., and Salafsky, J. (2015) Protein conformational changes are detected and resolved site specifically by second-harmonic generation. *Biophys. J.* **109,** 806 – 815
39. Salafsky, J. S. (2001) "SHG-labels" for detection of molecules by second harmonic generation. *Chem. Phys. Lett.* **342,** 485– 491
40. Fernandez, C. O., Hoyer, W., Zweckstetter, M., Jares-Erijman, E. A., Sub-ramaniam, V., Griesinger, C., and Jovin, T. M. (2004) NMR of *α*-synuclein-polyamine complexes elucidates the mechanism and kinetics of induced aggregation. *EMBO J.* **23,** 2039 –2046
41. Erlanson, D. A. (2012) Introduction to fragment-based drug discovery. *Top. Curr. Chem.* **317,** 1–32
42. Der-Sarkissian, A., Jao, C. C., Chen, J., and Langen, R. (2003) Structural organization of alpha-synuclein fibrils studied by site-directed spin labeling. *J. Biol. Chem.* **278,** 37530 –37535
43. Delaglio, F., Grzesiek, S., Vuister, G. W., Zhu, G., Pfeifer, J., and Bax, A. (1995) NMRPipe: a multidimensional spectral processing system based on UNIX pipes. *J. Biomol. NMR* **6,** 277–293
44. Lázaro, D. F., Rodrigues, E. F., Langohr, R., Shahpasandzadeh, H., Ribeiro, T., Guerreiro, P., Gerhardt, E., Kro¨hnert, K., Klucken, J., Pereira, M. D., Popova, B., Kruse, N., Mollenhauer, B., Rizzoli, S. O., Braus, G. H., Danzer,
    K. M., and Outeiro, T. F. (2014) Systematic comparison of the effects of *α*-synuclein mutations on its oligomerization and aggregation. *PLoS Genet.* **10,** e1004741
45. McLean, P. J., Kawamata, H., and Hyman, B. T. (2001) Alpha-synuclein-enhanced green fluorescent protein fusion proteins form proteasome sensitive inclusions in primary neurons. *Neuroscience* **104,** 901–912
46. Outeiro, T. F., Klucken, J., Strathearn, K. E., Liu, F., Nguyen, P., Rochet, J. C., Hyman, B. T., and McLean, P. J. (2006) Small heat shock proteins protect against *α*-synuclein-induced toxicity and aggregation. *Biochem. Biophys. Res. Commun.* **351,** 631– 638
47. Bence, N. F., Sampat, R. M., and Kopito, R. R. (2001) Impairment of the ubiquitin-proteasome system by protein aggregation. *Science* **292,** 1552–1555
48. Heinz, T. F. (1991) Second-Order Nonlinear Optical Effects at Surfaces and Interfaces. in *Nonlinear Surface Electromagnetic Phenomena* (Ponath,
    H. E., and Stegeman, G. I., eds) pp. 353– 416, Elsevier, Amsterdam
49. Lee, E.-N., Cho, H.-J., Lee, C.-H., Lee, D., Chung, K. C., and Paik, S. R. (2004) Phthalocyanine tetrasulfonates affect the amyloid formation and cytotoxicity of *α*-synuclein. *Biochemistry* **43,** 3704 –3715
50. Huahai, H., and Singh, A. K. (2006) GraphRank: Statistical Modeling and Mining of Significant Subgraphs in the Feature Space. in *Data Mining, 2006. ICDM '06. Sixth International Conference on IEEE.* pp. 885– 890, Hong Kong, China
51. Craik, D. J., and Wilce, J. A. (1997) Studies of protein-ligand interactions by NMR. *Methods Mol. Biol.* **60,** 195–232
52. Freund, I., Deutsch, M., and Sprecher, A. (1986) Connective tissue polarity: optical second-harmonic microscopy, crossed-beam summation, and small-angle scattering in rat-tail tendon. *Biophys. J.* **50,** 693–712
53. Campagnola, P. J., Millard, A. C., Terasaki, M., Hoppe, P. E., Malone, C. J., and Mohler, W. A. (2002) Three-dimensional high-resolution second-harmonic generation imaging of endogenous structural proteins in biological tissues. *Biophys. J.* **82,** 493–508
54. Campagnola, P. J., and Loew, L. M. (2003) Second-harmonic imaging microscopy for visualizing biomolecular arrays in cells, tissues and organ-isms. *Nat. Biotechnol.* **21,** 1356 –1360
55. Moreaux, L., Pons, T., Dambrin, V., Blanchard-Desce, M., and Mertz, J. (2003) Electro-optic response of second-harmonic generation membrane potential sensors. *Opt. Lett.* **28,** 625– 627
56. Ahmad, B., and Lapidus, L. J. (2012) Curcumin prevents aggregation in *α*-synuclein by increasing reconfiguration rate. *J. Biol. Chem.* **287,** 9193–9199
57. Tardiff, D. F., Tucci, M. L., Caldwell, K. A., Caldwell, G. A., and Lindquist,
    S. (2012) Different 8-hydroxyquinolines protect models of TDP-43 protein, *α*-synuclein, and polyglutamine proteotoxicity through distinct mechanisms. *J. Biol. Chem.* **287,** 4107– 4120
1. Baell, J., and Walters, M. A. (2014) Chemistry: chemical con artists foil drug discovery. *Nature* **513,** 481– 483
2. Christopoulos, A. (2002) Allosteric binding sites on cell-surface receptors: novel targets for drug discovery. *Nat. Rev. Drug Discov.* **1,** 198 –210
3. Hardy, J. A., and Wells, J. A. (2004) Searching for new allosteric sites in enzymes. *Curr. Opin. Struct. Biol.* **14,** 706 –715
4. Swinney, D. C., and Anthony, J. (2011) How were new medicines discovered? *Nat. Rev. Drug Discov.* **10,** 507–519
5. Goddard, T. D., and Kneller, D. G. (2007) *Sparky*, University of California, San Francisco

3.3. The effects of the novel A53E alpha-synuclein mutation on its oligomerization and aggregation

Diana F. Lázaro#, Mariana Castro Dias#, Anita Carija, Susanna Navarro, Carolina Silva Madaleno, Sandra Tenreiro, Salvador Ventura and Tiago F. Outeiro.
#equal contribution

Experiments	Done by
Aggregation process and study design, Figure 1	Diana F. Lázaro
A53E reduces aSyn oligomerization, Figure 3	Diana F. Lázaro, and Mariana Castro Dias
A53E does not change the inclusion pattern, in Figure 4	Diana F. Lázaro, and Mariana Castro Dias
Golgi morphology in the oligomerization and aggregation models, in Figure 5	Diana F. Lázaro, and Mariana Castro Dias
All other experiment were performed by the other authors	

Status of the manuscript: published (Acta Neuropathol Commun. 2016 Dec 9;4(1):128).

Acta Neuropathologica Communications

Lázaro et al. Acta Neuropathologica Communications (2016) 4:128

DOI 10.1186/s40478-016-0402-8

RESEARCH Open Access

The effects of the novel A53E alpha-synuclein mutation on its oligomerization and aggregation

Diana F. Lázaro[1†], Mariana Castro Dias[1†], Anita Carija[2], Susanna Navarro[2], Carolina Silva Madaleno[3], Sandra Tenreiro[3], Salvador Ventura[2] and Tiago F. Outeiro[1,3,4*]

Abstract

α-synuclein (aSyn) is associated with both sporadic and familial forms of Parkinson's disease (PD), the second most common neurodegenerative disorder after Alzheimer's disease. In particular, multiplications and point mutations in the gene encoding for aSyn cause familial forms of PD. Moreover, the accumulation of aSyn in Lewy Bodies and Lewy neurites in disorders such as PD, dementia with Lewy bodies, or multiple system atrophy, suggests aSyn misfolding and aggregation plays an important role in these disorders, collectively known as synucleinopathies. The exact function of aSyn remains unclear, but it is known to be associated with vesicles and membranes, and to have an impact on important cellular functions such as intracellular trafficking and protein degradation systems, leading to cellular pathologies that can be readily studied in cell-based models. Thus, understanding the molecular effects of aSyn point mutations may provide important insight into the molecular mechanisms underlying disease onset. We investigated the effect of the recently identified A53E aSyn mutation. Combining in vitro studies with studies in cell models, we found that this mutation reduces aSyn aggregation and increases proteasome activity, altering normal proteostasis.

We observed that, in our experimental paradigms, the A53E mutation affects specific steps of the aggregation process of aSyn and different cellular processes, providing novel ideas about the molecular mechanisms involved in synucleinopathies.

Keywords: Alpha-synuclein, Parkinson's disease, Oligomerization, Aggregation, Neurodegeneration

Introduction

Parkinson's disease (PD) is a highly debilitating and progressive neurodegenerative disorder affecting around seven million people worldwide. PD is typically known as a movement disorder, due to the characteristic motor manifestations associated with the loss of dopaminergic neurons from the substantia nigra, although it also affects other areas of the brain. PD and other neurodegenerative disorders, such as demential with Lewy bodies, and multiple system atrophy, are also characterized by the accumulation of aggregated alpha-synuclein (aSyn) in proteinaceous inclusions known as Lewy bodies (LBs) or Lewy neurites [54]. Together, these diseases are known as synucleinopathies [17, 55]. However, it is still unclear whether LBs are themselves toxic or protective [7, 43], with smaller oligomeric species of aSyn being the culprits as recent studies suggest [31, 45, 58, 63]. aSyn is a disordered and abundant neuronal protein whose normal function is still elusive. Familial forms of PD associated with duplication and triplication of the SNCA gene [53], along with studies of aSyn overexpression, in cellular and animal models, suggest the protein may acquire a toxic function. The cellular pathologies associated with increased levels and accumulation of aSyn include disruption of vesicular transport [6, 42], mitochondrial dysfunction, impairment of autophagy and proteasome, and oxidative stress [2, 21], suggesting aSyn plays a multitude of roles in the cell, perhaps due

* Correspondence: touteir@gwdg.de

†Equal contributors

[1]Department of Neurodegeneration and Restorative Research, University Medical Center Göttingen, Waldweg 33, 37073 Göttingen, Germany

[3]Chronic Disease Research Center (CEDOC), NOVA Medical School, Campo dos Mártires da Pátria, 130, 1169-056 Lisbon, Portugal

BioMed Central

© The Author(s). 2016 Open Access This article is distributed under the terms of the Creative Commons Attribution 4.0 International License (http://creativecommons.org/licenses/by/4.0/), which permits unrestricted use, distribution, and reproduction in any medium, provided you give appropriate credit to the original author(s) and the source, provide a link to the Creative Commons license, and indicate if changes were made. The Creative Commons Public Domain Dedication waiver (http://creativecommons.org/publicdomain/zero/1.0/) applies to the data made available in this article, unless otherwise stated.

to its intrinsically disordered nature. Under physiological conditions, aSyn is considered to be a pre-synaptic protein [37] that associates with vesicles and membranes [11].

According to the "Braak hypothesis", PD pathology is thought to start from the periphery (gut or nose), and progress until it reaches the brain [4, 5, 49], spreading in a prion-like manner [20, 29, 36]. However, this hypothesis is still controversial, and the molecular mechanisms underlying this phenomenon are not fully understood [25].

The vast majority of PD cases are sporadic but single point mutations in the gene encoding for aSyn (SNCA) cause familial forms of the disease [10]. The most recently identified aSyn mutation causes the substitution of alanine at position 53 by a glutamate residue (A53E), identified in a 36 year-old Finnish patient with atypical PD. The patient displayed a dense accumulation of SNCA inclusions in the striatum and a severe cortical pathology, affecting both the superficial and deep laminae [3]. In vitro, the A53E mutation was shown to reduce aSyn aggregation and fibril formation without changing the secondary structure content of the protein, when compared to WT aSyn [15]. These data suggest that the negatively charged glutamate residue may affect the folding and, consequently, the aggregation process of the protein.

In our study, we conducted a detailed study of the effects of the A53E mutation on aSyn using a combination of in vitro and cellular models of aSyn oligomerization and aggregation [40, 45]. Our results showed that the A53E mutation modulates aSyn aggregation in vitro and in vivo and impacts on distinct cellular pathways.

Altogether, the study of specific aSyn mutants provides novel insight into the spectrum of functions and cellular pathologies associated, opening novel avenues for the design of therapeutic strategies for PD and other synucleinopathies.

Materials and methods

Protein expression and purification

pET21a vectors (Novagen) encoding for WT aSyn and the A53E mutant were transformed into E. coli BL21 (DE3) cells. For protein expression, 10 ml overnight culture of transformed cells was used to inoculate 1 L of LB medium with 100 μg/mL ampicillin, which was further incubated at 37 °C and 250 rpm. At an OD_{600} 0.6, protein expression was induced with 1 mM of isopropyl-1-thio-β-D-galactopyranoside (IPTG) for 4 h at 37 °C. Afterwards, the cultures were centrifuged and the cell pellet frozen at −80 °C.

For cell lysis, pellets were resuspended in 15 mL of lysis buffer (50 mM Tris · HCl, 150 mM NaCl, 1 μg/mL Pepstatin A, 20 μg/ml Aprotinin, 1 mM Benzamidine, 1 mM PMSF and 1 mM EDTA) and sonicated on ice. The lysate was boiled for 10 min at 95 °C and soluble and insoluble fractions were separated by centrifugation at 48,384 × g, for 15 min. 136 μL/mL of 10% streptomycin sulfate and 228 μL/mL of glacial acetic acid was added to the supernatant. The resulting solution was centrifuged for 5 min at 48,384 × g, and the supernatant was collected and precipitated with saturated ammonium sulphate at 4 °C in a ratio 1:1 (v/v) with the supernatant. The pellets were washed with a 1:1 (v/v) solution of ammonium sulphate and water. The pellets were resuspended in 900 μL of ammonium acetate 100 mM and the same volume of 100% ethanol was added to precipitated aSyn.

Purification protocol was as adapted from [59]. Briefly, ethanol precipitated aSyn was resuspended in starting buffer (25 mM Tris · HCl at pH 8.0) and filtered through a Millex-HP filter syringe-driven filter unit (0.45 μm, Millipore). Anion exchange high-performance liquid-chromatography was carried out on an AKTA-FPLC (GE Healthcare). The sample was loaded, bounded to Hi-Trap column (GE Healthcare) and eluted with a NaCl linear gradient of elution buffer (25 mM Tris · HCl at pH 8.0, 1 M NaCl). The fractions containing aSyn were collected and buffer was exchanged for 20 mM ammonium acetate. The identity, and purity of the recombinant proteins was assessed by Mass Spectrometry and SDS-PAGE being higher than 99%.

Aggregation assays

The protein stocks were prepared by resuspending lyophilized protein in native buffer (10 mM sodium phosphate at pH 7.0) to a concentration of approximately 100 μM. Then, the protein stocks were filtered through 0.22 μm filter unit. The integrity of the protein and the absence of soluble oligomers at the beginning of the reaction was confirmed by gel filtration chromatography in a Superdex 75 10/300 column (GE Healthcare Life Sciences). Three aliquots of 300 μL of aSyn WT and A53E mutant were prepared from the protein stocks, in native buffer to a final concentration of 60 μM. Samples were incubated in an Eppendorf Thermomixer Comfort (Eppendorf, USA) with 0.02% sodium azide at 600 rpm and 37 °C.

Light scattering spectroscopy

The transition of aSyn from initial soluble monomeric form to aggregated state was determined by measuring light scattering in a Jasco FP-8200 spectrofluorometer (Jasco Inc, MD, USA) with an excitation wavelength of 330 nm and emission range from 320 to 340 nm at 25 °C. Final protein concentration was 10 μM in native buffer. Solutions without protein were used as negative controls. All experiments were carried out in triplicates

Thioflavin T binding assay

Th-T binding to amyloid fibrils was recorded using a JASCO FP-8200 spectrofluorometer (Jasco Inc, MD, USA) with an excitation wavelength of 445 nm and emission range from 460 to 600 nm at 25 °C, using a slit width of 5 nm for excitation and emission. The final concentration of Th-T was 25 μM and final protein concentration was 10 μM in native buffer. Solutions without protein were used as negative controls. All experiments were carried out in triplicates.

Congo red binding assay

CR binding to amyloid fibrils was tested using a Cary-400 Varian spectrophotometer (Varian Inc., Palo Alto, CA, USA) by recording the absorbance spectra from 375 to 675 nm, at 25 °C. A final concentration of 10 μM CR was added to 10 μM protein samples in native buffer. Protein solutions in the presence and absence of CR were used to calculate the differential CR spectra. All experiments were carried out in triplicates.

Transmission electron microscopy (TEM) assays

For negative staining, incubated samples were diluted in Mili-Q water to 10 μM and 10 μL were then placed on carbon-coated copper grids, and left to stand for 5 min. The grids were washed with distilled water and stained with 2% (w/v) uranyl acetate for 1 min. The morphology of aggregates of WT and A53E aSyn was observed using a JEOL JEM 1400 transmission electron microscope (JEOL, USA) at an accelerating voltage of 120 kV. The width of fibrils for WT and necklace-like structures for A53E was measured using ImageJ (250 measurements). Results are provided as Mean ± SE.

ATR-FTIR spectroscopy

Attenuated total reflectance Fourier transform infrared spectroscopy (ATR FT-IR) analysis of amyloid fibrils was performed using a Bruker Tensor 27 FTIR Spectrometer (Bruker Optics Inc.) with a Golden Gate MKII ATR accessory. Incubated samples were centrifuged and the insoluble fraction was resuspended in water. Each spectrum consists of 16 independent scans, measured at a spectral resolution of 4 cm^{-1} within the 1800–1500 cm^{-1} range. Second derivatives of the spectra were used to determine the frequencies at which the different spectral components were located. FTIR spectra were fitted to overlapping Gaussian curves using PeakFit package software (Systat Software).

Aggregation kinetics

Aggregation of aSyn, departing from soluble monomeric form, was monitored by measuring the transition from non-aggregated to aggregated state according to the Th-T fluorescence at 486 nm on a 96-wells microplate reader for 72 h at 37 °C (Victor Microplate reader, Perkin Elmer, USA). The reactions were carried out with 70 μM soluble purified WT and A53E aSyn in native buffer. Experiments were carried out in triplicates.

Sedimentation assay

aSyn aggregation was measured by sedimentation using centrifugation. The incubated samples of WT and A53E mutant were centrifuged at 48,384 × g for 30 min, and the supernatants were carefully removed. The amount of soluble aSyn was measured by absorbance at 280 nm using aSyn extinction coefficient $\varepsilon_{280} = 5960\ M^{-1}/cm^{-1}$, before and after centrifugation. All measurements were carried out in triplicates.

Primer design

The primers were designed according with the manufacturer's instructions (Table 1).

Generation of A53E aSyn constructs for expression in mammalian cells

A53E was inserted in the Venus-BiFC system [45] or SynT [40] by site-directed mutagenesis (QuickChange II Site-Directed Mutagenesis Kit, Agilent Technologies, SC, USA) following the manufacturer's instructions. All constructions were confirmed by sequencing.

Cell culture

Human Embryonic Kidney 293 (HEK) cells were grown in Dulbecco's Modified Eagle Medium (DMEM, Life Technologies- Invitrogen, Carlsbad, CA, USA), and human neuroglioma cells (H4) in Opti-MEM I with Glutamax (Life Technologies- Gibco, Carlsbad, CA, USA), both supplemented with 10% Fetal Bovine Serum Gold (PAA, Cölbe, Germany) and 1% Penicillin-Streptomycin (PAN, Aidenbach, Germany). Cells were grown at 37 °C, with 5% of CO2.

Cell transfection

HEK cells

The day before transfection, 100 000 cells were plated in 12-well plates (Costar, Corning, New York, USA). The cells were transfected with equimolar amounts of the plasmids using Metafectene (Biotex, Munich, Germany) as specified by the manufacturer. After twenty-four hours, the cells were collected or stained for further analysis.

Table 1 Primers used to perform site-directed mutagenesis and generate the A53E mutant

A53E forward	5′ GAGTGGTGCATGGTGTGGAAACAGTGGCTGAGAAGAC 3′
A53E reverse	5′ GTCTTCTCAGCCACTGTTTCCACACCATGCACCACTC 3′

H4 cells

Eighty thousand cells were plated in 12-well plates (Costar, Corning, New York, USA). After 24 h, equal amount of SynT and Synphilin-1 were transfected using FuGENE6 Transfection Reagent (Promega, Madison, USA) in a ratio of 1:3 according to the manufacturer's recommendation. Forty-eight hours after transfection, the cells were processed for different assays.

Immunocytochemistry

After transfection, cells were fixed with 4% paraformaldehyde at room temperature (RT), followed by a permeabilization with 0.5% Triton X-100 (SigmaAldrich, St. Louis, MO, USA). The cells were blocked in 1.5% normal goat serum (PAA, Cölbe, Germany)/1xPBS (1.37 M NaCl, 27 mM KCl, 101.4 mM $Na_2HPO_4 7 \cdot H_2O$, 16.7 mM KH_2PO_4), and then incubated with primary antibody. Primary antibodies used in this study were: mouse Syn1 (1:1000, BD Transduction Laboratory, New Jersey, USA) or rabbit anti-aSyn (1:1000, Abcam, Boston, USA), anti-Giantin (1:1000, Abcam, Boston, USA), aSyn-S129 1:1000 (Wako Chemicals USA, Inc., Richmond, USA) overnight, and secondary antibody (Alexa Fluor 488 donkey anti-mouse IgG and/or Alexa Fluor 555 goat anti rabbit IgG, (Life Technologies- Invitrogen, Carlsbad, CA, USA)) for 2 h at RT. Cells were finally stained with Hoechst 33258 (Life Technologies- Invitrogen, Carlsbad, CA, USA) (1:5000 in DPBS) for 5 min, and maintained in 1xPBS for imaging.

Yeast transformation and plasmids

The p426GAL-aSyn-GFP plasmid carries the human gene of aSyn with a C-terminal fusion to GFP, under the regulation of GAL1 inducible promoter [44]. This plasmid was used to generate aSyn A53E by site directed mutagenesis. The yeast cells W303-1A (MATa; can1-100; his3-11,15; leu2-3,112; trp1-1; ura3-1; ade2-1) were transformed with the indicated plasmids using lithium acetate standard method [16].

Yeast growth

For all experiments, an inoculum was prepared to obtain cells in log growth phase, using synthetic complete (SC) medium [0.67% (w/v) yeast nitrogen base without amino acids (Difco), 1% (w/v) raffinose and 0.79 $g.L^{-1}$ complete supplement mixture (CSM) (QBiogene)], 200 rpm, 30 °C, as we described [57]. To induce aSyn expression, in liquid medium, cells were grown ($OD_{600\ nm}$ 0.2) in SC selective medium 1% (w/v) galactose (aSyn ON) for 7 h at 30 °C, 200 rpm. aSyn cytotoxicity was evaluated by spotting assays. $OD_{600\ nm}$ was set to 0.1 ± 0.005 and 1:10 serially dilutions of each sample were prepared [57]. Then, 4 µL of each dilution was spotted in solid SC selective medium containing 2% glucose (aSyn OFF) or 1% (w/v) galactose (aSyn ON) and incubated at 30 °C for 36–42 h. Images were acquired using ChemiDoc Touch (Bio-Rad).

Fluorescence microscopy

HEK cells expressing the aSyn Venus-BiFC assay were visualized using the Olympus IX81-ZDC microscope system, with a 20× objective. One hundred images were randomly taken out of four independent experiments. Total intensity was measured using the Olympus Scan^R Image Analysis Software.

In order to determine the percentage of yeast cells with aSyn inclusions, cells were grown as described above and GFP fluorescence was visualized with a Zeiss Z2 Widefield Fluorescence microscope. The percentage of cells presenting aSyn inclusions was then determined by counting at least 300 cells for each treatment using ImageJ software.

Quantification of aSyn inclusions

Cells expressing aSyn were scored according with the presence or absence of inclusion on transfected cells. Three independent experiments were performed, and the results were expressed as the percentage of the total number of transfected cells.

Thioflavin S staining

Freshly prepared, 0.5% of Thio-S (Sigma-Aldrich, St. Louis, MO, USA) was incubated within the cells for 5 min. The cells were washed three times with 80% ethanol, and maintained in 1xPBS for fluorescence microscopy.

Quantification of Golgi fragmentation

Golgi morphology was assessed in transfected HEK and H4, and scored into three groups, was we previously published [32] (normal, diffused and fragmented). Three independent experiments were performed.

Western blot analysis

HEK and H4 cells were lysed with Radio-Immunoprecipitation Assay (RIPA) lysis buffer (50 mM Tris pH 8.0, 0.15 M NaCl, 0.1% SDS, 1% NP40, 0.5% Na-Deoxycholate), 2 mM EDTA and a Protease Inhibitor Cocktail (1 tablet/10 mL) (Roche Diagnostics, Mannheim, Germany). Protein concentration was determined by Bradford assay (BioRad Laboratories, Hercules, CA, USA), and the sample were denaturation for 5 min at 100 °C in protein sample buffer (125 mM of 1 M Tris HCl pH 6.8, 4% SDS 0,5% Bromophenol blue, 4 mM EDTA, 20% Glycerol, 10% b-Mercapto ethanol). The gels were loaded with 80 µg protein, and the samples separated on 12% SDS-polyacrylamide gels. The gel was transferred to a PVDF membrane using a Trans-Blot Turbo transfer system (BioRad), according to the manufacturer's instructions. Membranes were blocked with 5% (w/v) skim milk (Fluka,

Sigma-Aldrich St. Louis, MO, USA), and incubated with Syn1 (1:1000, BD Biosciences, San Jose, CA, USA), and 1:2000 anti-b-actin (Sigma-Aldrich, St. Louis, MO, USA) overnight at 4 °C. After washing, the membranes were incubated for 1 h with secondary antibody, anti-mouse IgG, or anti-rabbit IgG, horseradish peroxidase labeled secondary antibody (GE Healthcare, Bucks, UK) at 1:10,000. Proteins were detected by ECL chemiluminescent detection system (Millipore, Billerica, MA, USA) in Fusion FX (Vilber Lourmat). The band intensity was estimated using the ImageJ software (NIH, Bethesda, MD, USA) and normalized against b-actin.

For aSyn quantification total yeast protein extraction and western blot was performed following standard procedures as described before [57]. Antibodies used: aSyn (BD Transduction Laboratories, San Jose, CA, USA), pS129-aSyn (Wako Chemicals USA, Inc., Richmond VA, USA) PGK (Life Technologies, PaisleyUK). Triton soluble and insoluble fractions were processed and analyzed as described before [56].

Native PAGE

For native PAGE, HEK cells were lysed in 1xPBS pH 7.4 with Protease Inhibitor Cocktail tablet and separated in 4–16% gradient Native pre-cast gel (SERVA Electrophoresis GmbH, Heidelberg, Germany). Gels were run according to the manufacturer's instructions, and transferred as previously described.

Proteinase K digestion

H4 cells samples were digested with Proteinase K (2.5 μg/mL) (Roth, Carlsbad, Germany) for 1, 3, and 5 min at 37 °C. The enzyme reaction was stopped with protein sample buffer, and the samples were separated in a SDS-page gel, as described above.

Flow cytometry (FCM)

FCM was performed in a BD FACSCanto II. To analyze cell viability yeast cells transformed with the indicated plasmids were incubated with 5 $\mu g.mL^{-1}$ PI, for 15 min at 30 °C, 200 rpm and protected from light. Cells were then washed with PBS and used to FCM. A minimum of 10,000 events were collected for each experiment. Results were expressed as median fluorescence intensity (MFI) of a molecule.

Measurement of 26S Proteasome Catalytic Activity

The chymotrypsin-like activity of the 26S proteasome was determined has previously described [27]. Briefly, after 48 h transfected cells were collected in lysis buffer (50 mM Tris, pH 7.5, 250 mM Sucrose, 5 mM $MgCl_2$, 1 mM DTT, 0.5 mM EDTA, 0.025% Digitonin, 2 mM ATP). The reaction was initiated with 15 μg from the total protein lysates, together with the addition of reaction buffer (50 mM Tris (pH 7.5), 40 mM KCl_2, 5 mM $MgCl_2$, 1 mM DTT, 0.5 mM ATP, 100 μM Suc-LLVYAMC) were mix in 100 μl fina volume. The fluorescence of AMC (380 nm ex-Citation and 460 nm emission) was monitored in a microplate fluorometer (Infinite M1000, Tecan) at 37 °C. As control, proteasome was inhibited with 20 μM MG132 (Sigma, Hamburg, Germany) prior to the measurements.

Statistical analyses

Data were analyzed using GraphPad Prism 6 (San Diego California, USA) software and were expressed as the mean + − SD. Statistical differences from WT aSyn were calculated using unpaired Student t-test and one-way ANOVA with post-hoc Tukey's test. Significance was assessed for, where * corresponds to $p < 0.05$, ** corresponds to $p < 0.01$ and *** corresponds to $p < 0.001$.

Results

A53E mutant forms protofibrils by reducing aSyn fibrilization

To understand the effect of the A53E substitution in the aggregation process of aSyn (Fig. 1a), we assembled a pipeline of both in in vitro and cellular studies, in human and yeast cells (Fig. 1b), and conducted a battery of experiments to characterize the behavior of this recently identified aSyn mutant form.

We started to compare the in vitro aggregation properties of WT and A53E aSyn using synchronous light scattering, sedimentation and binding to amyloid-binding dyes. For these assays, the soluble forms of both proteins were incubated at 60 μM under agitation at 37 °C for two weeks. The light scattering signal was 6-fold higher for WT aSyn than for the A53E mutant, suggesting differences in aggregation process (Fig. 2a). Using spectrophotometry, we quantified the levels of aggregated protein in both solutions after separating aSyn in two fractions (soluble and insoluble), by centrifugation. The amount of protein in the insoluble fraction in the WT aSyn preparation was two times higher than with A53E (*$p < 0.05$, Fig. 2b).

The presence of amyloid fibrils can be detected in vitro using Thioflavin T (Th-T), a dye that specifically binds to amyloid fibrils [35, 51]. In agreement with light scattering and sedimentation data, we found that the Th-T fluorescence signal was 10 times lower for A53E than for WT aSyn (Fig. 2c). The presence of amyloid fibrils can be further detected by monitoring the increase of the absorbance of Congo Red (CR) and the red shift of the dye absorbance maximum [28]. The binding of A53E to CR was negligible, since the peak of absorbance in the presence of A53E aSyn was similar to that of free CR (Fig. 2d). In contrast, we observed a dramatic spectral change in CR for WT aSyn (Fig. 2d). To confirm the different amyloidogenic propensities of WT and A53E aSyn, we analyzed the morphological features of the aggregates formed using

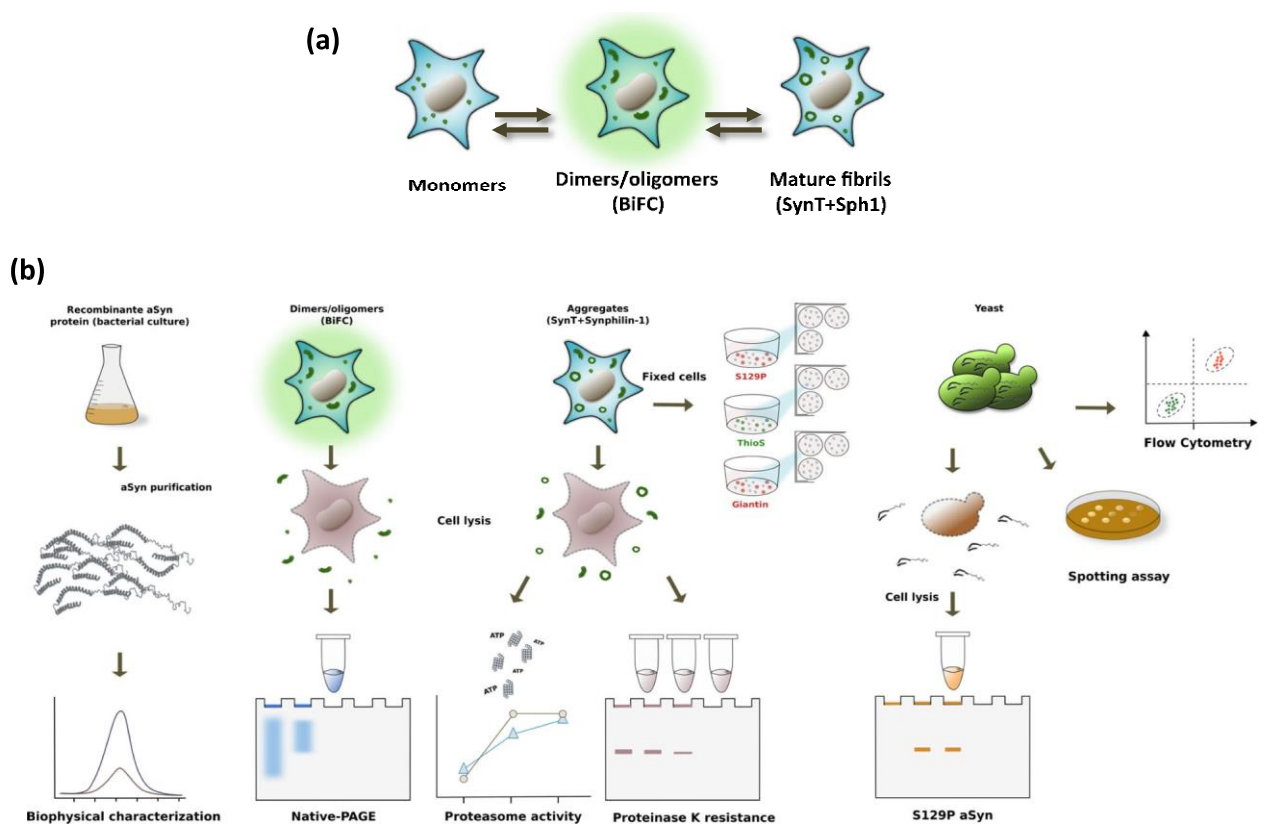

Fig. 1 Aggregation process and study design. **a** aSyn aggregation process in cell models. **b** Experimental design used in the study. In vitro studies and studies in cell models were used to assess the effect of the A53E mutation on aSyn

transmission electron microscopy (TEM). Although we detected the presence of higher order complexes in both preparations, their size and morphology was different. For WT aSyn, we observed the typical long and unbranched amyloid fibrils (Fig. 2e), 11.6 ± 0.4 nm with a width of 11.6 ± 0.4 nm (Fig. 2e). In contrast, the structures formed by A53E aSyn exhibited a protofibrillar appearance, with small round oligomeric structures that seemed to be linked in a necklace fashion, with a width of 28.5 ± 0.7 nm (Fig. 2f-g).

To assess the secondary structure content of the assemblies formed by WT and A53E aSyn, we analyzed the amide I region of the FTIR spectrum (1700–1600 cm^{-1}). This region of the spectrum corresponds to the absorption of the carbonyl peptide bond of the main amino acid chain of the protein, and is a sensitive marker of the protein secondary structure. After deconvolution of the FTIR spectra of the aSyn solutions, we were able to assign the individual secondary structure elements and their relative contribution to the main absorbance signal at the end of the aggregation reaction (Fig. 2g and h and Table 2). The absorbance spectra were radically different for WT and A53E aSyn. While the spectrum of WT aSyn was dominated by a peak at 1625 cm^{-1}, attributable to the presence of amyloid-like inter-molecular β–sheet structure (Fig. 2g), the spectrum of the A53E mutant was dominated by a peak at 1649 cm^{-1} corresponding to disordered/random coil conformation (Fig. 2h).

Next, we monitored how the mutation impacted on the aggregation kinetics of aSyn by continuously monitoring the changes in Th-T binding over time for WT and A53E variants. The kinetics of amyloid fibril formation usually follows a sigmoidal curve that reflects a nucleation-dependent growth mechanism. The aggregation of both proteins followed this pattern, with an apparent lag phase of 8 h (Fig. 2i). After this lag phase, the two aggregation reactions diverged significantly, with an exponential increase for WT aSyn that plateaued at around 55 h, and a steady and much slower increase for A53E aSyn, reaching a 3.5-times lower fluorescence intensity. Altogether, our data demonstrates that the A53E mutation reduces aSyn amyloid formation in vitro.

The A53E mutation decreases aSyn oligomerization in cellular models

We next investigated the effects of the A53E mutation on the behavior of aSyn in the context of living human cell models. First, we used the Bimolecular Fluorescence

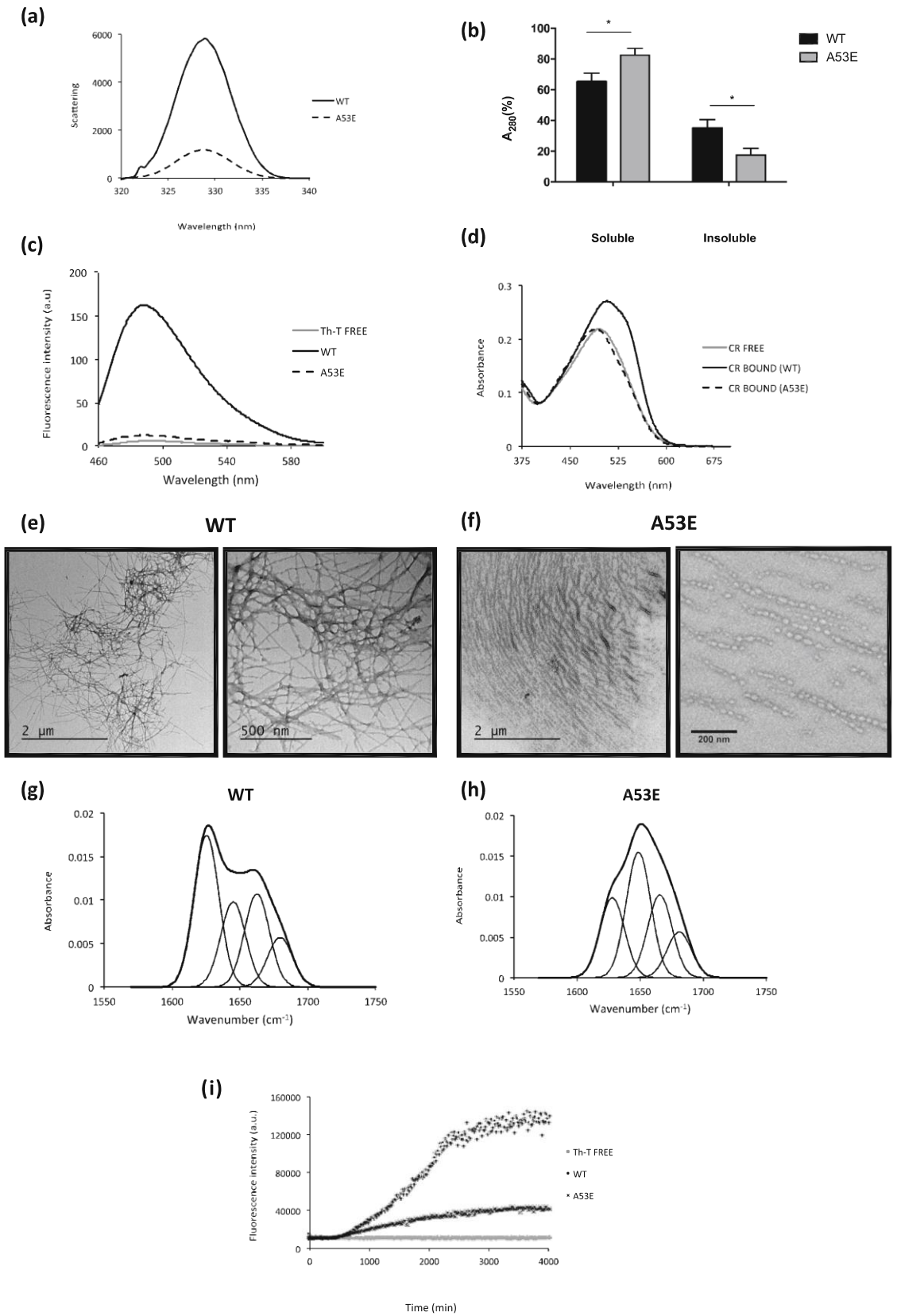

Fig. 2 (See legend on next page.)

(See figure on previous page.)

Fig. 2 Aggregation properties of WT and A53E aSyn variants. aSyn WT and A53E mutant, prepared at 60 μM in 10 mM sodium phosphate, pH 7.0, were incubated for 2 weeks under agitation at 37 °C. **a** Static light scattering of 10 μM aSyn in 10 mM sodium phosphate, WT (*solid line*) and A53E mutant (dashed line). **b** Distribution of aSyn between the soluble and insoluble fractions. **c** Fluorescence emission spectra of Th-T upon incubation with 10 μM aSyn WT (solid line) and A53E mutant (dashed line). Free Th-T emission spectrum is represented in grey. **d** CR absorbance spectra in the presence of 10 μM aSyn WT (solid line) and A53E mutant (dashed line). Free CR absorbance spectrum is represented in grey. **f-g** Morphology of WT and A53E aSyn aggregates TEM micrographs. Negatively stained aggregates formed by aSyn WT (left panel) and A53E mutant (right panel) incubated for two weeks. h-i Secondary structure of WT and A53E aSyn aggregates. Secondary structure content of the aSyn WT and A53E mutant after two weeks incubation. ATR-FTIR absorbance spectra in the amide I region was acquired (thick line) and the fitted individual bands after Gaussian deconvolution are shown (thin lines). **i** Aggregation kinetics of WT and A53E aSyn. Aggregation kinetics of aSyn were monitored by following the changes in relative ThioT fluorescence emission. Concentration of protein was 70 μM WT aSyn (crosses) and A53E mutant (dots) in a final volume of 150 μL. The evolution of Th-T fluorescence in the absence of protein is represented in grey, n = 3

Complementation (BiFC) assay to monitor aSyn oligomerization, as we previously described [45]. Briefly, non-fluorescence Venus fragments are fused to either the N- or C-terminus of aSyn and, upon dimerization/oligomerization of the protein, the fluorophore is reconstituted resulting in fluorescence signal. While this assay involves the tagging of aSyn with fragments of fluorescent proteins, it constitutes a powerful paradigm to assess aSyn oligomerization. We observed that A53E aSyn, similarly to WT, formed dimers/oligomers (Fig. 3a). However, the fluorescence signal was lower than that observed with WT aSyn, suggesting differences in the dimerization/oligomerization process (**$p < 0.01$) (Fig. 3b), since the levels of expression of WT and A53E aSyn were identical (Fig. 3c and d, Additional file 1: Figure S2.1 and Additional file 1: Figure S2.2). We also found that the A53E mutant produced high molecular weight species, similar to WT aSyn (Fig. 3e). Thus, we refer to the species formed as oligomers, for simplicity.

The A53E mutation alters the biochemical properties of aSyn inclusions

Next, we investigated if the later stages of the aSyn aggregation process were altered by the A53E mutation. For that, we used a well-established cell-based aggregation model that consists in the co-expression of SynT (C-terminally modified aSyn) and Synphilin-1 [40], since expression of aSyn alone does not result in inclusion formation. In this aSyn aggregation model, aSyn inclusions are readily detected by immunocytochemistry using antibodies against aSyn, allowing the characterization of different types of inclusions [32], and screening modulators of aSyn aggregation [41]. 48 h after transfection, we analyzed inclusion formation in the cells (Fig. 4a), and observed that the A53E mutation did not alter inclusion formation when compared to WT aSyn (Fig. 4b). Again, no differences in the levels of aSyn or Synphilin-1 were detected between WT and A53E mutant aSyn (Fig. 4c-e).

aSyn is phosphorylated on Serine 129 (pS129) in LBs found in the brains of PD patients, linking this post-translational modification with disease [14, 52]. We previously showed that specific aSyn mutations, such as the E46K, can alter pS129 on aSyn [39]. Thus we investigated the effect of the A53E mutation on S129 phosphorylation. We found that both WT and A53E aSyn inclusions were positive for pS129 (Fig. 4f).

To further investigate the biochemical nature of the inclusions formed by the A53E aSyn mutant, we stained the cells with Thioflavin S (Th-S), a dye that binds to β-sheet rich amyloid structures [33]. We observed that the larger inclusions formed by WT and A53E aSyn stained positive for Th-S (Fig. 4g). In addition, we also used proteinase K (PK) resistance as a marker of aggregate formation, as protein inclusions tend to be more resistance to PK digestion. Interestingly, we found that the A53E mutant was less resistant when compared to WT aSyn (Fig. 4h and i), suggesting the inclusions formed by the A53E mutant have a less-compact nature than those formed by the WT protein.

The ubiquitin-proteasome system (UPS) is the major non-lysosomal pathway for selective protein degradation. In cell models, it has been shown that aSyn accumulation can affect the activity of the UPS system [61]. In our experimental conditions, we observed that cells expressing A53E aSyn mutant display increased proteolytic activity of the proteasome (Fig. 4j and k).

Table 2 Assignment of secondary structure components of aSyn variants in the amide I region of the FTIR spectra

	WT			A53E		
	Band (cm^{-1})	Area (%)	Structure	Band (cm^{-1})	Area (%)	Structure
1	1625	40	β -sheet (inter)	1628	24	β -sheet (inter)
2	1645	22		1649	38	
3	1663	25	Loop/β-turn/bend/α-helix	1666	25	Loop/β-turn/bend/α-helix
4	1680	13	β-turn	1681	14	β-turn

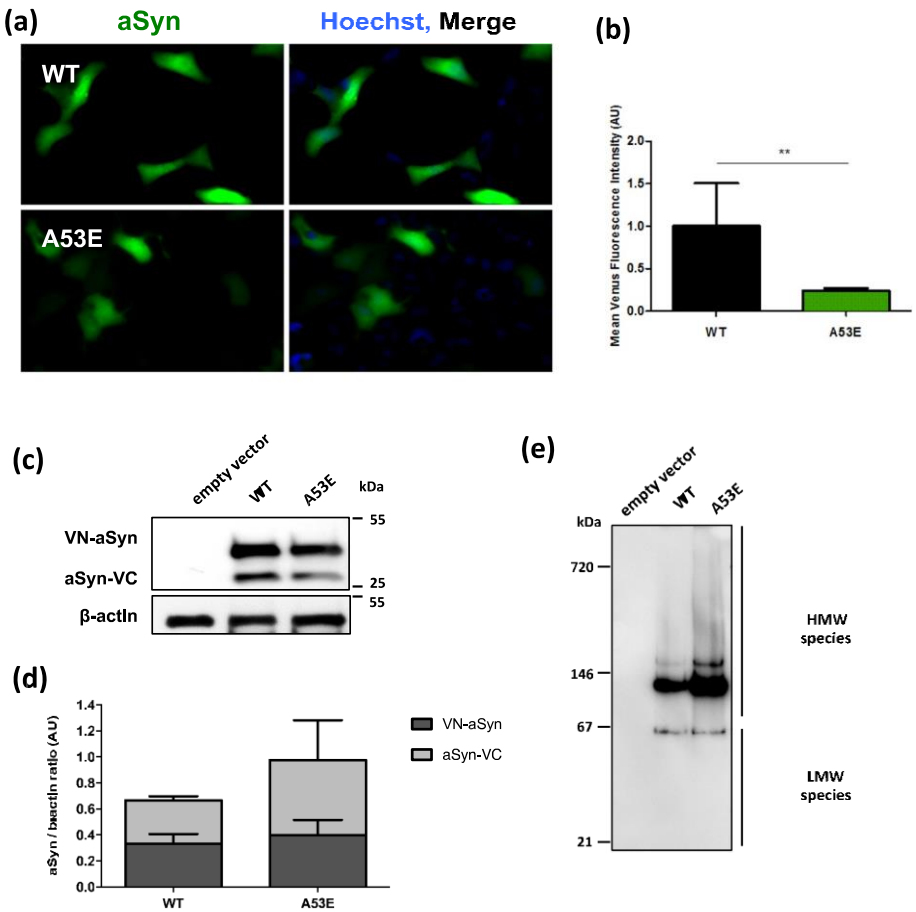

Fig. 3 A53E reduces aSyn oligomerization. **a** Fluorescent cells, expressing VN-aSyn and aSyn-VC constructs, as a result of the aSyn interaction. Scale bar: 30 μm. **b** Mean fluorescence intensity of cells were assessed 24 h post-transfection using an Olympus IX81-ZDC microscope. For each condition, 100 pictures were acquire in 4 independent experiments were conducted. Student's t test (**$p < 0.01$). **c-d** aSyn protein levels were assessed by immunoblot analysis and were found to similar between WT aSyn and the A53E mutant. n = 3. **e** Native-PAGE gel showed that the A53E mutant forms high molecular weight species similar to WT aSyn

aSyn aggregation leads to Golgi fragmentation

aSyn induces several cellular pathologies that have been documented over the years and are routinely used to assess the effect of specific mutations or genetic interactors [60]. One particular type of cellular pathology associated with aSyn toxicity is the fragmentation of the Golgi apparatus [13]. This is also evident in other neurodegenerative diseases [18], suggesting it might be a more general response to the proteotoxicity associated with protein misfolding and aggregation. To assess whether expression of A53E mutant aSyn affected the integrity of the Golgi, we analyzed the morphology of this organelle in both the aSyn oligomerization and aggregation models (Fig. 5a and c). We classified the morphology of the Golgi as normal, diffuse and fragmented, as we previously described [32].

In the oligomerization model, we observed that WT aSyn reduced the percentage of cells exhibiting normal Golgi morphology (~40%, ***$p < 0.001$ Fig. 5a and b and Additional file 1: Figure S3.1–3.3), as we previously reported [32]. However, in cells expressing the A53E mutant the effects were not as pronounced as with WT, and the phenotype was more similar to that of cells carrying an empty vector (~70% and 80% of the transfected cells displayed normal Golgi morphology for A53E, and empty vector, respectively) (*$p < 0.05$) (Fig. 5b and Additional file 1: Figure S3.1).

In the aSyn aggregation model, we observed the opposite effect. Around 50% of the cells expressing the A53E SynT displayed normal Golgi morphology whereas around 70% of the cells expressing WT SynT displayed normal Golgi (Fig. 5c and d and Additional file 1: Figure S2.4–2.6; ***$p < 0.001$ and *$p < 0.01$ for empty vector, and WT, respectively). This suggests that the aggregation of A53E aSyn induces Golgi alterations.

A53E aSyn behaves identically to WT aSyn in yeast cells

Yeast cells have been extremely useful to assess cellular pathologies associated with the expression of aSyn. Thus,

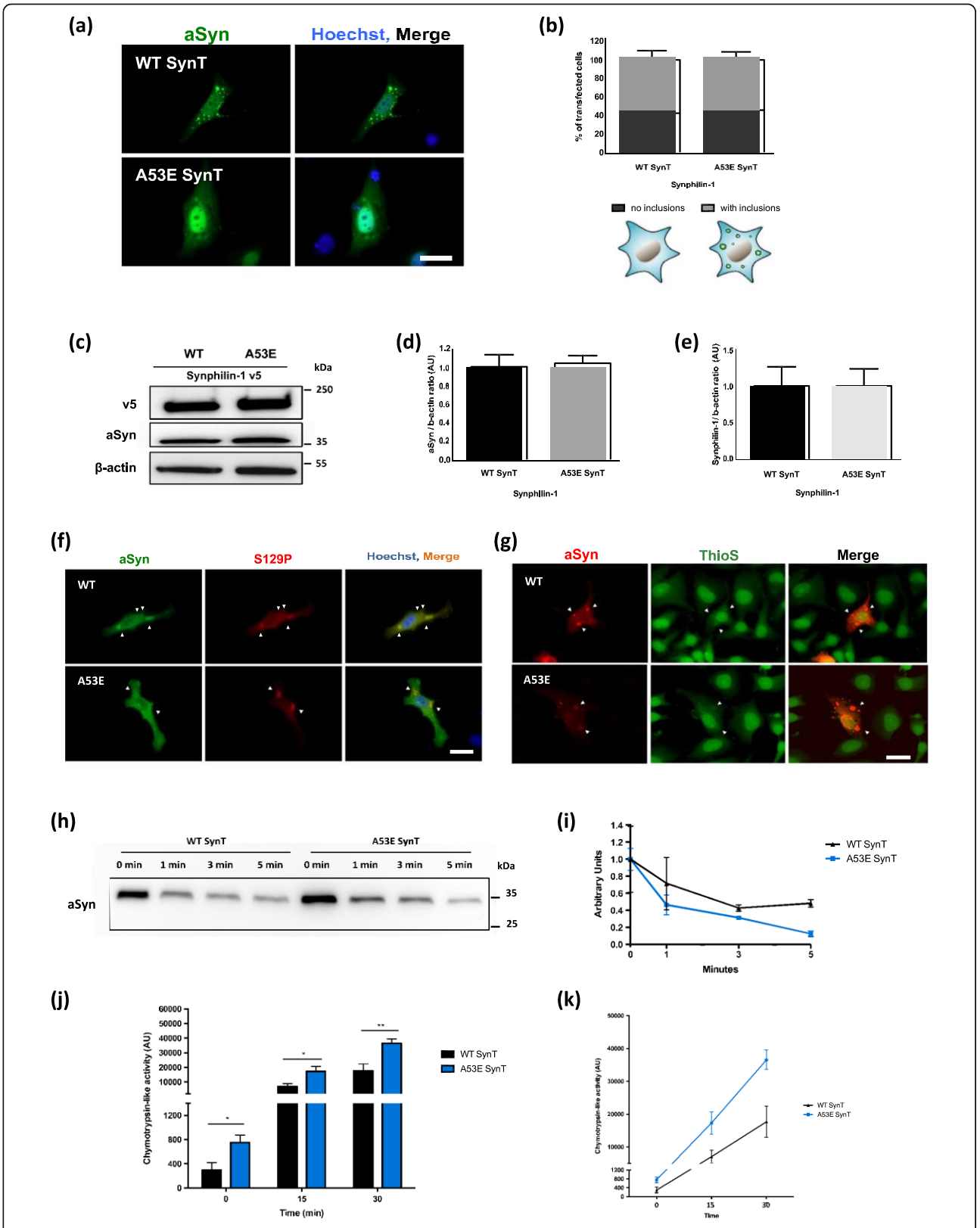

Fig. 4 (See legend on next page.)

(See figure on previous page.)

Fig. 4 A53E does not change the inclusion pattern. **a-b** At least 50 cells per condition were classified according to the pattern formed. We observed that A53E did not change the number of inclusions per cells. n = 3. Scale bar: 30 μm. **c-e** Immunoblot analysis of the aSyn and Synphilin-1 levels showed no significant differences in expression of WT or A53E aSyn. n = 3 (**f**) Inclusions formed by WT and A53E are positive for pS129. Positive inclusions are indicated with white arrows. Scale bar: 30 μm. **g** Inclusions were stained with Th-S and analyzed via fluorescence microscopy. As indicated with arrow heads, we observed that some inclusions displayed amyloid-like properties, by staining positive with Th-S. Scale bar: 30 μm. **h-i** WT and A53E aSyn protein lysates were digested with PD for different times (1, 3 and 5 min). After normalization of the values to the undigested condition, we observed that A53E inclusions are less resistant to PK-digestion. n = 2. **j-k** 48 h post-transfection the cells were collected and we assessed the activity of the proteasome. We observed that cells expressing A53E mutant increased proteolytic activity of the proteasome in comparison with WT. n = 3. Student's t test (*$p < 0.05$, **$p < 0.01$)

in order to assess if the A53E mutation alters the cytotoxicity and aggregation of aSyn, we expressed this mutant in S. cerevisiae and monitored phenotypes previously established [44]. We expressed WT or mutant A53E aSyn fused to eGFP using multi-copy (2 μ) plasmids and under the regulation of a galactose-inducible promoter (GAL1). aSyn cytotoxicity was first evaluated by a spotting assay. The growth of the cells expressing A53E aSyn was compared to that of cells expressing WT aSyn (Fig. 6a). As described before, expression of WT aSyn is toxic and results in reduced cell growth (Fig. 6a). We found that cells expressing A53E aSyn display a similar phenotype, suggesting that this familial mutation does not significantly affect aSyn toxicity in yeast (Fig. 6a). To further dissect the cytotoxicity of the A53E mutant, we performed propidium iodide (PI) staining and flow cytometry analysis, a readout of plasma membrane integrity (Fig. 6b). We observed that, 7 h after induction of aSyn expression, no significant differences were observed between cells expressing either WT or the A53E aSyn (Fig. 6b).

Next, we evaluated the subcellular distribution of the A53E mutant aSyn, using fluorescence microscopy. 7 h after induction of aSyn expression we assessed inclusion formation in the cells (Fig. 6c). The expression of A53E aSyn resulted in the formation of cytoplasmic inclusions that looked similar to those formed in cells expressing aSyn WT (Fig. 6c). In addition, no significant differences were observed in the percentage of cells with inclusions between WT and the A53E (Fig. 6c). We also evaluated the levels of aSyn expression by immunoblot analyses and found that both proteins were expressed at similar levels (Fig. 6d). The levels of phosphorylation on serine 129 were also indistinguishable between WT and A53E mutant aSyn (Fig. 6d).

Discussion

aSyn plays a major role in the pathological processes involved in neurodegenerative diseases, like PD or Dementia with Lewy Bodies [26]. When overexpressed in cells, to mimic familial forms of PD associated with multiplications of the aSyn gene, aSyn can promote cytotoxicity and impair vital processes, thereby contributing to cell death [9, 38, 44]. However, the precise molecular mechanisms underlying aSyn toxicity are still unclear, compromising our ability to intervene therapeutically. Both mutations and multiplications of the SNCA gene cause familial forms of PD [8, 22, 64]. Currently, six missense mutations in aSyn have been associated with autosomal dominant forms of parkinsonism (A30P, E46K, H50Q, G51D, A53E, A53T) [1, 30, 34, 46–48, 65]. Of these, the A53E was the last one to be identified and, therefore, has been less investigated.

In this study, we aimed to investigate the effect of the substitution of the alanine at position 53 by a glutamic acid residue that introduces an additional negative charge in the protein. For this purpose, we used in vitro techniques to characterize the biophysical effects of the mutation, and exploited cell-based models to assess the effects of the expression of the A53E mutant on the distribution, aggregation, and toxicity of the protein.

In vitro, we observed that A53E attenuates aSyn aggregation and reduces amyloid fibril formation when compared to WT aSyn. In fact, the formation of amyloid structures by the A53E mutant is marginal, since A53E is unable to bind CR. Overall, these observations are in line with a previous report showing that the presence of a negatively-charged residue can reduce the intrinsic aggregation propensity of aSyn [15]. Nevertheless, because the change in net charge in aSyn is small, −9 and −10 for the WT and A53E proteins, respectively, the effect this mutation has on aggregation has more likely a local origin. We used the Amylpred2 consensus aggregation predictor to analyze if the A53E mutation might have an impact in the intrinsic aggregation propensity of the aSyn sequence. Amylpred2 identifies a hot spot of aggregation corresponding to the 49–55 sequence stretch (VHGVATV), including Ala53. The A53E mutation shortens the aggregation region now including only residues 49–53 (VHGVE). The AGGRESCAN algorithm enables the comparison of the aggregation propensity of the two regions, showing that it is 2.1 lower for A53E than for WT aSyn.

In the context of a cell, the behavior of a protein is subjected not only to the crowded environment but also to the action of various protein quality control mechanisms. In human cells, we observed that the A53E mutation reduces aSyn oligomerization without changing the aggregation pattern. Interestingly, the inclusions formed

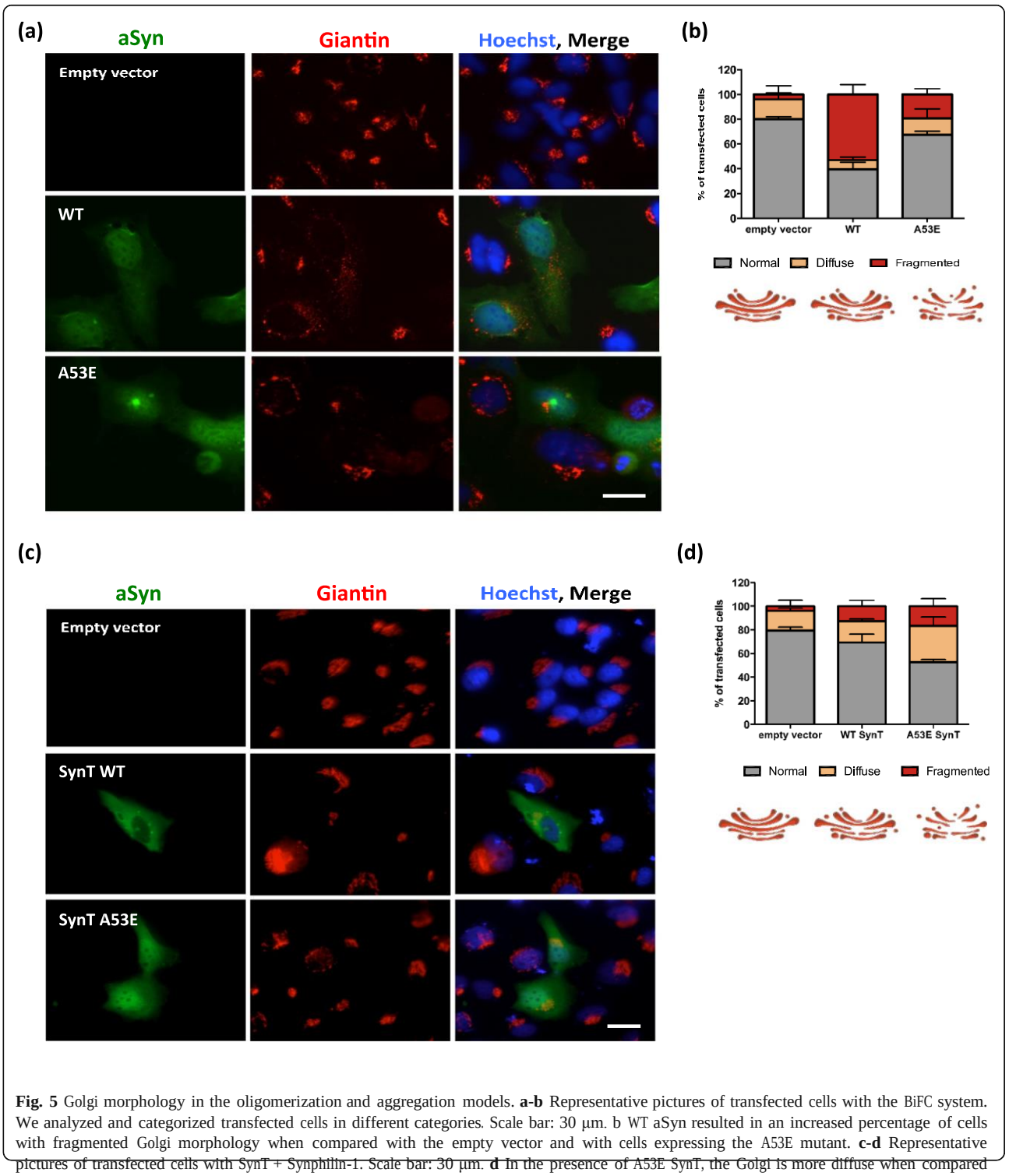

Fig. 5 Golgi morphology in the oligomerization and aggregation models. **a-b** Representative pictures of transfected cells with the BiFC system. We analyzed and categorized transfected cells in different categories. Scale bar: 30 μm. b WT aSyn resulted in an increased percentage of cells with fragmented Golgi morphology when compared with the empty vector and with cells expressing the A53E mutant. **c-d** Representative pictures of transfected cells with SynT + Synphilin-1. Scale bar: 30 μm. **d** In the presence of A53E SynT, the Golgi is more diffuse when compared with the control and with WT SynT. n = 3

by A53E aSyn are more sensitive to PK digestion than those formed by WT aSyn, suggesting that the inclusions formed are less compact or, possibly, more immature. The negative charge introduced by the glutamate residue can perhaps alter the intermolecular interactions between aSyn molecules, and prevent the formation of tighter inclusions. This may also correlate with the increase in proteasome activity that we observed, since this is an important degradation system to eliminate soluble proteins and smaller assemblies that are not degraded by autophagy.

In our previous studies, we did not observe major differences when comparing another PD-associated aSyn mutant

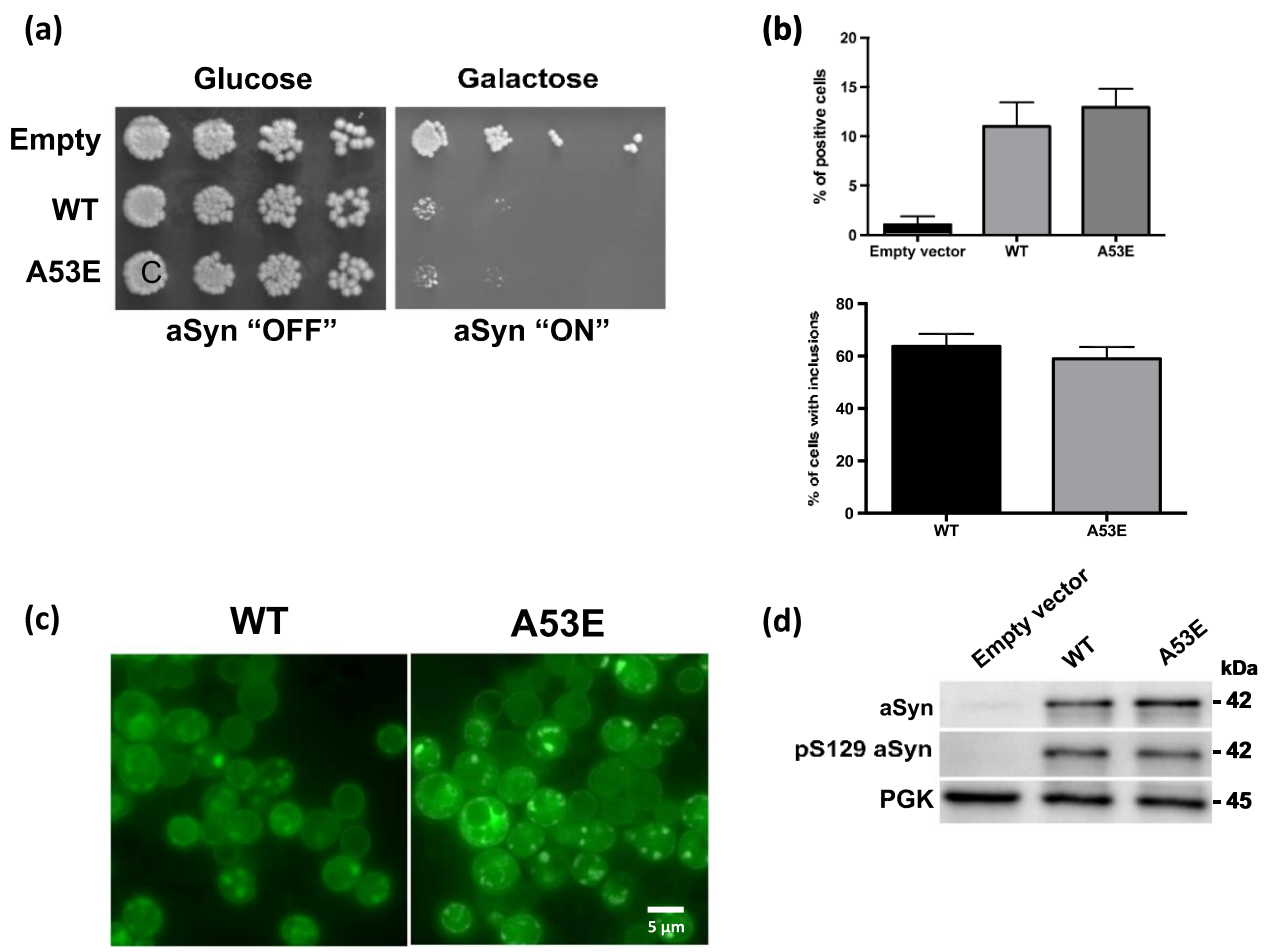

Fig. 6 Phenotypic characterization of yeast cells expressing the A53E aSyn mutant. **a** Cytotoxicity of WT and A53E aSyn in yeast cells compared to the empty vector, assessed by spotting assay. Photos were taken 3 days after incubation at 30 °C. **b** Frequency of PI positive cells assessed by flow cytometry, after 7 h of induction of expression of WT and A53E aSyn. c Fluorescence microscopy visualization (left panel) and percentage of cells with WT and A53E aSyn inclusions (right panel). **d** Expression levels of WT and A53E aSyn-GFP in yeast cells assessed by western blot analysis of total protein extracts. Results shown are from one representative experiment from at least three independent experiments. Values represent the mean ± SD of at least three independent measurements

at position 53 (A53T) with WT protein. We found that the aggregation of A53T aSyn was identical to that of WT aSyn [32], suggesting again that the change in charge at position 53 may influence the initial steps of the aggregation process (dimerization/oligomerization) of aSyn, and not the later steps that culminate with the formation of the mature inclusions. Also, the differences might result by difference spatial sequestration of aSyn. Misfolded proteins can be targetted to specific compartments, like aggresomes, to facilitate their degradation [23, 24, 62]. These compartments rely on filament network proteins like vimentin, actin, and tubulin, or proteins that can assist in the transportation of misfolded proteins through the microtubule network, such as p62 (24843142, 12093283, 14623963, 24086678). For example, Tubulin Polymerization Promoting Protein (TPPP/p25), belongs to the microtubule network, and associates with aSyn in pathological conditions, possibly affecting aSyn aggregation (17123092).

The Golgi apparatus plays a determinant role in the intracellular flow of several endogenous proteins and exogenous macromolecules, regulating the trafficking to their final destination inside or outside cells [12]. Fragmentation of the Golgi apparatus is a characteristic feature in several neurodegenerative diseases, including PD [13, 18, 19]. Interestingly, in our cell-based aggregation models, we observed a striking loss of the typical Golgi morphology in cells expressing A53E aSyn. Previous studies about the effect of this recently identified PD mutation in aSyn showed that A53E is as toxic as WT aSyn [15, 50]. While this was also the trend we observed in our cellular models, our findings suggest that the A53E mutant may cause specific alterations in cell physiology

that are still not understood and demand additional investigation.

Conclusions

Overall, our study demonstrates that the A53E aSyn mutation influences the ability of aSyn to aggregate in vitro and in vivo, and that it may induce different cellular pathologies that should be further investigated in vivo. Ultimately, a deeper understanding of the effect of aSyn mutations on the behavior of the protein will enable the design of novel models to assess the potential value of future therapeutic strategies for PD and other synucleinopathies.

Additional file

Additional file 1: Figure S1.1. Biochemical characterization of WT and A53E recombinant aSyn. Analysis of purified WT and A53E aSyn variants by SDS-PAGE (18%) stained with Coomassie Brilliant Blue. S1.2. MALDI-TOF mass spectrometry analysis of purified WT (up) and A53E (down) aSyn variants. A MW of 14462.98 Da was obtained for WT (theoretical of 14460.16 da) and of 14519.47 Da for A53E (theoretical of 14518.19 Da) aSyn variants. The peaks of 7231.82 and 7260.97 Da correspond to the M^{+2} ions of WT and A53E aSyn, respectively. Figure S2.1 and S2.2. Immunoblot quantifications. Levels of VN-aSyn (S2.1) and aSyn-VC (S2.1). n=3. Figure S3.1-S3.3. Morphological analysis of Golgi apparatus in the aSyn BiFC system. The morphology of the Golgi was analyzed as normal (S3.1), diffuse (S3.2) and fragmented (S3.3). One-way ANOVA with post-hoc Tukey's test (*p<0.05, **p<0.01, ***p<0.001). n=3. Figure S3.4-3.6 Morphological analysis of Golgi apparatus in the aSyn aggregation model. Transfected cells were analyzed according to the morphology of the Golgi: normal (S3.4), diffuse (S3.5) and fragmented (S3.6) One-way ANOVA with post-hoc Tukey's test (*p<0.05, **p<0.01, ***p<0.001). n=3. (PDF 389 kb)

Abbreviations

A53E: Substitution of alanine at position 53 by a glutamate residue; aSyn: alpha-synuclein; ATR FT-IR: Attenuated total reflectance Fourier transform infrared spectroscopy; BiFC: Bimolecular fluorescence complementation assay; CR: Congo red; H4: Human Neuroglioma cells; HEK: Human embryonic kidney cells; IPTG: isopropyl-1-thio-β-D-galactopyranoside; LBs: Lewy bodies; PD: Parkinson's disease; PI: Propidium iodide; PK: Proteinase K; RT: Room temperature; SC: synthetic complete medium; TEM: Transmission electron microscopy; Th-S: Thioflavin S; Th-T: Thioflavin T; UPS: Ubiquitin-proteasome system

Acknowledgements

TFO is supported by the DFG Center for Nanoscale Microscopy and Molecular Physiology of the Brain, by the German-Israeli Foundation for Scientific Research and Development (GIF), and by a grant from the Niedersachsisches Ministerium fur Wissenschaft und Kultur (MWK). TFO and SV are supported by a grant from Fundación La Marato de TV3 (Ref. 20144330). The funders had no role in study design, data collection and analysis, decision to publish, or preparation of the manuscript.

Authors' contributions

Conceived and designed the experiments: DFL, MD, SV, TFO. Performed the experiments: DFL, MD, AC, SN, CSM, ST. Analyzed the data: DFL, MD, SV, ST, TFO. Wrote the paper: DFL, MD, SV, TFO. All authors read and approved the final manuscript.

Competing interests

The authors declare that they have no competing interests.

Author details

[1]Department of Neurodegeneration and Restorative Research, University Medical Center Göttingen, Waldweg 33, 37073 Göttingen, Germany. [2]Institut de Biotecnologia i Biomedicina and Departament de Bioquímica i Biologia Molecular, Universitat Autònoma de Barcelona, 08193, Bellaterra, Barcelona, Spain. [3]Chronic Disease Research Center (CEDOC), NOVA Medical School, Campo dos Mártires da Pátria, 130, 1169-056 Lisbon, Portugal. [4]Max Planck Institute for Experimental Medicine, Göttingen, Germany.

Received: 29 October 2016 Accepted: 3 December 2016

Published online: 09 December 2016

References

1. Appel-Cresswell S, Vilarino-Guell C, Encarnacion M, Sherman H, Yu I, Shah B, Weir D, Thompson C, Szu-Tu C, Trinh J et al (2013) Alpha-synuclein p.H50Q, a novel pathogenic mutation for Parkinson's disease. Mov Disord 28:811–813
2. Auluck PK, Caraveo G, Lindquist S (2010) alpha-Synuclein: membrane interactions and toxicity in Parkinson's disease. Annu Rev Cell Dev Biol 26:211–233
3. Barona-Lleo L, Zulueta-Santos C, Murie-Fernandez M, Perez-Fernandez N (2014) Recent onset disequilibrium mimicking acute vestibulopathy in early multiple sclerosis. Am J Otolaryngol 35:529–534
4. Braak H, Del Tredici K, Rub U, de Vos RA, Jansen Steur EN, Braak E (2003) Staging of brain pathology related to sporadic Parkinson's disease. Neurobiol Aging 24:197–211
5. Braak H, Ghebremedhin E, Rub U, Bratzke H, Del Tredici K (2004) Stages in the development of Parkinson's disease-related pathology. Cell Tissue Res 318:121–134
6. Cai H, Reinisch K, Ferro-Novick S (2007) Coats, tethers, Rabs, and SNAREs work together to mediate the intracellular destination of a transport vesicle. Dev Cell 12:671–682
7. Chandra S, Gallardo G, Fernandez-Chacon R, Schluter OM, Sudhof TC (2005) Alpha-synuclein cooperates with CSPalpha in preventing neurodegeneration. Cell 123:383–396
8. Chartier-Harlin MC, Dachsel JC, Vilarino-Guell C, Lincoln SJ, Lepretre F, Hulihan MM, Kachergus J, Milnerwood AJ, Tapia L, Song MS et al (2011) Translation initiator EIF4G1 mutations in familial Parkinson disease. Am J Hum Genet 89:398–406
9. Cooper AA, Gitler AD, Cashikar A, Haynes CM, Hill KJ, Bhullar B, Liu K, Xu K, Strathearn KE, Liu F et al (2006) Alpha-synuclein blocks ER-Golgi traffic and Rab1 rescues neuron loss in Parkinson's models. Science 313:324–328
10. Coppede F (2012) Genetics and epigenetics of Parkinson's disease. Sci World J 2012:489830
11. Dikiy I, Eliezer D (2014) N-terminal acetylation stabilizes N-terminal helicity in lipid- and micelle-bound alpha-synuclein and increases its affinity for physiological membranes. J Biol Chem 289:3652–3665
12. Fan J, Hu Z, Zeng L, Lu W, Tang X, Zhang J, Li T (2008) Golgi apparatus and neurodegenerative diseases. Int J Dev Neurosci 26:523–534
13. Fujita Y, Ohama E, Takatama M, Al-Sarraj S, Okamoto K (2006) Fragmentation of Golgi apparatus of nigral neurons with alpha-synuclein-positive inclusions in patients with Parkinson's disease. Acta Neuropathol 112:261–265
14. Fujiwara H, Hasegawa M, Dohmae N, Kawashima A, Masliah E, Goldberg MS, Shen J, Takio K, Iwatsubo T (2002) alpha-Synuclein is phosphorylated in synucleinopathy lesions. Nat Cell Biol 4:160–164
15. Ghosh D, Sahay S, Ranjan P, Salot S, Mohite GM, Singh PK, Dwivedi S, Carvalho E, Banerjee R, Kumar A, Maji SK (2014) The newly discovered Parkinson's disease associated Finnish mutation (A53E) attenuates alpha-synuclein aggregation and membrane binding. Biochemistry 53:6419–6421
16. Gietz D, St Jean A, Woods RA, Schiestl RH (1992) Improved method for high efficiency transformation of intact yeast cells. Nucleic Acids Res 20:1425
17. Goedert M, Spillantini MG, Del Tredici K, Braak H (2013) 100 years of Lewy pathology. Nat Rev Neurol 9:13–24
18. Gonatas NK, Stieber A, Gonatas JO (2006) Fragmentation of the Golgi apparatus in neurodegenerative diseases and cell death. J Neurol Sci 246:21–30
19. Gosavi N, Lee HJ, Lee JS, Patel S, Lee SJ (2002) Golgi fragmentation occurs in the cells with prefibrillar alpha-synuclein aggregates and precedes the formation of fibrillar inclusion. J Biol Chem 277:48984–48992
20. Hardy J (2005) Expression of normal sequence pathogenic proteins for neurodegenerative disease contributes to disease risk: 'permissive templating' as a general mechanism underlying neurodegeneration. Biochem Soc Trans 33:578–581

21. Hernandez-Vargas R, Fonseca-Ornelas L, Lopez-Gonzalez I, Riesgo-Escovar J, Zurita M, Reynaud E (2011) Synphilin suppresses alpha-synuclein neurotoxicity in a Parkinson's disease Drosophila model. Genesis 49:392–402
22. Ibanez P, Bonnet AM, Debarges B, Lohmann E, Tison F, Pollak P, Agid Y, Durr A, Brice A (2004) Causal relation between alpha-synuclein gene duplication and familial Parkinson's disease. Lancet 364:1169–1171
23. Johnston JA, Ward CL, Kopito RR (1998) Aggresomes: a cellular response to misfolded proteins. J Cell Biol 143:1883–1898
24. Kaganovich D, Kopito R, Frydman J (2008) Misfolded proteins partition between two distinct quality control compartments. Nature 454:1088–1095
25. Kannarkat GT, Boss JM, Tansey MG (2013) The role of innate and adaptive immunity in Parkinson's disease. J Park Dis 3:493–514
26. Kim WS, Kagedal K, Halliday GM (2014) Alpha-synuclein biology in Lewy body diseases. Alzheimers Res Ther 6:73
27. Kisselev AF, Goldberg AL (2005) Monitoring activity and inhibition of 26S proteasomes with fluorogenic peptide substrates. Methods Enzymol 398:364–378
28. Klunk WE, Pettegrew JW, Abraham DJ (1989) Quantitative evaluation of congo red binding to amyloid-like proteins with a beta-pleated sheet conformation. J Histochem Cytochem 37:1273–1281
29. Kordower JH, Brundin P (2009) Propagation of host disease to grafted neurons: accumulating evidence. Exp Neurol 220:224–225
30. Kruger R, Kuhn W, Muller T, Woitalla D, Graeber M, Kosel S, Przuntek H, Epplen JT, Schols L, Riess O (1998) Ala30Pro mutation in the gene encoding alpha-synuclein in Parkinson's disease. Nat Genet 18:106–108
31. Lashuel HA, Overk CR, Oueslati A, Masliah E (2013) The many faces of alpha-synuclein: from structure and toxicity to therapeutic target. Nat Rev Neurosci 14:38–48
32. Lazaro DF, Rodrigues EF, Langohr R, Shahpasandzadeh H, Ribeiro T, Guerreiro P, Gerhardt E, Krohnert K, Klucken J, Pereira MD et al (2014) Systematic comparison of the effects of alpha-synuclein mutations on its oligomerization and aggregation. PLoS Genet 10:e1004741
33. Lee HJ, Lee SJ (2002) Characterization of cytoplasmic alpha-synuclein aggregates. Fibril formation is tightly linked to the inclusion-forming process in cells. J Biol Chem 277:48976–48983
34. Lesage S, Anheim M, Letournel F, Bousset L, Honore A, Rozas N, Pieri L, Madiona K, Durr A, Melki R et al (2013) G51D alpha-synuclein mutation causes a novel parkinsonian-pyramidal syndrome. Ann Neurol 73:459–471
35. LeVine H 3rd (1993) Thioflavine T interaction with synthetic Alzheimer's disease beta-amyloid peptides: detection of amyloid aggregation in solution. Protein Sci 2:404–410
36. Li JY, Englund E, Holton JL, Soulet D, Hagell P, Lees AJ, Lashley T, Quinn NP, Rehncrona S, Bjorklund A et al (2008) Lewy bodies in grafted neurons in subjects with Parkinson's disease suggest host-to-graft disease propagation. Nat Med 14:501–503
37. Maroteaux L, Campanelli JT, Scheller RH (1988) Synuclein: a neuron-specific protein localized to the nucleus and presynaptic nerve terminal. J Neurosci 8:2804–2815
38. Martin LJ, Pan Y, Price AC, Sterling W, Copeland NG, Jenkins NA, Price DL, Lee MK (2006) Parkinson's disease alpha-synuclein transgenic mice develop neuronal mitochondrial degeneration and cell death. J Neurosci 26:41–50
39. Mbefo MK, Fares MB, Paleologou K, Oueslati A, Yin G, Tenreiro S, Pinto M, Outeiro T, Zweckstetter M, Masliah E, Lashuel HA (2015) Parkinson disease mutant E46K enhances alpha-synuclein phosphorylation in mammalian cell lines, in yeast, and in vivo. J Biol Chem 290:9412–9427
40. McLean PJ, Kawamata H, Hyman BT (2001) Alpha-synuclein-enhanced green fluorescent protein fusion proteins form proteasome sensitive inclusions in primary neurons. Neuroscience 104:901–912
41. Moree B, Yin G, Lazaro DF, Munari F, Strohaker T, Giller K, Becker S, Outeiro TF, Zweckstetter M, Salafsky J (2015) Small molecules detected by second-harmonic generation modulate the conformation of monomeric alpha-synuclein and reduce its aggregation in cells. J Biol Chem 290: 27582–27593
42. Murphy DD, Rueter SM, Trojanowski JQ, Lee VM (2000) Synucleins are developmentally expressed, and alpha-synuclein regulates the size of the presynaptic vesicular pool in primary hippocampal neurons. J Neurosci 20:3214–3220
43. Olanow CW, Perl DP, DeMartino GN, McNaught KS (2004) Lewy-body formation is an aggresome-related process: a hypothesis. Lancet Neurol 3:496–503
44. Outeiro TF, Lindquist S (2003) Yeast cells provide insight into alpha-synuclein biology and pathobiology. Science 302:1772–1775
45. Outeiro TF, Putcha P, Tetzlaff JE, Spoelgen R, Koker M, Carvalho F, Hyman BT, McLean PJ (2008) Formation of toxic oligomeric alpha-synuclein species in living cells. PLoS One 3:e1867
46. Pasanen P, Myllykangas L, Siitonen M, Raunio A, Kaakkola S, Lyytinen J, Tienari PJ, Poyhonen M, Paetau A (2014) Novel alpha-synuclein mutation A53E associated with atypical multiple system atrophy and Parkinson's disease-type pathology. Neurobiol Aging 35:2180.e2181–2185
47. Polymeropoulos MH, Lavedan C, Leroy E, Ide SE, Dehejia A, Dutra A, Pike B, Root H, Rubenstein J, Boyer R et al (1997) Mutation in the alpha-synuclein gene identified in families with Parkinson's disease. Science 276:2045–2047
48. Proukakis C, Dudzik CG, Brier T, MacKay DS, Cooper JM, Millhauser GL, Houlden H, Schapira AH (2013) A novel alpha-synuclein missense mutation in Parkinson disease. Neurology 80:1062–1064
49. Rey NL, Steiner JA, Maroof N, Luk KC, Madaj Z, Trojanowski JQ, Lee VM, Brundin P (2016) Widespread transneuronal propagation of alpha-synucleinopathy triggered in olfactory bulb mimics prodromal Parkinson's disease. J Exp Med 213:1759–1778
50. Rutherford NJ, Giasson BI (2015) The A53E alpha-synuclein pathological mutation demonstrates reduced aggregation propensity in vitro and in cell culture. Neurosci Lett 597:43–48
51. Sabate R, Rodriguez-Santiago L, Sodupe M, Saupe SJ, Ventura S (2013) Thioflavin-T excimer formation upon interaction with amyloid fibers. Chem Commun 49:5745–5747
52. Saito Y, Kawashima A, Ruberu NN, Fujiwara H, Koyama S, Sawabe M, Arai T, Nagura H, Yamanouchi H, Hasegawa M et al (2003) Accumulation of phosphorylated alpha-synuclein in aging human brain. J Neuropathol Exp Neurol 62:644–654
53. Singleton AB, Farrer M, Johnson J, Singleton A, Hague S, Kachergus J, Hulihan M, Peuralinna T, Dutra A, Nussbaum R et al (2003) alpha-Synuclein locus triplication causes Parkinson's disease. Science 302:841
54. Spillantini MG, Schmidt ML, Lee VM, Trojanowski JQ, Jakes R, Goedert M (1997) Alpha-synuclein in Lewy bodies. Nature 388:839–840
55. Spillantini MG, Crowther RA, Jakes R, Hasegawa M, Goedert M (1998) alpha-Synuclein in filamentous inclusions of Lewy bodies from Parkinson's disease and dementia with lewy bodies. Proc Natl Acad Sci U S A 95:6469–6473
56. Tenreiro S, Reimao-Pinto MM, Antas P, Rino J, Wawrzycka D, Macedo D, Rosado-Ramos R, Amen T, Waiss M, Magalhaes F et al (2014) Phosphorylation modulates clearance of alpha-synuclein inclusions in a yeast model of Parkinson's disease. PLoS Genet 10:e1004302
57. Tenreiro S, Rosado-Ramos R, Gerhardt E, Favretto F, Magalhaes F, Popova B, Becker S, Zweckstetter M, Braus GH, Outeiro TF (2016) Yeast reveals similar molecular mechanisms underlying alpha- and beta-synuclein toxicity. Hum Mol Genet 25:275–290
58. Tsigelny IF, Sharikov Y, Wrasidlo W, Gonzalez T, Desplats PA, Crews L, Spencer B, Masliah E (2012) Role of alpha-synuclein penetration into the membrane in the mechanisms of oligomer pore formation. FEBS J 279:1000–1013
59. Volles MJ, Lansbury PT Jr (2007) Relationships between the sequence of alpha-synuclein and its membrane affinity, fibrillization propensity, and yeast toxicity. J Mol Biol 366:1510–1522
60. Wales P, Pinho R, Lazaro DF, Outeiro TF (2013) Limelight on alpha-synuclein: pathological and mechanistic implications in neurodegeneration. J Park Dis 3:415–459
61. Webb JL, Ravikumar B, Atkins J, Skepper JN, Rubinsztein DC (2003) Alpha-Synuclein is degraded by both autophagy and the proteasome. J Biol Chem 278:25009–25013
62. Weisberg SJ, Lyakhovetsky R, Werdiger AC, Gitler AD, Soen Y, Kaganovich D (2012) Compartmentalization of superoxide dismutase 1 (SOD1G93A) aggregates determines their toxicity. Proc Natl Acad Sci U S A 109:15811–15816
63. Winner B, Jappelli R, Maji SK, Desplats PA, Boyer L, Aigner S, Hetzer C, Loher T, Vilar M, Campioni S et al (2011) In vivo demonstration that alpha-synuclein oligomers are toxic. Proc Natl Acad Sci U S A 108:4194–4199
64. Xu W, Tan L, Yu JT (2015) Link between the SNCA gene and parkinsonism. Neurobiol Aging 36:1505–1518
65. Zarranz JJ, Alegre J, Gomez-Esteban JC, Lezcano E, Ros R, Ampuero I, Vidal L, Hoenicka J, Rodriguez O, Atares B et al (2004) The new mutation, E46K, of alpha-synuclein causes Parkinson and Lewy body dementia. Ann Neurol 55:164–173

4. Discussion

4.1. The urgency for standardization of models and observations

Many neurodegeneration disorders are associated with the misfolding and aggregation of proteins. However, the molecular events that underlie the aggregation process and that specifically dictate neuronal cell death in each disease are still unclear. Over the years, different *in vitro* and *in vivo* models were established and enabled tremendous progress in the field. However, due to the complexity of each disorder, we still lack a clear and fundamental understanding of the underpinning molecular mechanisms and cellular pathways. This is also due to the complexity and specificity of each model system, and our limited success in transposing findings across the various models.

The present study aimed at shedding light into the cellular pathologies associated with aSyn aggregation. To do this, we exploited two cell-based models of aSyn aggregation in order to compare the effect of genetic alterations in aSyn on its aggregation. For the first time, all reported familial and artificial mutations were systematically compared in well-established cell models. Our goal was to create a comprehensive and pivotal knowledge that can then be explored to screen and optimize novel compounds that interfere with pathological forms of aSyn. In addition, we tested the effect of small molecules selected based on *in vitro* assays, and found protective effects in the cell models.

4.2. Distinguishing aSyn species and their cellular effects

Artificial mutants of aSyn are useful tools to probe the behavior of the protein, since they can trap aSyn in specific conformations, therefore allowing us to assess their effects in different environments. The E35K and E57K aSyn mutants were specifically designed to form oligomers, by disrupting aSyn salt bridges. *In vitro* studies confirmed that they form ring/pore-like structures and not amyloid fibers (as the A30P, E46K and A53T aSyn mutants do). *In vivo*, E35K and E57K aSyn cause a stronger reduction in DA cells in the rat SN (Winner et al. 2011). Furthermore, those toxic oligomer-forming mutants display a higher affinity to bind to membranes in comparison with WT aSyn. The E46K mutant was been described to fibrillize more

rapidly than WT aSyn (Greenbaum et al. 2005; Ono et al. 2011), and the fibrils formed have a distinct twisted appearance (Choi et al. 2004), maybe because of the long-range interactions of the C-terminus with the N-terminus and NAC regions, producing more compact structures (Wise-Scira et al. 2013). Although this mutant occurs in PD patients, it was found to cause reduced cell death, and reduced calcium influx when compared with the artificial E35K and E57K mutants (Winner et al. 2011).

In our aSyn-aggregation cell model, we observed that E46K, E35K and E57K produce inclusions that are morphologically different (Fig.3B- Lázaro DF et al., PLoS Genet. 2014). The inclusions produced by E35K and E57K were smaller, appearing as puncta (Fig.3C- Lázaro DF et al., PLoS Genet. 2014), and were ThioS negative (Fig.6C- Lázaro DF et al., PLoS Genet. 2014). Furthermore, these two mutations increased aSyn oligomerization, as measured by the fluorescence intensity complementation of the BiFC assay, in line with what was reported in previous studies (Fig.1C- Lázaro DF et al., PLoS Genet. 2014). On the other hand, the E46K produces enlarged cytoplasmic inclusions enriched in amyloid structure, as indicated by the positive staining with ThioS (Fig.6C- Lázaro DF et al., PLoS Genet. 2014). A possible explanation for the formation of these large structures can be an inefficient clearance of aSyn by autophagy. E46K aSyn inactivates JNK1 by decreasing its phosphorylation, resulting in impairment of autophagy (Yan et al. 2014). Importantly, these three lysine substitution mutants produced the most extreme increase in aSyn inclusion formation from the whole panel tested.

The Golgi apparatus is an important organelle for transporting, processing, and targeting synthesized proteins, from the ER to their final destination in the cell (Nakagomi et al. 2008). However, different cellular insults can induce its fragmentation, leading to dysfunctional machinery and protein accumulation in the cytoplasm, or even to cell death (Nakagomi et al. 2008). It is now normally accepted in the field that oligomerized aSyn is more toxic to the cell, and our results strengthen this idea, since the aSyn E35K and E57K mutants promote fragmentation of the Golgi apparatus (Fig.10A and Fig S2A. Lázaro DF et al., PLoS Genet. 2014). These observations are important because they allow us to hypothesize additional scenarios that can be tested experimentally in future studies. For example, the ER is closely associated with several other organelles in the cell, especially with the Golgi. If the ER is afflicted by certain types of stress (such as glucose starvation, hypoxia, calcium

homeostasis disruption, oxidative stress (Omura et al. 2013)), or increased aSyn expression (Colla et al. 2012) it can result in Golgi fragmentation (Nakagomi et al. 2008) and, consequently, to cell death (Gonatas et al. 2006; Fan et al. 2008; Fujita et al. 2006).

Our results provide a simple readout to test new agents that may reduce ER damage, or that may even directly affect the Golgi apparatus. As proof of concept, Salubrinal could be tested, as it was shown to act as an anti-ER stress agent that attenuates A53T aSyn-mediated effects in mice and in a rat adeno-associated virus model (Colla et al. 2012).

4.3. Modulation of aSyn aggregation by proline residues

The aa proline is a potent breaker of both α-helical and β-sheet structures in soluble proteins (Li et al. 1996). Thus, a series of aSyn proline mutants (familial- A30P, and artificial- A56P, A75P, A56P/A75P-DP, A30P/A56P/A75P-TP) was designed based on the flexibility of the backbone in monomeric state (Bertoncini et al. 2005). Interestingly, the proline mutations slowed down fibril and β-sheet structure formation *in vitro* and *in vivo* (Karpinar et al. 2009; Taschenberger et al. 2012). Consistently, it was not entirely surprising that we observed similar effects in our cell-based aSyn aggregation models. All proline mutations reduce/abolish the propensity of aSyn to form inclusions (Fig.3B and C, Fig.5B and C- Lázaro DF et al., PLoS Genet. 2014). This was further validated by super resolution microscopy (STED), and biochemically, using Triton X-100 solubility assays (Fig.6B and E- Lázaro DF et al., PLoS Genet. 2014). Additionally, we observed a prominent increase in aSyn oligomerization for A56P and TP aSyn (Fig.2C- Lázaro DF et al., PLoS Genet.).

The TP mutant showed, so far, to be the most effective in promoting the accumulation of pre-fibrillar species of aSyn (Karpinar et al. 2009). Despite the impairment in amyloid fibril formation *in vitro*, it increases neurotoxicity in primary neurons, worms, and flies (Karpinar et al. 2009; Gajula Balija et al. 2011), reinforcing the idea that soluble aSyn oligomers have detrimental effects. However, in yeast the behavior of this mutant seems to be different. We and others (Petroi et al. 2012) observed that the TP aSyn mutant is not toxic in yeast cells (Fig.5A and C- Lázaro DF et al. PLoS Genet), suggesting that yeast cells may have a different strategy to deal with oligomeric aSyn species. Furthermore, the TP mutant can increase the number of

vacuoles, the compartments that are equivalent to lysosomes in yeast. The vacuoles are the major contributors to aggregate clearance in yeast and the TP induces the formation of tube-like structures that resemble autophagic tubes (Petroi et al. 2012), and are characteristic of yeast microautophagy (Muller et al. 2000). Thus, it is possible that the increase of these acidic structures assists the degradation machinery to eliminate the toxic forms of aSyn.

In vitro, A30P aSyn promotes the formation of non-fibrillar protofibrils (Conway et al. 2000), and its seeds accelerate WT fibrillization more effectively than WT seeds (Yonetani et al. 2009). Moreover, A30P disrupts α-helix formation, essential for lipid binding (Jo et al. 2002), and significantly reduces presynaptic targeting of aSyn (Burre et al. 2012), which might compromise SNARE-complex assembly. Thus, one can speculate that the A30P aSyn mutant disrupts the normal function of the protein, which is then no longer in its stable form, causing its accumulation. In turn, this accumulation will act as a positive loop that potentiates even more aSyn seeding, causing deposition of harmful protofibrillar species and cellular damage.

4.4. Position 53: the effect of the charge

Recently, a new point mutation in aSyn (A53E) was associated with familial forms of PD (Pasanen et al. 2014). The A53E was initially reported to attenuate aSyn aggregation, slow fibrillization and oligomerization, and to exhibit reduced membrane binding affinity when compared to WT aSyn (Ghosh et al. 2014). In addition, it was found to enhance toxicity upon mitochondrial stress (Rutherford et al. 2015).

Combining *in vitro* studies with recombinant aSyn and studies in cellular models, we showed that A53E forms higher order complexes (Fig.2f and Fig.3a, b and e- Lázaro DF et al. Acta Neuropathol Commun. 2016), displaying protofibrillar appearance (small round oligomers) (Fig.2f- Lázaro DF et al. Acta Neuropathol Commun. 2016). We also found that A53E aSyn inclusions are less compact or more immature than those formed by WT aSyn, since they are less resistant to PK digestion (Fig.4h and i- Lázaro DF et al. Acta Neuropathol Commun. 2016). This can explain the increase in proteasomal activity induced by A53E aSyn (Fig.4j- Lázaro DF et al. Acta Neuropathol Commun. 2016), since this degradation system eliminates mostly soluble proteins. These results were very interesting, since in our previous report,

A53T did not induce significant differences in terms of oligomerization (Fig.2C- Lázaro DF et al. Acta Neuropathol Commun. 2016) or aggregation (Fig.3C- Lázaro DF et al. Acta Neuropathol Commun. 2016). The negatively charged glutamate residue might disrupt the α-helical structure, similarly to the effect of the A30P mutation, resulting in altered fibrillation kinetics. Substitution for a positively charged aa, such as a lysine, induces a similar behavior in aSyn, delaying aggregation (Ghosh et al. 2014). Thus, one possibility is that the neutral side chain of threonine, in the A53T mutant aSyn, may facilitate hydrophobic interactions, with the -OH group participating in favoring fibril formation (Ghosh et al. 2014).

4.5. Phosphorylation and other PTMs: the need for additional in depth studies

Of all PTMs studied thus far, phosphorylation is perhaps the most widely investigated, since the majority of aSyn in LBs is thought to be phosphorylated on serine 129 (Fujiwara et al. 2002). Most of the known aSyn PTMs are located in the C-terminal region of the protein: phosphorylation (S87, Y125, S129, Y133 and Y136), truncation (D115, D119, P120, E130 and D135), ubiquitination (K96), or sumoylation (k96 and K102) (Schmid et al. 2009; Oueslati et al. 2010).

In PD patients, the levels of aSyn phosphorylation on S129 rise from 5% to 30%-100% (depending on the brain region and the severity of the pathology) (Zhou et al. 2011), and are thought to be useful for distinguishing between different synucleinopathies (Foulds et al. 2012; Swirski et al. 2014). However, in PD models there is a lot of controversy, due to conflicting data. This is partly due to the fact that artificial aSyn mutants are often used to mimic the phosphorylated state (S129D/E), and the dephosphorylated state of aSyn (S129A/G), but these fail to fully replicate the real phosphorylation of aSyn (Paleologou et al. 2008). This is also true for other phosphorylation sites (S87, or Y125, for example), or even other PTMs, such as sumoylation.

In our study, we did not observe major differences between mimicking or blocking aSyn phosphorylation on S129 (Fig. 2C and Fig.3C9- Lázaro DF et al. PLoS Genet. 2014 Nov). This suggests that different model systems likely handle the proteins slightly differently, and that other mechanisms may be involved in modulating the behavior of these mutant forms of aSyn.

Strikingly, despite all studies performed, whether aSyn phosphorylation is the cause or a consequence of PD is still unclear. To understand the relevance of phosphorylation it is important to determine the origins of its increases and the consequences it may have on cell function and survival. Three important aspects seem to be correlated with aSyn phosphorylation: (i) aSyn turnover, (ii) protein-protein interactions, and (iii) its subcellular localization. We can speculate that the accumulation of aSyn pS129 is an attempt of the cell to sequester toxic forms of aSyn when proteasome and the autophagy-lysosome pathway are compromised (Chau et al. 2009; Machiya et al. 2010). Furthermore, non-phosphorylated aSyn mainly interacts with proteins related to mitochondrial electron transport but when it is phosphorylated it has more affinity to specific cytoskeletal proteins and presynaptic proteins (McFarland et al. 2008). This can indicate that phosphorylation can participate in regulating the movement of in the cell, and also in synaptic transmission and vesicle trafficking. These are two major cellular aspects associated in PD, not only because different types of compartments have different fates (section 1.2.4) but also because aSyn pathology can be transmitted from neuron-to-neuron, afflicting surrounding cells.

Changes in the phosphorylation status of aSyn could also represent a response to other biochemical events. Several studies report the detection of aSyn in the nucleus of mammalian cell lines (Mbefo et al. 2010; Lee et al. 2013), primary neuronal cultures (McLean et al. 2000; Seo et al. 2002), tg mice (Goers et al. 2003; Schell et al. 2009), adeno-associated-based rat model of PD (Azeredo da Silveira et al. 2009), or in drosophila models (Takahashi et al. 2003). Our group showed that there is a continuous trafficking of aSyn between the cytoplasm and nucleus that is partially regulated by phosphorylation. Blocking phosphorylation of aSyn (S129A) significantly reduces aSyn translocation to the nuclear compartment (Goncalves et al. 2013). Thus, additional studies will be necessary to further dissect the effects of phosphorylation in the cell and on PD.

4.6. Better treatments for a brighter future

PD, as well as all the other synucleinopathies, is devastating disorders that cannot currently be prevented or reverted. Thus, seeking for better treatments that interfere with, or ultimately stop the progression of such complex disorders is

essential. For that, it is pivotal to study how drugs/compounds/small molecules affect aSyn aggregation and biology.

Using SHG-based approach, we identified a small molecule (BIOD303) that affects aSyn aggregation (Moree B, Yin G, Lázaro DF et al. J Biol Chem. 2015). BIOD303 is a potent conformational modulator of aSyn, by binding to monomeric aSyn (Fig.3 Moree B, Yin G, Lázaro DF et al. J Biol Chem. 2015), and strongly reducing aSyn aggregation in our cell model (Fig.7 Moree B, Yin G, Lázaro DF et al. J Biol Chem. 2015). Not only percentage of cells with inclusions diminished by BIOD303, but also the amount of insoluble aSyn is reduced in a dose dependent manner (Fig.9A and B Moree B, Yin G, Lázaro DF et al. J Biol Chem. 2015). These results indicate that the conformation of aSyn is highly associated with its aggregation, and suggest that it may be possible to develop novel therapeutic strategies for PD and other synucleinopathies based on compounds that modulate aSyn aggregation.

5. Conclusion

Protein misfolding and aggregation are linked to many neurodegenerative disorders but the precise molecular events that dictate the selective neuronal cell death in each disease are unclear. PD is a common and complex neurological disorder associated with the misfolding and aggregation of the protein aSyn, that was first described two centuries ago. It is a slowly progressive neurodegenerative disorder that begins years before the onset of motor symptoms. This complicates clinical diagnosis, especially at early stages of the disease. Currently, only symptomatic treatments are available, and these only aid with motor symptoms. Thus, there is a tremendous need for both a deeper understanding of the underlying causes of the disease, and for the development of novel and more effective therapeutic approaches.

Although cell-based models are minimalistic, and do not fully recapitulate the complexity of a complete living organism, they enable us to eliminate sources of variability that compromise our understanding of basic molecular mechanisms underlying protein aggregation. Therefore, these models can serve as first line of investigation, prior to *in vivo* studies (worms, flies, mice, or non-human primates), thereby accelerating drug discovery efforts.

Our studies establish, for the first time a common basis for the comparison of the effects of mutations on the aggregation behavior and on the biology of aSyn in cells. For this, we exploited two cellular models that model aSyn oligomerization (BiFC) and aggregation (SynT+Sph1).

The aggregation of aSyn is considered one of the key steps for the development of PD. Until recently, directly visualization of aSyn interactions in living cells was not possible. The BiFC assay, despite its limitations, affords a unique opportunity to visualize aSyn interactions and where these interactions take place (for example in the nucleus versus the cytoplasm). In the future, using techniques such as Fluorescence Recovery After Photobleaching (FRAP) or Fluorescence Loss in Photobleaching (FLIP) will enable additional questions to be addressed. For example, do different familial aSyn mutants have different mobilities in the cell? Or, does the increase of oligomerization affect the movement from one compartment to another? Tracking the movement of soluble aSyn oligomers, and how fast these processes occur is just one more aspect that can be investigated.

With few exceptions, the tested mutants promote the accumulation of a variety of cytoplasmic inclusions. However, conventional light microscopy has limit of resolution that does not allow to reliably distinguish structures smaller that this limit. Emerging super-resolution microscopy techniques, such expansion microscopy, promise to lead to new findings in the field by enabling the visualization of species that could not be previously resolved without an electron microscope, which is of course powerful, but has its own limitations, such as a much more cumbersome sample preparation. Thus, the use of these novel imaging techniques, in combination with the SynT + Sph1 model might enable a better characterization of the protein inclusions formed (e.g. in terms of size, volume, or intracellular localization).

In conclusion, I am confident we are living exciting moments in science. Every day there are reports of new findings or new tools that can be used in the field of neurodegeneration. Our findings add to our understanding of the molecular basis of devastating maladies and, ultimately, may enable the identification of molecules that could form the basis for future therapeutic strategies for synucleinopathies and other neurodegenerative disorders.

6. Annex

6.1. Supporting Information

Lázaro DF. et al. Plos Genetics 2014

Figure S1 Statistical analysis of ASYN inclusion formation.

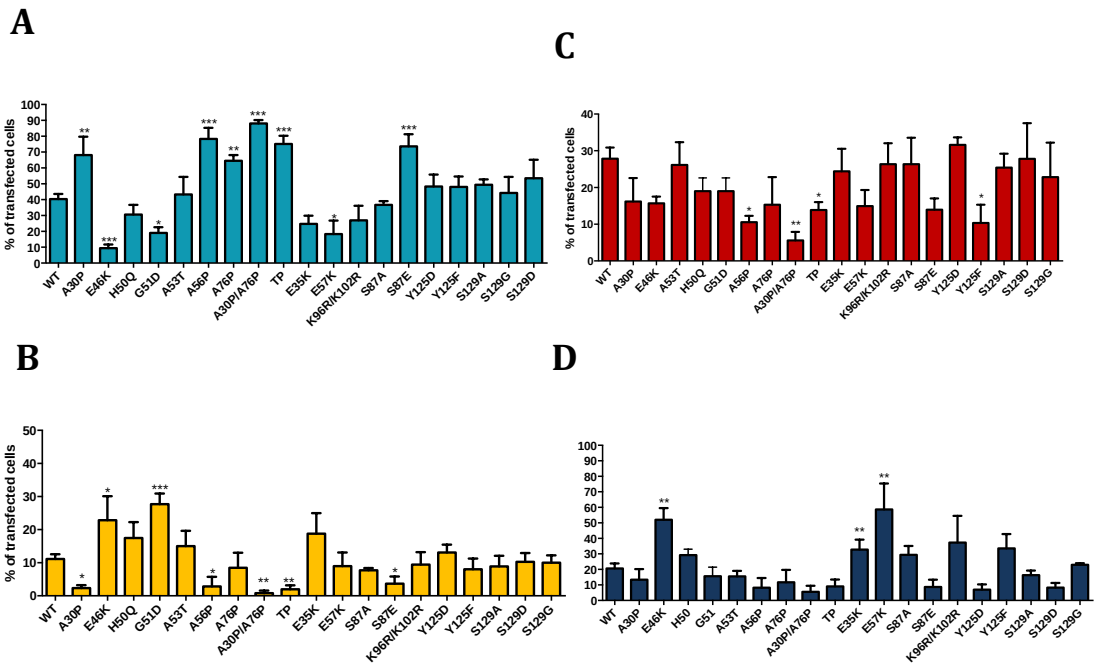

Figure S2 Morphological analysis of Golgi apparatus.

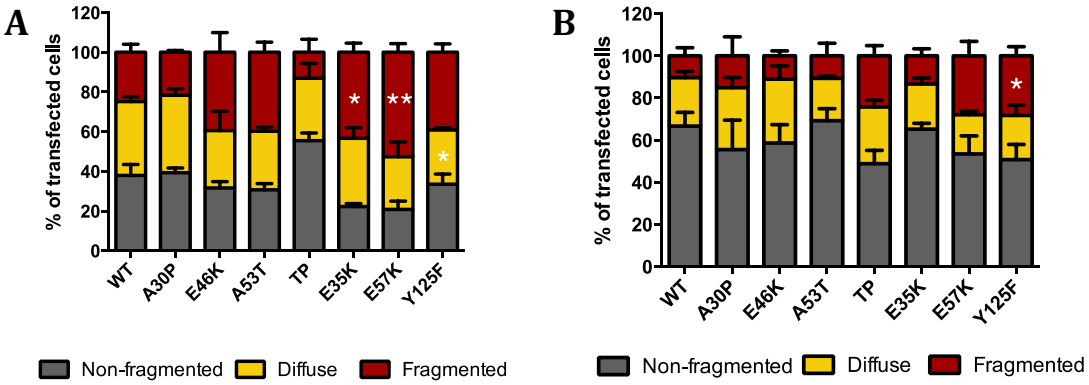

Figure S3 Phosphorylation state of ASYN on S129.

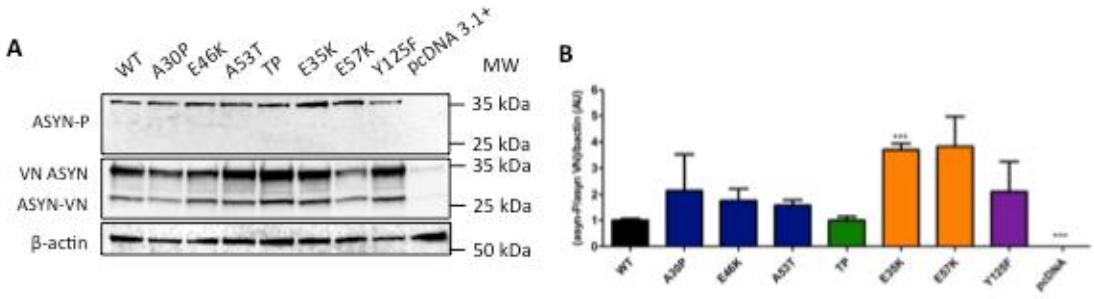

Table S1 Primers used in the site-directed mutagenesis**.**

Mutation	Primer
A30P	Forward: 5'-GGGTGTGGCAGAAGCACCAGGAAAGACAAAAGA-3' Reverse: 5'-TCTTTTGTCTTTCCTGGTGCTTCTGCCACACCC-3'
E46K	Forward: 5'-TAGGCTCCAAAACCAAGAAGGGAGTGGTGCATGG-3' Reverse: 5'-CCATGCACCACTCCCTTCTTGGTTTTGGAGCCTA-3'
H50Q	Forward: 5'-GGAGGGAGTGGTGCAGGGTGTGGCAACAG-3' Reverse: 5'- CTGTTGCCACACCCTGCACCACTCCCTCC-3'
G51D	Forward: 5'-GGGAGTGGTGCATGATGTGGCAACAGTGG-3' Reverse: 5'-CCACTGTTGCCACATCATGCACCACTCCC-3'
A53T	Forward: 5'-GAGTGGTGCATGGTGTGACGACAGTGGCTGAGAAGAC-3' Reverse: 5'-GTCTTCTCAGCCACTGTCGTCACACCATGCACCACTC-3'
E35K	Forward: 5'-CAGAAGCAGCAGGAAAGACAAAAAAGGGTGTTCTCT-3' Reverse: 5'-AGAGAACACCCTTTTTTGTCTTTCCTGCTGCTTCTG-3'
E57K	Forward: 5' GTGGCAACAGTGGCTAAGAAGACCAAAGAGC 3' Reverse: 5' GCTCTTTGGTCTTCTTAGCCACTGTTGCCAC 3'
A56P	Forward: 5'-GGTGTGGCAACAGTGCCTGAGAAGACCAAAG-3' Reverse: 5'-CTTTGGTCTTCTCAGGCACTGTTGCCACACC-3'
A76P	Forward: 5'-TGACGGGTGTGACACCAGTAGCCCAGAAG-3' Reverse: 5'-CTTCTGGGCTACTGGTGTCACACCCGTCA-3'
S129A	Forward: 5'CTTATGAAATGCCTGCTGAGGAAGGGTATC-3' Reverse: 5'GATACCCTTCCTCAGCAGGCATTTCATAAG-3'
S129D	Forward: 5'-GGCTTATGAAATGCCTGATGAGGAAGGGTATCAAG-3' Reverse: 5'-CTTGATACCCTTCCTCATCAGGCATTTCATAAG CC-3'
S129G	Forward: 5'-GACAATGAGGCTTATGAAATGCCTGGTGAGGAAGGGTATC-3' Reverse: 5'-GATACCCTTCCTCACCAGGCATTTCATAAGCCTCATTGTC-3'
S87A	Forward: 5'-AAGACAGTGGAGGGAGCAGGGGCCATTGCAGCAG-3' Reverse: 5'-CTGCTGCAATGGCCCCTGCTCCCTCCACTGTCTT-3'
S87E	Forward: 5'-ACAGTGGAGGGAGCAGGGGAAATTGCAGCAGC-3' Reverse: 5'-GCTGCTGCAATTTCCCCTGCTCCCTCCACTGT-3'
Y125F	Forward: 5'-GGATCCTGACAATGAGGCTTTTGAAATGCCTTCTGA-3' Reverse: 5'-TCAGAAGGCATTTCAAAAGCCTCATTGTCAGGATCC-3'
Y125D	Forward: 5'-GATCCTGACAATGAGGCTGATGAAATGCCTTCTGAGG-3' Reverse: 5'-CCTCAGAAGGCATTTCATCAGCCTCATTGTCAGGATC-3'
K96R	Forward: 5'-GCCACTGGCTTTGTCAGAAAGGACCAGTTGGGC-3' Reverse: 5'-GCCCAACTGGTCCTTTCTGACAAAGCCAGTGGC-3'
K102R	Forward: 5'-AAGGACCAGTTGGGCAGGAATGAAGAAGGAGCC-3' Reverse: 5'-GGCTCCTTCTTCATTCCTGCCCAACTGGTCCTT-3'

Table 2. Summary of the effects of the mutations on ASYN oligomerization and aggregation.

Mutation	Effects on oligomerization			Effects on aggregation	
	Flow Cytometry	Subcellular distribution		Number	Morphology
		Nucleus	Cytosol		
A30P	↔	↑	↓	↓	↔
E46K	↔	↔	↔	↑	Mix
A53T	↔	↑	↓	↔	↔
H50Q	↔			↑	↔
G51D	↔			↑	↔
A56P	↑	↔	↔	↓	↔
A76P	↑	↔	↔	↓	↔
A30P/A76P	↑	↑	↓	↓	↔
TP	↑	↔	↔	↓	↔
E35K	↑	↔	↔	↑	Mix
E57K	↑	↔	↔	↑	Small
S87A	↔	↔	↔	↔	↔
S87E	↓	↔	↔	↓	↔
K96R/K102R	↑	↔	↔	↔	Mix
Y125D	↔	↔	↔	↔	↔
Y125F	↔	↔	↔	↔	Mix
S129A	↔	↑	↓	↔	↔
S129G	↔	↔	↔	↔	↔
S129D	↔	↔	↔	↔	↔

6.2. Additional file

Lázaro DF. et al Acta Neuropathol Commun. 2016

Figure S1.1. Biochemical characterization of WT and A53E recombinant aSyn.

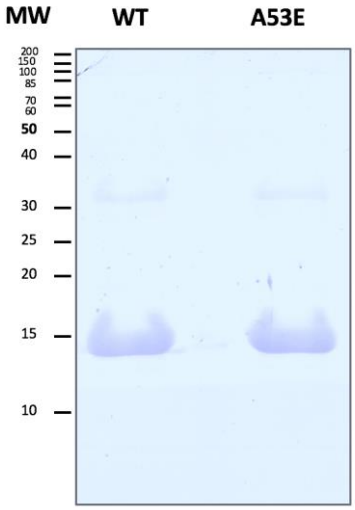

S1.2. MALDI-TOF mass spectrometry analysis of purified WT (up) and A53E (down) aSyn variants.

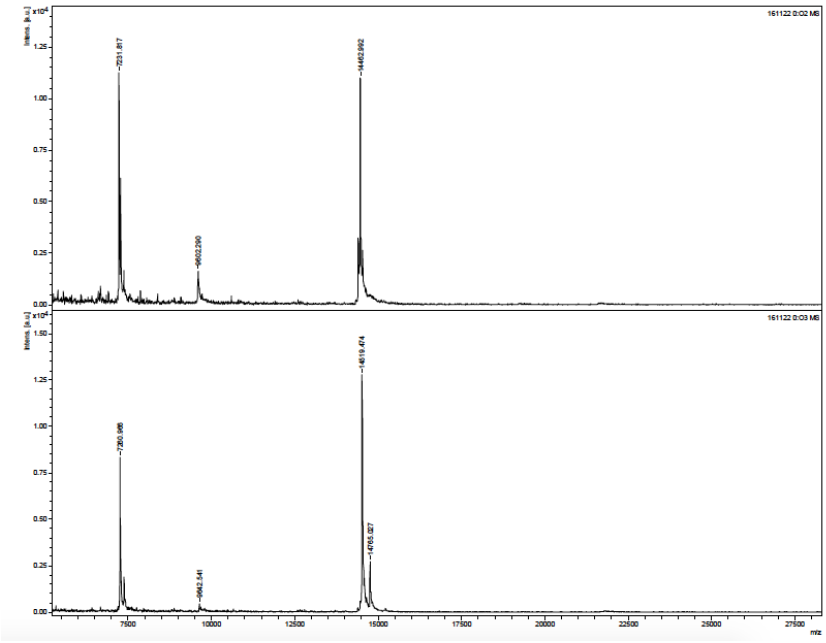

Figure S2.1 and S2.2. Immunoblot quantifications.

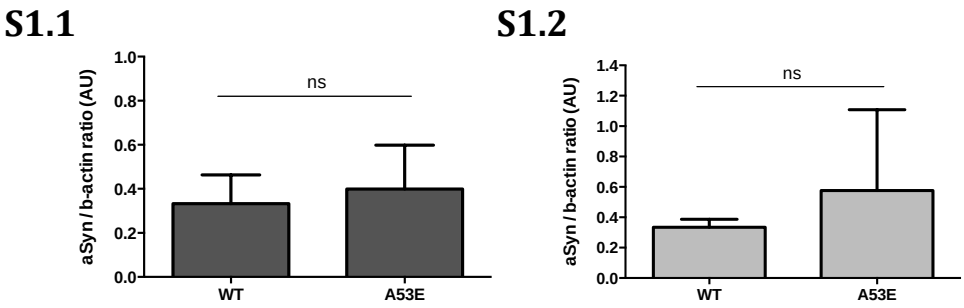

Figure S3.1-S3.3. Morphological analysis of Golgi apparatus in the aSyn BiFC system.

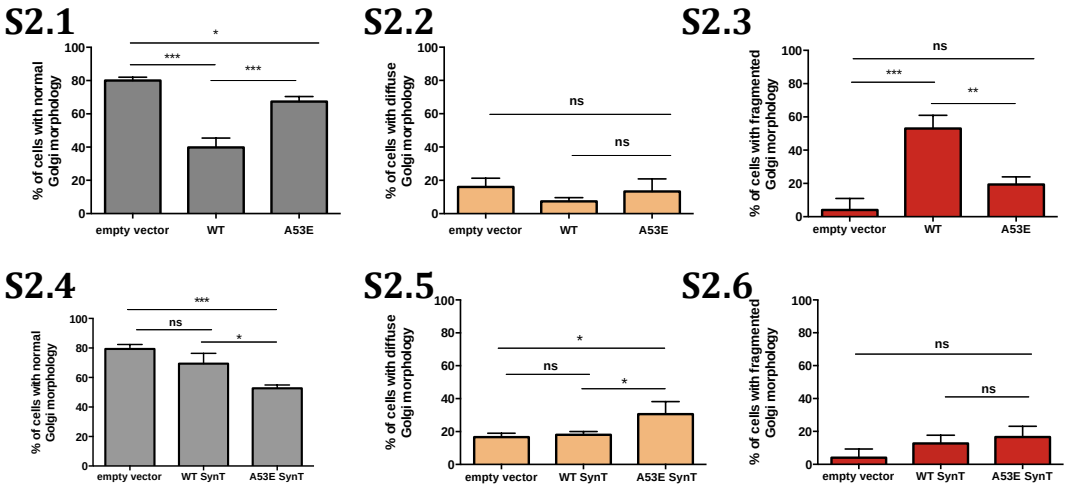

7. References

Abeliovich, A., Y. Schmitz, I. Farinas, D. Choi-Lundberg, W. H. Ho, P. E. Castillo, N. Shinsky, J. M. Verdugo, M. Armanini, A. Ryan, M. Hynes, H. Phillips, D. Sulzer and A. Rosenthal (2000). "Mice lacking alpha-synuclein display functional deficits in the nigrostriatal dopamine system." Neuron **25**(1): 239-252.

Adamczyk, A., M. Kacprzak and A. Kazmierczak (2007). "Alpha-synuclein decreases arachidonic acid incorporation into rat striatal synaptoneurosomes." Folia Neuropathol **45**(4): 230-235.

Aguilaniu, H., L. Gustafsson, M. Rigoulet and T. Nystrom (2003). "Asymmetric inheritance of oxidatively damaged proteins during cytokinesis." Science **299**(5613): 1751-1753.

Ahn, B. H., H. Rhim, S. Y. Kim, Y. M. Sung, M. Y. Lee, J. Y. Choi, B. Wolozin, J. S. Chang, Y. H. Lee, T. K. Kwon, K. C. Chung, S. H. Yoon, S. J. Hahn, M. S. Kim, Y. H. Jo and D. S. Min (2002). "alpha-Synuclein interacts with phospholipase D isozymes and inhibits pervanadate-induced phospholipase D activation in human embryonic kidney-293 cells." J Biol Chem **277**(14): 12334-12342.

Al-Nimer, M. S., S. F. Mshatat and H. I. Abdulla (2014). "Saliva alpha-Synuclein and A High Extinction Coefficient Protein: A Novel Approach in Assessment Biomarkers of Parkinson's Disease." N Am J Med Sci **6**(12): 633-637.

Amaya, C., C. M. Fader and M. I. Colombo (2015). "Autophagy and proteins involved in vesicular trafficking." FEBS Lett **589**(22): 3343-3353.

Amer, D. A., G. B. Irvine and O. M. El-Agnaf (2006). "Inhibitors of alpha-synuclein oligomerization and toxicity: a future therapeutic strategy for Parkinson's disease and related disorders." Exp Brain Res **173**(2): 223-233.

Anderson, J. P., D. E. Walker, J. M. Goldstein, R. de Laat, K. Banducci, R. J. Caccavello, R. Barbour, J. Huang, K. Kling, M. Lee, L. Diep, P. S. Keim, X. Shen, T. Chataway, M. G. Schlossmacher, P. Seubert, D. Schenk, S. Sinha, W. P. Gai and T. J. Chilcote (2006). "Phosphorylation of Ser-129 is the dominant pathological modification of alpha-synuclein in familial and sporadic Lewy body disease." J Biol Chem **281**(40): 29739-29752.

Anfinsen, C. B. (1973). "Principles that govern the folding of protein chains." Science **181**(4096): 223-230.

Angot, E., J. A. Steiner, C. Hansen, J. Y. Li and P. Brundin (2010). "Are synucleinopathies prion-like disorders?" Lancet Neurol **9**(11): 1128-1138.

Antony, T., W. Hoyer, D. Cherny, G. Heim, T. M. Jovin and V. Subramaniam (2003). "Cellular polyamines promote the aggregation of alpha-synuclein." J Biol Chem **278**(5): 3235-3240.

Appel-Cresswell, S., C. Vilarino-Guell, M. Encarnacion, H. Sherman, I. Yu, B. Shah, D. Weir, C. Thompson, C. Szu-Tu, J. Trinh, J. O. Aasly, A. Rajput, A. H. Rajput, A. Jon Stoessl and M. J. Farrer (2013). "Alpha-synuclein p.H50Q, a novel pathogenic mutation for Parkinson's disease." Mov Disord **28**(6): 811-813.

Arawaka, S., Y. Saito, S. Murayama and H. Mori (1998). "Lewy body in neurodegeneration with brain iron accumulation type 1 is immunoreactive for alpha-synuclein." Neurology **51**(3): 887-889.

Arawaka, S., M. Wada, S. Goto, H. Karube, M. Sakamoto, C. H. Ren, S. Koyama, H. Nagasawa, H. Kimura, T. Kawanami, K. Kurita, K. Tajima, M. Daimon, M. Baba, T. Kido, S. Saino, K. Goto, H. Asao, C. Kitanaka, E. Takashita, S. Hongo, T. Nakamura, T. Kayama, Y. Suzuki, K. Kobayashi, T. Katagiri, K. Kurokawa, M. Kurimura, I. Toyoshima, K. Niizato, K. Tsuchiya, T. Iwatsubo, M. Muramatsu, H. Matsumine and T. Kato (2006). "The role of G-protein-coupled receptor kinase 5 in pathogenesis of sporadic Parkinson's disease." J Neurosci **26**(36): 9227-9238.

Astashkina, A., B. Mann and D. W. Grainger (2012). "A critical evaluation of in vitro cell culture models for high-throughput drug screening and toxicity." Pharmacol Ther **134**(1): 82-106.

Auluck, P. K., G. Caraveo and S. Lindquist (2010). "alpha-Synuclein: membrane interactions and toxicity in Parkinson's disease." Annu Rev Cell Dev Biol **26**: 211-233.

Auluck, P. K., H. Y. Chan, J. Q. Trojanowski, V. M. Lee and N. M. Bonini (2002). "Chaperone suppression of alpha-synuclein toxicity in a Drosophila model for Parkinson's disease." Science **295**(5556): 865-868.

Azeredo da Silveira, S., B. L. Schneider, C. Cifuentes-Diaz, D. Sage, T. Abbas-Terki, T. Iwatsubo, M. Unser and P. Aebischer (2009). "Phosphorylation does not prompt, nor prevent, the formation

of alpha-synuclein toxic species in a rat model of Parkinson's disease." Hum Mol Genet **18**(5): 872-887.

Baptista, M. J., C. O'Farrell, S. Daya, R. Ahmad, D. W. Miller, J. Hardy, M. J. Farrer and M. R. Cookson (2003). "Co-ordinate transcriptional regulation of dopamine synthesis genes by alpha-synuclein in human neuroblastoma cell lines." J Neurochem **85**(4): 957-968.

Bartels, T., J. G. Choi and D. J. Selkoe (2011). "alpha-Synuclein occurs physiologically as a helically folded tetramer that resists aggregation." Nature **477**(7362): 107-110.

Bedford, L., S. Paine, P. W. Sheppard, R. J. Mayer and J. Roelofs (2010). "Assembly, structure, and function of the 26S proteasome." Trends Cell Biol **20**(7): 391-401.

Beltrao, P., P. Bork, N. J. Krogan and V. van Noort (2013). "Evolution and functional cross-talk of protein post-translational modifications." Mol Syst Biol **9**: 714.

Benabid, A. L., P. Pollak, A. Louveau, S. Henry and J. de Rougemont (1987). "Combined (thalamotomy and stimulation) stereotactic surgery of the VIM thalamic nucleus for bilateral Parkinson disease." Appl Neurophysiol **50**(1-6): 344-346.

Bertoncini, C. W., Y. S. Jung, C. O. Fernandez, W. Hoyer, C. Griesinger, T. M. Jovin and M. Zweckstetter (2005). "Release of long-range tertiary interactions potentiates aggregation of natively unstructured alpha-synuclein." Proc Natl Acad Sci U S A **102**(5): 1430-1435.

Bisaglia, M., E. Schievano, A. Caporale, E. Peggion and S. Mammi (2006). "The 11-mer repeats of human alpha-synuclein in vesicle interactions and lipid composition discrimination: a cooperative role." Biopolymers **84**(3): 310-316.

Bonifacino, J. S. and B. S. Glick (2004). "The mechanisms of vesicle budding and fusion." Cell **116**(2): 153-166.

Bonifati, V., P. Rizzu, M. J. van Baren, O. Schaap, G. J. Breedveld, E. Krieger, M. C. Dekker, F. Squitieri, P. Ibanez, M. Joosse, J. W. van Dongen, N. Vanacore, J. C. van Swieten, A. Brice, G. Meco, C. M. van Duijn, B. A. Oostra and P. Heutink (2003). "Mutations in the DJ-1 gene associated with autosomal recessive early-onset parkinsonism." Science **299**(5604): 256-259.

Braak, H., R. A. de Vos, J. Bohl and K. Del Tredici (2006). "Gastric alpha-synuclein immunoreactive inclusions in Meissner's and Auerbach's plexuses in cases staged for Parkinson's disease-related brain pathology." Neurosci Lett **396**(1): 67-72.

Braak, H., K. Del Tredici, U. Rub, R. A. de Vos, E. N. Jansen Steur and E. Braak (2003). "Staging of brain pathology related to sporadic Parkinson's disease." Neurobiol Aging **24**(2): 197-211.

Braakman, I. and N. J. Bulleid (2011). "Protein folding and modification in the mammalian endoplasmic reticulum." Annu Rev Biochem **80**: 71-99.

Brundin, P., R. Melki and R. Kopito (2010). "Prion-like transmission of protein aggregates in neurodegenerative diseases." Nat Rev Mol Cell Biol **11**(4): 301-307.

Burn, D. J., M. H. Mark, E. D. Playford, D. M. Maraganore, T. R. Zimmerman, Jr., R. C. Duvoisin, A. E. Harding, C. D. Marsden and D. J. Brooks (1992). "Parkinson's disease in twins studied with 18F-dopa and positron emission tomography." Neurology **42**(10): 1894-1900.

Burre, J. (2015). "The Synaptic Function of alpha-Synuclein." J Parkinsons Dis **5**(4): 699-713.

Burre, J., M. Sharma and T. C. Sudhof (2012). "Systematic mutagenesis of alpha-synuclein reveals distinct sequence requirements for physiological and pathological activities." J Neurosci **32**(43): 15227-15242.

Burre, J., M. Sharma and T. C. Sudhof (2014). "alpha-Synuclein assembles into higher-order multimers upon membrane binding to promote SNARE complex formation." Proc Natl Acad Sci U S A **111**(40): E4274-4283.

Burre, J., M. Sharma, T. Tsetsenis, V. Buchman, M. R. Etherton and T. C. Sudhof (2010). "Alpha-synuclein promotes SNARE-complex assembly in vivo and in vitro." Science **329**(5999): 1663-1667.

Caughey, B. and P. T. Lansbury (2003). "Protofibrils, pores, fibrils, and neurodegeneration: separating the responsible protein aggregates from the innocent bystanders." Annu Rev Neurosci **26**: 267-298.

Chandra, S., F. Fornai, H. B. Kwon, U. Yazdani, D. Atasoy, X. Liu, R. E. Hammer, G. Battaglia, D. C. German, P. E. Castillo and T. C. Sudhof (2004). "Double-knockout mice for alpha- and beta-synucleins: effect on synaptic functions." Proc Natl Acad Sci U S A **101**(41): 14966-14971.

Chartier-Harlin, M. C., J. C. Dachsel, C. Vilarino-Guell, S. J. Lincoln, F. Lepretre, M. M. Hulihan, J. Kachergus, A. J. Milnerwood, L. Tapia, M. S. Song, E. Le Rhun, E. Mutez, L. Larvor, A. Duflot, C. Vanbesien-Mailliot, A. Kreisler, O. A. Ross, K. Nishioka, A. I. Soto-Ortolaza, S. A. Cobb, H. L. Melrose, B. Behrouz, B. H. Keeling, J. A. Bacon, E. Hentati, L. Williams, A. Yanagiya, N. Sonenberg, P. J. Lockhart, A. C. Zubair, R. J. Uitti, J. O. Aasly, A. Krygowska-Wajs, G. Opala, Z. K. Wszolek, R. Frigerio, D. M. Maraganore, D. Gosal, T. Lynch, M.

Hutchinson, A. R. Bentivoglio, E. M. Valente, W. C. Nichols, N. Pankratz, T. Foroud, R. A. Gibson, F. Hentati, D. W. Dickson, A. Destee and M. J. Farrer (2011). "Translation initiator EIF4G1 mutations in familial Parkinson disease." Am J Hum Genet **89**(3): 398-406.

Chartier-Harlin, M. C., J. Kachergus, C. Roumier, V. Mouroux, X. Douay, S. Lincoln, C. Levecque, L. Larvor, J. Andrieux, M. Hulihan, N. Waucquier, L. Defebvre, P. Amouyel, M. Farrer and A. Destee (2004). "Alpha-synuclein locus duplication as a cause of familial Parkinson's disease." Lancet **364**(9440): 1167-1169.

Chau, K. Y., H. L. Ching, A. H. Schapira and J. M. Cooper (2009). "Relationship between alpha synuclein phosphorylation, proteasomal inhibition and cell death: relevance to Parkinson's disease pathogenesis." J Neurochem **110**(3): 1005-1013.

Checkoway, H. and L. M. Nelson (1999). "Epidemiologic approaches to the study of Parkinson's disease etiology." Epidemiology **10**(3): 327-336.

Chen, L. and M. B. Feany (2005). "Alpha-synuclein phosphorylation controls neurotoxicity and inclusion formation in a Drosophila model of Parkinson disease." Nat Neurosci **8**(5): 657-663.

Chen, L., M. Periquet, X. Wang, A. Negro, P. J. McLean, B. T. Hyman and M. B. Feany (2009). "Tyrosine and serine phosphorylation of alpha-synuclein have opposing effects on neurotoxicity and soluble oligomer formation." J Clin Invest **119**(11): 3257-3265.

Chi, Y. C., G. S. Armstrong, D. N. Jones, E. Z. Eisenmesser and C. W. Liu (2014). "Residue histidine 50 plays a key role in protecting alpha-synuclein from aggregation at physiological pH." J Biol Chem **289**(22): 15474-15481.

Chiti, F. and C. M. Dobson (2006). "Protein misfolding, functional amyloid, and human disease." Annu Rev Biochem **75**: 333-366.

Choi, W., S. Zibaee, R. Jakes, L. C. Serpell, B. Davletov, R. A. Crowther and M. Goedert (2004). "Mutation E46K increases phospholipid binding and assembly into filaments of human alpha-synuclein." FEBS Lett **576**(3): 363-368.

Ciechanover, A., H. Heller, S. Elias, A. L. Haas and A. Hershko (1980). "ATP-dependent conjugation of reticulocyte proteins with the polypeptide required for protein degradation." Proc Natl Acad Sci U S A **77**(3): 1365-1368.

Clayton, D. F. and J. M. George (1998). "The synucleins: a family of proteins involved in synaptic function, plasticity, neurodegeneration and disease." Trends Neurosci **21**(6): 249-254.

Coelho, M., A. Dereli, A. Haese, S. Kuhn, L. Malinovska, M. E. DeSantis, J. Shorter, S. Alberti, T. Gross and I. M. Tolic-Norrelykke (2013). "Fission yeast does not age under favorable conditions, but does so after stress." Curr Biol **23**(19): 1844-1852.

Colla, E., P. Coune, Y. Liu, O. Pletnikova, J. C. Troncoso, T. Iwatsubo, B. L. Schneider and M. K. Lee (2012). "Endoplasmic reticulum stress is important for the manifestations of alpha-synucleinopathy in vivo." J Neurosci **32**(10): 3306-3320.

Conway, K. A., J. D. Harper and P. T. Lansbury, Jr. (2000). "Fibrils formed in vitro from alpha-synuclein and two mutant forms linked to Parkinson's disease are typical amyloid." Biochemistry **39**(10): 2552-2563.

Conway, K. A., S. J. Lee, J. C. Rochet, T. T. Ding, R. E. Williamson and P. T. Lansbury, Jr. (2000). "Acceleration of oligomerization, not fibrillization, is a shared property of both alpha-synuclein mutations linked to early-onset Parkinson's disease: implications for pathogenesis and therapy." Proc Natl Acad Sci U S A **97**(2): 571-576.

Coskuner, O. and O. Wise-Scira (2013). "Structures and free energy landscapes of the A53T mutant-type alpha-synuclein protein and impact of A53T mutation on the structures of the wild-type alpha-synuclein protein with dynamics." ACS Chem Neurosci **4**(7): 1101-1113.

Dauer, W. and S. Przedborski (2003). "Parkinson's disease: mechanisms and models." Neuron **39**(6): 889-909.

Davidson, W. S., A. Jonas, D. F. Clayton and J. M. George (1998). "Stabilization of alpha-synuclein secondary structure upon binding to synthetic membranes." J Biol Chem **273**(16): 9443-9449.

de Lau, L. M. and M. M. Breteler (2006). "Epidemiology of Parkinson's disease." Lancet Neurol **5**(6): 525-535.

den Jager, W. A. (1969). "Sphingomyelin in Lewy inclusion bodies in Parkinson's disease." Arch Neurol **21**(6): 615-619.

Devic, I., H. Hwang, J. S. Edgar, K. Izutsu, R. Presland, C. Pan, D. R. Goodlett, Y. Wang, J. Armaly, V. Tumas, C. P. Zabetian, J. B. Leverenz, M. Shi and J. Zhang (2011). "Salivary alpha-synuclein and DJ-1: potential biomarkers for Parkinson's disease." Brain **134**(Pt 7): e178.

Di Monte, D. A., M. Lavasani and A. B. Manning-Bog (2002). "Environmental factors in Parkinson's disease." Neurotoxicology **23**(4-5): 487-502.

Dice, J. F. (1990). "Peptide sequences that target cytosolic proteins for lysosomal proteolysis." Trends Biochem Sci **15**(8): 305-309.

Dobson, C. M. (2001). "The structural basis of protein folding and its links with human disease." Philos Trans R Soc Lond B Biol Sci **356**(1406): 133-145.

Dobson, C. M. (2003). "Protein folding and misfolding." Nature **426**(6968): 884-890.

Dorval, V. and P. E. Fraser (2006). "Small ubiquitin-like modifier (SUMO) modification of natively unfolded proteins tau and alpha-synuclein." J Biol Chem **281**(15): 9919-9924.

Doty, R. L. (2012). "Olfactory dysfunction in Parkinson disease." Nat Rev Neurol **8**(6): 329-339.

Ebrahimi-Fakhari, D., L. Wahlster and P. J. McLean (2011). "Molecular chaperones in Parkinson's disease--present and future." J Parkinsons Dis **1**(4): 299-320.

Eckermann, K. (2013). "SUMO and Parkinson's disease." Neuromolecular Med **15**(4): 737-759.

Edvardson, S., Y. Cinnamon, A. Ta-Shma, A. Shaag, Y. I. Yim, S. Zenvirt, C. Jalas, S. Lesage, A. Brice, A. Taraboulos, K. H. Kaestner, L. E. Greene and O. Elpeleg (2012). "A deleterious mutation in DNAJC6 encoding the neuronal-specific clathrin-uncoating co-chaperone auxilin, is associated with juvenile parkinsonism." PLoS One **7**(5): e36458.

El-Agnaf, O. M., S. A. Salem, K. E. Paleologou, L. J. Cooper, N. J. Fullwood, M. J. Gibson, M. D. Curran, J. A. Court, D. M. Mann, S. Ikeda, M. R. Cookson, J. Hardy and D. Allsop (2003). "Alpha-synuclein implicated in Parkinson's disease is present in extracellular biological fluids, including human plasma." FASEB J **17**(13): 1945-1947.

El-Agnaf, O. M., S. A. Salem, K. E. Paleologou, M. D. Curran, M. J. Gibson, J. A. Court, M. G. Schlossmacher and D. Allsop (2006). "Detection of oligomeric forms of alpha-synuclein protein in human plasma as a potential biomarker for Parkinson's disease." FASEB J **20**(3): 419-425.

Eliezer, D., E. Kutluay, R. Bussell, Jr. and G. Browne (2001). "Conformational properties of alpha-synuclein in its free and lipid-associated states." J Mol Biol **307**(4): 1061-1073.

Ellis, R. J. (2001). "Macromolecular crowding: an important but neglected aspect of the intracellular environment." Curr Opin Struct Biol **11**(1): 114-119.

Emmer, K. L., E. A. Waxman, J. P. Covy and B. I. Giasson (2011). "E46K human alpha-synuclein transgenic mice develop Lewy-like and tau pathology associated with age-dependent, detrimental motor impairment." J Biol Chem **286**(40): 35104-35118.

Engelender, S., Z. Kaminsky, X. Guo, A. H. Sharp, R. K. Amaravi, J. J. Kleiderlein, R. L. Margolis, J. C. Troncoso, A. A. Lanahan, P. F. Worley, V. L. Dawson, T. M. Dawson and C. A. Ross (1999). "Synphilin-1 associates with alpha-synuclein and promotes the formation of cytosolic inclusions." Nat Genet **22**(1): 110-114.

Engelender, S., T. Wanner, J. J. Kleiderlein, K. Wakabayashi, S. Tsuji, H. Takahashi, R. Ashworth, R. L. Margolis and C. A. Ross (2000). "Organization of the human synphilin-1 gene, a candidate for Parkinson's disease." Mamm Genome **11**(9): 763-766.

Escusa-Toret, S., W. I. Vonk and J. Frydman (2013). "Spatial sequestration of misfolded proteins by a dynamic chaperone pathway enhances cellular fitness during stress." Nat Cell Biol **15**(10): 1231-1243.

Fares, M. B., N. Ait-Bouziad, I. Dikiy, M. K. Mbefo, A. Jovicic, A. Kiely, J. L. Holton, S. J. Lee, A. D. Gitler, D. Eliezer and H. A. Lashuel (2014). "The novel Parkinson's disease linked mutation G51D attenuates in vitro aggregation and membrane binding of alpha-synuclein, and enhances its secretion and nuclear localization in cells." Hum Mol Genet **23**(17): 4491-4509.

Farrer, M., A. Destee, C. Levecque, A. Singleton, S. Engelender, E. Becquet, V. Mouroux, F. Richard, L. Defebvre, R. Crook, D. Hernandez, C. A. Ross, J. Hardy, P. Amouyel and M. C. Chartier-Harlin (2001). "Genetic analysis of synphilin-1 in familial Parkinson's disease." Neurobiol Dis **8**(2): 317-323.

Fauvet, B., M. B. Fares, F. Samuel, I. Dikiy, A. Tandon, D. Eliezer and H. A. Lashuel (2012). "Characterization of semisynthetic and naturally Nalpha-acetylated alpha-synuclein in vitro and in intact cells: implications for aggregation and cellular properties of alpha-synuclein." J Biol Chem **287**(34): 28243-28262.

Fiske, M., S. Valtierra, K. Solvang, M. Zorniak, M. White, S. Herrera, A. Konnikova, R. Brezinsky and S. Debburman (2011). "Contribution of Alanine-76 and Serine Phosphorylation in alpha-Synuclein Membrane Association and Aggregation in Yeasts." Parkinsons Dis **2011**: 392180.

Forno, L. S. and E. C. Alvord, Jr. (1974). "Depigmentation in the nerve cells of the substantia nigra and locus ceruleus in Parkinsonism." Adv Neurol **5**: 195-202.

Foulds, P. G., O. Yokota, A. Thurston, Y. Davidson, Z. Ahmed, J. Holton, J. C. Thompson, H. Akiyama, T. Arai, M. Hasegawa, A. Gerhard, D. Allsop and D. M. Mann (2012). "Post mortem cerebrospinal fluid alpha-synuclein levels are raised in multiple system atrophy and

distinguish this from the other alpha-synucleinopathies, Parkinson's disease and Dementia with Lewy bodies." Neurobiol Dis **45**(1): 188-195.

Frydman, J. and F. U. Hartl (1996). "Principles of chaperone-assisted protein folding: differences between in vitro and in vivo mechanisms." Science **272**(5267): 1497-1502.

Fujita, Y., E. Ohama, M. Takatama, S. Al-Sarraj and K. Okamoto (2006). "Fragmentation of Golgi apparatus of nigral neurons with alpha-synuclein-positive inclusions in patients with Parkinson's disease." Acta Neuropathol **112**(3): 261-265.

Fujiwara, H., M. Hasegawa, N. Dohmae, A. Kawashima, E. Masliah, M. S. Goldberg, J. Shen, K. Takio and T. Iwatsubo (2002). "alpha-Synuclein is phosphorylated in synucleinopathy lesions." Nat Cell Biol **4**(2): 160-164.

Funayama, M., K. Ohe, T. Amo, N. Furuya, J. Yamaguchi, S. Saiki, Y. Li, K. Ogaki, M. Ando, H. Yoshino, H. Tomiyama, K. Nishioka, K. Hasegawa, H. Saiki, W. Satake, K. Mogushi, R. Sasaki, Y. Kokubo, S. Kuzuhara, T. Toda, Y. Mizuno, Y. Uchiyama, K. Ohno and N. Hattori (2015). "CHCHD2 mutations in autosomal dominant late-onset Parkinson's disease: a genome-wide linkage and sequencing study." Lancet Neurol **14**(3): 274-282.

Gai, W. P., H. X. Yuan, X. Q. Li, J. T. Power, P. C. Blumbergs and P. H. Jensen (2000). "In situ and in vitro study of colocalization and segregation of alpha-synuclein, ubiquitin, and lipids in Lewy bodies." Exp Neurol **166**(2): 324-333.

Gajula Balija, M. B., C. Griesinger, A. Herzig, M. Zweckstetter and H. Jackle (2011). "Pre-fibrillar alpha-synuclein mutants cause Parkinson's disease-like non-motor symptoms in Drosophila." PLoS One **6**(9): e24701.

Gallegos, S., C. Pacheco, C. Peters, C. M. Opazo and L. G. Aguayo (2015). "Features of alpha-synuclein that could explain the progression and irreversibility of Parkinson's disease." Front Neurosci **9**: 59.

Gao, N., Y. H. Li, X. Li, S. Yu, G. L. Fu and B. Chen (2007). "Effect of alpha-synuclein on the promoter activity of tyrosine hydroxylase gene." Neurosci Bull **23**(1): 53-57.

Gasser, T. (2009). "Molecular pathogenesis of Parkinson disease: insights from genetic studies." Expert Rev Mol Med **11**: e22.

Gasser, T., B. Muller-Myhsok, Z. K. Wszolek, R. Oehlmann, D. B. Calne, V. Bonifati, B. Bereznai, E. Fabrizio, P. Vieregge and R. D. Horstmann (1998). "A susceptibility locus for Parkinson's disease maps to chromosome 2p13." Nat Genet **18**(3): 262-265.

George, J. M., H. Jin, W. S. Woods and D. F. Clayton (1995). "Characterization of a novel protein regulated during the critical period for song learning in the zebra finch." Neuron **15**(2): 361-372.

Ghosh, D., M. Mondal, G. M. Mohite, P. K. Singh, P. Ranjan, A. Anoop, S. Ghosh, N. N. Jha, A. Kumar and S. K. Maji (2013). "The Parkinson's disease-associated H50Q mutation accelerates alpha-Synuclein aggregation in vitro." Biochemistry **52**(40): 6925-6927.

Ghosh, D., S. Sahay, P. Ranjan, S. Salot, G. M. Mohite, P. K. Singh, S. Dwivedi, E. Carvalho, R. Banerjee, A. Kumar and S. K. Maji (2014). "The newly discovered Parkinson's disease associated Finnish mutation (A53E) attenuates alpha-synuclein aggregation and membrane binding." Biochemistry **53**(41): 6419-6421.

Giasson, B. I., J. E. Duda, I. V. Murray, Q. Chen, J. M. Souza, H. I. Hurtig, H. Ischiropoulos, J. Q. Trojanowski and V. M. Lee (2000). "Oxidative damage linked to neurodegeneration by selective alpha-synuclein nitration in synucleinopathy lesions." Science **290**(5493): 985-989.

Giasson, B. I., I. V. Murray, J. Q. Trojanowski and V. M. Lee (2001). "A hydrophobic stretch of 12 amino acid residues in the middle of alpha-synuclein is essential for filament assembly." J Biol Chem **276**(4): 2380-2386.

Gibb, W. R. and A. J. Lees (1988). "The relevance of the Lewy body to the pathogenesis of idiopathic Parkinson's disease." J Neurol Neurosurg Psychiatry **51**(6): 745-752.

Goedert, M., M. G. Spillantini, K. Del Tredici and H. Braak (2013). "100 years of Lewy pathology." Nat Rev Neurol **9**(1): 13-24.

Goers, J., A. B. Manning-Bog, A. L. McCormack, I. S. Millett, S. Doniach, D. A. Di Monte, V. N. Uversky and A. L. Fink (2003). "Nuclear localization of alpha-synuclein and its interaction with histones." Biochemistry **42**(28): 8465-8471.

Gonatas, N. K., A. Stieber and J. O. Gonatas (2006). "Fragmentation of the Golgi apparatus in neurodegenerative diseases and cell death." J Neurol Sci **246**(1-2): 21-30.

Goncalves, S. and T. F. Outeiro (2013). "Assessing the subcellular dynamics of alpha-synuclein using photoactivation microscopy." Mol Neurobiol **47**(3): 1081-1092.

Gorbatyuk, O. S., S. Li, L. F. Sullivan, W. Chen, G. Kondrikova, F. P. Manfredsson, R. J. Mandel and N. Muzyczka (2008). "The phosphorylation state of Ser-129 in human alpha-synuclein

determines neurodegeneration in a rat model of Parkinson disease." Proc Natl Acad Sci U S A **105**(2): 763-768.

Greenbaum, E. A., C. L. Graves, A. J. Mishizen-Eberz, M. A. Lupoli, D. R. Lynch, S. W. Englander, P. H. Axelsen and B. I. Giasson (2005). "The E46K mutation in alpha-synuclein increases amyloid fibril formation." J Biol Chem **280**(9): 7800-7807.

Groiss, S. J., L. Wojtecki, M. Sudmeyer and A. Schnitzler (2009). "Deep brain stimulation in Parkinson's disease." Ther Adv Neurol Disord **2**(6): 20-28.

Guerriero, C. J. and J. L. Brodsky (2012). "The delicate balance between secreted protein folding and endoplasmic reticulum-associated degradation in human physiology." Physiol Rev **92**(2): 537-576.

Harper, J. D., S. S. Wong, C. M. Lieber and P. T. Lansbury (1997). "Observation of metastable Abeta amyloid protofibrils by atomic force microscopy." Chem Biol **4**(2): 119-125.

Harper, J. D., S. S. Wong, C. M. Lieber and P. T. Lansbury, Jr. (1999). "Assembly of A beta amyloid protofibrils: an in vitro model for a possible early event in Alzheimer's disease." Biochemistry **38**(28): 8972-8980.

Hartl, F. U., A. Bracher and M. Hayer-Hartl (2011). "Molecular chaperones in protein folding and proteostasis." Nature **475**(7356): 324-332.

Hatano, Y., Y. Li, K. Sato, S. Asakawa, Y. Yamamura, H. Tomiyama, H. Yoshino, M. Asahina, S. Kobayashi, S. Hassin-Baer, C. S. Lu, A. R. Ng, R. L. Rosales, N. Shimizu, T. Toda, Y. Mizuno and N. Hattori (2004). "Novel PINK1 mutations in early-onset parkinsonism." Ann Neurol **56**(3): 424-427.

Heise, H., W. Hoyer, S. Becker, O. C. Andronesi, D. Riedel and M. Baldus (2005). "Molecular-level secondary structure, polymorphism, and dynamics of full-length alpha-synuclein fibrils studied by solid-state NMR." Proc Natl Acad Sci U S A **102**(44): 15871-15876.

Herkenham, M., M. D. Little, K. Bankiewicz, S. C. Yang, S. P. Markey and J. N. Johannessen (1991). "Selective retention of MPP+ within the monoaminergic systems of the primate brain following MPTP administration: an in vivo autoradiographic study." Neuroscience **40**(1): 133-158.

Hershko, A. and A. Ciechanover (1998). "The ubiquitin system." Annu Rev Biochem **67**: 425-479.

Hershko, A., A. Ciechanover, H. Heller, A. L. Haas and I. A. Rose (1980). "Proposed role of ATP in protein breakdown: conjugation of protein with multiple chains of the polypeptide of ATP-dependent proteolysis." Proc Natl Acad Sci U S A **77**(4): 1783-1786.

Hilker, R., A. V. Thomas, J. C. Klein, S. Weisenbach, E. Kalbe, L. Burghaus, A. H. Jacobs, K. Herholz and W. D. Heiss (2005). "Dementia in Parkinson disease: functional imaging of cholinergic and dopaminergic pathways." Neurology **65**(11): 1716-1722.

Holzmann, C., R. Kruger, A. M. Saecker, I. Schmitt, L. Schols, K. Berger and O. Riess (2003). "Polymorphisms of the alpha-synuclein promoter: expression analyses and association studies in Parkinson's disease." J Neural Transm (Vienna) **110**(1): 67-76.

Honig, B. (1999). "Protein folding: from the levinthal paradox to structure prediction." J Mol Biol **293**(2): 283-293.

Hoyer, W., T. Antony, D. Cherny, G. Heim, T. M. Jovin and V. Subramaniam (2002). "Dependence of alpha-synuclein aggregate morphology on solution conditions." J Mol Biol **322**(2): 383-393.

Hoyer, W., D. Cherny, V. Subramaniam and T. M. Jovin (2004). "Impact of the acidic C-terminal region comprising amino acids 109-140 on alpha-synuclein aggregation in vitro." Biochemistry **43**(51): 16233-16242.

Hsu, L. J., M. Mallory, Y. Xia, I. Veinbergs, M. Hashimoto, M. Yoshimoto, L. J. Thal, T. Saitoh and E. Masliah (1998). "Expression pattern of synucleins (non-Abeta component of Alzheimer's disease amyloid precursor protein/alpha-synuclein) during murine brain development." J Neurochem **71**(1): 338-344.

Ibanez, P., A. M. Bonnet, B. Debarges, E. Lohmann, F. Tison, P. Pollak, Y. Agid, A. Durr and A. Brice (2004). "Causal relation between alpha-synuclein gene duplication and familial Parkinson's disease." Lancet **364**(9440): 1169-1171.

Ikeda, F. and I. Dikic (2008). "Atypical ubiquitin chains: new molecular signals. 'Protein Modifications: Beyond the Usual Suspects' review series." EMBO Rep **9**(6): 536-542.

Inobe, T. and A. Matouschek (2014). "Paradigms of protein degradation by the proteasome." Curr Opin Struct Biol **24**: 156-164.

Iseki, E., N. Takayama, Y. Furukawa, W. Marui, T. Nakai, S. Miura, K. Ueda and K. Kosaka (2002). "Immunohistochemical study of synphilin-1 in brains of patients with dementia with Lewy bodies - synphilin-1 is non-specifically implicated in the formation of different neuronal cytoskeletal inclusions." Neurosci Lett **326**(3): 211-215.

Ishizawa, T., P. Mattila, P. Davies, D. Wang and D. W. Dickson (2003). "Colocalization of tau and alpha-synuclein epitopes in Lewy bodies." J Neuropathol Exp Neurol **62**(4): 389-397.

Iwai, A., E. Masliah, M. Yoshimoto, N. Ge, L. Flanagan, H. A. de Silva, A. Kittel and T. Saitoh (1995). "The precursor protein of non-A beta component of Alzheimer's disease amyloid is a presynaptic protein of the central nervous system." Neuron **14**(2): 467-475.

Jaattela, M. (1999). "Heat shock proteins as cellular lifeguards." Ann Med **31**(4): 261-271.

Jahn, R. and R. H. Scheller (2006). "SNAREs--engines for membrane fusion." Nat Rev Mol Cell Biol **7**(9): 631-643.

Jakes, R., M. G. Spillantini and M. Goedert (1994). "Identification of two distinct synucleins from human brain." FEBS Lett **345**(1): 27-32.

Jao, C. C., A. Der-Sarkissian, J. Chen and R. Langen (2004). "Structure of membrane-bound alpha-synuclein studied by site-directed spin labeling." Proc Natl Acad Sci U S A **101**(22): 8331-8336.

Jao, C. C., B. G. Hegde, J. Chen, I. S. Haworth and R. Langen (2008). "Structure of membrane-bound alpha-synuclein from site-directed spin labeling and computational refinement." Proc Natl Acad Sci U S A **105**(50): 19666-19671.

Jensen, M. R., M. Zweckstetter, J. R. Huang and M. Blackledge (2014). "Exploring free-energy landscapes of intrinsically disordered proteins at atomic resolution using NMR spectroscopy." Chem Rev **114**(13): 6632-6660.

Jensen, P. H., M. S. Nielsen, R. Jakes, C. G. Dotti and M. Goedert (1998). "Binding of alpha-synuclein to brain vesicles is abolished by familial Parkinson's disease mutation." J Biol Chem **273**(41): 26292-26294.

Jo, E., N. Fuller, R. P. Rand, P. St George-Hyslop and P. E. Fraser (2002). "Defective membrane interactions of familial Parkinson's disease mutant A30P alpha-synuclein." J Mol Biol **315**(4): 799-807.

Johnston, J. A., M. E. Illing and R. R. Kopito (2002). "Cytoplasmic dynein/dynactin mediates the assembly of aggresomes." Cell Motil Cytoskeleton **53**(1): 26-38.

Johnston, J. A., C. L. Ward and R. R. Kopito (1998). "Aggresomes: a cellular response to misfolded proteins." J Cell Biol **143**(7): 1883-1898.

Jucker, M. and L. C. Walker (2013). "Self-propagation of pathogenic protein aggregates in neurodegenerative diseases." Nature **501**(7465): 45-51.

Kaganovich, D., R. Kopito and J. Frydman (2008). "Misfolded proteins partition between two distinct quality control compartments." Nature **454**(7208): 1088-1095.

Kanduri, C., T. Kuusi, M. Ahvenainen, A. K. Philips, H. Lahdesmaki and I. Jarvela (2015). "The effect of music performance on the transcriptome of professional musicians." Sci Rep **5**: 9506.

Kang, L., G. M. Moriarty, L. A. Woods, A. E. Ashcroft, S. E. Radford and J. Baum (2012). "N-terminal acetylation of alpha-synuclein induces increased transient helical propensity and decreased aggregation rates in the intrinsically disordered monomer." Protein Sci **21**(7): 911-917.

Karpinar, D. P., M. B. Balija, S. Kugler, F. Opazo, N. Rezaei-Ghaleh, N. Wender, H. Y. Kim, G. Taschenberger, B. H. Falkenburger, H. Heise, A. Kumar, D. Riedel, L. Fichtner, A. Voigt, G. H. Braus, K. Giller, S. Becker, A. Herzig, M. Baldus, H. Jackle, S. Eimer, J. B. Schulz, C. Griesinger and M. Zweckstetter (2009). "Pre-fibrillar alpha-synuclein variants with impaired beta-structure increase neurotoxicity in Parkinson's disease models." EMBO J **28**(20): 3256-3268.

Kawamata, H., P. J. McLean, N. Sharma and B. T. Hyman (2001). "Interaction of alpha-synuclein and synphilin-1: effect of Parkinson's disease-associated mutations." J Neurochem **77**(3): 929-934.

Kaylor, J., N. Bodner, S. Edridge, G. Yamin, D. P. Hong and A. L. Fink (2005). "Characterization of oligomeric intermediates in alpha-synuclein fibrillation: FRET studies of Y125W/Y133F/Y136F alpha-synuclein." J Mol Biol **353**(2): 357-372.

Kerppola, T. K. (2006). "Design and implementation of bimolecular fluorescence complementation (BiFC) assays for the visualization of protein interactions in living cells." Nat Protoc **1**(3): 1278-1286.

Khalaf, O., B. Fauvet, A. Oueslati, I. Dikiy, A. L. Mahul-Mellier, F. S. Ruggeri, M. K. Mbefo, F. Vercruysse, G. Dietler, S. J. Lee, D. Eliezer and H. A. Lashuel (2014). "The H50Q mutation enhances alpha-synuclein aggregation, secretion, and toxicity." J Biol Chem **289**(32): 21856-21876.

Khurana, R., V. N. Uversky, L. Nielsen and A. L. Fink (2001). "Is Congo red an amyloid-specific dye?" J Biol Chem **276**(25): 22715-22721.

Kiely, A. P., Y. T. Asi, E. Kara, P. Limousin, H. Ling, P. Lewis, C. Proukakis, N. Quinn, A. J. Lees, J. Hardy, T. Revesz, H. Houlden and J. L. Holton (2013). "alpha-Synucleinopathy associated with G51D SNCA mutation: a link between Parkinson's disease and multiple system atrophy?" Acta Neuropathol **125**(5): 753-769.

Kiely, A. P., H. Ling, Y. T. Asi, E. Kara, C. Proukakis, A. H. Schapira, H. R. Morris, H. C. Roberts, S. Lubbe, P. Limousin, P. A. Lewis, A. J. Lees, N. Quinn, J. Hardy, S. Love, T. Revesz, H. Houlden and J. L. Holton (2015). "Distinct clinical and neuropathological features of G51D SNCA mutation cases compared with SNCA duplication and H50Q mutation." Mol Neurodegener **10**: 41.

Kim, E. J., J. Y. Sung, H. J. Lee, H. Rhim, M. Hasegawa, T. Iwatsubo, S. Min do, J. Kim, S. R. Paik and K. C. Chung (2006). "Dyrk1A phosphorylates alpha-synuclein and enhances intracellular inclusion formation." J Biol Chem **281**(44): 33250-33257.

Kim, H. T., K. P. Kim, F. Lledias, A. F. Kisselev, K. M. Scaglione, D. Skowyra, S. P. Gygi and A. L. Goldberg (2007). "Certain pairs of ubiquitin-conjugating enzymes (E2s) and ubiquitin-protein ligases (E3s) synthesize nondegradable forked ubiquitin chains containing all possible isopeptide linkages." J Biol Chem **282**(24): 17375-17386.

Kim, T. D., S. R. Paik, C. H. Yang and J. Kim (2000). "Structural changes in alpha-synuclein affect its chaperone-like activity in vitro." Protein Sci **9**(12): 2489-2496.

Kim, W. S., K. Kagedal and G. M. Halliday (2014). "Alpha-synuclein biology in Lewy body diseases." Alzheimers Res Ther **6**(5): 73.

Kitada, T., S. Asakawa, N. Hattori, H. Matsumine, Y. Yamamura, S. Minoshima, M. Yokochi, Y. Mizuno and N. Shimizu (1998). "Mutations in the parkin gene cause autosomal recessive juvenile parkinsonism." Nature **392**(6676): 605-608.

Klein, T., R. I. Viner and C. M. Overall (2016). "Quantitative proteomics and terminomics to elucidate the role of ubiquitination and proteolysis in adaptive immunity." Philos Trans A Math Phys Eng Sci **374**(2079).

Knowles, T. P., M. Vendruscolo and C. M. Dobson (2014). "The amyloid state and its association with protein misfolding diseases." Nat Rev Mol Cell Biol **15**(6): 384-396.

Kordower, J. H., Y. Chu, R. A. Hauser, T. B. Freeman and C. W. Olanow (2008). "Lewy body-like pathology in long-term embryonic nigral transplants in Parkinson's disease." Nat Med **14**(5): 504-506.

Kordower, J. H., Y. Chu, R. A. Hauser, C. W. Olanow and T. B. Freeman (2008). "Transplanted dopaminergic neurons develop PD pathologic changes: a second case report." Mov Disord **23**(16): 2303-2306.

Kraft, C., M. Peter and K. Hofmann (2010). "Selective autophagy: ubiquitin-mediated recognition and beyond." Nat Cell Biol **12**(9): 836-841.

Kragh, C. L., L. B. Lund, F. Febbraro, H. D. Hansen, W. P. Gai, O. El-Agnaf, C. Richter-Landsberg and P. H. Jensen (2009). "Alpha-synuclein aggregation and Ser-129 phosphorylation-dependent cell death in oligodendroglial cells." J Biol Chem **284**(15): 10211-10222.

Krebs, C. E., S. Karkheiran, J. C. Powell, M. Cao, V. Makarov, H. Darvish, G. Di Paolo, R. H. Walker, G. A. Shahidi, J. D. Buxbaum, P. De Camilli, Z. Yue and C. Paisan-Ruiz (2013). "The Sac1 domain of SYNJ1 identified mutated in a family with early-onset progressive Parkinsonism with generalized seizures." Hum Mutat **34**(9): 1200-1207.

Krishnan, S., E. Y. Chi, S. J. Wood, B. S. Kendrick, C. Li, W. Garzon-Rodriguez, J. Wypych, T. W. Randolph, L. O. Narhi, A. L. Biere, M. Citron and J. F. Carpenter (2003). "Oxidative dimer formation is the critical rate-limiting step for Parkinson's disease alpha-synuclein fibrillogenesis." Biochemistry **42**(3): 829-837.

Kruger, R. (2004). "The role of synphilin-1 in synaptic function and protein degradation." Cell Tissue Res **318**(1): 195-199.

Kruger, R., W. Kuhn, T. Muller, D. Woitalla, M. Graeber, S. Kosel, H. Przuntek, J. T. Epplen, L. Schols and O. Riess (1998). "Ala30Pro mutation in the gene encoding alpha-synuclein in Parkinson's disease." Nat Genet **18**(2): 106-108.

Krumova, P., E. Meulmeester, M. Garrido, M. Tirard, H. H. Hsiao, G. Bossis, H. Urlaub, M. Zweckstetter, S. Kugler, F. Melchior, M. Bahr and J. H. Weishaupt (2011). "Sumoylation inhibits alpha-synuclein aggregation and toxicity." J Cell Biol **194**(1): 49-60.

Kuusisto, E., L. Parkkinen and I. Alafuzoff (2003). "Morphogenesis of Lewy bodies: dissimilar incorporation of alpha-synuclein, ubiquitin, and p62." J Neuropathol Exp Neurol **62**(12): 1241-1253.

Lai, C. Y., E. Jaruga, C. Borghouts and S. M. Jazwinski (2002). "A mutation in the ATP2 gene abrogates the age asymmetry between mother and daughter cells of the yeast Saccharomyces cerevisiae." Genetics **162**(1): 73-87.

Lan, S., L. Kang, D. T. Schoen, S. P. Rodrigues, Y. Cui, M. L. Brongersma and W. Cai (2015). "Backward phase-matching for nonlinear optical generation in negative-index materials." Nat Mater **14**(8): 807-811.

Larsen, K. E., Y. Schmitz, M. D. Troyer, E. Mosharov, P. Dietrich, A. Z. Quazi, M. Savalle, V. Nemani, F. A. Chaudhry, R. H. Edwards, L. Stefanis and D. Sulzer (2006). "Alpha-synuclein overexpression in PC12 and chromaffin cells impairs catecholamine release by interfering with a late step in exocytosis." J Neurosci **26**(46): 11915-11922.

Lashuel, H. A., D. Hartley, B. M. Petre, T. Walz and P. T. Lansbury, Jr. (2002). "Neurodegenerative disease: amyloid pores from pathogenic mutations." Nature **418**(6895): 291.

Lautier, C., S. Goldwurm, A. Durr, B. Giovannone, W. G. Tsiaras, G. Pezzoli, A. Brice and R. J. Smith (2008). "Mutations in the GIGYF2 (TNRC15) gene at the PARK11 locus in familial Parkinson disease." Am J Hum Genet **82**(4): 822-833.

Lee, B. R., Y. Matsuo, A. G. Cashikar and T. Kamitani (2013). "Role of Ser129 phosphorylation of alpha-synuclein in melanoma cells." J Cell Sci **126**(Pt 2): 696-704.

Lee, H. J., C. Choi and S. J. Lee (2002). "Membrane-bound alpha-synuclein has a high aggregation propensity and the ability to seed the aggregation of the cytosolic form." J Biol Chem **277**(1): 671-678.

Lesage, S., M. Anheim, F. Letournel, L. Bousset, A. Honore, N. Rozas, L. Pieri, K. Madiona, A. Durr, R. Melki, C. Verny, A. Brice and G. French Parkinson's Disease Genetics Study (2013). "G51D alpha-synuclein mutation causes a novel parkinsonian-pyramidal syndrome." Ann Neurol **73**(4): 459-471.

Lesage, S., V. Drouet, E. Majounie, V. Deramecourt, M. Jacoupy, A. Nicolas, F. Cormier-Dequaire, S. M. Hassoun, C. Pujol, S. Ciura, Z. Erpapazoglou, T. Usenko, C. A. Maurage, M. Sahbatou, S. Liebau, J. Ding, B. Bilgic, M. Emre, N. Erginel-Unaltuna, G. Guven, F. Tison, C. Tranchant, M. Vidailhet, J. C. Corvol, P. Krack, A. L. Leutenegger, M. A. Nalls, D. G. Hernandez, P. Heutink, J. R. Gibbs, J. Hardy, N. W. Wood, T. Gasser, A. Durr, J. F. Deleuze, M. Tazir, A. Destee, E. Lohmann, E. Kabashi, A. Singleton, O. Corti and A. Brice (2016). "Loss of VPS13C Function in Autosomal-Recessive Parkinsonism Causes Mitochondrial Dysfunction and Increases PINK1/Parkin-Dependent Mitophagy." Am J Hum Genet **98**(3): 500-513.

Levinthal, C. (1968). "Are there pathways for protein folding?" Extrait du Journal de Chimie Physique **65**(1): 44.

Li, S. C., N. K. Goto, K. A. Williams and C. M. Deber (1996). "Alpha-helical, but not beta-sheet, propensity of proline is determined by peptide environment." Proc Natl Acad Sci U S A **93**(13): 6676-6681.

Li, W., N. West, E. Colla, O. Pletnikova, J. C. Troncoso, L. Marsh, T. M. Dawson, P. Jakala, T. Hartmann, D. L. Price and M. K. Lee (2005). "Aggregation promoting C-terminal truncation of alpha-synuclein is a normal cellular process and is enhanced by the familial Parkinson's disease-linked mutations." Proc Natl Acad Sci U S A **102**(6): 2162-2167.

Li, Y. J., W. K. Scott, D. J. Hedges, F. Zhang, P. C. Gaskell, M. A. Nance, R. L. Watts, J. P. Hubble, W. C. Koller, R. Pahwa, M. B. Stern, B. C. Hiner, J. Jankovic, F. A. Allen, Jr., C. G. Goetz, F. Mastaglia, J. M. Stajich, R. A. Gibson, L. T. Middleton, A. M. Saunders, B. L. Scott, G. W. Small, K. K. Nicodemus, A. D. Reed, D. E. Schmechel, K. A. Welsh-Bohmer, P. M. Conneally, A. D. Roses, J. R. Gilbert, J. M. Vance, J. L. Haines and M. A. Pericak-Vance (2002). "Age at onset in two common neurodegenerative diseases is genetically controlled." Am J Hum Genet **70**(4): 985-993.

Lindner, A. B., R. Madden, A. Demarez, E. J. Stewart and F. Taddei (2008). "Asymmetric segregation of protein aggregates is associated with cellular aging and rejuvenation." Proc Natl Acad Sci U S A **105**(8): 3076-3081.

Lippa, C. F., H. Fujiwara, D. M. Mann, B. Giasson, M. Baba, M. L. Schmidt, L. E. Nee, B. O'Connell, D. A. Pollen, P. St George-Hyslop, B. Ghetti, D. Nochlin, T. D. Bird, N. J. Cairns, V. M. Lee, T. Iwatsubo and J. Q. Trojanowski (1998). "Lewy bodies contain altered alpha-synuclein in brains of many familial Alzheimer's disease patients with mutations in presenilin and amyloid precursor protein genes." Am J Pathol **153**(5): 1365-1370.

Litim, N., M. Morissette and T. Di Paolo (2015). "Neuroactive gonadal drugs for neuroprotection in male and female models of Parkinson's disease." Neurosci Biobehav Rev.

Liu, B., L. Larsson, A. Caballero, X. Hao, D. Oling, J. Grantham and T. Nystrom (2010). "The polarisome is required for segregation and retrograde transport of protein aggregates." Cell **140**(2): 257-267.

Liu, D., L. Jin, H. Wang, H. Zhao, C. Zhao, C. Duan, L. Lu, B. Wu, S. Yu, P. Chan, Y. Li and H. Yang (2008). "Silencing alpha-synuclein gene expression enhances tyrosine hydroxylase activity in MN9D cells." Neurochem Res **33**(7): 1401-1409.

Liu, Y., L. Fallon, H. A. Lashuel, Z. Liu and P. T. Lansbury, Jr. (2002). "The UCH-L1 gene encodes two opposing enzymatic activities that affect alpha-synuclein degradation and Parkinson's disease susceptibility." Cell **111**(2): 209-218.

Lowe, J., A. Blanchard, K. Morrell, G. Lennox, L. Reynolds, M. Billett, M. Landon and R. J. Mayer (1988). "Ubiquitin is a common factor in intermediate filament inclusion bodies of diverse type in man, including those of Parkinson's disease, Pick's disease, and Alzheimer's disease, as well as Rosenthal fibres in cerebellar astrocytomas, cytoplasmic bodies in muscle, and mallory bodies in alcoholic liver disease." J Pathol **155**(1): 9-15.

Luk, K. C., V. Kehm, J. Carroll, B. Zhang, P. O'Brien, J. Q. Trojanowski and V. M. Lee (2012). "Pathological alpha-synuclein transmission initiates Parkinson-like neurodegeneration in nontransgenic mice." Science **338**(6109): 949-953.

Luk, K. C., V. M. Kehm, B. Zhang, P. O'Brien, J. Q. Trojanowski and V. M. Lee (2012). "Intracerebral inoculation of pathological alpha-synuclein initiates a rapidly progressive neurodegenerative alpha-synucleinopathy in mice." J Exp Med **209**(5): 975-986.

Machiya, Y., S. Hara, S. Arawaka, S. Fukushima, H. Sato, M. Sakamoto, S. Koyama and T. Kato (2010). "Phosphorylated alpha-synuclein at Ser-129 is targeted to the proteasome pathway in a ubiquitin-independent manner." J Biol Chem **285**(52): 40732-40744.

Mahul-Mellier, A. L., B. Fauvet, A. Gysbers, I. Dikiy, A. Oueslati, S. Georgeon, A. J. Lamontanara, A. Bisquertt, D. Eliezer, E. Masliah, G. Halliday, O. Hantschel and H. A. Lashuel (2014). "c-Abl phosphorylates alpha-synuclein and regulates its degradation: implication for alpha-synuclein clearance and contribution to the pathogenesis of Parkinson's disease." Hum Mol Genet **23**(11): 2858-2879.

Maltsev, A. S., J. Ying and A. Bax (2012). "Impact of N-terminal acetylation of alpha-synuclein on its random coil and lipid binding properties." Biochemistry **51**(25): 5004-5013.

Maroteaux, L., J. T. Campanelli and R. H. Scheller (1988). "Synuclein: a neuron-specific protein localized to the nucleus and presynaptic nerve terminal." J Neurosci **8**(8): 2804-2815.

Marsden, C. D. (1983). "Neuromelanin and Parkinson's disease." J Neural Transm Suppl **19**: 121-141.

Marx, F. P., C. Holzmann, K. M. Strauss, L. Li, O. Eberhardt, E. Gerhardt, M. R. Cookson, D. Hernandez, M. J. Farrer, J. Kachergus, S. Engelender, C. A. Ross, K. Berger, L. Schols, J. B. Schulz, O. Riess and R. Kruger (2003). "Identification and functional characterization of a novel R621C mutation in the synphilin-1 gene in Parkinson's disease." Hum Mol Genet **12**(11): 1223-1231.

Mayer, M. P. and B. Bukau (2005). "Hsp70 chaperones: cellular functions and molecular mechanism." Cell Mol Life Sci **62**(6): 670-684.

Mbefo, M. K., M. B. Fares, K. Paleologou, A. Oueslati, G. Yin, S. Tenreiro, M. Pinto, T. Outeiro, M. Zweckstetter, E. Masliah and H. A. Lashuel (2015). "Parkinson disease mutant E46K enhances alpha-synuclein phosphorylation in mammalian cell lines, in yeast, and in vivo." J Biol Chem **290**(15): 9412-9427.

Mbefo, M. K., K. E. Paleologou, A. Boucharaba, A. Oueslati, H. Schell, M. Fournier, D. Olschewski, G. Yin, M. Zweckstetter, E. Masliah, P. J. Kahle, H. Hirling and H. A. Lashuel (2010). "Phosphorylation of synucleins by members of the Polo-like kinase family." J Biol Chem **285**(4): 2807-2822.

McFarland, M. A., C. E. Ellis, S. P. Markey and R. L. Nussbaum (2008). "Proteomics analysis identifies phosphorylation-dependent alpha-synuclein protein interactions." Mol Cell Proteomics **7**(11): 2123-2137.

McLean, P. J., H. Kawamata and B. T. Hyman (2001). "Alpha-synuclein-enhanced green fluorescent protein fusion proteins form proteasome sensitive inclusions in primary neurons." Neuroscience **104**(3): 901-912.

McLean, P. J., H. Kawamata, S. Shariff, J. Hewett, N. Sharma, K. Ueda, X. O. Breakefield and B. T. Hyman (2002). "TorsinA and heat shock proteins act as molecular chaperones: suppression of alpha-synuclein aggregation." J Neurochem **83**(4): 846-854.

McLean, P. J., S. Ribich and B. T. Hyman (2000). "Subcellular localization of alpha-synuclein in primary neuronal cultures: effect of missense mutations." J Neural Transm Suppl(58): 53-63.

Mezey, E., A. M. Dehejia, G. Harta, N. Tresser, S. F. Suchy, R. L. Nussbaum, M. J. Brownstein and M. H. Polymeropoulos (1998). "Alpha synuclein is present in Lewy bodies in sporadic Parkinson's disease." Mol Psychiatry **3**(6): 493-499.

Mihajlovic, M. and T. Lazaridis (2008). "Membrane-bound structure and energetics of alpha-synuclein." Proteins **70**(3): 761-778.

Miller, S. B., A. Mogk and B. Bukau (2015). "Spatially organized aggregation of misfolded proteins as cellular stress defense strategy." J Mol Biol **427**(7): 1564-1574.

Moree, B., K. Connell, R. B. Mortensen, C. T. Liu, S. J. Benkovic and J. Salafsky (2015). "Protein Conformational Changes Are Detected and Resolved Site Specifically by Second-Harmonic Generation." Biophys J **109**(4): 806-815.

Muller, O., T. Sattler, M. Flotenmeyer, H. Schwarz, H. Plattner and A. Mayer (2000). "Autophagic tubes: vacuolar invaginations involved in lateral membrane sorting and inverse vesicle budding." J Cell Biol **151**(3): 519-528.

Murphy, D. D., S. M. Rueter, J. Q. Trojanowski and V. M. Lee (2000). "Synucleins are developmentally expressed, and alpha-synuclein regulates the size of the presynaptic vesicular pool in primary hippocampal neurons." J Neurosci **20**(9): 3214-3220.

Murray, I. J., M. A. Medford, H. P. Guan, S. M. Rueter, J. Q. Trojanowski and V. M. Lee (2003). "Synphilin in normal human brains and in synucleinopathies: studies with new antibodies." Acta Neuropathol **105**(2): 177-184.

Nakagomi, S., M. J. Barsoum, E. Bossy-Wetzel, C. Sutterlin, V. Malhotra and S. A. Lipton (2008). "A Golgi fragmentation pathway in neurodegeneration." Neurobiol Dis **29**(2): 221-231.

Nakajo, S., K. Tsukada, K. Omata, Y. Nakamura and K. Nakaya (1993). "A new brain-specific 14-kDa protein is a phosphoprotein. Its complete amino acid sequence and evidence for phosphorylation." Eur J Biochem **217**(3): 1057-1063.

Nathan, J. A., H. T. Kim, L. Ting, S. P. Gygi and A. L. Goldberg (2013). "Why do cellular proteins linked to K63-polyubiquitin chains not associate with proteasomes?" EMBO J **32**(4): 552-565.

Negro, A., A. M. Brunati, A. Donella-Deana, M. L. Massimino and L. A. Pinna (2002). "Multiple phosphorylation of alpha-synuclein by protein tyrosine kinase Syk prevents eosin-induced aggregation." FASEB J **16**(2): 210-212.

Newton, K., M. L. Matsumoto, I. E. Wertz, D. S. Kirkpatrick, J. R. Lill, J. Tan, D. Dugger, N. Gordon, S. S. Sidhu, F. A. Fellouse, L. Komuves, D. M. French, R. E. Ferrando, C. Lam, D. Compaan, C. Yu, I. Bosanac, S. G. Hymowitz, R. F. Kelley and V. M. Dixit (2008). "Ubiquitin chain editing revealed by polyubiquitin linkage-specific antibodies." Cell **134**(4): 668-678.

Nollen, E. A., A. E. Kabakov, J. F. Brunsting, B. Kanon, J. Hohfeld and H. H. Kampinga (2001). "Modulation of in vivo HSP70 chaperone activity by Hip and Bag-1." J Biol Chem **276**(7): 4677-4682.

Nollen, E. A. and R. I. Morimoto (2002). "Chaperoning signaling pathways: molecular chaperones as stress-sensing 'heat shock' proteins." J Cell Sci **115**(Pt 14): 2809-2816.

Nussbaum, R. L. and M. H. Polymeropoulos (1997). "Genetics of Parkinson's disease." Hum Mol Genet **6**(10): 1687-1691.

Nystrom, T. and B. Liu (2014). "The mystery of aging and rejuvenation - a budding topic." Curr Opin Microbiol **18**: 61-67.

O'Farrell, C., D. D. Murphy, L. Petrucelli, A. B. Singleton, J. Hussey, M. Farrer, J. Hardy, D. W. Dickson and M. R. Cookson (2001). "Transfected synphilin-1 forms cytoplasmic inclusions in HEK293 cells." Brain Res Mol Brain Res **97**(1): 94-102.

Ogrodnik, M., H. Salmonowicz, R. Brown, J. Turkowska, W. Sredniawa, S. Pattabiraman, T. Amen, A. C. Abraham, N. Eichler, R. Lyakhovetsky and D. Kaganovich (2014). "Dynamic JUNQ inclusion bodies are asymmetrically inherited in mammalian cell lines through the asymmetric partitioning of vimentin." Proc Natl Acad Sci U S A **111**(22): 8049-8054.

Omura, T., M. Kaneko, Y. Okuma, K. Matsubara and Y. Nomura (2013). "Endoplasmic reticulum stress and Parkinson's disease: the role of HRD1 in averting apoptosis in neurodegenerative disease." Oxid Med Cell Longev **2013**: 239854.

Ono, K., T. Ikeda, J. Takasaki and M. Yamada (2011). "Familial Parkinson disease mutations influence alpha-synuclein assembly." Neurobiol Dis **43**(3): 715-724.

Onuchic, J. N., Z. Luthey-Schulten and P. G. Wolynes (1997). "Theory of protein folding: the energy landscape perspective." Annu Rev Phys Chem **48**: 545-600.

Oueslati, A., M. Fournier and H. A. Lashuel (2010). "Role of post-translational modifications in modulating the structure, function and toxicity of alpha-synuclein: implications for Parkinson's disease pathogenesis and therapies." Prog Brain Res **183**: 115-145.

Outeiro, T. F. and S. Lindquist (2003). "Yeast cells provide insight into alpha-synuclein biology and pathobiology." Science **302**(5651): 1772-1775.

Outeiro, T. F., P. Putcha, J. E. Tetzlaff, R. Spoelgen, M. Koker, F. Carvalho, B. T. Hyman and P. J. McLean (2008). "Formation of toxic oligomeric alpha-synuclein species in living cells." PLoS One **3**(4): e1867.

Paisan-Ruiz, C., K. P. Bhatia, A. Li, D. Hernandez, M. Davis, N. W. Wood, J. Hardy, H. Houlden, A. Singleton and S. A. Schneider (2009). "Characterization of PLA2G6 as a locus for dystonia-parkinsonism." Ann Neurol **65**(1): 19-23.

Paleologou, K. E., A. Oueslati, G. Shakked, C. C. Rospigliosi, H. Y. Kim, G. R. Lamberto, C. O. Fernandez, A. Schmid, F. Chegini, W. P. Gai, D. Chiappe, M. Moniatte, B. L. Schneider, P. Aebischer, D. Eliezer, M. Zweckstetter, E. Masliah and H. A. Lashuel (2010). "Phosphorylation at S87 is enhanced in synucleinopathies, inhibits alpha-synuclein oligomerization, and influences synuclein-membrane interactions." J Neurosci **30**(9): 3184-3198.

Paleologou, K. E., A. W. Schmid, C. C. Rospigliosi, H. Y. Kim, G. R. Lamberto, R. A. Fredenburg, P. T. Lansbury, Jr., C. O. Fernandez, D. Eliezer, M. Zweckstetter and H. A. Lashuel (2008). "Phosphorylation at Ser-129 but not the phosphomimics S129E/D inhibits the fibrillation of alpha-synuclein." J Biol Chem **283**(24): 16895-16905.

Pan-Montojo, F., O. Anichtchik, Y. Dening, L. Knels, S. Pursche, R. Jung, S. Jackson, G. Gille, M. G. Spillantini, H. Reichmann and R. H. Funk (2010). "Progression of Parkinson's disease pathology is reproduced by intragastric administration of rotenone in mice." PLoS One **5**(1): e8762.

Pankratz, N., W. C. Nichols, S. K. Uniacke, C. Halter, A. Rudolph, C. Shults, P. M. Conneally and T. Foroud (2002). "Genome screen to identify susceptibility genes for Parkinson disease in a sample without parkin mutations." Am J Hum Genet **71**(1): 124-135.

Park, S. M., H. Y. Jung, T. D. Kim, J. H. Park, C. H. Yang and J. Kim (2002). "Distinct roles of the N-terminal-binding domain and the C-terminal-solubilizing domain of alpha-synuclein, a molecular chaperone." J Biol Chem **277**(32): 28512-28520.

Parkinson, J. (2002). "An essay on the shaking palsy. 1817." J Neuropsychiatry Clin Neurosci **14**(2): 223-236; discussion 222.

Pasanen, P., L. Myllykangas, M. Siitonen, A. Raunio, S. Kaakkola, J. Lyytinen, P. J. Tienari, M. Poyhonen and A. Paetau (2014). "Novel alpha-synuclein mutation A53E associated with atypical multiple system atrophy and Parkinson's disease-type pathology." Neurobiol Aging **35**(9): 2180 e2181-2185.

Peng, X., R. Tehranian, P. Dietrich, L. Stefanis and R. G. Perez (2005). "Alpha-synuclein activation of protein phosphatase 2A reduces tyrosine hydroxylase phosphorylation in dopaminergic cells." J Cell Sci **118**(Pt 15): 3523-3530.

Petroi, D., B. Popova, N. Taheri-Talesh, S. Irniger, H. Shahpasandzadeh, M. Zweckstetter, T. F. Outeiro and G. H. Braus (2012). "Aggregate clearance of alpha-synuclein in Saccharomyces cerevisiae depends more on autophagosome and vacuole function than on the proteasome." J Biol Chem **287**(33): 27567-27579.

Piccini, P., D. J. Burn, R. Ceravolo, D. Maraganore and D. J. Brooks (1999). "The role of inheritance in sporadic Parkinson's disease: evidence from a longitudinal study of dopaminergic function in twins." Ann Neurol **45**(5): 577-582.

Pimentel, M. M., F. C. Rodrigues, M. A. Leite, M. Campos Junior, A. L. Rosso, D. H. Nicaretta, J. S. Pereira, D. J. Silva, M. V. Della Coletta, L. F. Vasconcellos, G. M. Abreu, J. M. Dos Santos and C. B. Santos-Reboucas (2015). "Parkinson disease: alpha-synuclein mutational screening and new clinical insight into the p.E46K mutation." Parkinsonism Relat Disord **21**(6): 586-589.

Plotegher, N., E. Greggio, M. Bisaglia and L. Bubacco (2014). "Biophysical groundwork as a hinge to unravel the biology of alpha-synuclein aggregation and toxicity." Q Rev Biophys **47**(1): 1-48.

Polymeropoulos, M. H., C. Lavedan, E. Leroy, S. E. Ide, A. Dehejia, A. Dutra, B. Pike, H. Root, J. Rubenstein, R. Boyer, E. S. Stenroos, S. Chandrasekharappa, A. Athanassiadou, T. Papapetropoulos, W. G. Johnson, A. M. Lazzarini, R. C. Duvoisin, G. Di Iorio, L. I. Golbe and R. L. Nussbaum (1997). "Mutation in the alpha-synuclein gene identified in families with Parkinson's disease." Science **276**(5321): 2045-2047.

Proukakis, C., C. G. Dudzik, T. Brier, D. S. MacKay, J. M. Cooper, G. L. Millhauser, H. Houlden and A. H. Schapira (2013). "A novel alpha-synuclein missense mutation in Parkinson disease." Neurology **80**(11): 1062-1064.

Prusiner, S. B. (1982). "Novel proteinaceous infectious particles cause scrapie." Science **216**(4542): 136-144.

Qin, Z., D. Hu, S. Han, D. P. Hong and A. L. Fink (2007). "Role of different regions of alpha-synuclein in the assembly of fibrils." Biochemistry **46**(46): 13322-13330.

Quadri, M., M. Fang, M. Picillo, S. Olgiati, G. J. Breedveld, J. Graafland, B. Wu, F. Xu, R. Erro, M. Amboni, S. Pappata, M. Quarantelli, G. Annesi, A. Quattrone, H. F. Chien, E. R. Barbosa, B. A. Oostra, P. Barone, J. Wang and V. Bonifati (2013). "Mutation in the SYNJ1 gene associated with autosomal recessive, early-onset Parkinsonism." Hum Mutat **34**(9): 1208-1215.

Quist, A., I. Doudevski, H. Lin, R. Azimova, D. Ng, B. Frangione, B. Kagan, J. Ghiso and R. Lal (2005). "Amyloid ion channels: a common structural link for protein-misfolding disease." Proc Natl Acad Sci U S A **102**(30): 10427-10432.

Ramirez, A., A. Heimbach, J. Grundemann, B. Stiller, D. Hampshire, L. P. Cid, I. Goebel, A. F. Mubaidin, A. L. Wriekat, J. Roeper, A. Al-Din, A. M. Hillmer, M. Karsak, B. Liss, C. G. Woods, M. I. Behrens and C. Kubisch (2006). "Hereditary parkinsonism with dementia is caused by mutations in ATP13A2, encoding a lysosomal type 5 P-type ATPase." Nat Genet **38**(10): 1184-1191.

Remy, I. and S. W. Michnick (2006). "A highly sensitive protein-protein interaction assay based on Gaussia luciferase." Nat Methods **3**(12): 977-979.

Rey, N. L., J. A. Steiner, N. Maroof, K. C. Luk, Z. Madaj, J. Q. Trojanowski, V. M. Lee and P. Brundin (2016). "Widespread transneuronal propagation of alpha-synucleinopathy triggered in olfactory bulb mimics prodromal Parkinson's disease." J Exp Med **213**(9): 1759-1778.

Ribeiro, C. S., K. Carneiro, C. A. Ross, J. R. Menezes and S. Engelender (2002). "Synphilin-1 is developmentally localized to synaptic terminals, and its association with synaptic vesicles is modulated by alpha-synuclein." J Biol Chem **277**(26): 23927-23933.

Riek, R., S. Hornemann, G. Wider, M. Billeter, R. Glockshuber and K. Wuthrich (1996). "NMR structure of the mouse prion protein domain PrP(121-231)." Nature **382**(6587): 180-182.

Roodveldt, C., C. W. Bertoncini, A. Andersson, A. T. van der Goot, S. T. Hsu, R. Fernandez-Montesinos, J. de Jong, T. J. van Ham, E. A. Nollen, D. Pozo, J. Christodoulou and C. M. Dobson (2009). "Chaperone proteostasis in Parkinson's disease: stabilization of the Hsp70/alpha-synuclein complex by Hip." EMBO J **28**(23): 3758-3770.

Roostaee, A., S. Beaudoin, A. Staskevicius and X. Roucou (2013). "Aggregation and neurotoxicity of recombinant alpha-synuclein aggregates initiated by dimerization." Mol Neurodegener **8**: 5.

Roy, S. (2009). "The paradoxical cell biology of alpha-Synucle." Results Probl Cell Differ **48**: 159-172.

Rutherford, N. J. and B. I. Giasson (2015). "The A53E alpha-synuclein pathological mutation demonstrates reduced aggregation propensity in vitro and in cell culture." Neurosci Lett **597**: 43-48.

Rutherford, N. J., B. D. Moore, T. E. Golde and B. I. Giasson (2014). "Divergent effects of the H50Q and G51D SNCA mutations on the aggregation of alpha-synuclein." J Neurochem **131**(6): 859-867.

Salafsky, J. S. (2006). "Detection of protein conformational change by optical second-harmonic generation." J Chem Phys **125**(7): 074701.

Sancenon, V., S. A. Lee, C. Patrick, J. Griffith, A. Paulino, T. F. Outeiro, F. Reggiori, E. Masliah and P. J. Muchowski (2012). "Suppression of alpha-synuclein toxicity and vesicle trafficking defects by phosphorylation at S129 in yeast depends on genetic context." Hum Mol Genet **21**(11): 2432-2449.

Satake, W., Y. Nakabayashi, I. Mizuta, Y. Hirota, C. Ito, M. Kubo, T. Kawaguchi, T. Tsunoda, M. Watanabe, A. Takeda, H. Tomiyama, K. Nakashima, K. Hasegawa, F. Obata, T. Yoshikawa, H. Kawakami, S. Sakoda, M. Yamamoto, N. Hattori, M. Murata, Y. Nakamura and T. Toda (2009). "Genome-wide association study identifies common variants at four loci as genetic risk factors for Parkinson's disease." Nat Genet **41**(12): 1303-1307.

Schell, H., T. Hasegawa, M. Neumann and P. J. Kahle (2009). "Nuclear and neuritic distribution of serine-129 phosphorylated alpha-synuclein in transgenic mice." Neuroscience **160**(4): 796-804.

Schmid, A. W., D. Chiappe, V. Pignat, V. Grimminger, I. Hang, M. Moniatte and H. A. Lashuel (2009). "Dissecting the mechanisms of tissue transglutaminase-induced cross-linking of alpha-synuclein: implications for the pathogenesis of Parkinson disease." J Biol Chem **284**(19): 13128-13142.

Schmid, A. W., B. Fauvet, M. Moniatte and H. A. Lashuel (2013). "Alpha-synuclein post-translational modifications as potential biomarkers for Parkinson disease and other synucleinopathies." Mol Cell Proteomics **12**(12): 3543-3558.

Selkoe, D. J. (2003). "Folding proteins in fatal ways." Nature **426**(6968): 900-904.

Seo, J. H., J. C. Rah, S. H. Choi, J. K. Shin, K. Min, H. S. Kim, C. H. Park, S. Kim, E. M. Kim, S. H. Lee, S. Lee, S. W. Suh and Y. H. Suh (2002). "Alpha-synuclein regulates neuronal survival via Bcl-2 family expression and PI3/Akt kinase pathway." FASEB J **16**(13): 1826-1828.

Serio, T. R., A. G. Cashikar, A. S. Kowal, G. J. Sawicki, J. J. Moslehi, L. Serpell, M. F. Arnsdorf and S. L. Lindquist (2000). "Nucleated conformational conversion and the replication of conformational information by a prion determinant." Science **289**(5483): 1317-1321.

Serpell, L. C., J. Berriman, R. Jakes, M. Goedert and R. A. Crowther (2000). "Fiber diffraction of synthetic alpha-synuclein filaments shows amyloid-like cross-beta conformation." Proc Natl Acad Sci U S A **97**(9): 4897-4902.

Sharon, R., M. S. Goldberg, I. Bar-Josef, R. A. Betensky, J. Shen and D. J. Selkoe (2001). "alpha-Synuclein occurs in lipid-rich high molecular weight complexes, binds fatty acids, and shows homology to the fatty acid-binding proteins." Proc Natl Acad Sci U S A **98**(16): 9110-9115.

Shimura, H., M. G. Schlossmacher, N. Hattori, M. P. Frosch, A. Trockenbacher, R. Schneider, Y. Mizuno, K. S. Kosik and D. J. Selkoe (2001). "Ubiquitination of a new form of alpha-synuclein by parkin from human brain: implications for Parkinson's disease." Science **293**(5528): 263-269.

Shojaee, S., F. Sina, S. S. Banihosseini, M. H. Kazemi, R. Kalhor, G. A. Shahidi, H. Fakhrai-Rad, M. Ronaghi and E. Elahi (2008). "Genome-wide linkage analysis of a Parkinsonian-pyramidal syndrome pedigree by 500 K SNP arrays." Am J Hum Genet **82**(6): 1375-1384.

Sin, O. and E. A. Nollen (2015). "Regulation of protein homeostasis in neurodegenerative diseases: the role of coding and non-coding genes." Cell Mol Life Sci **72**(21): 4027-4047.

Singleton, A. B., M. Farrer, J. Johnson, A. Singleton, S. Hague, J. Kachergus, M. Hulihan, T. Peuralinna, A. Dutra, R. Nussbaum, S. Lincoln, A. Crawley, M. Hanson, D. Maraganore, C. Adler, M. R. Cookson, M. Muenter, M. Baptista, D. Miller, J. Blancato, J. Hardy and K. Gwinn-Hardy (2003). "alpha-Synuclein locus triplication causes Parkinson's disease." Science **302**(5646): 841.

Smith, W. W., Z. Liu, Y. Liang, N. Masuda, D. A. Swing, N. A. Jenkins, N. G. Copeland, J. C. Troncoso, M. Pletnikov, T. M. Dawson, L. J. Martin, T. H. Moran, M. K. Lee, D. R. Borchelt and C. A. Ross (2010). "Synphilin-1 attenuates neuronal degeneration in the A53T alpha-synuclein transgenic mouse model." Hum Mol Genet **19**(11): 2087-2098.

Smith, W. W., R. L. Margolis, X. Li, J. C. Troncoso, M. K. Lee, V. L. Dawson, T. M. Dawson, T. Iwatsubo and C. A. Ross (2005). "Alpha-synuclein phosphorylation enhances eosinophilic cytoplasmic inclusion formation in SH-SY5Y cells." J Neurosci **25**(23): 5544-5552.

Souza, J. M., B. I. Giasson, V. M. Lee and H. Ischiropoulos (2000). "Chaperone-like activity of synucleins." FEBS Lett **474**(1): 116-119.

Spillantini, M. G., R. A. Crowther, R. Jakes, M. Hasegawa and M. Goedert (1998). "alpha-Synuclein in filamentous inclusions of Lewy bodies from Parkinson's disease and dementia with lewy bodies." Proc Natl Acad Sci U S A **95**(11): 6469-6473.

Spillantini, M. G., M. L. Schmidt, V. M. Lee, J. Q. Trojanowski, R. Jakes and M. Goedert (1997). "Alpha-synuclein in Lewy bodies." Nature **388**(6645): 839-840.

Strauss, K. M., L. M. Martins, H. Plun-Favreau, F. P. Marx, S. Kautzmann, D. Berg, T. Gasser, Z. Wszolek, T. Muller, A. Bornemann, H. Wolburg, J. Downward, O. Riess, J. B. Schulz and R. Kruger (2005). "Loss of function mutations in the gene encoding Omi/HtrA2 in Parkinson's disease." Hum Mol Genet **14**(15): 2099-2111.

Sunde, M. and C. C. Blake (1998). "From the globular to the fibrous state: protein structure and structural conversion in amyloid formation." Q Rev Biophys **31**(1): 1-39.

Swirski, M., J. S. Miners, R. de Silva, T. Lashley, H. Ling, J. Holton, T. Revesz and S. Love (2014). "Evaluating the relationship between amyloid-beta and alpha-synuclein phosphorylated at Ser129 in dementia with Lewy bodies and Parkinson's disease." Alzheimers Res Ther **6**(5-8): 77.

Sykes, E. and E. Epstein (1990). "Laboratory measurement of bilirubin." Clin Perinatol **17**(2): 397-416.

Takahashi, M., H. Kanuka, H. Fujiwara, A. Koyama, M. Hasegawa, M. Miura and T. Iwatsubo (2003). "Phosphorylation of alpha-synuclein characteristic of synucleinopathy lesions is recapitulated in alpha-synuclein transgenic Drosophila." Neurosci Lett **336**(3): 155-158.

Takahashi, M., L. W. Ko, J. Kulathingal, P. Jiang, D. Sevlever and S. H. Yen (2007). "Oxidative stress-induced phosphorylation, degradation and aggregation of alpha-synuclein are linked to upregulated CK2 and cathepsin D." Eur J Neurosci **26**(4): 863-874.

Tanner, C. M., R. Ottman, S. M. Goldman, J. Ellenberg, P. Chan, R. Mayeux and J. W. Langston (1999). "Parkinson disease in twins: an etiologic study." JAMA **281**(4): 341-346.

Taschenberger, G., M. Garrido, Y. Tereshchenko, M. Bahr, M. Zweckstetter and S. Kugler (2012). "Aggregation of alphaSynuclein promotes progressive in vivo neurotoxicity in adult rat dopaminergic neurons." Acta Neuropathol **123**(5): 671-683.

Taschenberger, G., J. Toloe, J. Tereshchenko, J. Akerboom, P. Wales, R. Benz, S. Becker, T. F. Outeiro, L. L. Looger, M. Bahr, M. Zweckstetter and S. Kugler (2013). "beta-synuclein aggregates and induces neurodegeneration in dopaminergic neurons." Ann Neurol **74**(1): 109-118.

Tenreiro, S., M. M. Reimao-Pinto, P. Antas, J. Rino, D. Wawrzycka, D. Macedo, R. Rosado-Ramos, T. Amen, M. Waiss, F. Magalhaes, A. Gomes, C. N. Santos, D. Kaganovich and T. F. Outeiro (2014). "Phosphorylation modulates clearance of alpha-synuclein inclusions in a yeast model of Parkinson's disease." PLoS Genet **10**(5): e1004302.

Thannickal, T. C., Y. Y. Lai and J. M. Siegel (2007). "Hypocretin (orexin) cell loss in Parkinson's disease." Brain **130**(Pt 6): 1586-1595.

Thomas, B. and M. F. Beal (2007). "Parkinson's disease." Hum Mol Genet **16 Spec No. 2**: R183-194.

Tokuda, T., S. A. Salem, D. Allsop, T. Mizuno, M. Nakagawa, M. M. Qureshi, J. J. Locascio, M. G. Schlossmacher and O. M. El-Agnaf (2006). "Decreased alpha-synuclein in cerebrospinal fluid of aged individuals and subjects with Parkinson's disease." Biochem Biophys Res Commun **349**(1): 162-166.

Tonges, L., E. M. Szego, P. Hause, K. A. Saal, L. Tatenhorst, J. C. Koch, D. H. Z, V. Dambeck, S. Kugler, C. P. Dohm, M. Bahr and P. Lingor (2014). "Alpha-synuclein mutations impair axonal regeneration in models of Parkinson's disease." Front Aging Neurosci **6**: 239.

Tosatto, L., M. H. Horrocks, A. J. Dear, T. P. Knowles, M. Dalla Serra, N. Cremades, C. M. Dobson and D. Klenerman (2015). "Single-molecule FRET studies on alpha-synuclein oligomerization of Parkinson's disease genetically related mutants." Sci Rep **5**: 16696.

Uryu, K., C. Richter-Landsberg, W. Welch, E. Sun, O. Goldbaum, E. H. Norris, C. T. Pham, I. Yazawa, K. Hilburger, M. Micsenyi, B. I. Giasson, N. M. Bonini, V. M. Lee and J. Q. Trojanowski (2006). "Convergence of heat shock protein 90 with ubiquitin in filamentous alpha-synuclein inclusions of alpha-synucleinopathies." Am J Pathol **168**(3): 947-961.

Varkey, J., J. M. Isas, N. Mizuno, M. B. Jensen, V. K. Bhatia, C. C. Jao, J. Petrlova, J. C. Voss, D. G. Stamou, A. C. Steven and R. Langen (2010). "Membrane curvature induction and tubulation are common features of synucleins and apolipoproteins." J Biol Chem **285**(42): 32486-32493.

Venda, L. L., S. J. Cragg, V. L. Buchman and R. Wade-Martins (2010). "alpha-Synuclein and dopamine at the crossroads of Parkinson's disease." Trends Neurosci **33**(12): 559-568.

Vilarino-Guell, C., A. Rajput, A. J. Milnerwood, B. Shah, C. Szu-Tu, J. Trinh, I. Yu, M. Encarnacion, L. N. Munsie, L. Tapia, E. K. Gustavsson, P. Chou, I. Tatarnikov, D. M. Evans, F. T. Pishotta, M. Volta, D. Beccano-Kelly, C. Thompson, M. K. Lin, H. E. Sherman, H. J. Han, B. L. Guenther, W. W. Wasserman, V. Bernard, C. J. Ross, S. Appel-Cresswell, A. J. Stoessl, C. A. Robinson, D. W. Dickson, O. A. Ross, Z. K. Wszolek, J. O. Aasly, R. M. Wu, F. Hentati, R. A. Gibson, P. S. McPherson, M. Girard, M. Rajput, A. H. Rajput and M. J. Farrer (2014). "DNAJC13 mutations in Parkinson disease." Hum Mol Genet **23**(7): 1794-1801.

Wakabayashi, K., S. Engelender, M. Yoshimoto, S. Tsuji, C. A. Ross and H. Takahashi (2000). "Synphilin-1 is present in Lewy bodies in Parkinson's disease." Ann Neurol **47**(4): 521-523.

Wales, P., R. Pinho, D. F. Lazaro and T. F. Outeiro (2013). "Limelight on alpha-synuclein: pathological and mechanistic implications in neurodegeneration." J Parkinsons Dis **3**(4): 415-459.

Walter, S. and J. Buchner (2002). "Molecular chaperones--cellular machines for protein folding." Angew Chem Int Ed Engl **41**(7): 1098-1113.

Wang, W., I. Perovic, J. Chittuluru, A. Kaganovich, L. T. Nguyen, J. Liao, J. R. Auclair, D. Johnson, A. Landeru, A. K. Simorellis, S. Ju, M. R. Cookson, F. J. Asturias, J. N. Agar, B. N. Webb, C. Kang, D. Ringe, G. A. Petsko, T. C. Pochapsky and Q. Q. Hoang (2011). "A soluble alpha-synuclein construct forms a dynamic tetramer." Proc Natl Acad Sci U S A **108**(43): 17797-17802.

Waxman, E. A. and B. I. Giasson (2008). "Specificity and regulation of casein kinase-mediated phosphorylation of alpha-synuclein." J Neuropathol Exp Neurol **67**(5): 402-416.

Weisberg, S. J., R. Lyakhovetsky, A. C. Werdiger, A. D. Gitler, Y. Soen and D. Kaganovich (2012). "Compartmentalization of superoxide dismutase 1 (SOD1G93A) aggregates determines their toxicity." Proc Natl Acad Sci U S A **109**(39): 15811-15816.

Weissman, A. M. (2001). "Themes and variations on ubiquitylation." Nat Rev Mol Cell Biol **2**(3): 169-178.

Wider, C., L. Skipper, A. Solida, L. Brown, M. Farrer, D. Dickson, Z. K. Wszolek and F. J. Vingerhoets (2008). "Autosomal dominant dopa-responsive parkinsonism in a multigenerational Swiss family." Parkinsonism Relat Disord **14**(6): 465-470.

Wille, H., W. Bian, M. McDonald, A. Kendall, D. W. Colby, L. Bloch, J. Ollesch, A. L. Borovinskiy, F. E. Cohen, S. B. Prusiner and G. Stubbs (2009). "Natural and synthetic prion structure from X-ray fiber diffraction." Proc Natl Acad Sci U S A **106**(40): 16990-16995.

Winner, B., R. Jappelli, S. K. Maji, P. A. Desplats, L. Boyer, S. Aigner, C. Hetzer, T. Loher, M. Vilar, S. Campioni, C. Tzitzilonis, A. Soragni, S. Jessberger, H. Mira, A. Consiglio, E. Pham, E. Masliah, F. H. Gage and R. Riek (2011). "In vivo demonstration that alpha-synuclein oligomers are toxic." Proc Natl Acad Sci U S A **108**(10): 4194-4199.

Wise-Scira, O., A. Dunn, A. K. Aloglu, I. T. Sakallioglu and O. Coskuner (2013). "Structures of the E46K mutant-type alpha-synuclein protein and impact of E46K mutation on the structures of the wild-type alpha-synuclein protein." ACS Chem Neurosci **4**(3): 498-508.

Wood, S. J., J. Wypych, S. Steavenson, J. C. Louis, M. Citron and A. L. Biere (1999). "alpha-synuclein fibrillogenesis is nucleation-dependent. Implications for the pathogenesis of Parkinson's disease." J Biol Chem **274**(28): 19509-19512.

Wu, B., Q. Liu, C. Duan, Y. Li, S. Yu, P. Chan, K. Ueda and H. Yang (2011). "Phosphorylation of alpha-synuclein upregulates tyrosine hydroxylase activity in MN9D cells." Acta Histochem **113**(1): 32-35.

Xiang, W., S. Menges, J. C. Schlachetzki, H. Meixner, A. C. Hoffmann, U. Schlotzer-Schrehardt, C. M. Becker, J. Winkler and J. Klucken (2015). "Posttranslational modification and mutation of histidine 50 trigger alpha synuclein aggregation and toxicity." Mol Neurodegener **10**: 8.

Xie, W. and K. K. Chung (2012). "Alpha-synuclein impairs normal dynamics of mitochondria in cell and animal models of Parkinson's disease." J Neurochem **122**(2): 404-414.

Yan, J. Q., Y. H. Yuan, Y. N. Gao, J. Y. Huang, K. L. Ma, Y. Gao, W. Q. Zhang, X. F. Guo and N. H. Chen (2014). "Overexpression of human E46K mutant alpha-synuclein impairs macroautophagy via inactivation of JNK1-Bcl-2 pathway." Mol Neurobiol **50**(2): 685-701.

Yang, Z. and D. J. Klionsky (2009). "An overview of the molecular mechanism of autophagy." Curr Top Microbiol Immunol **335**: 1-32.

Yavich, L., M. Oksman, H. Tanila, P. Kerokoski, M. Hiltunen, T. van Groen, J. Puolivali, P. T. Mannisto, A. Garcia-Horsman, E. MacDonald, K. Beyreuther, T. Hartmann and P. Jakala (2005). "Locomotor activity and evoked dopamine release are reduced in mice overexpressing A30P-mutated human alpha-synuclein." Neurobiol Dis **20**(2): 303-313.

Yonetani, M., T. Nonaka, M. Masuda, Y. Inukai, T. Oikawa, S. Hisanaga and M. Hasegawa (2009). "Conversion of wild-type alpha-synuclein into mutant-type fibrils and its propagation in the presence of A30P mutant." J Biol Chem **284**(12): 7940-7950.

Ysselstein, D., M. Joshi, V. Mishra, A. M. Griggs, J. M. Asiago, G. P. McCabe, L. A. Stanciu, C. B. Post and J. C. Rochet (2015). "Effects of impaired membrane interactions on alpha-synuclein aggregation and neurotoxicity." Neurobiol Dis **79**: 150-163.

Zarow, C., S. A. Lyness, J. A. Mortimer and H. C. Chui (2003). "Neuronal loss is greater in the locus coeruleus than nucleus basalis and substantia nigra in Alzheimer and Parkinson diseases." Arch Neurol **60**(3): 337-341.

Zarranz, J. J., J. Alegre, J. C. Gomez-Esteban, E. Lezcano, R. Ros, I. Ampuero, L. Vidal, J. Hoenicka, O. Rodriguez, B. Atares, V. Llorens, E. Gomez Tortosa, T. del Ser, D. G. Munoz and J. G. de Yebenes (2004). "The new mutation, E46K, of alpha-synuclein causes Parkinson and Lewy body dementia." Ann Neurol **55**(2): 164-173.

Zhou, J., M. Broe, Y. Huang, J. P. Anderson, W. P. Gai, E. A. Milward, M. Porritt, D. Howells, A. J. Hughes, X. Wang and G. M. Halliday (2011). "Changes in the solubility and phosphorylation of alpha-synuclein over the course of Parkinson's disease." Acta Neuropathol **121**(6): 695-704.

8. Curriculum vitae

Diana Lázaro

E-mail: dlazaro@gwdg.de

Personal Data

Name	Fernandes Lázaro, Diana
Date of Birthday	08 January 1987
Nationality	Portuguese
Sex	Female
Address	Boettingerstr. 5 37073 Göttingen, Germany
Telephone	+491 793805561

Education

2013-present	University Medical Center Gottingen CNMPB PhD Program, Graduate School GGNB: Neurosciences, Biophysics, Molecular Biosciences Studies conducted at the Department of Neurodegeneration and Restorative Research, University Medicine Göttingen, Germany PhD Thesis:
2010-2012	Faculty of Sciences, University of Lisbon Master of Human Biology and Environment, studies conducted at the Department of Neurodegeneration and Restorative Research, University Medicine Göttingen, Germany Master Thesis: "Systematic comparison of the effects of alpha-synuclein mutations on aggregation" (average 17)
2007-2010	Faculty of Sciences, University of Lisbon Bachelor of Science in Molecular Biology and Genetics (average 12)

Professional Experience

1/2014-present	PhD student Department of Neurodegeneration and Restorative Research, University Medicine, Göttingen, Germany
09/2012-12/2013	Technicial assistant Department of Neurodegeneration and Restorative Research, University Medicine, Göttingen, Germany
09/2011-2012	ERASMUS Scholarship Department of Neurodegeneration and Restorative Research, University Medicine, Göttingen, Germany
10/2008-05/2009	Internship BioFIG, Microbiology Laboratory
07/2006	Internship UNL, Department of Immunology

Additional qualifications

Laboratory skills (excerpt)	Cell Culture, Fluorescent Microscopy, PCR, SDS-PAGE, Native-PAGE, Molecular Biology, Density Gradient Centrifuge, FACS, Site-Directed Mutagenesis, Immunocytochemistry, FELASA B certificate, RNA extraction, Time-lapse imaging
Languages	Portuguese (native speaker), English (advanced speaker), Spanish (basic)
IT	Windows OS, MS Office, IMARIS, ImageJ, Inkscape, GraphPad, Cytoscape

Academic Awards and Scholarships

01/04-30/06/2017	GGNB Bridging Fund
3/2015	Travel Grant
9/2014	Second place for *Best Poster Presentation*, Summer School U4
09/2011-2012	ERASMUS Scholarship (Education and Culture DG, Lifelong Learning Programme)

Publications

Lázaro DF#, Turriani E#, Ryazanov S, Leonov A, Giese A, Schön M, Schön MP, Griesinger C, Outeiro TF, Arndt-Jovin DJ, Becker D. Treatment with diphenyl-pyrazole compounds anle138b/c reveals that α-synuclein protects melanoma cells from autophagic cell death. PNAS. 2017 Jun. (#equal contribution)

Lázaro DF#, Pavlou MAS#, Outeiro TF. Cellular models as tools for the study of the role of alpha-synuclein in Parkinson's disease. Experimental Neurology. 2017 May. (#equal contribution)

de Oliveira RM, Vicente Miranda H, Francelle L, Pinho R, Szegö ÉM, Martinho R, Munari F, **Lázaro DF**, Moniot S, Guerreiro P, Fonseca L, Marijanovic Z, Antas P, Gerhardt E, Enguita FJ, Fauvet B, Penque D, Pais TF, Tong Q, Becker S, Kügler S, Lashuel HA, Steegborn C, Zweckstetter M, Outeiro TF. The mechanism of sirtuin 2-mediated exacerbation of alpha-synuclein toxicity in models of Parkinson disease. PLoS Biol. 2017 Mar.

Lázaro DF#, Dias M#, Carija A, Navarro S, Madaleno CS, Tenreiro S, Ventura S, Outeiro TF. The effects of the novel A53E alpha-synuclein mutation on its oligomerization and aggregation. Acta Neuropathologica Communications. 2016 Dez. (#equal contribution)

Vicente Miranda H, Gomes M, Branco-Santos J, Breda C, **Lázaro DF**, Lopes LV, Herrera F, Giorgini F, Outeiro TF. Glycation potentiates neurodegeneration in models of Huntington's disease. Sci Rep. 2016 Nov.

Kleinknecht A, Popova B, **Lázaro DF**, Pinho R, Valerius O, Outeiro TF, Braus GH. C-Terminal Tyrosine Residue Modifications Modulate the Protective Phosphorylation of Serine 129 of α-Synuclein in a Yeast Model of Parkinson's Disease. PLoS Genet. 2016 Jun.

Amen T, **Lázaro DF**, Outeiro TF, Kaganovich D. Modeling Neuronal Pathology in Yeast: Insights into the Molecular Basis of Parkinson's Disease. Israel J Chemistry. 2015 Nov.

Lázaro DF#, Moree B#, Yin G#**,** Munari F, Strohäker T, Giller K, Becker S, Outeiro TF, Zweckstetter M, Salafsky J. Small Molecules Detected by Second-Harmonic Generation

Modulate the Conformation of Monomeric α-Synuclein and Reduce its Aggregation in Cells. J Bio Chem. 2015 Sep. (#equal contribution)

Ducic T, Carboni E, Lai B, Chen S, Michalke B, **Lázaro DF**, Outeiro TF, Bähr M, Barski E, Lingor P. Alpha-Synuclein Regulates Neuronal Levels of Manganese and Calcium. ACS Chem Neurosci. 2015 Aug.

Lázaro DF, Rodrigues EF et al. Systematic comparison of the effects of alpha-synuclein mutations on its oligomerization and aggregation. PLoS Genet. 2014 Nov.

Perfeito R, **Lázaro DF**, Outeiro TF, Rego AC. Linking alpha-synuclein phosphorylation to reactive oxygen species formation and mitochondrial dysfunction in SH-SY5Y cells. Mol Cell Neurosci. 2014 Sep.

Yin G, Lopes da Fonseca T, Eisbach SE, Anduaga AM, Breda C, Orcellet ML, Szegő ÉM, Guerreiro P, **Lázaro DF**, Braus GH, Fernandez CO, Griesinger C, Becker S, Goody RS, Itzen A, Giorgini F, Outeiro TF, Zweckstetter M. α-Synuclein interacts with the switch region of Rab8a in a Ser129 phosphorylation-dependent manner. Neurobiol Dis. 2014 Oct.

Wales P, Pinho R, **Lázaro DF**, Outeiro TF. Limelight on Alpha-Synuclein: Pathological and Mechanistic Implications in Neurodegeneration. J Parkinsons Dis. 2013 Nov.

Communication in scientific conferences

8-11/08/2016 Oral presentation in Propagation in Neurodegenerative Disease Conference, Dublin, Ireland
The Role of Synphilin-1 on the Spreading of Alpha-Synuclein Pathology

03/11/2015 Poster presentation in 3rd biennial CMPB Symposium Encephalon, Goettingen, Germany
Deciphering the role of Synphilin-1 as a modulator of alpha-synuclein aggregation and toxicity
DF. Lázaro, N. Kruse, D. Kaganovich, B. Mollenhauer, SO. Rizzoli, and TF. Outeiro

31-04/05/2015 Poster presentation in EMBO Workshop- Macromolecular assemblies at the crossroads of cell stress and function, Jerusalem, Israel
Systematic Comparison of the Effects of Alpha-synuclein Mutations on Oligomerization and Aggregation
D. Lázaro, E. Rodrigues, P. Guerreiro, E. Gerhardtn, T. Outeiro

11-13/02/2015 Poster presentation in Alpha-Synuclein: The Gateway To Parkinsonism, Innsbruck, Austria
Systematic Comparison of the Effects of Alpha-synuclein Mutations on Oligomerization and Aggregation
D. Lázaro, E. Rodrigues, P. Guerreiro, E. Gerhardtn, T. Outeiro

13-16/03/2013 Participation with a poster presentation in 10th Göttingen Meeting of the German Neuroscience Society, Goettingen, Germany
Systematic Comparison of the Effects of Alpha-synuclein Mutations on Oligomerization and Aggregation
D. Lázaro, E. Rodrigues, P. Guerreiro, E. Gerhardtn, T. Outeiro

Workshops

1-2/12/2016	GGNB Workshop on "Grant Writing for Scientists"
04-6/11/2015	Brain Clearing Imaging Mini-Symposium
04/2012-03/2013	Drugs and the Brain (online course from Caltech University)
18-19/12/2010	Course of Scientific Entertainers
16/09/2010	Workshop "Talking Science to Journalists"
19/03/2010	Workshop on "Protein Folding diseases- metabolic disorders to neurodegeneration" *Instituto de Tecnologia Química e Biologia*
4-5/03/2010	Program and European Network of Excellence on Alternative Splicing, EURASNET, Calouste Gulbenkian Foundation, Lisbon
18-19/11/2006	Workshop on Mycology